NOTE TO USERS

This reproduction is the best copy available.

UMI®

University of Alberta

Physicochemical and Structural Characterization of Hull-less Barley Starches

by

Jihong Li ©

A thesis submitted to the Faculty of Graduate Studies and Research in partial fulfillment of the requirements for the degree of **Doctor of Philosophy**

in

Food Science and Technology

Department of Agricultural, Food and Nutritional Science

Edmonton, Alberta

Spring 2004

Library and
Archives Canada

Published Heritage
Branch

395 Wellington Street
Ottawa ON K1A 0N4
Canada

Bibliothèque et
Archives Canada

Direction du
Patrimoine de l'édition

395, rue Wellington
Ottawa ON K1A 0N4
Canada

Your file Votre référence
ISBN: 0-612-96294-6
Our file Notre référence
ISBN: 0-612-96294-6

The author has granted a non-exclusive license allowing the Library and Archives Canada to reproduce, loan, distribute or sell copies of this thesis in microform, paper or electronic formats.

L'auteur a accordé une licence non exclusive permettant à la Bibliothèque et Archives Canada de reproduire, prêter, distribuer ou vendre des copies de cette thèse sous la forme de microfiche/film, de reproduction sur papier ou sur format électronique.

The author retains ownership of the copyright in this thesis. Neither the thesis nor substantial extracts from it may be printed or otherwise reproduced without the author's permission.

L'auteur conserve la propriété du droit d'auteur qui protège cette thèse. Ni la thèse ni des extraits substantiels de celle-ci ne doivent être imprimés ou aturement reproduits sans son autorisation.

In compliance with the Canadian Privacy Act some supporting forms may have been removed from this thesis.

Conformément à la loi canadienne sur la protection de la vie privée, quelques formulaires secondaires ont été enlevés de cette thèse.

While these forms may be included in the document page count, their removal does not represent any loss of content from the thesis.

Bien que ces formulaires aient inclus dans la pagination, il n'y aura aucun contenu manquant.

Canada

ABSTRACT

Waxy, normal, and high-amylose types of starches (0-6%, 24-29%, and 42-45% amylose, respectively) were extracted from ten hull-less barley (HB) grain genotypes and were physicochemically and structurally characterized in terms of composition, morphology, gelatinization, pasting, susceptibility to acid, branch chain length distribution of amylopectin, and granule ultrastructure. Morphological and ultrastructural changes in waxy, normal, and high-amylose starches during heating in water and α-amylolysis were also examined. The studies showed the following major results: (1) The amylose contents in this set of starches ranged from 0-45% with 0.3-1.7% of amylose bound lipids and the average chain length and degree of branching ranged from 17.6-22.7 anhydro-glucose units and 4.4-5.5% in amylopectin; (2) The starch composition, granule size and shape differed, but the amylose/amylopectin ratio and amylopectin branch chain length had high correlations with granule size and size distribution; (3) Gelatinization parameters and other physicochemical properties were highly correlated with some structural starch characteristics; (4) Two distinct regions, densely packed granule growth rings alternating with inter-crystalline amorphous growth rings and semi-crystalline growth rings in the periphery and a loose filamentous network in the central granule, were present in varying number and width. Granule bound proteins (mainly integral proteins) existed in the central and growth ring regions of the granule; (5) The swelling and melting/solubilization patterns of waxy HB starch were different from those of non-waxy types under electron microscope. The macromolecular solution formed in waxy starch while "ghost" structure (shell of starch granule) was formed and embedded in soluble starch matrix, whereas, a web network within ghosts of non-waxy starches at 90-100°C was also observed; (6) The patterns of

amylolysis, such as surface erosion, endoerosion, and erosion at the equatorial groove plane of granules, were dependent on enzyme source and starch type. The outer layers of normal and high-amylose HB starch granules were more resistant to enzyme hydrolysis. Waxy starch has a more open ultrastructure leading to easier gelatinization and higher susceptibility to acid and enzymes than do non-waxy starches. In general, the structural features of HB starch determine its physicochemical properties. A new model for HB starch granule ultrastructure is postulated.

Dedicated to my parents, wife, and
children for their love and
encouragement.

ACKNOWLEDGEMENTS

I would like to express my sincere appreciation to my supervisors, Dr. Thava Vasanthan and Dr. Brian G. Rossnagel (University of Saskatchewan) for their invaluable guidance and advice throughout my Ph.D. study. Thanks to Drs. Peter Sporns, Feral Temelli, and Buncha Ooraikul for their advice as supervisory committee members. I thank Dr. Ratnajothi Hoover (Memorial University of Newfoundland), who is an active research collaborator in the starch research program of my supervisor, Dr. T. Vasanthan, for his input into this research and critical review of my manuscripts for publication and thesis. Appreciation is extended to Prof. Ling-cheng Jian (University of Minnesota) for his valuable advice in TEM techniques, Mr. Doug Hassard for his assistance in DSC analysis, and Mr. George Braybrook and Dr. Min Chen for their assistance in SEM and TEM examination. Also to Dr. Gao-Song Jiang, Dr. Jian Wang, Dr. Wettasinghe Mahinda, Dr. You Jin Jeon, Abdul Faraj, Judy Yeung, Xin-Hua Wang, Sandip Gill, Jing Yu, Hai-yan Zhang, Vivian Gee, Jun Gao, Baljit Ghotra, Shi-yu Li, Mei Sun, and Gordon Grant for their friendly assistance and support given throughout this study. I acknowledge the financial support from the Natural Sciences and Engineering Research Council of Canada (NSERC) and the Alberta Agricultural Research Institute (AARI) to Dr. T. Vasanthan's research program for which I performed my research and fellowships awarded by the Canadian Wheat Board (CWB), and the Province of Alberta as well as the travel grant from the Faculty of Graduate Studies and Research, Department of Agricultural, Food and Nutritional Science, University of Alberta, and the Carbohydrate Division, American Association of Cereal Chemists (AACC). Thanks to Jody Forslund and other staff in our department and all friends for their routine support and creating a pleasant environment in which to work. My sincere thanks are also to my loving wife, parents and children helping me in all possible ways to succeed.

TABLE OF CONTENTS

ABSTRACT ....

ACKNOWLEDGEMENTS ....

LIST OF TABLES ....

LIST OF FIGURES ....

LIST OF ABBREVIATIONS ....

CHAPTER 1 Literature Review 1

- 1.1 Barley grain 1
  - 1.1.1 Classification and production 1
  - 1.1.2 Grain structure and composition 2
  - 1.1.3 Barley utilization and potential 6
- 1.2 Starch 8
  - 1.2.1 General 8
    - 1.2.1.1 Starch sources 8
    - 1.2.1.2 Starch production and starch derivatives 9
    - 1.2.1.3 Application of starch and starch derivatives in food and non-food industries 13
  - 1.2.2 Chemical composition 16
    - 1.2.2.1 Amylose and amylopectin 16
    - 1.2.2.2 Minor components 16
      - 1.2.2.2.1 Starch proteins 19
      - 1.2.2.2.2 Starch lipids 20
      - 1.2.2.2.3 Minerals 21
  - 1.2.3 Morphology 22
    - 1.2.3.1 Granule shape and size 22
    - 1.2.3.2 Granule size distribution 25
    - 1.2.3.3 Surface features 27
  - 1.2.4 Ultrastructure 28
    - 1.2.4.1 Macromolecules 32
      - 1.2.4.1.1 Amylose 32
      - 1.2.4.1.2 Amylopectin 36
    - 1.2.4.2 Molecular orientation 45

1.2.4.3 Double helices, crystallites, and crystallinity 47
1.2.4.4 Polymorphic patterns 53
1.2.4.5 Lamellae 57
1.2.4.6 Growth rings 58
1.2.4.7 Channels and central cavity 62
1.2.4.8 Structure of amorphous region 63
1.2.4.8.1 Location and distribution of amylose 63
1.2.4.8.2 Lipid-complexed amylose 66
1.2.5 Physicochemical properties of starch 66
1.2.5.1 Gelatinization 68
1.2.5.1.1 Gelatinization and loss of granular order 71
1.2.5.1.2 Gelatinization and amylose/amylopectin ratio 72
1.2.5.1.3 Gelatinization, branch chain length and distribution of amylopectin 74
1.2.5.1.4 Gelatinization and crystalline type 74
1.2.5.1.5 Swelling and solubilization 75
1.2.5.2 Pasting 78
1.2.5.3 Acid hydrolysis 80
1.2.5.3.1 Acid hydrolysis kinetics 81
1.2.5.3.2 Effect on the degree of crystallinity and X-ray diffraction pattern 83
1.2.5.3.3 Effect on amylopectin molecular structure 84
1.2.5.3.4 Effect on gelatinization parameters 85
1.2.5.4 *In vitro* enzyme amylolysis 87
1.2.5.4.1 Hydrolysis kinetics 88
1.2.5.4.2 Hydrolysis products and their effects on hydrolysis 91
1.2.5.4.3 Action pattern revealed by EM 93
1.2.5.5 Retrogradation 95
1.3 Objectives of thesis 97
1.4 References 99
CHAPTER 2 Granule Morphology, Composition and Amylopectin Structure 140
2.1 Introduction 140
2.2 Materials and methods 142

2.2.1 Materials 142
2.2.2 Starch isolation 142
2.2.3 Chemical composition of grain and starch 143
2.2.4 Granule morphology 143
2.2.5 Granule size analysis 144
2.2.6 Molecular characterization of amylopectin 144
2.2.7 Statistical analysis 145
2.3 Results and discussion 145
2.3.1 Chemical composition of barley grains 145
2.3.2 Isolation and chemical composition of HB starches 147
2.3.3 Granule morphology 149
2.3.4 Granule size distribution 149
2.3.5 Amylopectin structure 156
2.4 Conclusion 159
2.5 References 160
CHAPTER 3 Thermal, Rheological and Acid Hydrolysis Characteristics 163
3.1 Introduction 163
3.2 Materials and methods 164
3.2.1 Materials 164
3.2.2 Starch isolation 164
3.2.3 Gelatinization characteristics 164
3.2.4 Brabender viscoamylography 165
3.2.5 Swelling power and solubility 165
3.2.6 Acid hydrolysis 165
3.2.7 Statistical analysis 165
3.3 Results and discussion 166
3.3.1 Gelatinization characteristics 166
3.3.2 Swelling power and solubility 169
3.3.3 Pasting properties 174
3.3.4 Acid hydrolysis 177
3.4 Conclusion 181
3.5 References 182

CHAPTER 4 Ultrastructure and Distribution of Granule-bound Proteins 186
4.1 Introduction.. 186
4.2 Materials and methods 189
4.2.1 Starch source.. 189
4.2.2 Starch localization.. 189
4.2.3 Protease treatment prior to starch localization 190
4.2.4 Protein localization... 190
4.2.5 Transmission electron microscopy... 191
4.2.6 Scanning electron microscopy 191
4.3 Results 192
4.3.1 Starch granule structure.. 192
4.3.2 Growth rings 196
4.3.3 Proteins in starch granules.. 199
4.4 Discussion.. 199
4.4.1 Architecture of starch granules 199
4.4.2 Growth rings 202
4.4.3 Starch granule-bound proteins.. 203
4.4.4 Periodic acid - thiosemicarbazide - silver protenate and ammoniacal silver reactions in starch granules.. 204
4.5 Conclusion.. 206
4.6 References 207
CHAPTER 5 Morphological and Structural Changes in Waxy, Normal and High-amylose Starch Granules during Heating 213
5.1 Introduction.. 213
5.2 Materials and methods 214
5.2.1 Materials 214
5.2.2 Sample preparation.. 215
5.2.3 Scanning electron microscopy 215
5.2.4 Transmission electron microscopy.. 216
5.2.5 Matrix-assisted laser desorption/ionisation mass spectrometry................. 216
5.3 Results and discussion.. 216
5.3.1 Morphology and ultrastructure of native HB starch granules 216

5.3.2 Morphological and ultrastructural changes during heating of waxy starch granules 218
5.3.3 Morphological and ultrastructural changes during heating of non-waxy HB starch granules 222
5.3.4 Detection of amylopectin in the leached exudates at 65°C and 100°C by MALDI-MS........ 233
5.4 Conclusion........ 235
5.5 References 237
CHAPTER 6 *In vitro* Susceptibility of Waxy, Normal, and High-amylose Starches towards Hydrolysis by Alpha-amylases and Amyloglucosidase........ 240
6.1 Introduction........ 240
6.2 Materials and methods 242
6.2.1 Starch sources........ 242
6.2.2 Enzymes........ 243
6.2.3 Enzyme hydrolysis........ 243
6.2.4 Quantification of glucose, maltose, and maltotriose 244
6.2.5 Scanning electron microscopy 244
6.2.6 Transmission electron microscopy........ 244
6.3 Results and discussion........ 246
6.3.1 Granule morphology of native HB starches........ 246
6.3.2 Hydrolysis kinetics 246
6.3.3 Scanning electron microscopy 251
6.3.4 Transmission electron microscopy........ 256
6.3.5 Hydrolysis products........ 261
6.4 Conclusion........ 263
6.5 References 264
CHAPTER 7 Conclusions and Recommendations 269
7.1 References 276
PUBLICATIONS........ 277
APPENDIX A 278
APPENDIX B 279

LIST OF TABLES

Table 1-1 Chemical composition of hulled and hull-less barley grains 5

Table 1-2 World starch production by source in 2000 10

Table 1-3 Applications of starch and starch derivatives in food and non-food industries 14

Table 1-4 Chemical composition of starches from various sources 17

Table 1-5 Shape and size of starch granules from different botanical sources 23

Table 1-6 Granule size distribution of some cereal starches 26

Table 1-7 General characteristics of amylose and amylopectin 30

Table 1-8 Molecular characteristics of amylose from various starches 33

Table 1-9 Molecular characteristics of amylopectin from various starches 37

Table 1-10 Branch chain length distributions of amylopectin from various starches 43

Table 1-11 Unit cell structures of A- and B-type crystallites 51

Table 1-12 Degree of crystallinity of starches determined by different methods 52

Table 1-13 Thermal properties of starch gelatinization determined by differential scanning calorimetry 70

Table 2-1 Chemical composition of hull-less barley grain 146

Table 2-2 Chemical composition of hull-less barley and maize starches 148

Table 2-3 Granule size and size distribution of hull-less barley and maize starches 155

Table 2-4 Chain length distribution of debranched amylopectins of hull-less barley and maize starches 158

Table 3-1 Thermal characteristics of hull-less barley and maize starches................ 167

Table 3-2 Correlations between physicochemical properties and structural characteristics of hull-less barley starches.. 176

Table 4-1 Widths of granule growth rings of HB starches.. 198

LIST OF FIGURES

Figure 1-1 Cross section of barley grain..3

Figure 1-2 Products derived from starch...12

Figure 1-3 Structure of amylose and amylopectin..29

Figure 1-4 Illustration of the length scale of starch granule structure levels together with technology used for characterization of starch structural features...31

Figure 1-5 Gel-permeation chromatograms of debranched amylopectins.................41

Figure 1-6 Cluster models of amylopectin...46

Figure 1-7 Double helix model of starch chain...48

Figure 1-8 Double helix packing arrangement of amylopectin crystallites in A- and B-type unit cells...50

Figure 1-9 X-ray diffraction patterns of A-, B-, and C-type starches with their characteristic d-spacing..54

Figure 1-10 Proposed models for branching patterns of A- and B-type starches.......56

Figure 1-11 A starch granule structure model...59

Figure 1-12 Schematic diagram of starch granule structure...............................61

Figure 1-13 A possible mechanism to explain the disruption of amylopectin double helical packing by amylose...65

Figure 1-14 Schematic illustration of amylose-lipid complex.............................67

Figure 2-1 Scanning electron micrographs of hull-less barley and maize starches...150

Figure 2-2 Scanning electron micrographs of hull-less barley and maize starches...151

Figure 2-3 Scanning electron micrographs of hull-less barley starches from SB 94917, SR 93102, and SB 94860 152

Figure 2-4 Transmission electron micrographs of hull-less barley starch granules from SR 93102 153

Figure 2-5 Granule size distribution of hull-less barley and maize starches. 154

Figure 2-6 MALDI-MS spectrum and chain length distribution of debranched starch (SB 94893) 157

Figure 3-1 Swelling power of native hull-less barley and maize starches 170

Figure 3-2 Solubility curves of native hull-less barley and maize starches. 171

Figure 3-3 Pasting properties of native hull-less barley and maize starches 175

Figure 3-4 Acid hydrolysis of native hull-less barley and maize starches 178

Figure 4-1 Schematic diagram of amylopectin structure showing growth rings and areas for amorphous and crystalline lamellae formation 187

Figure 4-2 Transmission electron micrographs of ultrathin sections of HB starch granules treated with PATAg 193

Figure 4-3 Transmission electron micrographs of ultrathin sections of maize starch granules treated with PATAg 194

Figure 4-4 Scanning electron micrographs of HB starch granules hydrolyzed by α-amylase from porcine pancreas at 37°C for 1h and cracked mechanically 195

Figure 4-5 Transmission electron micrographs of ultrathin sections of high-amylose barley starch granule and normal maize starch granule hydrolyzed by protease 197

Figure 4-6 Transmission electron micrographs of ultrathin sections of HB starch granules treated with AS 200

Figure 5-1 Scanning and transmission electron micrographs of native waxy (CDC Alamo), normal (CDC Dawn), and high-amylose (SB 94893) HB starch granules........217

Figure 5-2 Scanning electron micrographs of waxy HB starch granules (CDC Alamo) heated in water to various temperatures........219

Figure 5-3 Scanning electron micrographs of waxy HB starch granules (CDC Alamo) heated in water to various temperatures........220

Figure 5-4 Transmission electron micrographs of waxy HB starch granules (CDC Alamo) heated in water to various temperatures........221

Figure 5-5 Scanning electron micrographs of normal HB starch granules (CDC Dawn) heated in water to various temperatures........223

Figure 5-6 Scanning electron micrographs of normal HB starch granules (CDC Dawn) heated in water to various temperatures........224

Figure 5-7 Scanning electron micrographs of high-amylose HB starch granules (SB 94893) heated in water to various temperatures........225

Figure 5-8 Scanning electron micrographs of high-amylose HB starch granules (SB 94893) heated in water to various temperatures........226

Figure 5-9 Transmission electron micrographs of normal HB starch granules (CDC Dawn) heated in water to various temperatures........229

Figure 5-10 Transmission electron micrographs of high-amylose HB starch granules (SB 94893) heated in water to various temperatures........230

Figure 5-11 Scanning electron micrographs of HB starch granule remnants heated in water to 100°C........232

Figure 5-12 MALDI-MS spectra of debranched HB starch heated in water to 65°C and 100°C........234

Figure 6-1 Scanning and transmission electron micrographs of HB starch granules from waxy (CDC Alamo), normal (CDC Dawn), and high-amylose (SB 94893) types 247

Figure 6-2 Hydrolysis of HB starches from waxy (CDC Alamo), normal (CDC Dawn) and high-amylose (SB 94893) types by PPA, BAA, and AAG 250

Figure 6-3 Scanning electron micrographs of HB starch granules from waxy (CDC Alamo), normal (CDC Dawn), and high-amylose (SB 94893) types hydrolyzed by PPA at 37°C for 1 h........ 252

Figure 6-4 Scanning electron micrographs of HB starch granules from waxy (CDC Alamo), normal (CDC Dawn), and high-amylose (SB 94893) types hydrolyzed by PPA at 37°C for 3 h and 6 h........ 254

Figure 6-5 Scanning electron micrographs of HB starch granules from waxy (CDC Alamo), normal (CDC Dawn), and high-amylose (SB 94893) types hydrolyzed by PPA at 37°C for 21 h........ 255

Figure 6-6 Scanning electron micrographs of HB starch granules from waxy (CDC Alamo), normal (CDC Dawn), and high-amylose (SB 94893) types hydrolyzed by AAG at 55°C for 21 h 257

Figure 6-7 Transmission electron micrographs of HB starch granules from waxy (CDC Alamo), normal (CDC Dawn), and high-amylose (SB 94893) types hydrolyzed by PPA at 37°C for 3 h........ 258

Figure 6-8 Transmission electron micrographs of HB starch granules from waxy (CDC Alamo), normal (CDC Dawn), and high-amylose (SB 94893) types hydrolyzed by AAG at 55°C for 21 h 259

Figure 6-9 The contents of glucose, maltose, and maltotriose produced during HB starch hydrolysis by PPA and BAA........ 262

Figure 7-1 Schematic diagram of a HB starch granule detailing the ultrastructural features 274

LIST OF ABBREVIATIONS

ΔH	Enthalpy
AAG	*Aspergillus niger* amyloglucosidase
AM	Amylose
AP	Amylopectin
AS	Ammoniacal silver
BAA	*Bacillus species* alpha-amylase
BD	Bound lipids
BP	Branch points
BV	Blue value
CL	Average chain length
CM	$CHCl_3$-CH_3OH
DE	Dextrose equivalent
DHB	2, 5-Dihydroxybenzoic acid
DMSO	Dimethyl sulfoxide
DP	Degree of polymerization
DSC	Differential scanning calorimetry
EU	European Union
FACE	Fluorophore-assisted carbohydrate electrophoresis
FAM	Lipid-free amylose
LAM	Lipid-complexed amylose
GBSS	Granule-bound starch synthase
GNP	Gross national product
GPC	Gel permeation chromatography
HB	Hull-less barley
HPAEC-PAD	High performance anion-exchange chromatography with pulsed amperometric detection
HPLC	High performance liquid chromatography
IA	Iodine affinity
ICAGR	Inter-crystalline amorphous growth ring
MALDI-MS	Matrix-assisted laser desorption/ionization-mass spectrometry

NMR	Nuclear magnetic resonance
PAGE	Polyacrylamide gel electrophoresis
PATAg	Periodic acid–thiosemicarbazide–silver protenate
PAS	Periodic acid-Schiff
PPA	Porcine pancreatic alpha-amylase
PW	n-Propanol-water
RVA	Rapid visco-analyzer
SAXS	Small-angle X-ray scattering
SDS	Sodium dodecyl sulfate
SEC	Size-exclusion chromatography
SEM	Scanning electron microscopy
$T_c - T_o$	Transition temperature range
T_c	Conclusion temperature
TEM	Transmission electron microscopy
T_o	Onset temperature
T_p	Peak temperature
UK	United Kingdom
USA	United States of America

CHAPTER 1

Literature Review

1.1 Barley grain

1.1.1 Classification and production

Barley belongs to the grass family *Poaceae*, the tribe *Triticeae*, and the genus *Hordeum* (Nilan and Ullrich, 1993). Cultivated varieties of barley (*Hordeum vulgare* L.) are commonly classified as six-row or two-row, describing the physical arrangement of kernels on the spike/panicle of the plant. In six-rowed barley, all three spikelets at each node of the flat rachis of the spike (head) are fertile, while in two-rowed barley, only the central spikelet is fertile. Two-rowed barley is usually plump and has a greater uniformity in kernel size, which is preferable for malting/brewing and food processing (e.g. milling and rolling). Currently, over 50 barley varieties are registered for production in Canada, including 8 hull-less and 13 malting varieties (Alberta Barley Commission, 2003). Traditional two-row and six-row barley grains are covered with hulls, which adhere tightly to kernels (the lemma and palea adhere to the caryopsis and do not thresh free). Hull-less or naked barley (HB) has been developed for food, feed and potential industrial applications. The availability of genotypes (waxy, normal and high-amylose starch, low and high lysine, low and high β-glucan) makes HB uniquely suitable for use in feed and food products.

Barley is the fourth largest grain crop after wheat, rice, and maize in the world with annual production of about 132 million metric tons (FAO, 2003). The leading producing countries are Canada, Russian Federation, Germany, Spain, France, United States of

America (USA), Turkey, United Kingdom (UK), Australia, Denmark, and China. Canada is the world's largest barley producer, with production of 13.5 million metric tons, accounting for 10.2% of the total world production (FAO, 2003). As the second major cereal in Canada, approximately 88% of barley is grown in the prairie provinces of Alberta, Saskatchewan and Manitoba (Jadhav et al., 1998). HB production was estimated to be between 300,000 and 350,000 ha in 1998, with an estimated grain production of about 800,000 tons (Bhatty, 1999).

1.1.2 Grain structure and composition

The spindle-shaped barley grain is comprised of the caryopsis and a hull or husk (Figure1-1). The hull, the outermost part of hulled barley, consists of the lemma and palea. In hulled barley grain, the hull is strongly adhered to the caryopsis/kernel, whereas in HB grain, the hull is easily removed during threshing. The hull occupies about 10-13% of the grain and is rich in cellulose, insoluble arabinoxylan, lignin, polyphenols, and minerals (MacGregor, 1998). The caryopsis consists of the pericarp, testa, aleurone layer, endosperm, and embryo. The pericarp, about 2% of total kernel weight, is attached to the husk by a "cementing" layer (associated with an unknown lipid layer) (MacGregor, 1998). It contains cellulose, arabinoxylans, and lignin, but no protein and carbohydrates. The testa comprises 1-3% of the total kernel weight (MacGregor, 1998). It contains cellulose, waxes and pigments (i.e. anthocyanogens). The aleurone layer separates the endosperm from other grain tissues. It comprises 5-10% of the total kernel (MacGregor, 1998). The main components of aleurone cell walls are arabinoxylans (60%), β-glucan (22%), and protein (16%) (MacGregor, 1998). Aleurone cells are rich in lipids (30%) (mainly triacylglycerides) and protein (20%), with

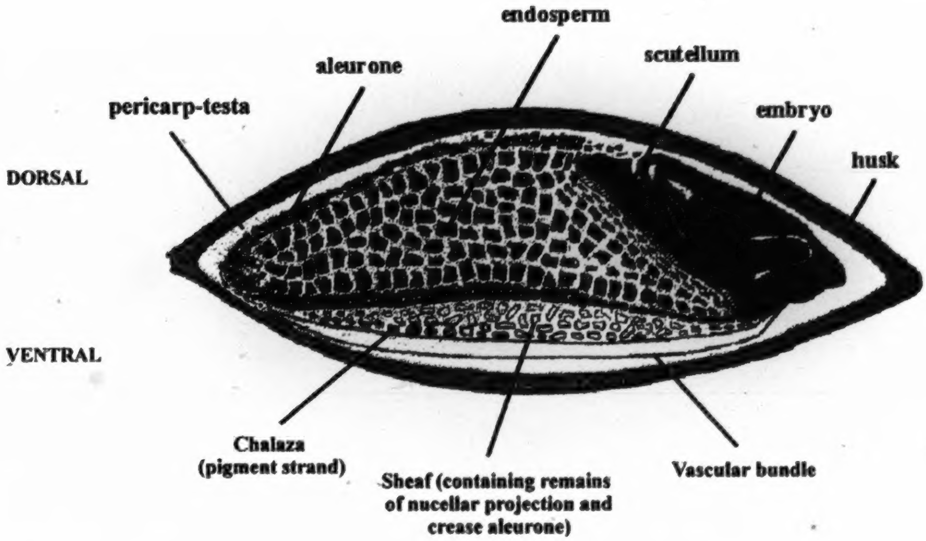
endosperm
scutellum
aleurone
embryo
pericarp-testa
husk
DORSAL
VENTRAL
Chalaza (pigment strand)
Sheaf (containing remains of nucellar projection and crease aleurone)
Vascular bundle

Figure 1-1 Cross section of barley grain (modified from Duffus and Cochrane, 1996; CRC, 2003).

minor components phytic acid, minerals, sucrose, and anthocyanogens (MacGregor, 1998). Vitamins, including thiamin, riboflavin, niacin, pathothenic acid, tocotrienols, and biotin are shared between the aleurone and embryo (MacGregor, 1998). Tocotrienols (isomers of vitamin E) are found in the aleurone and endosperm. The embryo comprises 2-4% of the kernel (MacGregor, 1998). The germ is rich in lipids (13-17%), protein and free amino acids (34%), sucrose (14%), raffinose (5-10%), arabinoxylan, cellulose and pectin (8-10%), and ash (5-10%). It also contains fructans/fructo-oligosaccharides (polymers of fructose) (0.2-0.9%) and trace of tocopherols (MacGregor, 1998). During pearling, outer layers of the grain (bran), including pericarp, testa, aleurone layer and embryo are gradually removed by abrasive action. Within the endosperm, starch, which comprises of 75-80% of the kernel weight, is embedded in a protein matrix (MacGregor, 1998). The cell walls in the endosperm are mainly composed of β-glucan (70-75%), arabinoxylans (20-25%), and protein (5-6%) with minor amount of glucomannans, cellulose, and phenolic compounds (MacGregor, 1998; Jadhav et al., 1998).

The chemical composition of hulled and hull-less barley grains are shown in Table 1-1. The major components are starch (52-72%), protein (9-14%), lipids (2-3%), and non-starch polysaccharides (MacGregor, 1998). Of the total proteins, albumins, globulins, hordein, and glutelins represent 3-5%, 20-30%, 35-50%, and 15-25%, respectively (MacGregor, 1998). Barley lipids are comprised of nonpolar lipids (67-78%) (mainly triacylglycerol with minor amounts of sterols and free fatty acids), glycolipids (8-13%), and phospholipids (14-21%) (Morrison, 1996). Lipids are distributed in the endosperm (63-72%) and in the embryo (28-37%) (Morrison, 1996). Non-starch polysaccharides contribute the major portion of the total dietary fibre, including cellulose/lignin (4-6%), β-

Table 1-1 Chemical composition of hulled and hull-less barley grains

	Hulled (%, db)			Hull-less (%, db)			
Starch	52.1-63.8	49.4-63.1	53.7	23.9-64.4	49.4-66.2	60.1-73.8	59.7
Protein	8.7-10.5	9.3-15.5	15.9	11.3-18.1	10.6-21.9	12.8-17.8	16.5
Dietary fiber	18.9-23.8	18.1-27.5	18.6	13.5-34.5	13.6-20.2	11.0-16.6	13.8
β-Glucan	2.8-6.9	3.8-6.3	5.2	4.6-14.9	4.7-7.9	4.1-8.0	5.6
Lipid	2.2-3.5	2.1-3.1	-	2.9-6.2	2.1-3.7	-	-
Ash	2.3-2.6	1.9-2.3	2.8	2.0-2.3	1.3-2.1	1.8-2.2	2.1
Cellulose	3.5-4.7	3.1-7.0	4.1	1.4-4.1	1.7-5.0	-	2.0
Arabinoxylans	7.5-9.0	0.4-0.7[a]	6.5	4.8-12.2	0.7-0.9[a]	-	4.5
Lignin	1.4-1.7	1.0-1.9	2.0	0.7-1.1	0.5-0.9	-	9.0
Uronic acids	4.4-5.2	0.5-1.1[a]	-	3.4-5.7	0.5-0.7[a]	-	-
LMWC[b]	-	0.8-1.4	1.4	-	0.9-2.2	-	1.6
Reference	Andersson et al., 1999	Oscarsson et al., 1996	Xue et al., 1997	Andersson et al., 1999	Oscarsson et al., 1996	Bhatty and Rossnagel, 1998	Xue et al., 1997

[a] Water soluble fraction.

[b] LMWC, low molecular weight carbohydrates including glucose, fructose, sucrose, maltose, raffinose, and fructans.

glucan (3-6%), hemicellulose/pentosans (mainly arabinoxylans) (4-7%), and fructans (0.2-0.9%). Sugars (glucose, 0.1-0.6%; fructose, 0.1-0.2%; sucrose, 0.3-2.0%; maltose, trace-0.1%; and raffinose, 0.1-0.8%), vitamins (mainly vitamin B complex, niacin, biotin, and folacin), and minerals (mainly phosphorous, potassium, calcium, chlorine, magnesium, sulfur, and sodium) are minor components (MacGregor, 1998; Newman and Newman, 1991). Tocols (tocopherols and tocotrienols), which are natural antioxidants, are present mainly in the bran fraction. The tocol content of barley has been reported to be 42-80 mg/kg (Peterson and Qureshi, 1993). The chemical composition of barley grain differs with variety and growing conditions. In general, HB contains more protein, starch, and total and soluble β-glucan than hulled barley (Bhatty, 1999).

1.1.3 Barley utilization and potential

Barley is grown for feed, malting and food. Of the total world barley production, about 50-57% of barley is used as animal feed, 30% for malt (to produce whiskey and beer), 3-5% for seed, and 10% is for food (World Crops and Cropping Systems, 2003). In Canada, 15% of the total barley production is exported as feed and for malting, 75% is used domestically as feed, and 10% is used as food and seed (Agriculture and Agri-Food Canada, 2003). Barley is popularly used as a staple food, such as pearled grain in soups, flour in flat bread, and ground grain in cooked porridge in China, Japan, Korea, West Asia and North Africa (Bhatty, 1996). Japan and Korea have been increasing pearled barley use for human consumption as a rice extender, roasted barley tea, alcoholic beverage, and barley-wheat composite flour for making cookies, cakes, and noodles. In Western countries, very small quantities of barley are used in breakfast cereals, soups, stews, porridge, bakery blends, and for baby foods. Barley products such as pot and pearled barley, grits, flakes, and barley and malt flours are also available commercially.

HB has major advantages over conventional hulled barley in transportation (increased energy/unit weight), processing and storage. Also, increased crude protein content (1-2% greater than comparable hulled types), improved digestibility, less manure handling for the animal industry using a HB diet (Saskatchewan Agriculture and Food, 2003), and equal feed value to wheat and maize (Salunkhe et al, 1985) are beneficial for the feed industry. Husk contributes unpalatability to the diet, leading to reduced feed intake and influences the biological parameters and protein utilization in animals, whereas, β-glucan has little effect on such protein quality parameters (Kalra and Jood, 1998). During the past decade, research on barley, especially HB, has been carried out in order to increase the utilization of barley grain for human foods and other industrial applications. Such research includes pearling and milling of barley grain, incorporation of barley flour into baked and pasta products, extraction and characterization of β-glucan, starch, protein, lipids, and tocols, production of malt, chemical modification of barley starch and fuel alcohol production (Bhatty, 1986; Newman and Newman, 1991; Bhatty, 1999; Berglund et al., 1992; Edney and Rossnagel, 2000; Keagy et al., 2001). High levels of β-glucan in barley is undesirable in the malting and brewing process due to filtration difficulties, haze formation, and precipitation during beer storage. Also, β-glucan interferes with digestion of the diet and decreases the nutritive value of barley for poultry (Jadhav et al., 1998). However, its high viscosity and solubility, similar to other polysaccharide gums, contributes textural, water retention, and fat replacement characteristics to food and beverage products, with added health promoting functions

(Temelli, 2001). As a soluble dietary fiber component, β-glucan offers health benefits, such as cholesterol lowering effect, reduction in insulin requirement for diabetics, and anticarcinogenic effects (Bhatty, 1999). The nutritional value of barley, based on amino acid content, is greater than that of maize (Tibelius and Trenholm, 1996). Incorporation of barley into human diet as a nutritive and high dietary fiber ingredient and fractionation of valuable components from barley grain will contribute to value-added barley processing, enhancement of barley utilization in foods, pharmaceuticals, cosmetics and the biotechnology industry (Tibelius and Trenholm, 1996), as well as the profitability and sustainability of the barley industry in Canada. Barley is a unique grain of the future with its advantages in processing and diversification in industrial utilization.

1.2 Starch

1.2.1 General

1.2.1.1 Starch sources

Starch is abundant in all major agricultural crops. Starch content (dry basis) ranges from 40-90%, 65-85%, and 30-70% in cereals, roots and tubers, and pulses (legumes), respectively (Guilbot and Mercier, 1985). Over the years, maize has been the world's major source of starch, followed by potato, cassava and wheat. Minor amounts of starch from rice, sorghum, sago, pea, and amaranth are also produced commercially. Maize is cultivated in warmer climates with annual world production of 602.5 million metric tons (30% of total cereals) (FAO, 2003). The USA (38%) and China (20%) are the two largest maize producers. Sixty three percent of the world's potato supply is grown in the cool, moist climate of northern Europe and Russia. Wheat, requiring a more temperate climate, is primarily grown in Europe (42%) and North America (11%). Approximately 90% of the world rice production comes from South and South East Asia. Cassava is cultivated in a narrow tropical band about the equator with a total production of 184.9 million metric tons (FAO, 2003). Today, about 10% of the total maize production, and over 5% of each of cassava, potato, and wheat production, are used for starch manufacture (Shukla, 2003). Legume starches are not utilized widely in the food industry due to their poor functional properties (Sosulski et al., 1997; Ratnayake et al., 2002). Barley starch has been commercialized in Finland. Canada is the leading producer of barley in the world, but at present there is no commercial production and usage of barley starch in Canada. A number of consultative reports (personal communication) have indicated that the use of HB for grain fractionation and production of β-glucan, starch, protein, and fiber is promising. To this end, further understanding of the structure and physicochemical properties of HB starches from different genotypes is important.

1.2.1.2 Starch production and starch derivatives

The total world production of starch in 2000 was 48.5 million metric tons (Table 1-2). Maize supplies over 80% of the global starch market. More than 8% of the world starch production is derived from wheat, 5% from potato, and 5% from cassava. The USA has the largest starch industry with 51% of the world starch production, almost entirely depending upon maize. Starches from maize, wheat, and potato share the starch industry in the European Union (EU). Cassava starch is produced mainly in South East Asia. Starches are also commercially produced in Asia from rice, sorghum, sweet

Table 1-2 World starch production by source in 2000

(million metric tons)

Location	Starch source				
	Maize	Potato	Wheat	Other	Total
European Union	3.9	1.8	2.8	0.0	8.4
USA	24.6	0.0	0.3	0.0	24.9
Other countries	10.9	0.8	1.1	2.5	15.2
World	39.4	2.6	4.1	2.5	48.5

Reference: LMC International, 2002

potato, arrowroot, mungbean, and sago. Legume starch is only produced by Parrish and Heimbecker Co. in Canada and its production is very small (1-2 thousand tons only, personal communication).

Starch has been converted into many derivatives (Figure 1-2). Continuous starch conversion with modern enzyme technology has facilitated large-scale production of starch hydrolysates [dextrins and syrups with various dextrose equivalent (DE) values], lower molecular weight oligosaccharides, maltose, and glucose. Glucose is becoming an important new intermediate in the fructose-based sweetener industry and its use in large-scale production of biofuel (ethanol) and organic chemicals is expanding. Today, more than 100 starch derivatives converted by specific enzymes are commercially available (Holló and Hoschke, 1993) and more economical and environmentally friendly carbohydrate derivatives are synthesized from maltose and glucose through enzymatic and chemical means. In Finland, the integrated industrial barley process for production of starch and starch derivatives has been established with a daily processing capacity of 450 tons (Stelwagen et al, 1988).

Overall demand for starch and starch derivatives has grown at an annual rate of 4.1% in the USA, 4.3% in the EU and 4.0% for the rest of the world (LMC International, 2002). Demand for syrups has grown more rapidly than that for starch worldwide, under the lead of the USA. It is expected that significant growth in starch demand and starch production will continue over the next decade. The absolute growth in the demand for syrups is expected to be 3.5 times greater than that for starches (LMC International, 2002). By 2010, production of syrups in the USA will be approximately 37 million tons due to strong increases in fuel ethanol use and 5.3 million tons in the EU

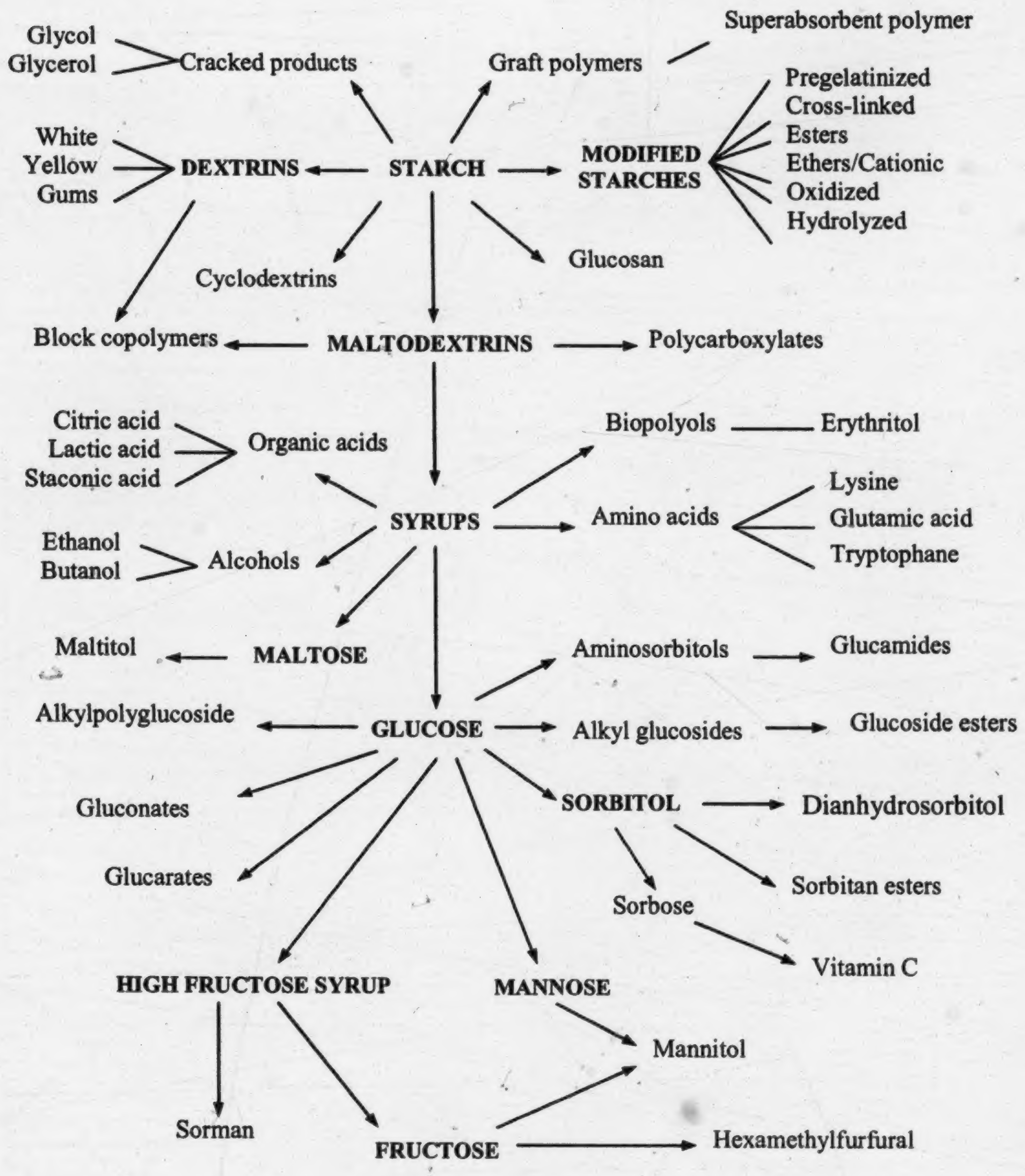
Glycol
Glycerol
Cracked products
Graft polymers
Superabsorbent polymer
Pregelatinized
Cross-linked
Esters
Ethers/Cationic
Oxidized
Hydrolyzed
White
Yellow
Gums
DEXTRINS
STARCH
MODIFIED STARCHES
Cyclodextrins
Glucosan
Block copolymers
MALTODEXTRINS
Polycarboxylates
Citric acid
Lactic acid
Staconic acid
Organic acids
Biopolyols
Erythritol
Lysine
Glutamic acid
Tryptophane
SYRUPS
Amino acids
Ethanol
Butanol
Alcohols
Maltitol
MALTOSE
Aminosorbitols
Glucamides
Alkylpolyglucoside
GLUCOSE
Alkyl glucosides
Glucoside esters
Gluconates
SORBITOL
Dianhydrosorbitol
Glucarates
Sorbitan esters
Sorbose
Vitamin C
HIGH FRUCTOSE SYRUP
MANNOSE
Mannitol
Sorman
FRUCTOSE
Hexamethylfurfural

Figure 1-2 Products derived from starch (modified from Röper, 2002).

with annual growth rate of 3.2% for syrups (LMC International, 2002). The global production of specialty chemicals from starches (Figure 1-2) may grow from today's 11-12 million metric tons to 15-20 million metric tons by 2010 (Shukla, 2003). Large-scale starch production and conversion from specialty starch sources, such as barley and oat, is of great potential in North America but has to compete with maize starch.

1.2.1.3 Application of starch and starch derivatives in food and non-food industries

Starch, as a renewable and biodegradable resource, is abundant, environmentally friendly, cost competitive, and versatile. The variation in starch source, composition and structure, and the diversities in properties, make starches suitable for various applications contributing to different functionalities. Native starches have diverse properties, which meet different application requirements; however, physical and chemical modifications greatly improve the properties of native starches and extend the range of starch applications in food, paper and board, textile, and pharmaceuticals. Also, numerous starch derivatives produced by enzyme technology, including dextrins and various DE syrups, have been used for the production of organic acids, solvents, alcohols, amino acids, biopolymers, and other products. Applications for starch and starch derivatives in various industries are summarized in Table 1-3.

The USA and the EU are the two largest starch producers and consumers. In the USA in 2000, 15% of the total starch production was used in native and modified forms, 32% was used to produce high fructose syrups, 13% went for conversion to syrup-based products (glucose syrups, crystalline dextrose, maltodextrin, as well as high maltose

Table 1-3 Application of starch and starch derivatives in food and non-food industries

Industry	Uses	Type used
Food	Thickener for pie filling, puddings Stabilizer for salad dressings, frozen foods Binder for meat and pet foods Moisture retainer for bakery and meat Fat replacer for desserts, spreads, sauces Adhesive for food packing and meat gluing Glaze for cakes, donuts, fruit and nuts	Native starches, Modified starches, Maltodextrins, High fructose syrups
Beverage	Soft drinks, beer, alcohol, instant coffee	Sweeteners
Confectionery	Ice cream, candy, gums, marshmallows, canning, marmalade and jams	Starch, maltodextrins, maltose syrups
Adhesive	Case sealing, laminating, tube winding, corrugated board	Starch and dextrins
Paper & cardboard	Wet end additives, spraying, surface sizing, coating	Native, cationic, and hydroxyethyl starches
Textile	Sizing, finishing, printing, fire resistances	Starch and modified
Cosmetic	Emulsifiers, humectants, face powders	Starch, sorbitan esters
Detergent	Surfactants, builders, bleach activators	Sucrose derivatives
Pharmaceuticals	Diluents, binders, drug delivery, encapsulation	Starch, malto- and cyclodextrins, glucose syrup syrups, polyols
Plastics	Biodegradable filler	Starch
Biochemistry	Organic acids, amino acids, biopolymers, polyols, enzymes, alcohols, antibiotics	Starch hydrolysates
Other	Ceramics, coal, water treatment, gypsum and mineral fiber, oil drilling, concrete	Starch and modified starches

References: Ellis et al. (1998); Guzmán-Maldonado and Paredes-López (1995).

and dextrose syrups that are processed into amino acids and other organic chemicals), and 40% for ethanol production (fermentation of starch syrups). In contrast, the corresponding percentages of starch usage in the EU, Japan, South Africa, and Australia were approximately 53%, 3%, 43%, and 1%, respectively (LMC International, 2003). In other parts of Asia and Africa, native starch constitutes a much larger proportion of the total starch consumption. In many low Gross National Product (GNP) countries, starch sweeteners are practically absent. In the EU, the usage of starch in paper, chemical and fermentation, cardboard, confectionary, beverages, and other foods accounted for 20%, 13%, 8%, 15%, 13%, and 27%, respectively (Röper, 1996).

The world starch market is expanding with new sources, new uses, and new products. Currently, improvements in starch functional properties by means of classical plant breeding and modern genetic engineering techniques, developments of new products based on starch and starch derivatives, and potential uses of starch in foods, detergents, cosmetics, pharmaceuticals, fermentation, and biodegradable packaging are the targets for the starch industry (Röper, 1996). Large-scale production and conversion of starches from other grains have great potential. Barley starches with waxy (0-5%), normal (20-30%), and high-amylose (> 30%) types are available from new barley varieties and have comparable properties with maize starches (Vasanthan and Bhatty, 1996) as well as great suitability for industrial production, conversion, and application (Jadhar et al., 1998). However, there are still some wide gaps in our knowledge of the relationship between starch structure and starch properties due to the inherently complex architecture of the starch granule, which is under genetic control and is significantly affected by environmental conditions during starch deposition (Ellis et al., 1998). Further research on starch structure and physicochemical properties is needed to better understand starch functionality in different application systems and to efficiently produce high quality products by choosing proper starch types for specific formulations. Also, increasing demand for starch as a biodegradable polymer and as a feedstock for chemicals will promote HB starch utilization.

1.2.2 Chemical composition

The chemical composition of starches from various sources is presented in Table 1-4. Usually, starch contains 10-15% moisture, 85-90% polysaccharides (amylose and amylopectin), and traces of non-starch components (protein, lipid, and minerals) (Tester, 1997).

1.2.2.1 Amylose and amylopectin

Amylose and amylopectin together represent the major portion of isolated pure starch, accounting for 97-99% by dry weight. The ratio between them varies depending on the starch source, i.e. species and cultivar (Galliard and Bowler, 1987). In non-mutant normal starches, amylose constitutes about 15-30% of total starch (Table 1-4). Waxy starches from maize, barley, wheat, potato, sorghum, and rice mutants have approximately 0-10% amylose, whereas the amylose contents of high-amylose starches from barley and maize mutants are in the range of 35-70% (Shannon and Garwood, 1984).

1.2.2.2 Minor components

In addition to amylose and amylopectin, starch granules contain small quantities of surface and integral proteins and lipids as well as a trace amount of minerals (Table 1-

Table 1-4 Chemical composition of starches from various sources

Source	Amylose %			Lipid			Phosphorus %	Protein %	Ash %
	Total	Apparent	LAM[a]	FFA[b] mg/100g	LPL[c] mg/100g	Total %			
Barley									
Waxy	1.7-7.4	0.8-5.2	37-59	28-43	120-751	0.3-0.49	0.022	0.15	0.15
Normal	25.3-32.7	20.3-25.9	18-32	31-51	469-1136	0.68-1.14	0.048	0.20	0.11
High-amylose	38.4-44.1	30.8-35.4	18-24	51-92	864-1360	1.05-1.36	0.051-0.068	0.18	0.13
Wheat									
Waxy		1.2-2.0	-	-	-	0.12-0.29	-	0.33	0.04
Normal	27.2-31.2	26.0-28.4	18-22	22-66	729-1047	0.77-1.17	0.054-0.058	0.1-0.6	0.1-0.4
Maize									
Waxy	1.4-2.7	1.3-2.7	0-7	5-46	3-29	0.08	0.002-0.004	0.25	0.007
Normal	25.8-32.5	21.7-26.9	13-22	290-454	170-248	0.60-0.72	0.016-0.018	0.2-0.4	0.05-0.1
High-amylose	42.6-67.8	35.3-59.9	8-17	375-671	262-602	0.81-1.15	0.028-0.033	-	0.07
Oat	25.2-29.8	17.3-22.0	28-33	262-462	977-1081	1.2-2.45	0.056	-	-
Rye	20.3-25.8	16.9-22.7	12.0-17.3	-	-	1.00	0.023-0.026	0.14-0.47	-
Rice									
Waxy	0-2.32	0-0.2	0-25	15-60	0	0.02-0.06	0.005	0.2	0.10
Normal	12.2-28.6	8.1-23.8	15-43	291-500	552-831	0.97-1.30	0.066	0.45	0.1
References	Data of waxy wheat from Yasui et al., 1996; oat from Sowa and White, 1992; rye from Radosta et al., 1991; others from Morrison, 1988, 1995; Morrison et al., 1984,1993a; Tester and Morrison, 1990, 1992; Tester and Karkalas, 1996; protein and ash from Galliard and Bowler, 1987; Swinkels, 1985b; Vasanthan et al., 1997; phosphorus from Kasemsuwan and Jane, 1996; Lim et al., 1994; Song and Jane, 2000.								

Table 1-4 Cont.

Source	Amylose^{d} %			Total Lipid %	Protein %	Ash %	Phosphorus %	Reference
	Total	Apparent	LAM					
Tubers & roots								
Waxy potato	0		-	-	-	-	0.069-0.075	McPherson anbd Jane, 1999
Potato	21.1-25.1	19.4-23.7	3.3-8.1	0.08-0.17	0.07-0.14	0.18-0.32	0.075-0.091	Vasanthan et al., 1999
Yam	27.1	26.5	2.2	0.13	0.44	-	0.012	Hoover and Vasanthan, 1994
Sweet potato	8.5-32.4			0.05-0.60	0.04-0.54	0.1	0.012-0.021	Tian et al., 1991
Arrowroot	19.4-38		-	0.30-0.32	-	-	0.022	Hoover, 2001
Sago	24-31		-	0.10-0.13	0.19-0.25	0.06-0.43	-	Ahmad et al., 1999
Taro	18.1-22.2		-	0.24-0.52	0.09-0.16	-	0.017-0.025	Jane et al., 1992
Tapioca	13.6-23.8		-	0.10-1.0	0.03-0.61	0.02-0.49	0.009	Rickard et al., 1991
Legume								
Kidney bean	34.4-35.0		-	0.18	0.13-0.30	0.18	-	Hoover and Sosulski, 1991
Navy bean	36		-	0.09-0.60	0.13-0.34	0.06-0.14	-	Hoover and Sosulski, 1991
Cow pea	33.0		-	0.21-0.33	0.12-0.50	0.06	-	Hoover and Sosulski, 1991
Pinto bean	25.8-30.2		-	0.16-0.51	0.37-0.52	0.05-0.09	-	Hoover and Sosulski, 1991
Smooth pea	32.5-33		-	0.01-0.1	0.52-0.70	0.07	-	Hoover and Sosulski, 1991
Wrinkled pea	62.8-75.4		-	0.01-0.19	0.34-0.46	0.08	-	Hoover and Sosulski, 1991
Pigeon pea	29.3	28.5	2.7	0.13	0.13	0.03	-	Hoover et al., 1993
Lentil	35.4-39.4	33.0-34.5	5.6-12.4	0.27-0.38	0.94-1.25	0.10	0.009	Hoover and Manuel, 1995
Mung bean	45.3	39.8	12.1	0.32	0.31	0.11	0.012-0.013	Hoover et al., 1997
Field pea	48.8-49.6	42.9-43.7	10.9-12.0	0.28-0.34	0.25-0.44	0.03-0.14	-	Ratnayake et al., 2001

[a] LAM, percentage of lipid-complexed amylose [(Total amylose-Apparent amylose)/Total amylose]; [b] FFA, free fatty acids; [c] LPL, lysophospholipids;

[d] The amylose contents of tuber, root, and legume starches were determined by calorimetric procedures without prior defatting in many instances (Hoover, 2001).

4). The starch-bound proteins and lipids have been reported to influence starch digestibility, swelling during gelatinization, solubilization, retrogradation, and granular integrity (Galliard and Bowler, 1987; Appelqvist and Debet, 1997; Han and Hamaker, 2002). Surface components are associated with the surface of granules and could be readily removed by appropriate treatment without granule damage/disruption. Integral components are deeply embedded within the starch matrix and can only be extracted near or above the starch gelatinization temperature (Galliard and Bowler, 1987; Baldwin, 2001).

1.2.2.2.1 Starch proteins

Typical protein content of thoroughly washed starches is 0.2-0.3%, 0.35%, and 0.06% in wheat, maize, and potato, respectively (Swinkels, 1985a; Skerritt et al., 1990). About 8% of proteins in wheat (Lowy et al., 1981) and 5-6% in rice starches (Baldwin, 2001) are surface proteins. Surface proteins are easily extracted by washing with either dilute NaCl (Lowy et al., 1981) or 1-2% sodium dodecyl sulfate solution at room temperature (Seguchi and Yamada, 1989). Sodium dodecyl sulfate extracted surface proteins, when subjected to polyacrylamide gel electrophoresis (SDS-PAGE), were of low molecular weight ranging from 5 to 30 kDa, with a predominant 30 kDa protein, and were distinct from the endosperm storage proteins (Lowy, 1981). Of these surface proteins, friabilin (a group of polypeptides with molecular weights of 15 kDa) has been reported to be associated with grain hardness (Darlington et al., 2000; Greenwell and Schofield, 1986). A 60 kDa waxy protein (a granule-bound starch synthase) is found both within and on the surface of the granule (Baldwin, 2001). It is hypothesized that the high levels of starch surface components, including proteins and lipids, influence granule surface chemistry and have a structural role in maintaining granule integrity and resistance (Baldwin, 2001). Integral proteins are higher molecular weight proteins (30-149 kDa), which can be extracted only near or above the gelatinisation temperature. Most are starch synthases and their isoforms (isozymes) involved in starch biosynthesis, and thus become entrapped within the granule structure during granule synthesis at an approximately constant protein-starch ratio (Rahaman et al., 1995; Baldwin, 2001). Internal proteins appear to be randomly interspersed within the starch matrix as monomers, whereas surface proteins are deposited on the granule surface as aggregates (Mu-Forster and Wasserman, 1998). High levels of basic, hydrophilic amino acids are believed to be responsible for the strong binding of surface proteins to the starch molecules (Baldwin, 2001).

1.2.2.2.2 Starch lipids

Starch lipids are found both on the surface and the inside of granules. Surface lipids include those that may have been present on the starch granule surface *in situ* within the plant tissues and non-starch lipids, mainly membrane and spherosome (oil storage bodies) lipids from the endosperm, aleurone and germ, and some free fatty acids and monoacylglycerols resulted from lipolysis during grain storage and absorbed into the granule surface during isolation (Galliard and Bowler, 1987; Morrison, 1988). It is likely that surface lipids are distributed unevenly at the granule surface and would be present in multimolecular droplet or micellar forms (Galliard and Bowler, 1987). Commonly, classification of starch lipids as surface and integral refers to cold and hot solvent extractability. Only integral lipids are considered to be true starch lipids (Morrison, 1995, 1988). However, both free and bound lipids may be present on the surface and inside of granules, thus, solvent extractable lipids at ambient temperature mainly represent free surface lipids whilst those lipids extracted at elevated temperatures represent surface and bound lipids (Vasanthan and Hoover, 1992). Free surface lipids content accounts for 5% of total starch lipids in cereals (maize, rice, and wheat), 18-42% in tubers and roots (potato and tapioca), and 22-62% in legumes (lentil and faba bean) (Vasanthan and Hoover 1992), which are mainly triacylglyceriols, followed by free fatty acids, glycolipids, and phospholipids (Galliard and Bowler, 1987; Vasanthan and Hoover, 1992). Integral lipids are predominantly monoacyl lipids (free fatty acids and lysophospholipids) normally comprising 0.6-1% of cereal starches, compared with tuber, root, and legume starches, which comprise only 0.05-0.1% (Swinkels, 1985a,b). Some oat starches have higher lipid contents (up to 2.45%) than other starches (Morrison, 1988; Sowa and White, 1992). In wheat, barley, rye, and triticale starches, integral lipids are entirely lysophospholipids, while in oat, rice, and maize starches, free fatty acids make up 30-60% of the integral lipids (Morrison, 1988, 1995). Linoleic (18:2) and palmitic (16:0) acids are the major fatty acid components in starch lipids (Morrison, 1988; Vasanthan and Hoover, 1992). Cereal starch lipids are proportional to the amylose content and are fully complexed with a portion of amylose, but the relationship between starch lipids and amylose content is quite different among starches (Morrison, 1995, 1988).

1.2.2.2.3 Minerals

Starches contain minor quantities of minerals such as calcium, sodium, potassium, magnesium and phosphorus. Normal cereal starches contain phosphorus (0.02-0.06%), mainly as phospholipids, whereas waxy starches contain only a trace of phosphorus (0.002-0.003%) mainly in the form of phosphate monoesters (Lim et al., 1994; Kasemsuwan and Jane, 1996). Amylomaize contains three forms of phosphorus:

phospholipids (0.015%), phosphate monoesters (0.005%), and inorganic phosphate (0.0076%). Tuber, root and legume starches are phospholipid-free and of those, the phosphorus is present mainly in the form of phosphate monoesters (0.002-0.02%) with an exceptionally high level in potato (0.089%) (Lim et al., 1994; Kasemsuwan and Jane, 1996).

1.2.3 Morphology

Starch is synthesised in plants as minute granules with its inherent characteristics. The source of starch can be identified from its microscopic shape, size, as well as the surface features, while the granule size distribution in terms of number, volume/weight, and surface area can be measured by particle size counters (Morrison and Scott, 1986), image analyzers (Jane et al., 1994; Harrigan, 1997), laser light scattering (Cornell et al., 1994), and sedimentation field flow fractionation (Moon and Giddings, 1993). Despite their wide variety of morphologies, starch granules from different botanical sources show some common features specific to each species.

1.2.3.1 Granule shape and size

The shape and size of starch granules from different botanical sources are presented in Table 1-5. Various shaped granules, such as oval/ellipsoidal, round/spherical, polygonal, lenticular, disk/plate shaped, and irregular, are found in various starches with size ranges of 0.5-110 µm in diameter (Jane et al., 1994; Hoover, 2001). Generally, starch granules from tubers and roots are relatively large in size with a diameter up to 100 µm (canna and potato). Most of the granules are oval with length of 5-100 µm and width of 5-65 µm, except starches from Chinese taro, Iliuana dasheen,

Table 1-5 The shape and size of starch granules from different botanical sources

Source	Shape	Size range^a µm			Reference
		Length	Width	Thickness	
Tubers and roots					Jane et al., 1994
Canna	Oval, round	30-100	25-65		
Potato	Oval, round	15-75	12-60		
Lotus root	Oval, round, irregular	10-50	10-35		
Arrow root	Oval, round	8-30	8-22		
Sago	Oval, round	20-50	15-40		
Tapioca	Oval, round, irregular	5-25			
Sweet potato	Round, polygonal, irregular	5-25			
Yam	Round, oval				
Chinese taro	Polygonal, irregular	1-4			
Iliuaua dasheen	Polygonal, irregular	0.5-3			
Parsnip	Polygonal, irregular	1-6			
Cereals					Jane et al., 1994
Wheat	Round, disk shaped	2-36		6-10	
Triticali	Round, disk-shaped	5-36		6-10	
Rye	Round, oval	22-36			
Barley	Round, oval, disk	2-32		6-10	
Sorghum	Polygonal, irregular	5-30			
Millet	Polygonal, irregular	2-15			
Oat	Polygonal, irregular, compound	3-15			
Rice	Polygonal, irregular, compound	3-8			
Maize	Polygonal, irregular	5-20			
Amylomaize	Irregular, rod/snake shaped	6-15			

Table 1-5 cont.

Source	Shape	Size range[a] µm			Reference
		Length	Width	Thickness	
Legumes					Hoover and Sosulski, 1991
Kidney	Oval, elliptical	16-60	16-42		
Navy bean	Oval, irregular, round	12-49	12-40		
Black bean	Oval, round, elliptical	8-55	8-34		
Mung bean	Oval, irregular, round	10-32	7-20		
Pinto bean	Oval, irregular, round	12-48	10-30		
Horse bean	Oval, irregular	6-31			
Red bean	Oval, irregular	25-67			
Wrinkled bean	Round	6-80			
Smooth bean	Oval, round	20-40			
Chick pea	Oval, spherical	8-54			
Cow pea	Oval, spherical	4-40			
Lentil	Oval, round, ellipsoid	10-36	15-30		
Other					Jane et al., 1994
Banana	Oval, irregular, disk shaped	15-45	10-20		
Avocado	Oval, barrel shaped	10-27	10-12		
Pineapple	Polygonal, irregular, compound	3-10			
Amaranth	Polygonal, irregular	0.5-2			
Cow cockle	Polygonal, irregular	0.5-2			
Small pigweed	Polygonal, irregular	1-2			

[a] Starch granules could be measured in one, two, or three dimensions. For starch granules that are symmetrical spheres, only one dimension (length) is measured; for those that are unsymmetrical spheres, two dimensions are measured (length and width); others that are unsymmetrical disk-shaped granules are measured in three dimensions (length, width, and thickness).

and parsnip, which have very small granules with a diameter of 0.5-6 µm. Among cereal starches, large round disk shaped granules are found in wheat, barley, and rye starches with a size of 15-36 µm in diameter and 6-10 µm in thickness, while the very small spherical granules with a diameter of 2-3 µm are present in small amounts (Jane et al., 1994). Oat and rice starches are a mixture of irregularly shaped single and compound granules (a cluster of several single granules, which could be verified by the presence of a maltese cross in each granule segment in polarized light micrographs) (Hoseney, 1986) with a relatively small size (2-15 µm). Maize starch granules are irregularly shaped with a number of polyhedral faces in the size of 5-15 µm. However, in amylomaize starch, granules are rod-shaped or snake-shaped. Compound granules are also found in wrinkled pea (Colonna et al., 1982), tapioca, taro (Hoover, 2001) and breadfruit (Hood and Liboff, 1983) starches.

1.2.3.2 Granule size distribution

Most of the cereal starches, including wheat, barley, rye, and sorghum, show a distinct bimodal granule size distribution (Table 1-6), whereas other starches (maize, legumes, tubers and roots) give mono modal distribution. The large and small granules are referred to as A- and B-granules, which are commonly distinguished at 10µm in diameter. The number proportion of A-granules is always lower than those of B-granules (each amyloplast of endosperm contains one large granule and a variable number of small granules) but represent the major proportion of the starch mass (Parker, 1985). For example, in wheat, rye (Stoddard, 1999), and barley (Goering et al., 1973) starches, A-granules account for 50-77%, 60-80%, and 69-94% of the total starch weight, respectively, but generally only 10-20% of the total number, depending

Table 1-6 Granule size distribution of some cereal starches

Source	Type	Large			Small			Reference
		Mean diameter µm	Weight %	Number %	Mean diameter µm	Weight %	Number %	
Wheat		13.9-16.0	-	-	3.7-5.1	13.0-37.3	-	Soulaka and Morrison, 1985
		-	60-76.8	-	-	-	-	Dengate and Meredith, 1984
		-	57.9-76.9	-	-	26.9-38.1	-	Raeker et al., 1998
		-	-	-	-	23.7-35.9	-	Karlsson et al., 1983
Barley	Waxy	10.2-13.6	-	-	2.1-3.1	3.5-13.6	72.4-90.2	Morrison et al., 1986
		20-25	-	-	4-5	10.2-26.3	89-97	Goering et al., 1973
	Normal	12.5-15.0	-	-	2.9-3.6	3.7-15.1	80.7-90.8	Morrison et al., 1986
		20-40	-	-	3-5	6.2-30.6	84.6-97	Goering et al., 1973
	High-amylose	10.8-12.2	-	-	3.9-4.4	29.2-46.3	82.9-93.8	Morrison et al., 1986
		24	-	-	3	14.3	83	Goering et al., 1973
Oat		6.4-7.4	-	-	3.0	-	-	Mäkelä and Laakso, 1984
Rye		-	85	-	-	15	-	Schierbaum et al., 1991
		-	-	-	-	36	-	Karlsson et al., 1983

on genotype, environment, starch extraction method, and analysis techniques. Both A- and B-granules from barley are smaller than those from wheat and rye (Table 1-6). Variations in the composition and physicochemical properties between A- and B-granules have been reported by several researchers (Kulp, 1973; Karlsson et al., 1983; Soulaka and Morrison, 1985; Morrison et al., 1986; Vasanthan and Bhatty, 1996; Tang et al., 2000). Trimodal distributions of granule sizes have also been reported in wheat and barley starches (Mäkelä et al., 1982; Bechtel et al., 1990; Raeker et al., 1998).

1.2.3.3 Surface features

Scanning electron microscopy (SEM) has been extensively used to study starch granule surfaces (Fitt and Snyder, 1984; Jane et al, 1994). Most starch granules (i.e. legumes, tubers, and roots) appears relatively smooth with no evidence of pores, cracks or fissures (Hoover and Sosulski, 1991; Jane et al., 1994; Hoover, 2001). However, indentations/cuts in many legume starches, sharp-edges in wild type and waxy rice and normal maize starches, pocks in wheat, oat, millet, and triticale starches, and rough surfaces in waxy maize starch were reported by Jane et al. (1994). These surface features are partly due to close packing of granules or packing with protein bodies within the plant cells (Hood and Liboff, 1983) Recently, studies on high resolution imaging of granule surface using atomic force microscopy (Baldwin et al., 1997, 1998) revealed that potato and wheat starches possess a rough granule appearance with many protrusions (10-300 nm) on the granule surface. Ohtani et al. (2000) examined physically damaged starch granules (ground with water in a glass homogenizer) from maize, potato, rice, sweet potato, and wheat and found that fine particles of approximately 30 nm in diameter were present on the bare inner granule surfaces of all starches. This protrusion/particle feature is believed to be the ends of the starch polymers within the crystalline amylopectin side-chain clusters at the granule surface (Baldwin et al., 1998; Ohtani et al., 2000).

Randomly distributed pinholes have also been observed on the surface of maize, sorghum, and millet starch granules and along the equatorial groove of large wheat, barley, and rye starch granules (Hall and Sayre 1970a; Fannon et al., 1992). These pinholes are exterior openings to internal channels that penetrate into the granule interior (Fannon et al., 1993). They, together with internal channels, are true architectural features of starch granules, potentially increasing the granule surface area available for chemical and enzymatic reactions (Huber and BeMiller, 2000).

1.2.4 Ultrastructure

Amylose and amylopectin are two major components of starch. Their molecular structures are shown in Figure 1-3 and their general molecular characteristics are summarised in Table 1-7. Despite of the simple composition of starch (polymers of glucose), the structural complexity and heterogeneity at different levels of scale both within a single granule and the natural variation inherent among granule populations make starch one of the most complex materials in nature (Myers et al., 2000; Gidley, 2001). At least four levels of structural scales are present within a starch granule (Figure 1-4): molecules (~Å), lamellae (~9 nm), growth ring (~100s nm), and whole granule morphology (µm) (Waigh et al., 1998; Myers et al., 2000; Gidley, 2001).

Starch is biosynthesized as semicrystalline granules with varying polymorphic types and degree of crystalinity. Within a starch granule, amylopectin molecules are arranged

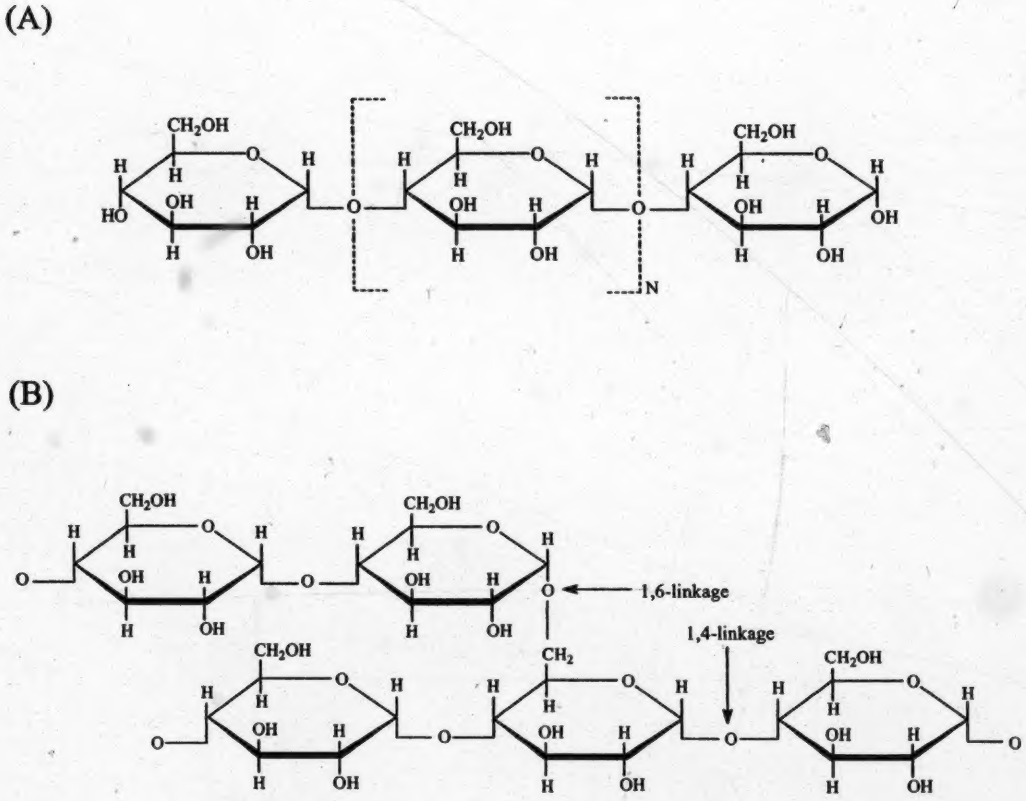
(A)
CH₂OH
H
OH
HO
O
N
(B)
1,6-linkage
1,4-linkage
CH₂

Figure 1-3 Structure of amylose (A) and amylopectin (B).

Table 1-7 General characteristics of amylose and amylopectin

Property	Amylose	Amylopectin
Molecular structure	Essentially linear, α-1,4-glucosidic linkage	Branched, α-1,4 and α-1,6-glucosidic linkage
Degree of branching, %	0.2-0.7	4-5.5
Degree of polymerization	700-5000	10^4-10^5
Molecular weight, Da	10^5-10^6	10^7-10^9
Average chain length	100-550	18-25
Structural conformation	Partly complexed with lipids, amorphous	Double helix, partly crystalline
Iodine complex		
Iodine affinity, g/100g	19-20.5	0-1.2
λmax, nm	640-660	530-570
Blue value	1.2-1.6	0-0.2
Color	Blue	Purple
β-Amylosis limit, %	70-85	55-60
Stability of dilute aqueous solutions	Unstable (retrogrades)	Stable
Gel texture	Stiff, thermally irreversible (<100°C)	Soft, thermally reversible (<100°C)
Film properties	Strong, coherent	Brittle
Reference	Biliaderis, 1991; Hizukuri, 1996	

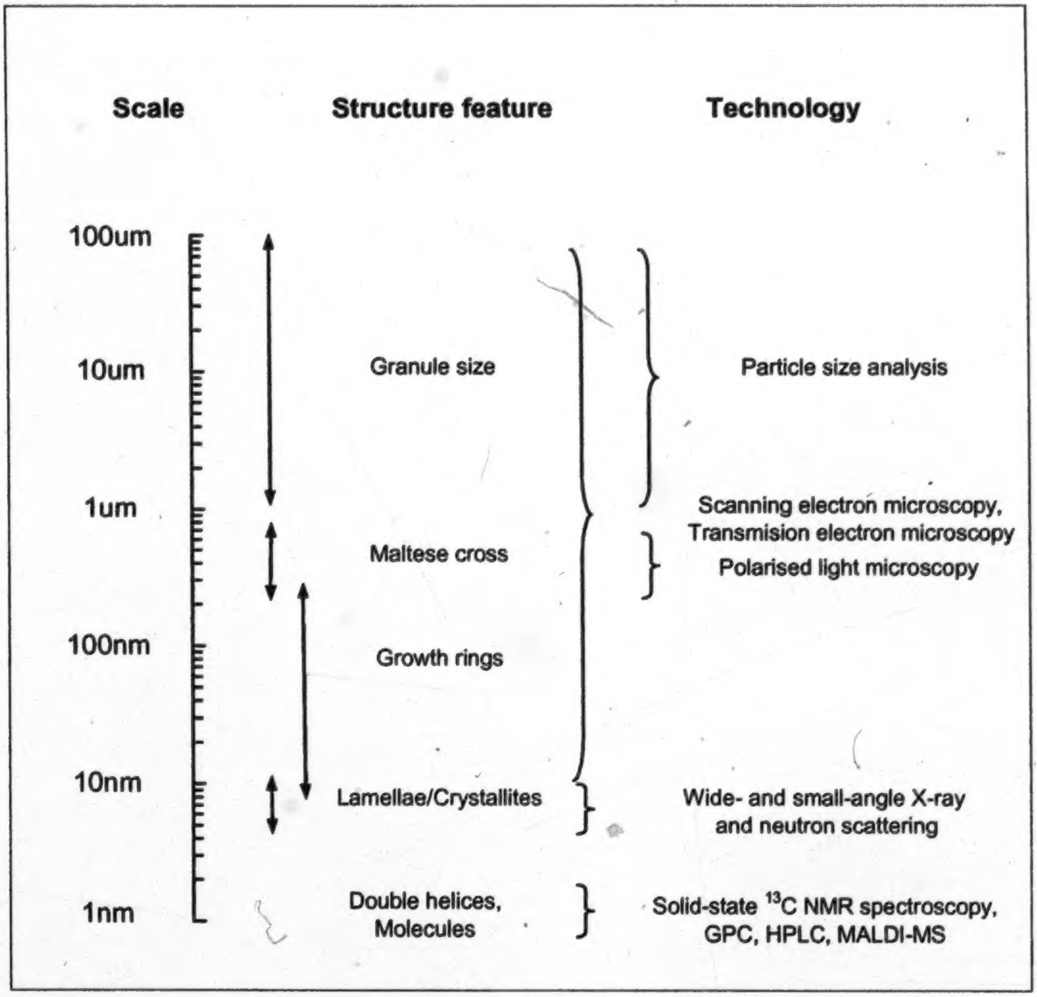
Scale
Structure feature
Technology
100um
10um
1um
100nm
10nm
1nm
Granule size
Maltese cross
Growth rings
Lamellae/Crystallites
Double helices, Molecules
Particle size analysis
Scanning electron microscopy, Transmision electron microscopy
Polarised light microscopy
Wide- and small-angle X-ray and neutron scattering
Solid-state 13C NMR spectroscopy, GPC, HPLC, MALDI-MS

Figure. 1-4 Illustration of the length scale of starch granule structure levels together with technology used for characterization of starch structural features (modified from Tester and Doben, 2000).

into clusters with short chains and are oriented perpendicular to the granule surface. Neighboring short amylopectin chains form double helices and are further packed into crystallites. Crystallites fall within crystalline lamellae while amylopectin branch points are located in the amorphous lamellae. The stacks of crystalline and amorphous lamellae form semicrystalline growth rings alternating with completely amorphous growth rings of a similar size. Amylose is interspersed in amorphous regions of the granule.

1.2.4.1 Macromolecules

1.2.4.1.1 Amylose

Amylose is an essentially linear α-1,4-D-glucan chain with a low degree of α-1,6 linked branch points. Structural and physicochemical properties of amylose from various starch sources are shown in Table 1-8. The molecular weight and degree of polymerization (DP) of amylose are usually in the range of 10^5-10^6 Da and 700-5000 anhydro-glucose units, respectively. The molecular size of amylose decreases with the increase of amylose content in maize and barley starches (Shi et al., 1998; Yoshimoto et al., 2000, 2002). Amylose from cereal starches has a much smaller average molecular size than those from tuber and root starches. The molecular weight distribution of amylose is monomodal but amyloses from tuber and root starches show narrower distribution with less small molecules than those from cereal starches (Hizukuri, 1996; Hizukuri and Takagi, 1984). About 25-55% of the total amylose (mole basis) in starch granules is branched with 4-18 branch points per molecule and branch chain length of 4 to over 100 (Hizukuri et al., 1981, 1997). In rice, the molecular size of

Table 1-8 Molecular characteristics of amylose from various starches

Property[a]	Rice	Wheat	Maize	Sweet potato	Potato	Tapioca
BV	1.40-1.47	1.13-1.31	1.35-1.39	1.48	1.38-1.41	1.47
IA, g/100g	20.0-21.1	19.0-19.5	20.0-20.1	19.9-20.2	20.0-20.9	20.0
λmax, nm	653-658	636-648	643-645	-	-	662
η, ml/g	180-249	118-237	183	324-334	384	384
β-Limit, %	73-87	79-85	81-84	72-73	80-87	75
DP_w range	210-13000	290-25200	400-14700	840-19100	560-21800	580-22400
DP_w	2750-3420	2360-5450	2270-2550	5430	5130-6360	6680
DP_n	920-1100	830-1570	930-990	3400-4100	2110-4920	2660
DP_w/DP_n	2.64-3.70	2.84-4.98	2.44-2.66	1.31	1.29	2.51
CL	250-450	135-255	295-335	330-380	630	340
Chain number per molecule						
Whole molecule	1.3-3.3	5.5-6.5	2.8-3.4	7.8-13	3.9-6.3	6.8
Branched molecule	4.7-8.7	12.9-20.7	5.3-5.4	-	-	16.1
Branched molecule, mol%	25-49	26-44	44-48	70	-	42
Reference	Hizukuri, 1996; Morrison and Karkalas, 1990					

Table 1-8 cont.

Property	Amylomaize	Barley		
		Waxy	Normal	High-amylose
Amylose content in starch, %	48-68	4-11.9	25.7-28.2	37.4-40.5
BV	1.32-1.39	1.35-1.42	1.33-1.63	18.8-20.0
IA, g/100g	19.4-19.6	19.5-19.8	20.0-20.1	1.36-1.43
λmax, nm	645-650	643-655	643-664	643-646
η, ml/g	139-147	-	257-344	-
β-Limit, %	75-78	77-82	76-87	70-73
DP_w range	210-8940	-	180-17200	130-19000
DP_w	1810-1990	-	3440-5580	4080-4920
DP_n	690-740	1560-1680	940-1570	950-1080
DP_w /DP_n	2.45-2.88	-	3.56-4.1	4.3-4.6
CL	215-255	460-510	210-530	350-450
Chain number per molecule				
Whole molecule	2.9-3.2	3.3-3.4	1.8-5.3	2.4-2.7
Branched molecule	4.9-6.1	6.1-10.4	5.8-12.0-13.8	9.5-10.6
Branched molecule, mol %	42-47	26-45	17-35	15-20
Reference	Takeda et al., 1989	Yoshimoto et al., 2002	Takeda et al., 1999, Schulman et al., 1995 Yoshimoto et al., 2000,2002	Yoshimoto et al., 2000

Table 1-8 cont.

Property	Navy bean	Mung bean	Faba bean	Smooth pea	Wrinkled pea	Lentil
BV						
IA, g/100g	18.5	19.4	19.6	18.8-19.2	18-19.2	19.6
λmax, nm						
η, ml/g	174	251	188	180-194	136-150	188
β-Limit, %	86.2	78.4	85.6	81.6-86.9	79-84.7	89.2
DP_n	1300	1900	1400	1300-1400	1000-1100	1400
Reference	Hoover and Sosulski, 1991					

[a] BV, blue value; IA, iodine affinity; λmax, maximum wavelength of the spectrum of iodine coloration; η, limiting viscosity number; DP, degree of polymerization; DP_w, weight average DP; DP_n, number average DP; CL, average chain length.

the branched amylose (average chain length 800) is 1.5-3.0 times larger than that of linear amylose (average chain length 140-250) (Hizukuri et al., 1997). Overall, amylose molecules contain 0.27-0.68% branching points with an average chain length of 100-550 anhydro-glucose units. Large amylose molecules have been shown to have more branched linkages than small amylose molecules (Hizukuri et al., 1997). The presence of branched chains (predominant DP10-30) does not significantly influence the general properties of amylose. In general, branched amylose molecules from various sources differ with respect to molecular size, side chain length, and the number of chains. Amylose in neutral, aqueous solution tends to be slightly helical due to the natural twist present in the chair conformation of the glucose units. It behaves as a random, flexible coil, which consists of extended helical segments (helical regions stabilized by intermolecular hydrogen bonds) interspaced by non-helical segments (Appelqvist and Debet, 1997) with a typical hydrodynamic radius (a measure of the volume occupied by the polymer in solution depending on the molecule weight) of 7-22nm (Buléon et al., 1998).

1.2.4.1.2 Amylopectin

Amylopectin is the major component of most starches. It is a highly branched macromolecule composed of thousands of linear α-1,4-D-glucan unit chains and 4-5.5% of α-1,6-glucosidic branch points (Hizukuri, 1997). Molecular characteristics of amylopectin from different starch sources are summarized in Table 1-9. The average chain length is 18-25 anhydro-glucose units. However, these unit chains are linked in a unique way to make up an average molecular weight of about 10^7-10^9 Da with a hydrodynamic radius of 21-75nm (Buléon et al., 1998). Compared with amylose,

Table 1-9 Molecular characteristics of amylopectin from various starches

Property[a]	Rice	Wheat	Maize	Sweet potato	Potato	Tapioca
BV	0.049-0.232	0.098-0.115	0.110	0.160-0.176	0.193-0.245	0.104
IA, g/100g	0.39-2.57	0.66-1.12	1.10	0.38-0.44	0.06-0.08	-
λmax, nm	531-575	547-560	554	-	-	-
η, ml/g	134-170	116-148	168	175-193	125	-
β-Limit, %	56-59	56-59	59	55-56	56	57
DP_n	4700-12800	5000-9400	10200	-	-	10000-100000
CL	19-22	20-21	22	21-22	23	21-26
Phosphorus, μg/g	8-29	9-13	15-27	117-144	650-900	-
Reference	Hizukuri, 1996; Morrison and Karkalas, 1990					

Table 1-9 cont.

Property	Amylomaize	Barley		
		Waxy	Normal	High-amylose
Amylopectin in starch, %	32-52	88.1-100	72.5	59.5-62.6
BV	0.427-0.441	0.04-0.12	0.07-0.12	0.07-0.12
IA, g/100g	3.60-4.63	0.00-0.55	0.64-0.69	0.66-1.22
λmax, nm	573-575	522-537	541-550	556-578
η, ml/g	-	-	155	-
β-Limit, %	61-62	53-54	55-56	56-57
DP_n	-	5700-8700	6000-12000	6200-7500
CL	30-32	17-20	18-20	19
Phosphorus, μg/g	75-261	19-69	14-45	41-214
Reference	Takeda et al., 1993	Tang et al., 2001 Yoshimoto et al., 2002	Takeda et al., 1999 Schulman et al., 1995 Yoshimoto et al., 2000, 2002	Yoshimoto et al., 2000

[a] BV, blue value; IA, iodine affinity; λmax, maximum wavelength of the spectrum of iodine coloration; η, limiting viscosity number; DP, degree of polymerization; DP_n, number average DP; CL, average chain length.

amylopectin has a low Blue Value (BV) (< 0.2), Iodine Affinity (IA) (< 0.1), and β-amylolysis limit (β-limits) (55-60%), but a much wider molecular weight distribution. Amylopectin in high-amylose starches has a lower degree of branching, higher average chain length, and a large proportion of long chains than that in waxy and normal starches (Takeda et al., 1993a,b; Salomonsson and Sundberg, 1994; Cheetham and Tao, 1997; Shi et al., 1998).

Amylopectin contains a small amount of covalently-bound phosphate monoester groups. Potato amylopectin contains 200-1000 ppm ester phosphorus and those from other tubers, roots and legumes 40-150 ppm, whereas cereal amylopectin contains less than 20 ppm (with the exception of 110-260 ppm in amylomaize) (Hizukuri, 1996). Phosphate monoesters, which are mainly linked to long B-chains (Takeda and Hizukuri, 1982), are located at C-6 (primary hydroxyl group) and at C-3 (secondary alcohol group) in amylopectins of tubers, roots, and legume starches (Tabada and Hizukuri, 1971; Lim et al., 1994) with 1 phosphate group per 200-400 glucose units (Galliard and Bowler, 1987). These phosphate monoesters in amylopectin may play important roles in starch, such as enhanced paste clarity, high paste viscosity, low gelatinization temperature, significant shear-thinning and slow retrogradation rate (Kasemsuwan and Jane, 1996).

Amylopectin structure has been extensively studied in terms of molecular size, branching chain length (inner and outer) distribution, branch points, and crystalinity using various techniques, such as chemical and enzymatic analysis including chromatography, matrix-assisted laser desorption/ionization mass spectrometry (MALDI-MS), fluorophore-assisted carbohydrate electrophoresis (FACE) (Manners, 1989; Morrison and Karkalas, 1990; Hizukuri, 1996; Morell et al., 1998; Broberg et al., 2000; Wang et al., 2000), optical and electron microscopy (French, 1984; Gallant et al., 1997), nuclear magnetic resonance (NMR) spectroscopy (Gidley and Bociek, 1985; Morgan et al., 1995; Gidley, 2001), and X-ray and neutron scattering (Donald et al., 1997, 2001), A number of reviews on amylopectin structure have been published (Banks and Greenwood, 1975; Sarko and Zugenmaier, 1980; Zobel, 1988b, Manners, 1989; Gidley and Cooke, 1991; Imberty et al.,1991; Zobel, 1992; Hizukuri, 1996; Ball et al., 1996; Gallant, 1997; Oates, 1997; Gidley, 2001; Tester et al., 2001).

Chain length distribution

Complete debranching of amylopectin using isoamylase and pullulanase (debranching enzymes that hydrolyze α-1,6 branch linkages of amylopectin and produce short linear chains) followed by fractionation of the linear chains using chromatography revealed that debranched amylopectin normally has a tri-modal distribution (MacGregor and Morgan, 1984; Takeda et al., 1987b, 1988; Tang et al., 2001a,b) or a poly-modal distribution (Hizukuri, 1986; Manners, 1989; Hizukuri and Maehara, 1990; Shibanuma et al., 1994; Takeda et al., 1999; Yashimoto et al., 2000, 2002). As shown in Figure1-5, fractions A, B1, B2, B3, and B4 represent different chain groups of amylopectin with average chain lengths (CL) of 12-16, 20-24, 42-48, and 69-75, respectively. The relative molar ratio of chain length among B1, B2, and B3 fractions is 1:2:3, implying one to three or more clusters that may be formed from these chains (Hizukuri, 1986). The A- and B1-chains account for 80-90% (mole basis) of total chains, which represent outer short chains in a single molecule, and B2-chains 10%, B3-chains 1-3%, and B4-chains 0.1-0.6%, which connect 2, 3 or more clusters (Hizukuri, 1986). Further analysis

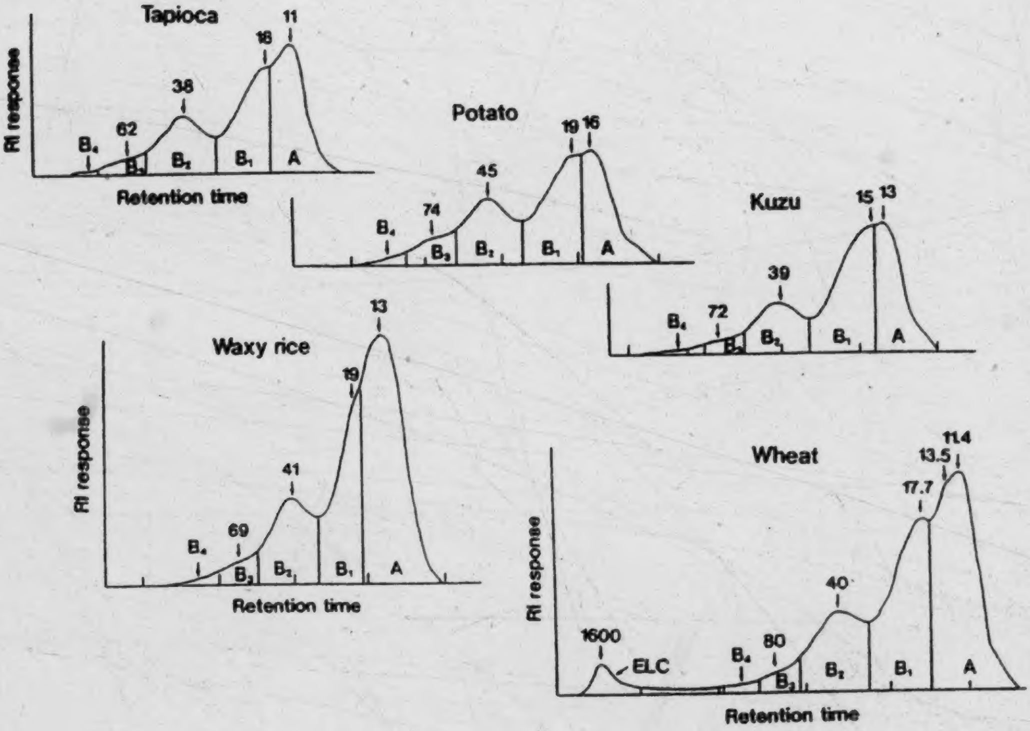

Figure 1-5 Gel-permeation chromatograms of debranched amylopectins. Fractions of A, B1, B2, B3, B4, and ELC (extra-long chains) are different groups of branch chains. The peak DP is labeled on the top of each fraction (adapted from Hizukuri, 1996, with permission from Marcel Dekker).

of the connection mode of branching (Hizukuri and Machara, 1990; Hizukuri, 1996) indicated that the average span length (the number of glucose units linked through two adjacent branch points in a chain) is in the range of 3-12 and one B-chain carries 0-3 A- or other B-chains while 37% of B-chains have no A-chains and carry only B-chains. In general, the average CL for most amylopectins is in the range of 18-25, but its distribution is characteristic of a source. Potato and other B-type crystalline/polymorph (in X-ray diffraction pattern) starches contain less short (A- and B1-) chains and more long B-chains (B2-B4) than cereal starches, with a mole ratio of 5 for potato and 8-10 for cereal starch amylopectins (Hizukuri, 1996). In mutant maize starches, A-type crystalline amylopectin contains larger clusters, more short branch chains, and more branching points than B-type crystalline amylopectin (Gérard et al., 2000).

High-performance anion-exchange chromatography with pulsed amperometric detection (HPAEC-PAD) has been used for quantifying debranched amylopectin chains (Jane et al., 1999). As shown in Table 1-10, the branch chain length distribution of amylopectin is related to the crystalline polymorphs and its profile is characteristic for each starch even in the same polymorph type (Hizukuri, 1985; Hanashiro et al., 1996; Jane et al., 1999). A-type starches have shorter peak DP and shorter average chain length than B-type starches. Also, A-type starches have relatively higher proportions of short chains (DP6-12) than B-type starches, and C-type starches have intermediate amounts. In addition, amylopectins from amylomaize starches have relatively longer average chain length and higher proportions of long chains (DP $\geq$ 37) compared to those from waxy and normal maize starches (Jane and Chen, 1992; Shi et al., 1998; Jane et al., 1999). Branch chain length distribution of amylopectin has been shown to influence starch physicochemical properties such as gelatinization temperature, pasting

Table 1-10 Branch chain length distributions of amylopectin from various starches

Source	Peak DP		Average CL	Distribution %				Reference
	I	II		DP6-12	DP13-24	DP25-36	DP≥37	
A-type starch								Jane et al., 1999
Waxy maize	14	48	23.5	17.0	49.4	17.1	16.5	Jane et al., 1999
du Waxy maize	14	51	23.1	16.7	51.9	17.4	14	Jane et al., 1999
Normal maize	13	48	24.4	17.9	47.9	14.9	19.3	Jane et al., 1999
	13	-	22	24	54	13	9	Hanashiro et al., 1996
Waxy barley	12	48	24.2	21.6	43.0	16.1	19.2	Song and Jane, 2000
Normal barley	12	50	26.6	18.0	40.9	17.2	23.7	Song and Jane, 2000
	12	43	22.1	20.8	48.9	17.7	12.6	Jane et al., 1999
	11	-	19.3	27	50	14	9	Hanashiro et al., 1996
High-amylose barley	12	48	24.5-25.5	16.5-17.4	44.9-47.9	17.2-17.9	17.8-20.7	Song and Jane, 2000
Waxy rice	12	41	18.8	27.4	53.4	12.6	6.6	Jane et al., 1999
	12	-	18.9	29	50	11	9	Hanashiro et al., 1996
Normal rice	12	46	22.7	19.0	52.2	12.3	16.5	Jane et al., 1999
	12	-	21.6	27	52	12	9	Hanashiro et al., 1996
Wheat	12	41	22.7	19.0	41.7	16.2	13.0	Jane et al., 1999
	11	-	20.1	27	49	14	10	Hanashiro et al., 1996
	12	46-51	25.6-26.9	18.9-21.0	40.9-42.7	14.4-17.7	20.4-23.4	Franco et al. 2002
Tapioca	12	49	27.6	17.3	40.4	15.6	26.7	Jane et al., 1999
Sweet potato	13	-	22.1	21	47	17	15	Hanashiro et al., 1996

Table 1-10 cont.

Source	Peak DP		Average CL	Distribution %				Reference
	I	II		DP6-12	DP13-24	DP25-36	DP≥37	
B-type starch								
Amylomaize V	16	48	28.9	9.7	43.9	20.3	26.1	Jane et al., 1999
Amylomaize VII	16	48	30.7	8.5	40.7	21.3	29.5	Jane et al., 1999
Waxy potato	14	49	25.8	14.8	48.4	14.4	22.4	McPherson and Jane, 1999
Potato	14	52	29.4	12.3	43.3	15.5	28.9	Jane et al., 1999
	13	-	22.1	21	47	17	15	Hanashiro et al., 1996
	14	51	28.6	13.1	44.4	14	28.5	McPherson and Jane, 1999
Yam	14	-	23.2	18	56	15	11	Hanashiro et al., 1996
C-type starch								
Field pea	13-15	40-43	22.9-24.2	16.2-19.6	48.2-52.9	13.9-17.5	16.2-19.4	Ratnayake et al., 2001
Lotus	13	52	25.4	16.4	47.2	15.4	21.0	Jane et al., 1999
	13	-	22.6	23	55	13	9	Hanashiro et al., 1996
Arrowhead	12	-	20.5	25	53	13	9	Hanashiro et al., 1996
Sweet potato	13	48	26.3	17.1	48.1	13.6	23.4	McPherson and Jane, 1999
Yam	13	52	25.8	19.1	44.8	14.3	21.8	McPherson and Jane, 1999
Water chestnut	13	50	26.7	5.9	17.8	43.7	15.3	Jane et al., 1999
Green banana	13	48	26.4	16.8	46.3	12.9	24.0	Jane et al., 1999

properties, retrogradation, and acid hydrolysis (Jane and Chen, 1992; Shi and Seib, 1992, 1995; Shi et al., 1998; Jane et al., 1999; McPherson and Jane, 1999;; Franco et al., 2002).

Structural model

One of the most widely accepted models for amylopectin is the cluster model (Figure 1-6) that was proposed by Robin et al. (1974) and modified by Hizukuri (1986). In the cluster model, the amylopectin molecule consists of three types of unit chains, referred to as A-, B-and C-chains (Figure 1-6). A-chains are unbranched and linked to B-chains through α-1,6-bonds at their reducing end-group. B-chains are linked to other B-chains or C-chain in the same manner, carrying either A-chains or B-chains. C-chain is the only reducing end-group carrying numerous B-chains. Unit chains are arranged in groups/clusters, where A- and B1-chains are located within individual clusters, whereas B2- and B3-chains connect 2 and 3 clusters. The ratio of A- to B-chains is in the range of 1.1-1.5 to 1 depending on amylopectin source (Manners, 1989).

1.2.4.2 Molecular orientation

When viewed under polarized light, starch granules show birefringence in the form of the typical maltese cross at the hilum (the original growing point of the granule, normally near the center of elliptical granules or positioned on the axis of symmetry at the far end of pear-shaped granules). This implies a radial molecular orientation within the granule due to higher radial refractive index than tangential refractive index along the molecular axes of starch granules (Banks and Greenwood, 1975; French, 1984). Transmission electron microscopy (TEM) and small-angle light scattering have also

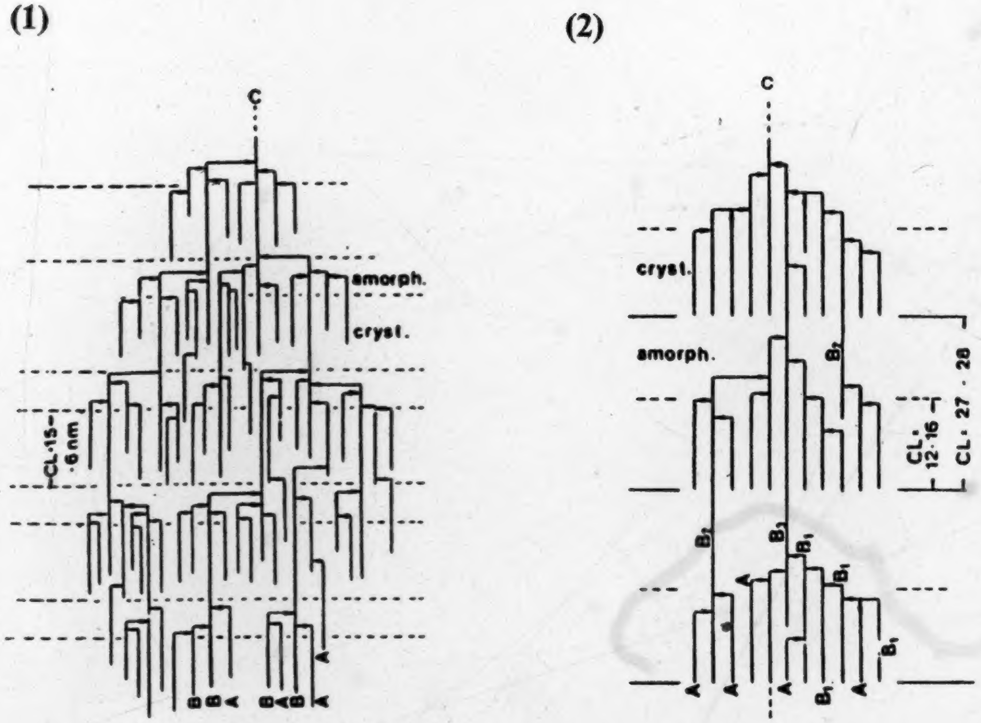

(1)
(2)
C
amorph.
cryst.
CL·15-·6nm
B
B
A
B
A
B
A
A
C
cryst.
amorph.
B2
CL·12·16
CL·27·28
B2
B1
B1
B1
A
A
A
A
A
B1
A
B1

Figure 1-6 Cluster models of amylopectin proposed by (1) Robin et al. (1974) and (2) Hizukuri (1986). A: outer most branches, B: inter branches, C: the chain that carries the reducing group. Amorph. = amorphous region, Cryst. = crystalline region, CL = chain length (adapted with permission from American Association of Cereal Chemists and Elsevier Science).

shown that both amylose and amylopectin molecular orientation is perpendicular to the surface of the granule (French, 1984; Blanshard, 1987). Labeling starch granules by tritium bombardment (Nordin, 1970) confirmed that the non-reducing ends of macromolecules are oriented toward the granule surface. A recent study (Waigh et al., 1997) using X-ray microfocus diffraction with a 2 µm beam revealed that, by analysis of the direction of the helical reflections, amylopectin helices in the periphery region of the potato starch granule were perpendicularly oriented to the surface of the granule.

1.2.4.3 Double helices, crystallites, and crystallinity

Within starch granules, about 40-50% of chains on a weight basis exist as double helices with approximately half of these helical chains present in the form of crystallites, which are large and perfect enough to diffract X-rays (Gidley and Bociek, 1985; Gidley, 2001). Double helices are formed between the outer branch chains (A- and B1-chains) of amylopectin (French, 1972). Two neighboring short chains fit together compactly, with the hydrophobic parts of the opposed glucose units in close contact inside the structure, and the hydroxyl groups at the outside of the double helix resulting in strong interchain hydrogen bonding (helical order or short-range order). French and Murphy (1977) proposed the first detailed computer model (Figure 1-7) for the starch double helix with no intra-chain hydrogen bonds. The stability of the helix is attained by interchain hydrogen bonding between hydroxyl groups at positions C2 and C6 and from Van der Waal's forces. The helical core is highly hydrophobic and compact so that there is no room for water or any other molecule to reside in it. Close packing of neighboring double helices (crystalline order or long range order) via direct or indirect

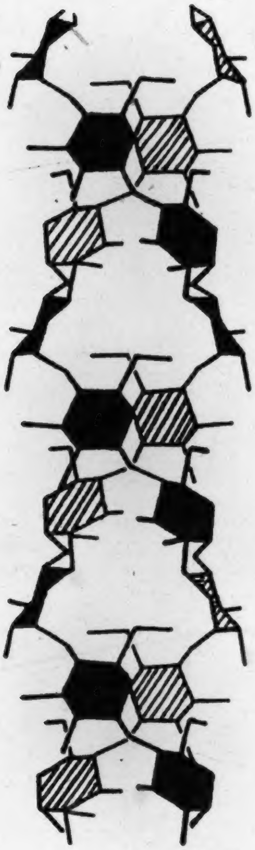

Figure 1-7 Doule helix model of starch chain (adapted from French and Murphy, 1977, with permission from American Association of Cereal Chemists).

(through a bridge of water molecules) hydrogen bonding forms granule crystallites (Wu and Sarco 1978a,b; Imberty et al., 1988; Imberty and Pérez 1988; Imberty et al., 1991).

Crystallites, which are roughly spherical in shape with a diameter of about 10 nm in wheat starch and somewhat smaller in potato starch (Muhrbeck, 1991), may occur either between adjacent branch chains in the same amylopectin branch cluster or between adjacent clusters in three dimensions (Oates, 1997). The most recent model (Figure 1-8) was proposed by Wu and Sarko (1978). The unit cell structures of crystallites (Table 1-11) are classified as A- and B-type (Imberty et al., 1988; Imberty and Pérez, 1988). The double helices are identical for both A and B types but their packing manner (helix geometry) and water content differ. The left-handed, parallel-stranded double helices are packed in hexagonal arrays and stabilized by a network of hydrogen bonds (Imberty et al., 1988; Imberty and Pérez, 1988; Gidley and Bociek, 1988, 1985).

Double helical content and degree of crystallinity determined by ^{13}C-NMR and X-ray diffraction, respectively, are presented in Table 1-12. Degree of crystallinity ranges from 15 to 45% by weight depending on starch origin, hydration, and method used (Zobel, 1988b). The degree of crystallinity is inversely proportional to the amylose content and average branch chain length in maize starches (Cheetham and Tao, 1998). Gidley and Bociek (1985) and Cooke and Gidley (1992) showed that the double helical content determined by NMR (corresponds to crystalline and non-crystalline domains) is higher than the crystalline order determined by X-ray diffraction (which corresponds only to the crystalline order of the double helices), suggesting that a

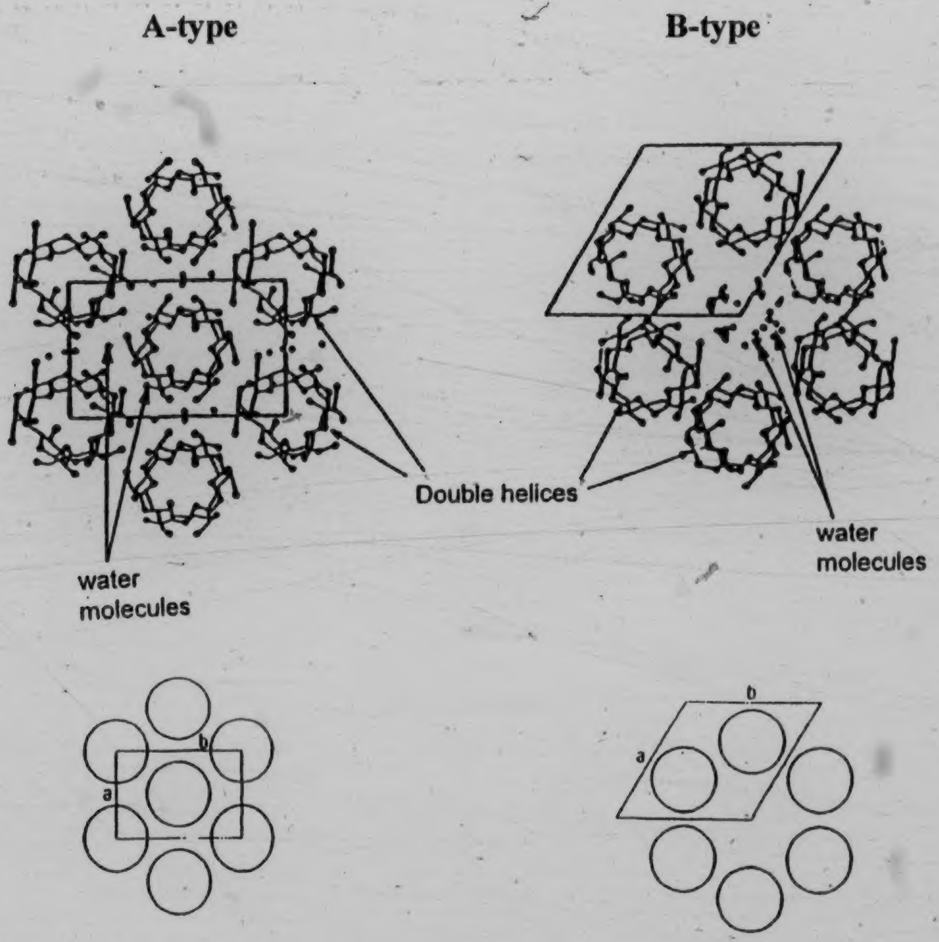
A-type
B-type
Double helices
water molecules
water molecules
b
a
b
a

Figure 1-8 Double helix packing arrangement of amylopectin crystallites in A- and B-type unit cells (adapted from Wu and Sarko, 1978a,b, with permission from Elsevier Science).

Table 1-11 Unit cell structures of A- and B-type crystallites

Parameter	A-type	B-type
Dimension (nm)	a = 2.214	a = 1.85
	b = 1.172	b = 1.85
	c = 1.069	c = 1.04
	$\gamma = 123.5°$	
Density	d = 1.48	
Space group	B2	$P6_1$
Geometry	Monoclinic	Hexagonal
Glucose number	12	12
Repeat unit	Maltotriose	Maltose
Water	4 (3.6%)	36 (25%)

Reference: Imberty et al. (1991).

Table 1-12 Degree of crystallinity (%) of starches determined by different methods

Starch	X-ray diffraction	^{13}C NMR
A-type		
Normal maize	36-40	42-43
Waxy maize	39-40	48-53
Oat	33	-
Wheat	36	39
Rice	38	49
Sorghum	37	-
Rye	34	-
B-type		
Amylomaize	15-24	38
Potato	25-28	40-50
Edible canna	26	--
C-type		
Sweet potato	31-37	-
Tapioca	31-39	44
Reference	Zobel, 1988, Nara et al., 1981	Cooke and Gidley, 1992

portion of the double helices exist individually and not further ordered to form crystalline order within the starch granule.

1.2.4.4 Polymorphic patterns

The crystalline types within starch granules from various botanical sources are shown as one of three well defined X-ray diffraction patterns, classified as A-, B-, and C-type polymorphs. The A-type occurs in most cereal starches (e.g. normal maize, rice, wheat, barley, and oat) as well as in some root and tuber starches (e.g. taro, some sweet potatoes, tapioca, and iris) (Hizukuri, 1996; Cheetham and Tao, 1998; Hoover, 2001). The B-type occurs in tuber and root starches (e.g. potato, lily, canna, and tulip) and high-amylose (> 40%) cereal starches (e.g. amylomaize, high-amylose barley, and high-amylose rice) (Eliasson and Gudmundsson, 1996; Hizukuri, 1996; Cheetham and Tao, 1998). The A- and B-types are believed to be independent, whereas, the C-type, which is commonly observed in legume starches, is a mixture of A- and B-type crystallites in varying proportions (Sarko and Wu, 1978; Gernat et al., 1990; Hizukuri, 1996). Further subclassification of C-type as Ca-, Cb-, and Cc-types is on the basis of their resemblance to A- and B-types or in between the two types, respectively (Hizukuri, 1996). Mutant maize starches containing A- and B-type polymorphs in various ratios (Gérard et al., 2001) and wheat and rye starches, containing low levels of the B-type polymorph (up to 10%) (Gernat et al., 1993) have been reported. Cheetham and Tao (1998) have reported that a transition of crystalline types in maize starches from A- to B-types via C-type occurs at approximately 40% amylose. Typical X-ray diffraction patterns are shown in Figure 1-9.

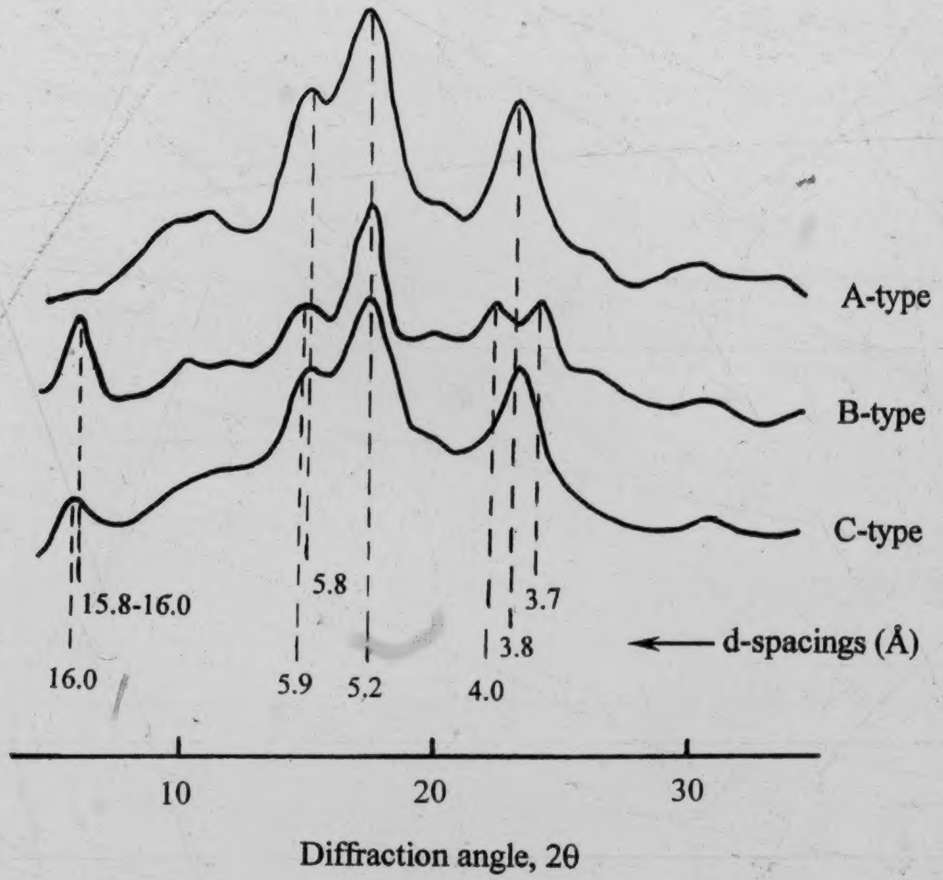

Figure 1-9 X-ray diffraction patterns of A-, B-, and C-type starches with their characteristic d-spacing. (modified from Zobel, 1988a). A-type pattern shows three strong peaks at 2θ 15.27° (d=5.8Å), 17.05° (d=5.2 Å), and 23.40° (d=3.8 Å). B-type pattern shows strong peaks at 5.52-5.6° (d=15.8-16.0 Å) and 17.05° (d=5.2 Å), and medium intensity peaks at 15.01° (d=5.9 Å), 22.22°(d=4.0 Å), and 24.04° (d=3.7 Å). C-type pattern is the same as that of A-type except for the addition of the medium to strong peak at about 5.52 (d=16.0). The d-spacing at 4.4 Å (2θ=20°) is characteristic of amylose-lipid complex (Zobel, 1988a; Vasanthan and Bhatty, 1996; Cheetham and Tao, 1998).

Except for the differences in their crystallite arrangements and water content (Figure 1-8, Table 1-12), the amylopectin chain length (Pfannemüeller, 1987; Gidley and Cooke, 1991; Hizukuri, 1996) and branching pattern (Jane et al., 1997) also differ with each other. Relatively shorter branch chains lead to A-type; whereas longer branch chains show B-type and intermediate branch chains are associated with C-type polymorph (Hizukuri et al., 1983; Hizukuri, 1996). The difference in the average chain length between A- and B-types can be as little as one glucose unit (Hizukuri et al., 1983; Hizukuri, 1996). These are probably due to mixtures of A- and B-type crystallites either within individual granules or as mixtures of A- and B-type granules (Lineback, 1984). The extent of α-amylase hydrolysis of mutant maize starches with various A and B polymorph ratios indicated that heterogeneous distributions of A- and B-type crystallites were present within the granule (Gérard et al., 2001). In C-type pea starches, Bogracheva et al. (1998) found that B-type was present in the granule interior, while A-type was located in the periphery of the granule. Synthesis of both polymorphs from linear α-glucans (Gidley and Bulpin, 1987; Pfannemüeller, 1987) showed that at least 10 glucose units of a linear chain is required for the crystallization of double helices, but that a chain length of more than DP50 did not form crystallites. Also, shorter chain length, higher crystallization temperature, greater polysaccharide concentration, and slower crystallization favor formation of the A-type polymorph.

Jane et al. (1997) reported the different branching patterns for A- and B-type crystalline starches (Figure 1-10). In A-type amylopectin, the α-1,6 branch linkages are more scattered and mainly located within the crystalline region (crystalline lamellae), whereas others are in the amorphous region (amorphous lamellae). In B-type

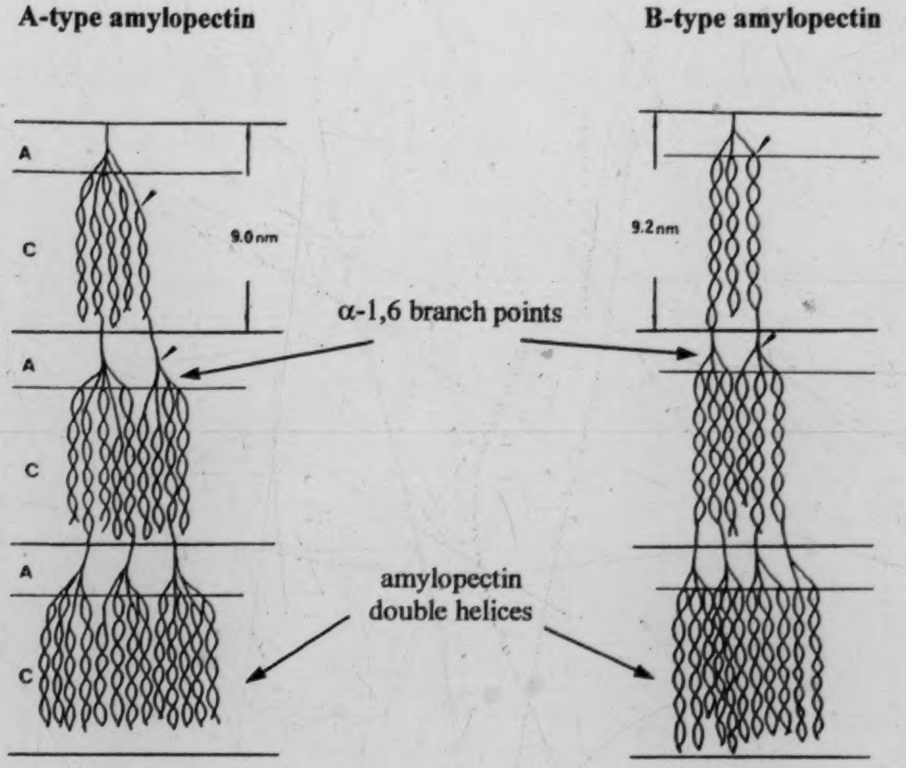
A-type amylopectin
B-type amylopectin
A
C
A
C
A
C
9.0 nm
9.2 nm
α-1,6 branch points
amylopectin double helices

Figure 1-10 Proposed models for branching patterns of A-type starch and B-type starch. A and C stand for the amorphous and crystalline regions, respectively (adapted from Jane et al., 1997, with permission from Elsevier Science).

amylopectin, most of the α-1,6 branch linkages are clustered in the amorphous region. In A-type amylopectin, due to the scattered branch points, there are likely more short A-chains derived from branch linkages located inside the crystalline region, which produces an inferior crystalline structure. This inferior crystalline structure containing α-1,6 branch linkages and the short double helices is more susceptible to enzyme hydrolysis. Clustered branch points and relatively fewer short chains in B-type amylopectin lead to the development of a superior crystalline structure, which is more resistant to enzyme attack.

1.2.4.5 Lamellae

Kassenbeck (1975, 1978) and Yamaguchi et al. (1979) observed rippled fibrillar structures with a periodicity of 6-8 nm in the growth rings of maize and wheat starch granules using electron microscopy. After extensive acid hydrolysis, the residual starch granules (acid resistant amylodextrins) showed lamellar structures of 5 nm thickness, which stacked together side-by-side and oriented tangentially to the growth rings and to the granule surface (Yamaguchi et al., 1979). These lamellar structures were believed to be the crystalline region of the ripples alternating with amorphous lamellae. The sizes of crystalline lamellae and the combined period (repeat distance) of crystalline and amorphous lamellae corresponded to the linear chain length and a single amylopectin cluster, respectively, as proposed by French (1972) and Robin et al. (1974). By optical diffraction analysis of electron micrographs, Oostergetel and van Bruggen (1989) found that the repeat distance agreed with the value determined by small angle X-ray diffraction at approximately 10 nm (at an angle of approximately 25° along the molecular axis). Jenkins et al. (1993) confirmed that the lamellae spacing is maintained across starch sources with A-, B-, and C-type X-ray diffraction patterns and is consistent at 9 nm, despite differing lengths of the amylopectin side chains formed among the species (Hizukuri, 1986) and variations in the size of crystalline lamellae in starches with various amylose contents (Jenkins and Donald, 1995).

Oosteregetel and van Bruggen (1993) modeled the crystalline lamellae as a continuous, left-hand twisted, super-helical structure. Each superhelix is interlocked to neighbouring superhelices to give a tetragonal array, which is filled with amorphous materials. Gallant et al. (1997) further modified this model in which the spherical blocklets range from 20-500 nm in size (Figure 1-11).

1.2.4.6 Growth rings

Growth rings represent periodic growth, and in cereal starches, daily fluctuations in carbohydrates available for starch deposition (French, 1984). During day time, carbohydrates from photosynthesis are abundant and a dense packing of starch molecules results, whereas during the night, the supply of carbohydrates becomes lower and packing gets looser (Tester, 1997). Therefore, starch deposition during granule development seems to be in a diurnal rhythm and is related to the development of granule growth rings.

Growth rings are easily visible under the optical microscope in large, fully hydrated starch granules (e.g. potato and canna), and can be observed by SEM and TEM only after chemical and enzymatic treatments (French, 1984). These more or less concentric layers, namely semicrystalline growth rings and amorphous growth rings (Jenkins et al., 1994), alternate within the granule. They represent two distinct regions

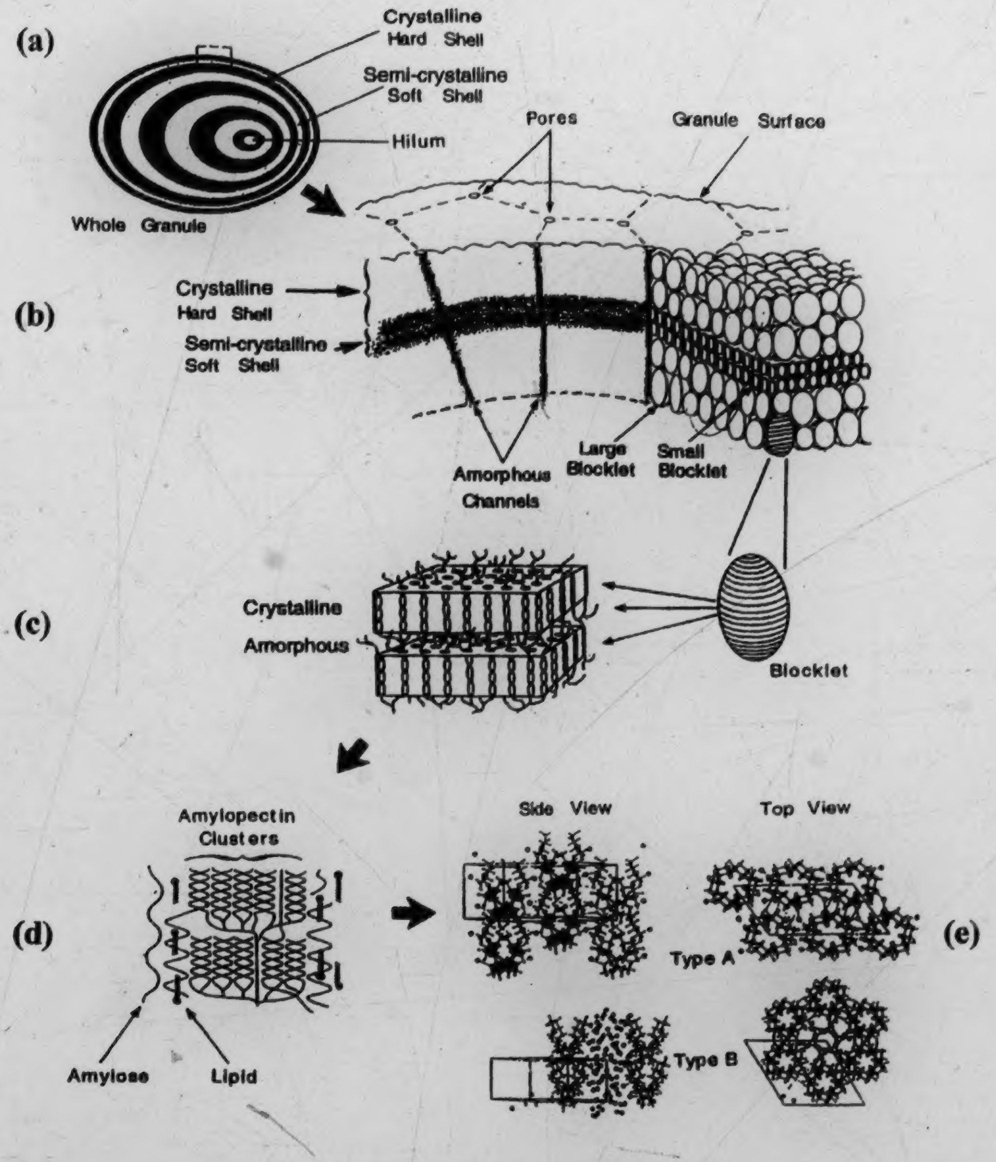
(a)
Crystalline Hard Shell
Semi-crystalline Soft Shell
Hilum
Whole Granule
Pores
Granule Surface
(b)
Crystalline Hard Shell
Semi-crystalline Soft Shell
Amorphous Channels
Large Blocklet
Small Blocklet
(c)
Crystalline
Amorphous
Blocklet
Amylopectin Clusters
(d)
Amylose
Lipid
Side View
Top View
Type A
Type B
(e)

Figure 1-11 A starch granule structure model proposed by Gallant et al. (1997). (a) A whole starch granule showing the alternating growth rings. (b) The blocklet structure within growth rings. (c) Amorphous and crystalline lamellae are arranged within the blocklet structure. (d) The structure of amylopectin clusters with amylose (b) and lipid within lamellae. (e) Crystallite structure of amylopectin (adapted from Gallant et al., 1997, with permission from Elsevier Science).

of the granule with high and low refractive indices, densities, crystallinities, and resistances to acid and enzymatic hydrolysis, respectively (French, 1984).

Both semicrystalline and amorphous growth rings have a similar width, 120-400 nm (French, 1984). Each semicrystalline growth ring contains 16 periodic crystalline and amorphous lamellae corresponding to a distance of about 140 nm, while amorphous growth rings contain mostly amylose (Cameron and Donald, 1992). In a granule structure model (Figure 1-12) proposed by Jenkins et al. (1994), the semicrystalline growth rings, which alternate with the amorphous growth rings, are composed of crystalline and amorphous lamellae fitting the current cluster model of the amylopectin molecule. More recently, Gallant et al. (1997) proposed another granule structure model (Figure 1-11) based on EM examinations of partly hydrolyzed (α-amylazed) starches from different sources. They showed that growth rings are composed of spherical structures, namely blocklets, stacked on top of each other and having sizes between 20-500 nm in diameter depending on the starch source and the location in the granule. Semicrystalline rings contain large blocklets of about 100 nm in diameter, compared to 20-50 nm blocklets in the less organized amorphous rings. A-type starches have smaller blocklets (80-120 nm), whereas potato and other B- and C-type starches show much larger blocklets (200-500 nm) at the granule surface to a depth of about 10 µm (Gallant et al., 1992, 1997). The width of the growth rings becomes progressively thinner toward the exterior of the starch granule.

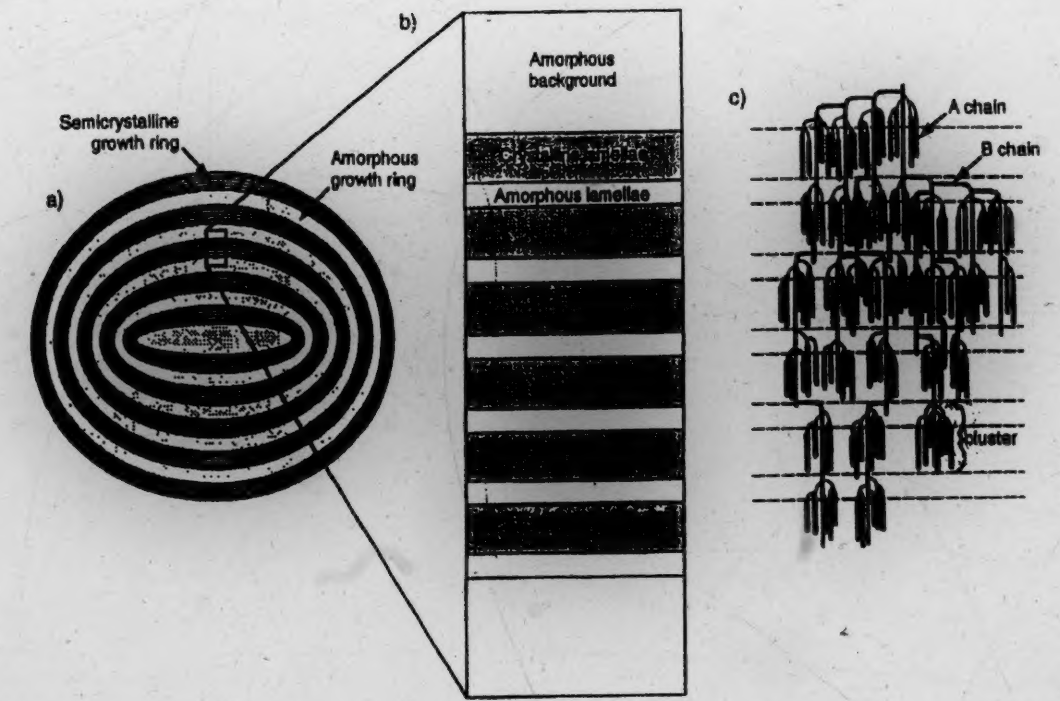
b)
Amorphous background
Crystalline lamellae
Amorphous lamellae
c)
A chain
B chain
cluster
Semicrystalline growth ring
Amorphous growth ring
a)

Figure 1-12 Schematic diagram of starch granule structure. (a) A single granule, comprising of concentric rings of alternating amorphous and semi-crystalline composition. (b) Expanded view of the internal structure. The semi-crystalline growth ring contains stacks of amorphous and crystalline lamellae. (c) The currently accepted cluster structure for amylopectin within the semi-crystalline growth ring. Branch points for both A- and B-chains are predominantly located within the amorphous lamellae (adapted from Jenkins and Donald, 1995, with permission from Elsevier Science).

1.2.4.7 Channels and central cavity

Channels and central cavities are visible under SEM, TEM, and fluorescent microscope, and co-exist with growth rings within granules in some starches. Fannon et al. (1993) observed that channels are serpentine at a roughly radial direction within sorghum starch granules and their size was estimated to be in the range of 0.07-0.1µm in diameter. Huber and BeMiller (1997, 2000) have shown the presence of radial, internal channels in maize and sorghum starch granules. These channels have been shown to penetrate from the external surface inward toward a cavity at the hilum with various depths of penetration. Central cavities with a variety of shapes and sizes at the hilum of starch granules have also been observed by Hall and Sayre (1970b, 1973), Chabot et al. (1978), Baldwin et al. (1994), and Huber and BeMiller (1997, 2000) in maize, sorghum, waxy maize, potato, rice, and wheat starches (using SEM, TEM, confocal scanning laser microscopy, and light and fluorescence microscopy). No direct relationships have been found among surface pinholes, granule size, cavity size, and internal channels. For instance, potato starch granules have no visible holes and no channels, but still have central cavities. Huber and BeMiller (1997, 2000) suggested that channels and cavities are more likely voids, which are formed by crystallization of amylopectin molecules and concurrent shrinkage of the matrix as the granule grows and develops. The above authors have postulated that channels and cavities could influence reactions (i.e. dye penetration) within granules by providing direct access of reagents to a loosely organized region at the hilum and increasing the surface area available for reagent infiltration into the granule matrix.

1.2.4.8 Structure of amorphous region

Only a small portion of the starch granule is believed to be crystalline. Thus, a large portion of the granule is in an amorphous or gel phase. Kainuma and French (1972) have visualized the granule as a gel matrix where the crystalline regions are embedded. The amorphous phase is interdependent but incompatible with crystalline phase within granules. There is no sharp demarcation between these two phases (French, 1984). To date, the structure of amorphous phase has not been clearly revealed.

1.2.4.8.1 Location and distribution of amylose

The major component of the amorphous region in starch granules is amylose. However, its exact location relative to the amylopectin crystallites is not fully understood. Amylose has been located in bundles between amylopectin clusters (Blanshard, 1987; Zobel, 1992). However chemical modifications (cross-linking) (Jane et al., 1992a; Kasemsuwan and Jane, 1994) have shown that amylose was randomly interspersed as individual molecules in both the amorphous and crystalline regions of the granule instead of being in bundles (because no cross-linking was found between amylose molecules whilst it was found only between amylopectin molecules and between amylose and amylopectin molecules). The possible locations of amylose within granules may be in: 1) amorphous growth rings; 2) inter-crystalline amorphous lamellae (including amylopectin branching zone); 3) between crystallites/blocklets within crystalline lamellae; and 4) radial channels and central cavities (Gallant et al., 1997). Therefore, in the amorphous region, amylose may exist individually or mixed together with the branch portions of amylopectin.

A number of studies have indicated that the distribution of amylose is uneven within the granule. Increased values of BV, λmax, IA and the amount of amylose fraction during the granule development of maize (Inouchi et al., 1984), wheat (Morrison and Gadan, 1987), barley (McDonald et al., 1991), rice (Asaoka et al., 1985), and pea (Biliaderis, 1982) starches imply a richer amylose region in the periphery than in the center of granules. However, a number of studies (Schwatz, 1982; Yun and Matheson, 1992; Kuipers et al., 1994; Tatge et al., 1999) reported reverse amylose distribution after examinations of the amylose distribution of potato and maize hybrid *ae/wx* starch granules with reduced amylose contents. The independent localization of amylose and amylopectin in starches with a wide range of amylose content (0-70%) by enzyme-gold labeling (Atkin et al., 1999) revealed that location of amylose within granules differed with different amylose content. In starches with low amylose content (e.g. potato), amylase was mainly localized in amorphous growth rings alternating with semicrystalline growth rings, whereas with high-amylose content (e.g. amylomaize), amylose was encapsulated by an amylopectin surface but separated with an amylopectin center, suggesting that an increase in amylose content causes more separation of amylopectin molecules. Because an increase of amylose content increases the crystalline lamellae size but reduces the electron density of Small-angle X-ray scattering (SAXS), Jenkins and Donald (1995) suggested that amylose acts to disrupt the packing of the amylopectin double helices within the crystalline lamellae through co-crystallizing with the amylopectin and the penetration into the amorphous lamellae (Figure 1-13). However, direct evidence is still lacking to reveal the exact interrelationship between amylose and amylopectin.

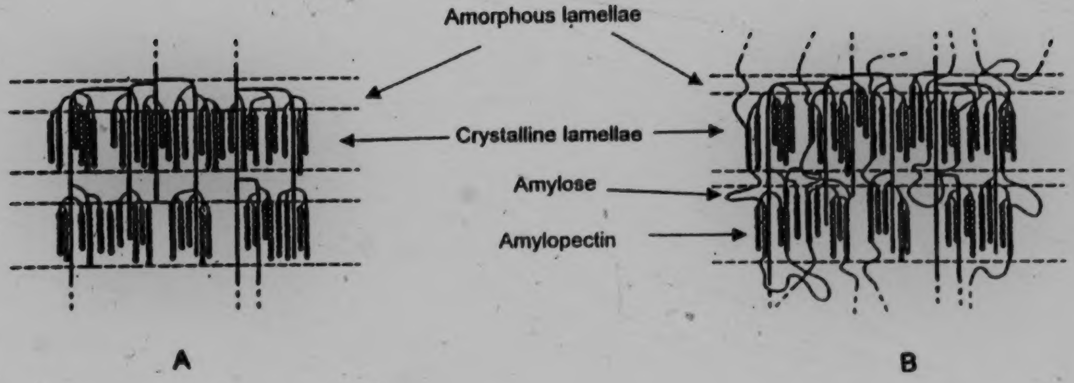
Amorphous lamellae
Crystalline lamellae
Amylose
Amylopectin
A
B

Figure 1-13 A possible mechanism to explain the disruption of amylopectin double helical packing by amylose. (A) Amylopectin structure without amylose presence showing small crystalline lamellar size; (B) Cocrystallinity between amylose and amylopectin pulls a number of the amylopectin chains out of register (adapted from Jenkins and Donald, 1995, with permission from Elsevier Science).

1.2.4.8.2 Lipid-complexed amylose

The relationship between amylose and starch internal lipids has been extensively studied and reviewed by Morrison (1988, 1993, 1995). There are two forms of amylose, lipid-free amylose (FAM) and lipid-complexed amylose (LAM), in cereal starches (Morrison et al., 1993a). Within LAM, the amylose is coiled around monoacyl lipids located within a hydrophobic core surrounded by single polysaccharide helices (V-helix/conformation) (Figure 1-14), where the lipid accounts for about 12.5% of the complex (Morrison et al., 1993a). Lipid-complexed amylose is amorphous in native starches but could be annealed into crystalline form to show strong V-type of X-ray pattern (Biliaderis, 1991; Morrison, 1995). Different levels of V-type X-ray pattern has been found in wrinkled pea, amylomaize, and maize mutant starches (Gérard et al., 2001; Cheetham and Tao, 1998; Gernat et al., 1993; Zobel, 1988a).

1.2.5 Physicochemical properties of starch

The physicochemical properties of starch are closely related to its functional attributes in starch and starch-containing processed products. These properties include aspects of thermal behavior during gelatinization, rheological changes following gelatinization, stability of gelatinized starch to continued heating and shearing action, tendency to retrograde, and susceptibility to acid and enzymatic hydrolysis as well as interaction with other components.

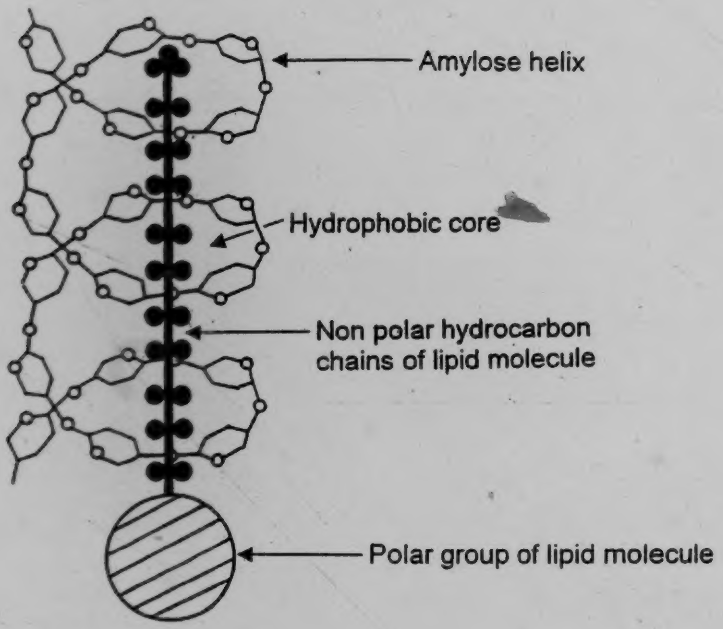
Amylose helix
Hydrophobic core
Non polar hydrocarbon chains of lipid molecule
Polar group of lipid molecule

Figure 1-14 Schematic illustration of amylose-lipid complex (adapted from Carlson et al., 1979, with permission from Wiley-VCH Verlag GmbH & Co. KGaA).

1.2.5.1 Gelatinization

Starch, when heated in the presence of excess water (the volume fraction of water v > 0.7) (Donovan, 1979) to a high enough temperature, undergoes an irreversible order-disorder phase transition termed gelatinization, which involves granule hydration and swelling, uptake of heat, loss of birefringence, crystallite melting, uncoiling/dissociation of double helices (in crystalline regions and those not located with ordered crystallites), and leaching of amylose and amylopectin (French, 1984; Tester, 1997). Of the various methods, which have been used for the characterization of starch gelatinization, such as polarized light microscopy, X-ray diffractionmetry, differential scanning calorimetry (DSC), NMR spectroscopy, enzymatic digestibility, viscoamylography, and small-angle light-scattering, DSC has been more widely used for evaluating gelatinization parameters (onset temperature T_o, peak temperature T_p, and conclusion temperature T_c) as well as energy change (enthalpy ΔH) characteristic for each starch (Appendix A) (Zobel, 1984; Tester and Debon, 2000). The T_c-T_o represents the gelatinization temperature range. According to Jenkins and Donald (1997, 1998) and Donovan (1979), gelatinization in excess water is primarily a swelling driven process. The swelling within the amorphous regions destabilizes the amylopectin crystallites within the crystalline lamellae via ripping apart the edges of crystallites (smaller crystallites are destroyed first), leading to a disruption of the crystallinity of starch granule. This process occurs rapidly for an individual crystallite, but over a limited temperature range for a single granule (1-2°C) and a wide range (10-15°C) for a whole population of granules with endothermic enthalpy values in the range of 10-20 J/g (French, 1984; Liu and Lelievre, 1993; Eliasson and Gudmundsson, 1996). However, at intermediate or lower water content, there is insufficient water present for hydration and gelatinization of all crystallites resulting in simply melting of remaining crystallites at high temperature and consequently increasing the gelatinization temperature range. Gelatinization is primarily a property of amylopectin of starch (Tester and Morrision, 1990a,b), in which gelatinization temperature reflects crystalline perfection (Tester, 1997) and gelatinization enthalpy is a measure of the overall crystallinity of amylopectin (i.e. the quality and quantity of crystallites) mainly reflecting the loss of double helical order (Cooke and Gidley, 1992). Therefore, the enthalpy value has been calculated on amylopectin content basis (Fredriksson et al., 1998). The thermal properties of various starches are illustrated in Table 1-13.

Tester (1997) has suggested that gelatinization and swelling properties are controlled in part by the molecular structure of amylopectin (unit chain length, the degree and pattern of branching, molecular weight, and polydispersity), starch composition (amylose to amylopectin ratio, lipid-complexed amylose chains, and phosphorous content), and granule architecture (crystalline to amorphous ratio). However, other factors also influence starch gelatinization. Increasing the heating rate increases endotherm temperature (Donovan, 1979; Shiotsubo and Takahashi, 1984). The presence of sugars, polyhydric alcohols, and salts may increase gelatinization temperature with invariant ΔH (Evans and Haisman, 1982). Heat-moisture treatment at 95-110°C and moisture level of 18-30% causes an increase in gelatinization temperature, broadening of the gelatinization temperature range, and a decrease in enthalpies with a transformation of B- or C-type polymorphs to more stable A-type polymorph (Jacobs and Delcour, 1998; Biliaderis, 1991). Annealing at water content above 40% and below the gelatinization temperature for a certain period of time

Table 1-13 Thermal properties of starch gelatinization determined by differential scanning calorimetry

Source	Type	T_o (°C)	T_p (°C)	T_c (°C)	T_c-T_o (°C)	ΔH (J/g)	Reference
Maize	Waxy	64.2	69.2	74.6	10.4	15.4	Jane et al., 1999
	Normal	64.1	69.4	74.9	10.8	12.3	Jane et al., 1999
	Amylomaize V	71.0	81.3	112.6	41.6	19.5	Jane et al., 1999
	Amylomaize VII	70.6	-	129.4	58.8	16.2	Jane et al., 1999
Rice	Waxy	56.9	63.2	70.3	13.4	15.4	Jane et al., 1999
	Normal	70.3	76.2	80.2	9.9	13.2	Jane et al., 1999
Wheat	Waxy	55.6	66.0	79.6	24.0	11.8	Abdel-Aal et al., 2002
	Normal	54.6	62.5	73.4	18.8	11.5	Abdel-Aal et al., 2002
Barley	Waxy	55.4	60.3	-	-	13.0	Song and Jane, 2000
	Normal	55.0	59.0	-	-	9.2	Song and Jane, 2000
	High-amylose	55.5	62.8	-	-	7.7	Song and Jane, 2000
Potato	Waxy	62.5	66.6	70.2	3.6	18.2	McPherson and Jane, 1999
	Normal	60.8	65.2	70.6	5.4	17.3	McPherson and Jane, 1999
Sweet potato		57.9	63.1	71.9	8.8	13.5	McPherson and Jane, 1999
Tapioca		64.3	68.3	74.4	10.1	14.7	Jane et al., 1999
Smooth pea		61.1	67.1	75.3	14.7	11.3	Ratnayake et al., 2002

increases gelatinization temperature and enthalpy, narrowing the gelatinization temperature range. Heat-moisture treatment and annealing may be associated with crystallite growth or perfection of already existing crystallites, rearrangement of double helices, partial melting and realignment of polymer chains, formation of crystalline amylose-lipid complexes, interaction between amylose chains or between amylose and amylopectin, and reorientation of the crystallites within the amorphous matrix (Jacobs and Delcour, 1998). Partial acid hydrolysis increases gelatinization temperature and gelatinization temperature range with varied enthalpy depending on starch source and hydrolysis time (Hoover, 2000). Chemical modification methods such as hydroxypropylation and acetylation also decrease gelatinization parameters and enthalpy (Hoover et al., 1988; White et al., 1989; Kim and Eliasson, 1993).

1.2.5.1.1 Gelatinization and loss of granular order

During gelatinization, various forms of order (orientational, lamellar, crystalline, and double helical) are lost over a broadly similar temperature range (Parker and Ring, 2001). Loss of birefringence (measured by polarized light microscopy) occurs in a narrower temperature range while crystalline order (measured by X-ray diffractionmetry) and molecular order (measured by NMR spectroscopy) are lost concurrently with the endotherm change (Liu et al. 1991; Gidley and Cooke, 1991; Cooke and Gidley, 1992; Liu and Lelievre, 1993). The melting disruption of crystallinity starts from the area around the hilum and spreads along the granule, accompanied by swelling of disrupted areas (French, 1984; Garcia et al., 1997; Bogracheva et al., 1998). Jenkins and Donald (1997, 1998) and Donald et al. (1997) have shown by a combination of X-ray and small angle neutron scatting studies, that initial swelling following rapid uptake of water in the amorphous regions imposes a stress upon the double helices within the amylopectin crystallites. Consequently, the amylopectin crystallites are disrupted, but do not completely correspond to the gelatinization endotherm, even at excess water content (most but not all crystallinity loss occurs throughout the gelatinization endotherm). The lamellar order remains unchanged (the crystalline lamellae dos not expand radially) as long as the crystallites can still be identified and rather beyond the end of the endotherm revealed by DSC.

1.2.5.1.2 Gelatinization and amylose/amylopectin ratio

The relationship between thermal properties and the ratio of amylose to amylopectin has been studied extensively (Knutson, 1990; Czuchajowska et al., 1998; Fredriksson et al., 1998; Yuryev et al., 1998; Sasaki et al., 2000; Matveev et al., 2001). Gelatinization temperature (T_p) increases and endotherm enthalpy (ΔH) gradually decreases with increasing amylose content in maize starches with a range of 1-70% amylose (Matveev et al., 2001) and pea starches with a range of 36-86% amylose content (Czuchajowska et al., 1998). High-amylose maize starches (57-90%) have broader gelatinization range (T_c-T_o) up to 58.8°C compared to waxy and normal maize starches (Shi et al., 1998; Jane et al., 1999). Sasaki et al. (2000) found that the conclusion temperature (T_c) and ΔH are negatively correlated with wheat amylose contents (0.8-20.3%). Further investigation (Fujita et al., 1993, 1998) indicated that T_p is strongly correlated with ΔH in various cereal starches with waxy phenotypes (i.e. rice, barley, wheat, and millet). Fredriksson and coworkers (1998) reported that T_o and T_p were negatively correlated to amylose content in a set of starches from different sources (using a principal component statistical method). Generally, waxy starches from wheat (Yasui et al., 1996; Fujita et al., 1998; Abdel-Aal et al., 2002), barley

(Gudmundsson and Eliasson, 1992; Yoshimoto et al., 2002), maize (Yasui et al., 1996; Jane et al., 1999), and potato (McPherson and Jane, 1999) show higher gelatinization temperatures and enthalpy than their normal counterparts. The high gelatinization temperature and enthalpy are closely related with a high degree of crystallinity caused by high amylopectin content (Gernat et al., 1993; Cheetham and Tao, 1998; Fujita et al. 1998; Matveev et al., 2001). Therefore, waxy starches require higher gelatinization temperature and more energy for gelatinization compared to non-waxy starches. No correlation was found between thermal parameters and the amylose to amylopectin ratio in sweet potato (14-24% amylose) and buckwheat (21-27%) starches (Noda et al., 1998) as well as normal wheat starch (29-33%) (Wootton et al., 1998). However, gelatinization temperatures are significantly correlated with the volume proportion of small granules in wheat starches (Wootton et al., 1998). The T_c-T_o range increases and ΔH decreases with increasing granule size in waxy, normal, and high-amylose barley starches (Vasanthan and Bhatty, 1996; Tang et al., 2000, 2001a, b). Thermal properties of starches are also influenced by amylose molecular size, amylopectin chain length (Cheetham and Tao, 1997), crystalline (polymorph) type and the ratio of A- and B-types and distribution within C-type starch granules (Cheetham and Tao, 1998; Gérard et al., 2001; Matveev et al., 2001), co-crystallinity of a part of amylose with the short amylopectin chains (forming double helices and crystalline lamellae) (Jenkins and Donald, 1995), and arrangement of part of amylose chains between the crystalline lamellae (acting as defects and does not contribute to the melting enthalpy of starches) (Matveev et al., 1998, 2001).

1.2.5.1.3 Gelatinization, branch chain length and distribution of amylopectin

A larger proportion of long branch chains of amylopectin in starches (e.g. amylomaize and *ae* waxy maize) has been shown to display a higher gelatinization temperature and enthalpy (due to large and more ordered double-helical crystallites, which require higher temperature and energy to uncoil and dissociate) (Sanders et al., 1990; Yuan et al, 1993; Shi et al., 1998; Sasaki and Matsuki, 1998; Jane et al., 1999; McPherson and Jane, 1999; Franco et al., 2002). Potato starch has higher proportion of long branch chains than cereal starches but contains high phosphate monoester derivatives, which contribute to low gelatinization temperature (Jane et al., 1999; McPherson and Jane, 1999). Starches with short average branch chain length (e.g. waxy rice) and a large proportion of short branch chain length (DP6-12) as well as those with relatively short second peak chain length (DP41-43) (e.g. wheat and barley) contribute to low gelatinization temperature and enthalpy (Jane et al., 1999). In sweet potato and buckwheat starches, the amount of shorter branch chains (DP6-11) is negatively correlated with all gelatinization parameters while that of longer branch chains with DP12-17 is positively correlated (Noda et al., 1998). High-amylose barley starch does not show significantly higher gelatinization temperature and enthalpy than waxy and normal barley starches, corresponding to their similar amylopectin branch chain distribution and small amount of long branch chains (Song and Jane, 2000; Yashimoto et al., 2000, 2002).

1.2.5.1.4 Gelatinization and crystalline type

Amylopectin branch chain length is highly correlated to the crystalline polymorphs of starch (Hizukuri, 1985; Hanashiro et al., 1996; Gérard et al., 2000). Generally, A-polymorph starches (most cereals), which contain shorter average branch chain length and large portion of short chains with densely packed cluster structure, show lower transition temperatures and enthalpy change than B-polymorph starches (amylomaize and most tubers and roots), which contain longer average branch chain length and high proportion of long chains with loosely packed clusters (Fredriksson et al., 1998; Jane et al., 1999; McPherson and Jane, 1999). In a study of C-polymorph pea starch, Bogracheva et al. (1998) found that the B-polymorph is present in the granule interior while the A-polymorph is located at the periphery. During gelatinization of starches in excess KCl solution, B-polymorph in the interior of the granule loses crystallinity first accompanied by loss of birefringence compared to A-polymorph in the periphery region. DSC showed a wider gelatinization temperature with two endothermic peaks in C-polymorph starch corresponding to the disruption of B-polymorph and A-polymorph.

1.2.5.1.5 Swelling and solubilization

Swelling and subsequent solubilization of amylose and amylopectin are the most important structural changes during and after gelatinization of starch granules. The irreversible swelling starts at a temperature corresponding to onset temperature (T_o) in DSC measurements and continues to a much higher temperature than conclusion temperature (T_c) (Tester and Morrison, 1990a,b). During granule swelling, macromolecules leach out of granules resulting in a parallel increase in starch solubility. In general, starches from tubers and roots show a rapid single-stage swelling and solubilization pattern (Kawabata et al., 1984; Rickard et al., 1991; Hoover, 2001). Of these, potato starch has the highest swelling power due to a high phosphate ester content of amylopectin (repulsion between phosphate groups on adjacent chains will increase hydration by weakening the extent of bonding with the crystalline domain)

(Swinkels, 1985b; Galliard and Bowler, 1987). Most legume starches also exhibit a restricted single-stage swelling and low solubility pattern (Hoover and Sosulski, 1991). In contrast to tuber, root, and legume starches, normal cereal starches show a two-stage swelling and solubilization pattern (Leach et al., 1959; Doublier et al., 1987; Langton and Hermansson, 1989). Amylose-free waxy starches swell much faster without the formation of typical swollen granules (Hermansson and Svegmark, 1996) and show unrestricted swelling and great solubility (Wang et al., 1993b). But amylose-containing waxy starches have lower solubility than normal and high-amylose starches (Lorenz and Collins, 1995). A starch granule could swell 100-fold its original volume in potato and up to 30-fold in cereal starches (Hermansson and Svegmark, 1996) but cooking at high temperatures (above 95°C) or the influence of shear forces breaks down the swollen granules. Swelling is a property of amylopectin, which is regulated by the crystallinity of the starch before full gelatinization, and amylose is believed to act as a diluent of amylopectin (Tester and Morrison, 1990a,b; Tester and Karkalas, 1996). Lipid-free amylose contributes to swelling and lipid-complexed amylose restrains swelling (Morrison et al., 1993). In addition to amylose-amylopectin ratio, molecular weight, branch chain length and distribution of amylopectin, and degree of crystallinity (Wang et al., 1993; Sasaki and Matsuki, 1998), physical (heat-moisture treatment and annealing) and chemical modification also influence swelling and solubilization properties (Deshpande et al., 1982). Also, physical granule damage (i.e. milling) causes amylopectin to fragment and become soluble resulting in an increase in granule swelling and a decrease in gelatinization parameters (Craig and Stark, 1984; Karkalas et al., 1992; Morrison and Tester, 1994a,b; Tester and Morrison, 1994)

During heating (50-70°C), amylose is mainly leached out of granules in potato and most cereal starches (Doublier, 1981; Tester and Morrison, 1990a,b; Svegmark and Hermansson, 1991). In the first stage of swelling, the amount of amylose leached from granules is limited and an amylose-rich phase is formed in the center of the granule (Langton and Hermansson, 1989). Once amylose-lipid complexes dissolve at the second stage, amylose leaching is enhanced and amylopectin-rich granules start to deform and lose their original shape (Doublier, 1981; Ghiasi et al., 1982; Eliasson, 1986; Zeleznak and Hoseney, 1987). For most cereal starches, amylose leaches before amylopectin solubilizes (Doublier, 1981); however, in oat starch, both amylose and amylopectin co-leach from granules (Doublier, 1987). The solubilized molecules increase in molecular weight and become more branched with increasing temperature (Ellis and Ring, 1985; Doublier, 1987; Prentice and Stark, 1992). Further heating (above 95°C) increases solubility substantially, enhances degradation of the granules and separation into amylose phase continues where amylopectin fragments are dispersed (Langton and Hermansson, 1989; Virtanen et al, 1993). The residue of swollen granules (ghosts) contain mainly amylopectin without any crystalline order and amylose content decrease to 16% in pea starch, 8.3% in wheat, and 8.0% in maize starches (Ellis et al., 1988). Amylose-lipid complexes dissociate into lipid-free amylose and dispersed lipids (Morrison et al., 1993a,b; Shamekh et al., 1999). True solubilization of all the starch substance does not occur unless the paste is cooked at 100-160°C (in an autoclave or in a commercial steam-jet cooker) to give a low-viscosity starch macromolecular solution (Swinkels, 1985b) or by dissolution of starch in dimethyl sulfoxide (DMSO) (French, 1984).

1.2.5.2 Pasting

The term pasting is used to describe the phenomenon following gelatinization in the dissolution of starch (Atwell et al., 1988). Gelatinization induces substantial rheological behavior of starch suspension as a result of structural changes at both molecular and granular levels. During gelatinization, starch granules swell with progressive hydration, but the more tightly bound crystalline lamellae of amylopectin remain intact, holding the granules together. As the granules continue to expand, more water is imbibed and swollen granules occupy the most space. The movement of swollen granules is restricted and viscosity increases rapidly. When maximum swelling is reached, granules start to rupture with further heating and shearing, which induces a viscosity reduction. Upon cooling and storage, the solubilized macromolecules will then reassociate into an ordered structure, a phenomenon known as retrogradation, and the viscosity rebuilds. Depending on the starch source, type and concentration, heating and shearing result in a dispersed phase (swollen granules or granule remnants) embedded in a continuous solution (rich in amylose) phase, whilst cooling causes the gelatinized starch suspension to turn into a turbid viscoelastic paste or an opaque elastic gel (Ring, 1985; Morris, 1990; Eliasson and Gudmundsson, 1996). In such a paste or gel matrix, the structure of swollen starch granule and granule remnants (rich in amylopectin) predominantly affect the rheological behavior of starch during heating, whereas leached amylose reinforces the gel structure during cooling (Lii et al., 1996; Tsai, et al., 1997). The formation of starch paste or gel is very important for the texture, acceptability, and digestibility of starch-containing foods (Biliaderis, 1991).

The Brabender Visco-Amylography has been the most common method for evaluation of starch pasting properties (Appendix B). The viscosity measured in Brabender Units

(BU) or torque (g.cm) is recorded as a function of temperature and time during a programmed heating-holding-cooling cycle at a specified rotational speed (rpm/min). The starch paste is subjected to both thermal and mechanical treatment to reveal the paste stability during heating (Breakdown) and the consistency (retrogradation tendency) during cooling (Setback) (Shuey and Tipples, 1980; Dengate, 1984). Pasting temperature (where a perceptible increase in viscosity occurs and thus is always higher than gelatinization temperature) and peak viscosity (reflects the ability of starch granules to swell freely before their physical breakdown at a given concentration) are also recorded. Most recently, the Rapid Visco-Analyzer (RVA), which has a high viscosity correlation with Brabender Visco-Amylograph, is used to rapidly characterize starch pasting with a small sample requirement (Deffenbaugh and Walker, 1989; Thiewes and Steeneken, 1997).

Starches with higher amylose and lipid/phospholipid contents have higher pasting temperature, lower peak viscosity and breakdown viscosity (shear thinning), and higher setback viscosity, whereas starches with more amylopectin long branch chains (DP ≥ 37) display lower pasting temperature, higher peak and breakdown viscosities (Zeng et al, 1997; Jane et al, 1999; Franco, 2002). Also, the long chain length amylopectin and intermediate molecular size amylose produce the synergistic effect on the viscosity of starch pastes (Jane and Chen, 1992). Both significant negative correlations between amylose content and pasting parameters (Zeng et al., 1997; Wootton et al., 1998) and significant positive correlations between long branch chain length and pasting temperature as well as peak viscosity (Franco et al., 2002) are found in wheat starches. In general, waxy cereal starches have lower pasting temperatures, higher peak viscosity, and lower setback viscosity than normal cereal starches (Vasanthan and Bhatty, 1996; Zheng et al., 1998; Jane et al., 1999; Abdel-Aal et al., 2002). Increase in pasting temperature, reduction of peak viscosity, and high resistance to shear thinning are more pronounced in normal wheat and barley starches than in normal maize and rice starches resulted from a larger amount of lipid-complexed amylose (Jane et al., 1999). Oat starches with high lipid contents have lower lipid-complexed amylose than wheat and maize starches, which show higher pasting temperature, lower peak viscosity, and higher setback viscosity (Jane et al., 2002; Hoover et al., 2003). Among tuber starches, potato starch has a very high peak viscosity as a result of the high phosphate monoester content and long branch chains (McPherson and Jane, 1999; Jane et al., 1999, 2002). Tuber and root starches have lower pasting value than normal cereal starches due to absence of lipids and phospholipids (Lim et al, 1994; Kasemsuwan and Jane, 1996; Jane et al., 1999; Hoover, 2001; Jane et al., 2002). In contrast to most waxy and normal cereal starches, waxy potato starch displays a lower peak viscosity than normal potato starch due to free swelling and rapid dispersion under shearing as well as a lower proportion of long branch chains and high phosphate monoester (McPherson and Jane, 1999; Jane et al., 2002). Legume starches show restricted swelling, the absence of peak viscosity, constant or increasing hot paste viscosity, a high setback, and a constant cold paste viscosity during cold holding (Hoover and Sosulski, 1991; Ratnayake et al., 2002).

1.2.5.3 Acid hydrolysis

Acids cause scission of the glucosidic linkages, thereby altering the structure and properties of the native starch. Starch treated with sulphuric acid (15% v/v) is referred to as *Nägeli* amylodextrins, whilst starch treated with hydrochloric acid (7.5% v/v) is referred to as lintnerized starch (Rohwer and Klem, 1984). Other acids such as HNO_3

and H_3PO_4 have also been used for starch degradation (Singh and Ali, 2000). Acid-modified starch, without substantially changing the granular form, is used commercially for the production of cationic and substituted starches (as a premodification step to improve fluidities) and for the manufacture of textile, building products, gum candy, paper and paperboard (Rohwer and Klem, 1984).

In acid hydrolysis, the hydronium ion (H_3O^+) carries out an electrophilic attack on the oxygen atom of the α $(1\rightarrow4)$ glycosidic bond. Then the electrons in one of the carbon-oxygen bonds move onto the oxygen atom to generate an unstable, high-energy carbocation intermediate. The carbocation intermediate is a Lewis acid, so it subsequently reacts with water, a Lewis base, leading to regeneration of a hydroxyl group (Hoover, 2000).

1.2.5.3.1 Acid hydrolysis kinetics

Studies have already shown a two-stage acid hydrolysis pattern (the extent of hydrolysis as a function of time) in various cereal, tuber and root, and legume starches (Biliaderis et al., 1981; Shi and Seib, 1992; Hoover and Vasanthan, 1994; Vasanthan and Bhatty, 1996; Jane et al., 1997; Jacobs et al., 1998; McPherson and Jane, 1999; Gérard et al., 2002;). The extent and rate of hydrolysis depend on starch source, acid type and concentration, and hydrolysis duration. Generally, a relatively fast hydrolysis stage is followed by a slow hydrolysis stage. The fast stage mainly corresponds to the hydrolysis of the amorphous region of the starch granule, whereas, the second stage corresponds to the hydrolysis of crystalline region within the granule (Kainuma and French, 1971; Robin et al., 1974; Biliaderis et al., 1981). Differences in the extent and rate of hydrolysis among the starches during the first stage of hydrolysis have been mainly attributed to: (1) the amount of lipid complexed amylose in lipid-containing starches (which is hardly observed after extensive hydrolysis in DSC endotherm at near 100°C) (Jacobs et al., 1998; Hoover et al., 2003); (2) the extent of interaction between starch chains (retrograded amylose) within the amorphous regions of the granule (Morrison et al., 1993c; Hoover and Manuel, 1996; Perera et al., 2001; Hoover et al., 2003); and (3) the amount of very short amylopectin branch chains (DP2-8, which exist as dangling chains on the surface of crystallites or at weak point of the crystallites) (Biliaderis et al., 1981; Jane et al., 1997; Gérard et al., 2002), Lipids within the amylose helix may decrease the extent and rate of hydrolysis by hindering the conformational transformation (chair → half chair) required for protonation of the glycosidic oxygens (Hoover, 2000). However, Gérard et al. (2002) have shown that V-type amylose-lipid complex was preferentially degraded by acid in mutant maize starches (revealed by the disappearance of the 19.9° reflection, specific for V-type in X-ray diffractogram) and related to the initial high hydrolysis rate in *dusu*, *su*, and *aedu* mutant maize starches. Differences in hydrolysis at the second stage have been attributed to the degree of packing of the double helices that form the crystalline lamellae. Closely packed double helices within the crystallites could slow the rate of hydrolysis by (1) decreasing the extent of penetration of hydronium ions (H_3O^+) into the crystalline lamellae; (2) slow down the reaching of hydrogen ions to the glycosidic oxygens, which are buried in the interior of the double helix; (3) sterically hindering the change in conformation (chair → half chair) of the D-glucopyranosyl unit (French, 1972; Biliaderis et al., 1981; Hoover et al., 2003). B-polymorph starches are usually less susceptible to acid hydrolysis than A-polymorph starches (Kainuma and French, 1971; Robin et al., 1974; Jane et al., 1997; Gérard et al., 2002). Increasing amylose content also decreases the extent and rate of hydrolysis in barley (Vasanthan and Bhatty, 1996; Song et al., 2000), maize (Hoover and Manuel, 1996; Shi et al., 1998), and oat (Hoover et al., 2003) starches.

1.2.5.3.2 Effect on the degree of crystallinity and X-ray diffraction pattern

The degree of crystallinity of acid hydrolyzed starches increases with increasing hydrolysis time in wheat (Muhr et al., 1984), maize (Komiya et al., 1987; Raja, 1994), mutant maize (Gérard et al., 2002), potato (Muhr et al., 1984), and Cassava (Raja, 1994; Atichokudomchai et al., 2002) starches. Morrison et al. (1993c) reported that the hydrolyzed starches from non-waxy barley have higher double helix content and degree of crystallinity compared to non-waxy native barley starches, whereas, not much change in double helix content and degree of crystallinity was found from waxy barley starches after hydrolysis, reflecting the overall transformation from a double-helix/non-ordered composite to a predominantly double-helix/V-type-conformation composite following lintnerization. Therefore, the increase in the degree of crystallinity during hydrolysis is attributed to the removal of amorphous parts (mainly amylose at the first hydrolysis stage) within the granule and retrograded lipid-free amylose (Morrison et al., 1993c; Atichokudomchai et al., 2002). Recently, Gérard et al. (2002) found that the B-polymorphic crystallites within the starch granule constitute an intrinsic limitation to acid hydrolysis in mutant maize starches with various proportions of A-, B-, and V-polymorphs and a wide range of amylose content (1-63%). No correlation was found between hydrolysis and amylose content or the crystallinity level of the native starches.

For most starches, X-ray pattern does not change after acid hydrolysis. However, the changes from A-polymorph in some barley cultivars such as Midas and Hector

(Morrison et al., 1993c) and B-polymorph in cassava starch (Garcia et al., 1996) to C-polymorph have been reported. The C-polymorph in barley starches is consistent with an A-polymorph from amylopectin residue and a B-polymorph from the retrograded amylose residue (Morrison et al., 1993). C-polymorph in cassava starch was postulated to be due to a crystalline transformation resulting from removal of the constraints exerted by the amorphous region on starch crystallites and/or the existence of B-polymorph crystallites in native starch granules that are present in small amounts and hence undetectable by X-ray diffraction.

1.2.5.3.3 Effect on amylopectin molecular structure

It has been shown that the insoluble acid-resistant starch residue after extensive acid hydrolysis is mainly the acid-resistant crystalline parts of amylopectin, which consist of two major populations of amylopectin molecules (a linear fraction at peak DP14 and a singly branched fraction at peak DP28) in waxy barley starch (Lauro et al., 1997). Similar distributions have been reported for waxy maize (Watanabe and French, 1980; Jane et al., 1997), waxy, normal maize, amylomaize (Jane et al., 1997; Perera et al. 2001), rice (Maningat and Juliano, 1979), wheat (Jacobs et al., 1998), potato (Robin et al., 1974; Jane et al., 1997; Jacobs et al., 1998), cassava (Jane et al., 1997), and pea (Jacobs et al., 1998) starches. Morrison et al. (1993c) found that, in addition to short amylopectin chains (DP16), two higher molecular weight fractions of amylopectin (DP46 and DP77-130) were present in lintnerized waxy and non-waxy barley starches. These two fractions were attributed to the formation of double helices (with B-type polymorph) from retrograded amylose after partial hydrolysis of lipid-free amylose during the early stage of hydrolysis and the acid-resistant amylose-lipid complex segments, respectively. Perera et al. (2001) also reported a higher molecular weight fraction (peak DP up to 38) in *su2* maize Nägeli dextrins, which could not be debranched and are attributed to retrograded amylose. A multiple branched fraction was also identified in maize starches but was gradually reduced by extensive hydrolysis (Watanabe and French, 1980; Umeki and Kainuma, 1981; Perera et al., 2001). Jane et al. (1997) found that, at a comparable degree of hydrolysis, Naegeli dextrins from A-polymorph starches (waxy and normal maize) contained higher proportion of the single branched amylopectin chains than those from B-polymorph starches (*ae* waxy maize and potato) and the proportion of single branched amylopectin chains in A-polymorph starches increase greatly with hydrolysis time, suggesting a structural difference (branching pattern) between A- and B-type starches. Substantial branching points with a higher proportion of short A- and B1-chains in A-polymorph starches are scattered within the crystalline region, which form an inferior crystalline structure but are not available for acid hydrolysis (at the vicinity of α-(1→6) linkages) at the first hydrolysis stage. However, most branching points in B-polymorph starches are clustered in the amorphous region, which are more susceptible to acid hydrolysis. But B-polymorph starches have long A and B1 branch chains, which are resistant to acid hydrolysis (Hanashiro and Hizukuri, 1996; Jane, 1997).

1.2.5.3.4 Effect on gelatinization parameters

Compared to native starches, the gelatinization temperatures (T_o, T_p, and T_c) and the temperature range (T_c-T_o) increase and the endotherm shift to higher temperatures in acid hydrolyzed starches from cassava (Garcia et al., 1996; Atichokudomchai et al., 2002), potato (Donovan and Mapes, 1980; Komiya and Nara, 1986; Jenkins and Donald, 1997; Jacobs et al., 1998), barley (Shi and Seib, 1992; Morrison et al., 1993c), rice (Chun et al., 1997), maize (Shi and Seib et al., 1998), wheat (Jacobs et al., 1998), pea (Jacobs et al., 1998) starches, which are attributed to the loss of cooperative melting between amorphous and crystalline regions by removal of the amorphous region of the granule (swelling of amorphous region destabilize crystallites), consequently, the starch residue melts at higher temperature (Donovan and Mapes, 1980; Jacobs et al., 1998; Hoover, 2000). It was suggested that the broadening of gelatinization temperature in hydrolyzed starches was related to disordering of different fractions (short amylopectin chains, retrogradation of partly hydrolyzed amylose, and amylose-lipid complex) at different temperatures (Morrison et al., 1993; Shi and Seib, 1998; Perera et al., 2001). However, extensive hydrolysis reduces the gelatinization temperatures (T_o and T_p) of hydrolyzed starches (Komiya and Nara, 1986; Shi and Seib, 1992; Chun et al., 1997; Jenkins and Donald, 1997; Atichokudomchai et al., 2002). Broadening the endotherms could be due to the increase in the short chain length of amylopectin by extensive hydrolysis, the difference in melting point of different amylopectin chain length, and the variation in the thermal stability of crystallites (Atichokudomchai et al., 2002) The gelatinization enthalpy has been reported to vary with starch source, acid concentration, and hydrolysis temperature and time (Biliaderis et al., 1981; Muhr et al., 1984; Komiya and Nara, 1986; Hoover and Vasanthan, 1994; Garcia et al., 1996; Jenkins and Donald, 1997; Jacobs et al., 1998; Atichokudomchai et al., 2002). Atichokudomchai et al. (2002) and Jenkins and Donald (1997) have shown that the enthalpy increases at fist hydrolysis stage and was not significantly decreased at the second stage in hydrolyzed cassava and potato starches when compared with that of native starch, implying that the increasing amylose retrogradation assisted in leveling the double helix content.

1.2.5.4 In vitro enzyme amylolysis

In vitro enzyme hydrolysis of starches is not only an important industrial process for production of sweeteners, syrups, ethanol, and other chemicals, but also a probe for understanding starch granule structure and better control of enzymatic susceptibility. α-Amylases and amyloglucosidases from various sources (i.e. malt, bacterial, fungal, and pancreas) are the most common enzymes used in hydrolysis. The differences in susceptibility of starches mainly depend on the nature of the starch with its inherent composition and structure, enzyme source, and hydrolysis conditions.

α-Amylase (α-1,4-D-glucan glucanohydrolase, EC 3.2.1.1) is an endohydrolase, which catalyzes the hydrolysis of the α-1,4-glycosidic bond in the interior of amylose and amylopectin molecules and can bypass but cannot hydrolyze the α-1,6-glucosidic branch points. α-Amylase hydrolyzes starch by a multiple attack mechanism (Robyt, 1984). The direction of multiple attack is from the reducing end towards the nonreducing end, that is, once the enzyme forms a complex with the substrate and produces the first cleavage, the fragment with the nonreducing end dissociates from the active site while the fragment with the newly formed hemiacetal reducing end remains associated with the active site end repositions itself to give another cleavage and the formation of maltose and maltotriose (Robyt, 1984). The active site of porcine pancreatic α-amylase has been shown to contain five subsites with catalytic groups (glutamine acid as acid/base catalyst and an aspartate as the nucleophile) between the second and third subsite from the reducing end subsite, whereas, *Bacillus amyloliquefaciens* α-amylase contains nine subsites in which the catalytic groups are positioned between the third and fourth subsites from the reducing end subsites (Robyt and French, 1970; Robyt, 1984). Due to the structural barrier of amylase at the active site preventing an attack on α-1,4-bonds next to the branch point, the major end products from the hydrolysis of starch by α-amylases are glucose, maltose, maltotriose, maltotetraose, maltopentaose, and maltohexaose (Reilly, 1985; Nigam and Singh, 1995). Amyloglucosidase (α-1,4-D-glucan glucoamylase, EC 3.2.1.3) is an exo-acting amylase, which catalyzes the hydrolysis of both α-1,4-D- and α-1,6-D-linkages from the nonreducing end of starch chain and produces β-D-glucose (the cleavage point is located between the first and second subsites).

1.2.5.4.1 Hydrolysis kinetics

The hydrolysis of various starches by amylases normally proceeds in an initially rapid hydrolysis stage followed by a progressively decreased or more constant hydrolysis stage. The two-stage hydrolysis is more pronounced at higher enzyme concentrations (Bertoft and Manelius, 1992; Planchot et al., 1995; Kimura and Robyt, 1995). Generally, A-polymorph (most cereals and cassava) starches are more readily hydrolyzed than B-polymorph (amylomaize and potato) starches (Gallont et al., 1992; Planchot et al., 1995; Oates, 1997). Waxy starches are hydrolyzed faster than normal starches (Leach and Schoch, 1961; MacGregor and Ballance, 1980; Bertoft and Manelius, 1992). The hydrolysis rates at the initial stage are similar in waxy and normal maize, barley (large granules), and wheat (large granules) but initial hydrolysis products differ (Bertoft et al., 2000). Among tuber and root starches, potato, yam, and taro starches are more resistant to amylases (Valetudie et al., 1993; Hoover, 2001). Legume starches are more susceptible than potato or high-amylose maize, but less digestible than cereal and cassava starches (Hoover and Sosulski, 1991; Ratnayake et al., 2002). Wrinkled pea starch is more susceptible to amylases than smooth pea starch (Bertoft et al., 1993a,b).

For hydrolysis by a certain enzyme, the diversities in composition and structural features of starches among and within species, such as inter-chain association (e.g. amylose-amylose and/or amylose-amylopectin) (Leach and Schoch, 1961; Vasanthan and Bhatty, 1996), type and degree of crystallinity (double helical packing) (Gérard et al., 2001), the number of the crystalline and amorphous lamellae in each growth ring (Gallant et al., 1997; Li et al., 2003), and amylose-lipid interaction (Anger et al., 1994; Appelqvist and Debet, 1997; Lauro et al., 1999; Morrison, 1995) determine the rate and extent of hydrolysis. Pre-treatment of starches, such as physical (Lauro et al., 1993; Kurakake et al., 1996) and chemical (Tharanathan and Ramadas Bhat, 1988; Wolf et al., 1999; Manelius et al., 2000) modification of starch prior to hydrolysis also influence amylolysis. For a given starch, the rate and extent of hydrolysis depend on enzyme source and hydrolysis conditions, including enzyme concentration, pH, temperature, ion/salt concentration, and media system (Blakeney and Stone, 1985; Franco and Ciacco, 1987; Manelius and Bertoft, 1996; Textor et al., 1998; Liakopoulou-Kyriakides et al., 2001). An early study indicates that pancreatic alpha-amylase is most effective towards native starches followed in order by malt, bacterial, and fungal alpha-amylases (Kimura and Robyt, 1995). Compared with alpha-amylase from *Bacillus subtilis* or from porcine pancreas, the alpha-amylase from A. *fumigatus*, which only produces glucose as an end hydrolysis product, displays a very high hydrolytic efficiency on starches at the same enzyme conditions (Planchot et al., 1995). *Bacillus licheniformis* alpha-amylase is one of the most efficient enzymes among alpha-amylases (Liakopoulou-Kyriakides et al., 2001).

Enzyme hydrolysis involves an enzyme in solution acting on a solid starch substrate with several steps, such as diffusion of enzyme to the solid surface, adsorption on the susceptible sites of the accessible starch surface, and finally catalysis, thus, the porosity and accessibility of the granule surface to enzyme and the efficiency of adsorption of enzyme onto this surface are critical kinetic parameters (Bertoft and Manelius, 1992; Leloup et al., 1991). However, the hydrolysis rate is not correlated to enzyme concentration or adsorption (Bertoft and Manelius, 1992; Chatterjee et al., 1992; Manelius and Bertoft, 1996). Also, a wide variation is present between susceptibility of starch to enzymes and starch granule morphology (Kimura and Robyt, 1995). The hydrolysis rate is positively correlated with the granule surface area in waxy, normal, and high-amylose maize starches (Knutson et al, 1982b). The granule surface area, which is closely related to the adsorption of enzyme, is inversely related to granule size to volume ratio (MacGregor, 1979). Thus, the initial hydrolysis rate is faster in small granules than in large granules in barley (MacGregor and Ballance, 1980; MacGregor and Morgan, 1986), wheat (Manelius et al., 1997), and pea (Bertoft et al., 1993a) starches. However, oat starch, which has a comparable granule size but different granule shape (polyhedral compound granules) with the small granules of wheat and barley starches, is hydrolyzed even faster by alpha-amylase (Bertoft et al, 2000). Also, waxy maize starch possesses similar size and shaped granules but a large number of pinholes with a higher hydrolysis rate compared to normal maize starch (Bertoft et al., 1992). These morphological features of starch granules seem to contribute to the hydrolysis rate, resulting from the high efficiency of adsorption of enzymes onto the already existing surface areas and substantially increased areas on the granule surface and within granules after initial hydrolysis.

1.2.5.4.2 Hydrolysis products and their effects on hydrolysis

By pumping *Bacillus subtilis* alpha-amylase solution through a thin layer of starch packed column and an ion-exchanger and charactering solubilized dextrins in the enzyme-removed solution, Bertoft and co-workers have studied the molecular weight distribution of the initial hydrolysis products and molecular changes of the partly hydrolyzed granule residue in normal and waxy maize (Bertoft and Manelius, 1992), barley (Bertoft et al., 2000), wheat (Manelius et al., 1997), oat (Manelius and Bertoft, 1996), and pea (Bertoft et al., 1993a, b) starches. The initial solubilized dextrins have a boarder molecular weight distribution in maize and oat starches (DP2-6000) followed by wheat and barley starches (DP2-500), and pea starches (DP2-100), whereas, a large number of high molecular weight dextrins (DP>3000) are found in solubilized waxy maize starch. The molecular size of solubilized dextrins varies with the enzyme concentration and flow rate and reduces rapidly with successive hydrolysis stages. The initial solubilized dextrins are from both amylose and amylopectin in all starches.

The composition and concentration of hydrolysis products may have an inhibitory effect on alpha-amylolysis. Franco and Ciacco (1987) reported that the elimination of soluble hydrolysis products by dialysis increased the degree of hydrolysis by 10% for cassava starch and 5% for maize starch. A gradual reduction of the rate of hydrolysis may be partly caused by the inhibition of oligosaccharides on alpha-amylase activities (Leloup et al., 1991; Colonna et al., 1992). During hydrolysis, the concentration increase in maltose and maltotriose, rather than in glucose or maltotetraose, may change the molar ratio of oligosaccharide to enzyme and thus influence the adsorption equilibrium by the formation of oligosaccharide-enzyme complex (Leloup et al., 1991; Colonna et al., 1992). However, if amyloglucosidase is used in combination with alpha-amylase, amyloglucosidase could hydrolyze maltose and maltotriose into glucose and thereby continuously transform the reaction products of alpha-amylolysis (Colonna et al., 1992; Liakopoulou-Kyriakides et al., 2001).

The molecular weight distribution of granule residue after amylolysis in cereal starches remains unchanged or changed slightly with an increase of a small amount of low molecular weight molecules (DP<200) at low extent of hydrolysis (<20%). The amylose chain length decreases while amylopectin chain length remains unchanged. However, the small molecules with DP<200 increase and the chain length decreases significantly in pea starches at this stage. The amylose to amylopectin ratio of maize, wheat, oat, and barley starches were not clearly changed or slightly decreased in the granule residue, which is consistent with other results (Leach and Schoch, 1961; Sargeant, 1980; Lauro et al., 1993, 1999). No changes in the crystalinity (Lauro et al., 1999) and in gelatinization behavior (Sargeant, 1980) are observed when up to 50% solubilization occurs in barley and wheat starches. However, lipid-complexed amylose is less susceptible to alpha-amylase than free amylose and amylopectin and remains in the granule residue until 40-50% of the barley starch is solubilized (Lauro et al, 1999). Subsequent hydrolysis produces much smaller dextrins with a narrow molecular weight distribution indicating that enzyme attack on starch is more random on large molecules and less random as the molecules become smaller. Gérard et al. (2001) have shown that amorphous material co-exists with B-polymorph of crystallites in the residues of maize mutant starches (with a wide range of crystallinity levels and various ratios of A-, B-, and V-polymorph types) although the ultimate extent of hydrolysis was highly correlated with the amount of B-polymorph crystallites. These studies suggest that there is a strong molecular association between amylopectin and/or amylose chains in the residue (mainly in the semi-crystalline regions) of the starch granule. In batch-wise hydrolysis, the originally produced dextrins are substantially hydrolyzed into smaller molecules in enzyme solutions, which are predominantly glucose, maltose, maltotriose with minor other low molecular weight oligosaccharides depending on enzyme types.

1.2.5.4.3 Action pattern revealed by EM

Kinetic analysis only gives a mean hydrolysis value for the whole population of starch granules. However, action patterns differ not only between starch types and enzyme sources, but also within the same population of granules. Scanning and transmission electron microscopy are useful means to approach individual starch granules on the surface and from the granule internal in more detail.

For most starches, electron microscopy has revealed that enzyme pits the starch granule surface first and then penetrates through pinholes/internal channels and subsequently hydrolyzes the granule from inside-out. However, the rapid corrosion of the peripheral region and then endocorrosion in *aedu* mutant maize starch by alpha-amylase (Gérard et al., 2001) showed a completely different enzyme action pattern. Wheat, barley, and rye starches, as well as cassava starch granules have specific zones that rapidly become pitted and then pores are randomly formed all over the granule surface, which deepen into the granule interior (Gallant et al., 1992). Maize and rice starches show random pitting with the pits enlarging through the granules at each subsequent layer while in waxy maize starch, deep pitting is present with more tangential corrosion in the semi-crystalline region. Amylomaize starch is undigested externally except for the formation of small protuberances with a pore of each on the top and a cavity in the granule center. However, potato starch is slowly but progressively eroded by exo-corrosion, without the apparent formation of surface pores (Gallant et al., 1992, 1997). Random erosion and enlargement of pores, elongation of channels, and appearance of internal layered structure are more pronounced in waxy and normal maize starches than in high-amylose maize starch (Planchot et al., 1995; Helbert et al., 1996). Channels in the granule periphery provide a pathway for the entry of enzymes into the granule interior (Leach and Schoch, 1961; Valetudie et al., 1993; Herbert et al., 1996). These channels may be derived from inherent surface pores/internal channels in starch granules and enlarged by enzyme hydrolysis (Kimura and Robyt, 1995). The action patterns of alpha-amylase are similar between cereal starches (Gallant et al., 1972; Gallant et al., 1992; Planchot et al., 1995), but differed with respect to some tuber starches (Gallant et al., 1992; Valetudie et al., 1993; Planchot et al., 1995). The differences in enzymatic action between bacterial and pancreatic α-amylases are found in yam starch (Valetudie et al., 1993). A sponge-like structure (numerous radial pores/canals) with bacterial α-amylase was formed in yam starch granules at the initial stage of hydrolysis, and fragmentation occurred at the final stage, whereas, a filamentous structure was retained with the resistant outer layer of the granule in the residue of starch hydrolyzed by pancreatic α-amylase. Under SEM at high magnification and high image resolution, spherical blocklets with up to 100 nm in diameter in crystalline regions are present in wheat, maize, and potato starches (Gallant et al., 1992).

1.2.5.5 Retrogradation

The behavior of gelatinized starches on cooling and storage, in which the molecular interactions (mainly hydrogen bonding between hydroxyl groups of starch chains) occur, has been termed retrogradation (Karim et al., 2000; Hoover, 2001). Retrogradation influences the texture of starch-containing foods such as bread and other starch-based products. It has been found to be time and temperature dependent, and do involve elastic gel formation in the presence of sufficient starch concentration (~6%, w/w) upon cooling, followed by increasing gel turbidity, firmness, degree of crystallinity, and phase separation between polymer and solvent (syneresis) during storage (Morris, 1990; Vasanthan, 1994). During retrogradation, amylose crystallization occurs quickly to form a gel network by nucleation (formation of double helices of 40-70 glucose units between the ends of amylose molecules, favoring chain elongation) and propagation (packing of double helical regions by chain folding), contributing to the initial development of gel firmness (Jane and Robyt, 1984; Miles et al., 1985; Ring et al., 1987; Leloup et al., 1992). However, amylopectin recrystallization occurs more slowly (continuing over a period of several days or weeks) by association of the outmost short branches, contributing to the subsequent slow increase in gel firmness (Ring et al., 1987). While recrystallized amylopectin melts in the temperature range of 40-100°C, amylose crystallites do so only at much higher temperature (120-170°C) (Sievert and Pomeranz, 1989; Eerlingen et al., 1994).

Retrogradation of starch has mainly been investigated by X-ray diffraction, DSC, spectroscopic methods, and rheological techniques (Karim et al., 2000; Eliasson and Gudmundsson, 1996). The retrograded starch, which shows a B-type X-ray diffraction pattern, contains both crystalline and amorphous regions (Zobel, 1988b). The transition temperatures and retrogradation enthalpy of retrogradated starch are usually 10-26°C lower and 60-80% smaller but temperature ranges are wider than those for gelatinization of native starch (White et al., 1989; Yuan et al., 1993; Baker and Rayas-Duarte, 1998) due to the weaker ordered crystallinity and a large amount of crystals of varying stability in retrograded starch than those existing in the native starch granules (Cooke and Gidley, 1992; Shi and Seib, 1992; Fredriksson et al., 1998; Sasaki et al., 2000). The retrogradation tendency of starches from different origins varies greatly. The rate and extent of retrogradation of starches are mainly influenced by starch composition and structure, starch concentration, storage condition, and the presence of other substances (i.e. lipids and surfactants) (Kalichevsky et al., 1990; Shi and Seib, 1992; Eliasson and Gudmundsson, 1996; Fredriksson et al., 1998; Lai et al., 2000). The rate and extent of retrogradation increase with increasing amylose, possibly with a synergistic interaction between amylose and amylopectin in high-amylose starches (75-90%) (Russell, 1987; Gudmundsson and Eliasson, 1990). Amylopectin from cereal starches has been shown to retrograde to a lesser extent than those from pea, potato, and canna starches, which has been attributed to shorter average chain length in the cereal amylopectin (Orford et al., 1987; Kalichevsky et al., 1990). A large amount of short chains over 15 glucose units and an increased ratio of A-chains to B-chains promote retrogradation, whereas, very short chains (6-9 glucose units) retard retrogradation of starch gels (Kalichevsky et al., 1990; Shi and Seib, 1992). Observations of two-stage retrogradation behavior in rice amylopectins (Lai et al., 2000) and multistage retrogradation behavior in waxy maize and potato starches (Bulkin et al., 1987; van Soest et al., 1994) appear to involve complicated crystallization mechanisms caused by amylose and amylopectin molecules (Miles et al., 1985; Orford et al., 1987; van Soest et al., 1994)

1.3 Objectives of thesis

Canada is the leading producer and has generated the major source of published information on HB. Several HB cultivars have been registered in Canada during the last two decades and recently, a series of new HB genotypes with a wide range of amylose contents have been developed through a breeding program at the Crop Development Centre, University of Saskatchewan. HB starch has great potential in the starch industry and has properties comparable to those of maize starch (Vasanthan and Bhatty, 1996) which, at present, is extensively used in a large number of food and industrial applications in North America. However, there is a paucity of information on the relationships between the structural and physicochemical properties of HB starches, which directly relates to their functionality in food and other industrial products. A preliminary study showed that starch granules from these new HB genotypes differed widely in their composition, granule morphology, and physicochemical characteristics. Thus, a fundamental study of the structure-property relationships of HB starches is needed to understand their functionality in food systems. With such information and available genetic variation, it should be possible to produce HB starches for specific uses.

The objectives of the thesis, as listed below, are formulated with the primary focus of advancing scientific knowledge in the area of structure-functionality relationships of HB starches from waxy, normal, and high-amylose genotypes:

Objective 1) To isolate starches from different HB genotypes, evaluate their chemical composition and physicochemical properties, and compare their properties to those of commercial waxy and normal maize starches (Chapters 2 and 3);

Objective 2) To characterize the amylopectin molecules from different genotypes of HB starches using MALDI-MS (Chapter 2);

Objective 3) To probe the ultrastructure of starch granules by scanning electron microscopy (SEM) and transmission electron microscopy (TEM) techniques (Chapters 2 and 4);

Objective 4) To study granule morphological and ultrastructural changes during heating and gelatinization of HB starches in order to correlate the information to the properties of HB starches (Chapter 5);

Objective 5) To study the susceptibility of HB starches towards hydrolysis by different amylases in order to probe the effect of enzyme hydrolysis on HB starch morphology and ultrastructure (Chapter 6).

1.4 References

Abdel-Aal, E.-S., Hucl, P., Chibbar, R. N., Han, H. L., and Demeke, T. 2002. Physicochemical and structural characteristics of flours and starches from waxy and nonwaxy wheats. *Cereal Chem.* 79: 458-464.

Agriculture and Agri-Food Canada. 2003. http://www.agr.ca/policy/winn/biweekly/index.htm. (accessed in September).

Ahmad, F. B., Williams, P. A., Doublier, J. L., Durand, S., and Buleon, A. 1999. Physico-chemical characterization of sago starch. *Carbohydr. Polym.* 38: 361-370.

Alberta Barley Commission, 2003. http://www.albertabarley.com. (accessed in September).

Andersson, A. A., Elfverson, C., Andersson, R., Regnér, S., and Åman, P. 1999. Chemical and physical characteristics of different barley samples. *J. Sci. Food Agric.* 79: 979-986

Anger, H., Richter, M., Kettlitz, B., and Radosta, S. 1994. Hydrothermische Behandlung von Stärke in Gegenwart von α-Amylase Teil 1: Hydrolyse von Stärke mit α-Amylase in heterogener Phase (Hydrothermal treatment of starch in presence of α-amylase. Part 1. Hydrolysis of starch with α-amylase in heterogeneous phase). *Starch/Stärke*, 46, 182-186.

Appelqvist, I. A. M., and Debet, M. R. M. 1997. Starch-biopolymer interaction—a review. *Food Rev. Int.* 13: 163-224.

Asaoka, M., Okuno, K., Sugimoto, Y., and Fuwa, H. 1985. Developmental changes in the structure of endosperm starch of rice (*Oryza sativa* L.). *Agric. Biol. Chem.* 49: 1973-1978.

Atichokudomchai, N., Varavinit, S., and Chinachoti, P. 2002. Gelatinization transitions of acid-modified tapioca starches by differential scanning calorimetry (DSC). *Starch/Stärke* 54: 296-302.

Atkin, N. J., Cheng, S. L., Abeysekera, R. M., and Robards, A. W. 1999. Localization of amylose and amylopectin in starch granules using enzyme-gold labeling. *Starch/Stärke* 51: 163-172.

Atwell, W. A., Hood, L. F., Lineback, D. R., Varriano-Marston, E., and Zobel, H. F. 1988. The terminology and methodology associated with basic starch phenomena. *Cereal Foods World* 33: 306-311.

Autio, K. 1990. Rheological and micro-structural changes of oat and barley starches during heating and cooling. *Food Structure* 9: 297-304.

Baker, L. A. and Rayas-Duarte, P. 1998. Freeze-thaw stability of amaranth starch and the effects of salt and sugars. *Cereal Chem.* 75: 301-307.

Baldwin, P. M. 2001. Starch granule-associated proteins and polypeptides: a review. *Starch/Stärke* 53: 475-503.

Baldwin, P. M., Adler, J., Davies, M. C., and Melia, C. D. 1994. Holes in starch granules: confocal, SEM and light microscopy studies of starch granule structure. *Starch/Stärke* 46: 341-346.

Baldwin, P. M., Adler, J., Davies, M. C., and Melia, C. D. 1998. High resolution imaging of starch granule surfaces by atomic force microscopy. *J. Cereal Sci.* 27: 255-265.

Baldwin, P. M., Davies, M. C., and Melia, C. D. 1997. Starch granule surface imaging using low-voltage scanning electron microscopy and atomic force microscopy. *Int. J. Biol. Marcromol.* 21: 103-107.

Ball, S., Guan, H. P., James, M., Myers, A., Keeling, P., Mouille, G., Buléon, A., Colonna, P., and Preiss, J. 1996. From glycogen to amylopectin: a model for the biogenesis of the plant starch granule. *Cell.* 86: 349-352.

Banks, W. and Greenwood, C. T. 1975. In: *Starch and its Components.* p.5-66. Edinburgh University Press, Edinburgh.

Bechtel, D. B., Zayas, I., Kaleikau, L., and Pomeranz, Y. 1990. Size-distribution of wheat starch granules during endosperm development. *Cereal Chem.* 67: 59-63.

Berglund, P. T., Fastnaught, C. E., and Holm, E. T. 1992. Food uses of hull-less barley. *Cereal Foods World.* 37: 707-714.

Bertoft, E. and Manelius, R. 1992. A method for the study of the enzyme hydrolysis of starch granules. *Carbohydr. Res.* 227: 269-283.

Bertoft, E., Manelius, R., and Qin, Z. 1993a. Studies on the structure of pea starches. Part 1: Initial stages in α-amylolysis of granular smooth pea starch. *Starch/Stärke* 45: 215-220.

Bertoft, E., Manelius, R., and Qin, Z. 1993b. Studies on the structure of pea starches. Part 2: α-Amylolysis of granular wrinkled pea starch. *Starch/Stärke* 45: 258-263.

Bertoft, E., Manelius, R., Myllärinen, P., and Schulman, A. H. 2000. Characterization of dextrins solubilized by α-amylase from barley starch granules. *Starch/Stärke* 52: 160-163.

Bhatty, R. S. 1986. The potential of hull-less barley — a review. *Cereal Chem.* 63: 97-103.

Bhatty, R. S. 1996. Nonmalting uses of barley. In: *Barley Chemistry and Technology*, A. W. McGregor and R. S. Bhatty eds. p.355-417. American Association of Cereal Chemists, St. Paul, MN.

Bhatty, R. S. 1999. The potential of hull-less barley. *Cereal Chem.* 76: 589-599.

Bhatty, R. S. and Rossnagel, B. G. 1998. Composition of pearled and unpearled Canadian and Japanese barleys. *Cereal Chem.* 75: 15-21.

Biliaderis, C. G. 1982. Characteristics of starch in developing pea seeds. *Phytochem.* 21: 37-39.

Biliaderis, C. G. 1991. The structure and interactions of starch with food constituents. *Can. J.* Physiol. *Pharmacol.* 69: 60-78.

Biliaderis, C. G., Grant, D. R., and Rose, J. R. 1981. Structural characterization of legume starches. II. Starch on acid treated starches. *Cereal Chem.* 58: 502-507.

Blakeney, A. B. and Stone, B. A. 1985. Activity and action pattern of *Bacillus licheniformis* α-Amylase in aqueous ethanol. *FEBS Letters* 186: 229-232.

Blanshard, J. M. V. 1987. Starch granule structure and function: a physicochemical approach. In: *Starch: Properties and Potential.* T. Galliard ed. p.16-54. John Wiley and Sons, Chichester.

Bogracheva, T. Ya., Morris, V. J., Ring, S. G., and Hedley, C. L. 1998. The granular structure of C-type pea starch and its role in gelatinization. *Biopolymers* 45: 323-332.

Broberg, S., Koch, K., Andersson, R., and Kenne, L. 2000. A comparison between MALDI-TOF mass spectrometry and HPAEC-PAD analysis of debranched starch. *Carbohydr. Polym.* 43: 285-289.

Buléon, A., Colonna, P, Planchot, V., and Ball, S. 1998. Starch granules: structure and biosynthesis. *Int. J. Biol. Macromol.* 23:85-112.

Bulkin, B. J., Kwak, Y., and Dea, I. C. M. 1987. Retrogradation kinetics of waxy-corn and potato starches: a rapid, Raman-spectroscopic study. *Carbohydr. Res.* 160: 86-92.

Cameron, R. E., and Donald, A. M. 1992. A small-angle X-ray scattering study of the annealing and gelatinization of starch. *Polymer* 33: 2628-2635.

Carlsberg Research Center homepage. 2003. http://www.crc.dk/flab/malting.htm. (accessed in September).

Carlson, T. L. G., Larsson, K., Dinh-Nguyen, N., and Krog, N. 1979. A study of the amylase-monoglyceride complex by Raman Spectroscopy. *Starch/Stärke* 31: 222-224.

Chabot, J. F., Allen, J. E., and Hood, L. F. 1978. Freeze-etch ultrastructure of waxy maize and acid hydrolyzed waxy maize starch granules. *J. Food Sci.* 43: 727-730, 734.

Chatterjee, J., Ghosh, A., and Das, A. 1992. Starch digestion and adsorption by β-amylase of *Emericella nidulans (Aspergillus nidulans)*. *J. Applied Bacteriology* 72: 208-213.

Cheetham, N. W. H. and Tao, L. 1997. The effects of amylose content on the molecular size of amylose, and on the distribution of amylopectin chain length in maize starches. *Carbohydr. Polym.* 33: 251-261.

Cheetham, N. W. H. and Tao, L. 1998. Variation in crystalline type with amylose content in maize starch granules: an X-ray powder diffraction study. *Carbohydr. Polym.* 36: 277-284.

Chrastil, J. 1987. Improved colorimetric determination of amylose in starches or flours. *Carbohydr. Res.* 159: 154-158.

Chun, J., Lim, S., Takeda, Y., and Shoki, M. 1997. Properties of high-crystalline rice amylodextrins prepared in acid-alcohol media as fat replacers. *Cereal Foods World* 42: 813-819.

Colonna, P., and Mercier, C. 1985. Gelatinization and melting of maize and pea starches with normal and high-amylose genotypes. *Phytochem.* 24: 1667-1674.

Colonna, P., Buléon, A., LeMaguer, M., and Mercier, C. 1982. Pisum sativum and Vicia faba carbohydrates. Part IV. Granular structure of wrinkled pea starch. *Carbohydr. Polym.* 2: 43-59.

Colonna, P., Leloup, V, and Buléon, A. 1992. Limiting factors of starch hydrolysis. *Eur. J. Clin. Nutr.* 46: S17-S32.

Cooke, D. and Gidley, M. J. 1992. Loss of crystalline and molecular order during starch gelatinization: origin of the enthalpic transition. *Carbohydr. Res.* 227: 103-112.

Cornell, H. J., Hoveling, A. W., Chryss, A., Rogers, M. 1994. Particle size distribution in wheat starch and its importance in processing. *Starch/Stärke* 46: 203-207.

Craig, S. A. S., and Stark, J. R. 1984. The effect of physical damage on the molecular structure of wheat starch (breadmaking). *Carbohydr. Res.* 125: 117-125.

Czuchajowska, Z., Otto, T., Paszczynska, B., and Baik, B.-K. 1998. Composition, thermal behavior, and gel texture of prime and tailings starches from garbanzo beans and peas. *Cereal Chem.* 75: 466-472.

Danilenko, A. N., Shtykova, Ye. V., and Yur'ev, V. P. 1994 Equilibrium and the cooperative unit of the process of melting of native starches with different packing of the macromolecular chains in the crystallites. *Biophysics* 39: 427-432.

Darlington, H. F., Tecsi, L., Harris, N., Griggs, D. L., Cantrell, I. C., and Shewry, P. R. 2000. Starch granule associated proteins in barley and wheat. *J. Cereal Sci.* 32: 21-29.

Deffenbaugh, L. B. and Walker, C. E. 1989. Comparison of starch pasting properties in the Brabender Viscoamylograph and the Rapid Visco-Analyzer. *Cereal Chem.* 66: 493-499.

Demeke, T., Hucl, P., Abdel-Aal, E.-S. M., Båga, M., and Chibbar, R. N. 1999 Biochemical characterization of the wheat waxy protein and its effect on starch properties. *Cereal Chem.* 76: 694-698.

Dengate, H. N. 1984. Swelling, pasting, and gelling of wheat starch. In: *Advances in Cereal Science and Technology*. Y. Pomeranz ed. Vol. VI. p.49-82, Am. Assoc. Cereal Chem., St. Paul, MN.

Dengate, H., and Meredith, P. 1984. Variation in size distribution of starch granules from wheat grain. *J. Cereal Sci.* 2: 83-90.

Deshpande, S. S., Sathe, S. K., Rangnekar, P. D., and Salunkhe, D. K. 1982. Functional properties of modified black gram (*Phaseolus mungo* L.) starch. *J. Food Sci.* 47: 1528-1533, 1602.

Donald, A. M., Kato, K. L., Perry, P. A., and Waigh, T. A. 2001. Scattering studies of the internal structure of starch granules. *Starch/Stärke* 53: 504-512.

Donald, A. M., Waigh, T. A., Jenkins, P. J., Gidley, M. J., Debet, M., and Smith, A. 1997. Internal structure of starch granules revealed by scattering studies. In: *Starch Structure and Functionality*. P. J. Frazier, P. Richmond, and A. M. Donald eds. p.173-179. The Royal Society of Chemistry, Cambridge.

Donovan, J. 1979. Phase transitions of the starch — water system. *Biopolymers* 18: 263-275.

Donovan, J. W. and Mapes, C. J. 1980. Multiple phase transitions of starches and Nägeli amylodextrins. *Starch/Stärke* 32: 190-193.

Doublier, J. L. 1981. Rheological studies on starch-flow behavior of wheat starch pastes. *Starch/Stärke* 33: 415-420.

Doublier, J. L. 1987. A rheological comparison of wheat, maize, faba bean and smooth pea starches. *J. Cereal Sci.* 5: 247-262.

Doublier, J. L., Paton, D., and Llamas, G. 1987. A rheological investigation of oat starch pastes. *Cereal Chem.* 64: 21-26.

Duffus, C. M. and Cochrane, M. P. 1996. Formation of the barley grain —Morphology, physiology, and biochemistry. In: *Barley Chemistry and Technology*. A. W. MacGregor and R. S. Bhatty eds. p.31-72. American Association of Cereal Chemists, St. Paul, MN.

Edney, M. J. and Rossnagel, B. G. 2000. Producing a quality malt from hull-less barley. Proceedings of the 8th International Barley Genetics Symposium, Adelaide, Australia. p.91-93.

Eerlingen, R. C., Jacobs, H., and Delcour, J. A. 1994. Enzyme-resistant starch. V. Effect of retrogradation of waxy maize starch on enzyme susceptibility. *Cereal Chem.* 71: 351-355.

Eliasson, A. C. 1986. Viscoelastic behavior during gelatinization of starch. I. Comparison of wheat, maize, potato and waxy-barley starches. *J. Texture Studies* 27: 253-265.

Eliasson, A.-C. and Gudmundsson, M. 1996. Starch: physicochemical and functional aspects. In: *Carbohydrates in Food*. A.-C. Eliasson ed. p.431-504. Marcel Dekker.

Ellis, H. S., and Ring, S. G. 1985. A study of some factors influencing amylose gelatin. *Carbohydr. Polym.* 5: 201-213.

Ellis, H. S., Ring, S. G., and Whittam, M. A. 1988. Time-dependent changes in the size and volume of gelatinized starch granules on storage. *Food Hydrocoll.* 2: 321-328.

Ellis, R. P., Cochrane, M. P., Dale, M. F. B., Duffus, C. M., Lynn, A., Morrison, I. M., Prentice, R. D. M., Swanston, J. S., and Tiller, S. A. 1998. Starch production and industrial use. *J. Sci. Food Agric.* 77: 289-311.

Evans, I. D. and Haisman, D. R. 1982. The effect of solutes on the gelatinization temperature range of potato starch. *Starch/Stärke* 34: 224-231.

Fannon, J. E., Hauber, R. J., and BeMiller, J. N. 1992. Surface pores of starch granules. *Cereal Chem.* 69: 284-288.

Fannon, J. E., Shull, J. M., and BeMiller, J. N. 1993. Interior channels of starch granules. *Cereal Chem.* 70: 611-613.

FAO, 2003, http://apps.fao.org/default.htm. (accessed in September).

Fitt, L. E. and Snyder, E. M. 1984. Photomicrographs of starches. in: *Starch Chemistry and Technology*, R. L. Whistler, J. N. Miller, and E. F. Paschall eds. p.675-689. Academic Press, Orlando, Florida

Franco, C. M. L. and Ciacco, C. F. 1987. Studies on the susceptibility of granular cassava and corn starches to enzymatic attack. *Starch/Stärke*, 39, 432-435.

Franco, C. M. L., Wong, K. S., Yoo, S., and Jane, J. 2002. Structural and functional characteristics of selected soft wheat starches. *Cereal Chem.* 79: 243-248.

Fredriksson, H., Silverio, J., Andersson, R., Eliasson, A.-C., and Åman, P. 1998. The influence of amylose and amylopectin characteristics on gelatinization and retrogradation properties of different starches. *Carbohydr. Polym.* 35: 119-134.

French, A. D. and Murphy, V. G. 1977. Computer modeling in the study of starch. *Cereal Foods World* 22: 61-70.

French, D. 1972. Fine structure of starch and its relationship to the organisation of starch granules. *J. Jap. Soc. Starch Sci.* 19: 8-25.

French, D. 1984. Organization of starch granules. In: *Starch Chemistry and Technology*. R. L. Whistler, J. N. BeMiller, and E. F. Paschall eds. p.183-247. Academic Press, Orlando, Florida.

Fujita, S., Morita, T. and Fujiyama, G. 1993. The study of melting temperature and enthalpy of starch from rice, barley, wheat, foxtail- and proso-millets. *Starch/Stärke* 45: 436-441.

Fujita, S., Yamamoto, H., Sugimoto, Y., Morita, N., and Yamamori, M. 1998. Thermal and crystalline properties of waxy wheat (*Triticum aestivum* L.) starch. *J. Cereal Sci.* 27: 1-5.

Gallant, D, Mercier, C. and Guilbot, A. 1972. Electron microscopy of starch granules modified by bacterial α-amylase. *Cereal Chem.* 49, 354-365.

Gallant, D. J., Bouchet, B., and Baldwin, P. M. 1997. Microscopy of starch: evidence of a new level of granule organization. *Carbohydr. Polym.* 32: 177-191.

Gallant, D. J., Bouchet, B., Buléon, A., and Pérez, S. 1992. Physical characteristics of starch granules and susceptibility to enzymatic degradation. *Eur. J. Clin. Nutr.* 46: S3-S16

Galliard, T. and Bowler, P. 1987. Morphology and composition of starch. In: *Starch: Properties and Potential*. T. Galliard ed. p.55-78. John Wiley and Sons, Chichester.

Garcia, V., Colonna, P., Bouchet, B., and Gallant, D. J. 1997. Structural changes of cassava starch granules after heating at intermediate water contents. *Starch/Stärke* 49: 171-179.

Garcia, V., Colonna, P., Lourden, D., Buléon, A., Bizot, H., and Ollivon, M. 1996. Thermal transitions of cassava starch at intermediate water contents. *J. Therm. Anal.* 47: 1213-1228.

Gérard, C., Colonna, P., Buléon, A., and Planchot, V. 2000. Relationship between branching density and crystalline structure of A- and B-type maize mutant starches. *Carbohydr. Res.* 326: 130-144.

Gérard, C., Colonna, P., Buléon, A., and Planchot, V. 2001. Amylolysis of maize mutant starches. *J. Sci. Food Agric.* 81: 1281-1287.

Gérard, C., Colonna, P., Buléon, A., and Planchot, V. 2002. Order in maize mutant starches revealed by mild acid hydrolysis. *Carbohydr. Polym.* 48: 131-141.

Gernat, C. Radosta, S., Damaschun, G., and Schierbaum, F. 1990. Supramolecular structure of legume starches revealed by X-ray scattering. *Starch/Stärke* 42: 175-178.

Gernat, C., Radosta, S., Aanger, H., Damaschun, G. 1993. Crystalline parts of three different conformations in native and enzymatically degraded starches. *Starch/Stärke* 45: 309-314.

Ghiasi, K., Hoseney, R. C., and Varriano-Marston, E. 1982. Gelatinization of wheat starch. I. Excess-water systems. *Cereal Chem.* 59: 81-85.

Gibson, T. S., Solah, V. A., and McCleary, B. V. 1997. A procedure to measure amylose in cereal starches and flours with concanavalin A. *J. Cereal Sci.* 25: 111-119.

Gidley, M. J. 2001. Starch structure/function relationships: achievements and challenges. In: *Starch Advances in Structure and Function*, T. L. Barsby, A. M. Donald, and P. J. Frazier eds. p.1-7. The Royal Society of Chemistry, Cambridge.

Gidley, M. J. and Cooke, D. 1991. Aspects of molecular organization and ultrastructure in starch granules. *Biochem. Soc. Trans.* 19: 551-555.

Gidley, M. J., and Bociek, S. M. 1985. Molecular organisation in starches: a ^{13}C CP/MAS NMR study. *J. Am. Chem. Soc.* 107: 7040-7044.

Gidley, M. J., and Bociek, S. M. 1988. ^{13}C CP/MAS NMR studies of amylose inclusion complexes, cyclodextrins, and the amorphous phase of starch granules:

relationships between glycosidic linkage conformation and solid-state ^{13}C chemical shifts. *J. Am. Chem. Soc.* 110: 3820-3829.

Gidley, M. J., and Bulpin, P. V. 1987. Crystallization of malto-oligosaccharides as models of the crystalline forms of starch minimum chain-length requirement for the formation of double helices. *Carbohydr. Res.* 161: 291-300.

Goering, K. J., Fritts, D. H., and Eslick, R. F. 1973. A study of starch granule size and distribution in 29 barley varieties. *Starch/Stärke* 25: 297-302.

Greenwell, P., and Schofield, J. D. 1986. A starch granule protein associated with endosperm softness in wheat. *Cereal Chem.* 63: 379-380.

Gudmundsson, M. and Eliasson, A. -C. 1990. Retrogradation of amylopectin and the effects of amylose and added surfactants/emulsifiers. *Carbohydr. Polym.* 13: 295-316.

Gudmundsson, M. and Eliasson, A.-C. 1992. Some physical properties of barley starches from cultivars differing in amylose content. *J. Cereal Sci.* 16: 95-105.

Guilbot, A. and Mercier, C. 1985. Starch. In: *The polysaccharides*. G. O. Aspinall ed., Vol. 3, p209-282. Academic Press, Orlando.

Guzmán-Maldonado, H. and Paredes-López, O. 1995. Amylolytic enzymes and products derived from starch: a review. *Crit. Rev. Food Sci. Nutr.* 35: 373-403.

Hall, D. M., and Sayre, J. G. 1970a. A scanning electron-microscope study of starches. Part II: Cereal starches. *Text. Res. J.* 40: 256-266.

Hall, D. M., and Sayre, J. G. 1970b. Internal architecture of potato and canna starch. Part I: Crushing studies. *Text. Res. J.* 40: 147-157.

Hall, D. M., and Sayre, J. G. 1973. A comparison of starch granules as seen by both scanning electron and ordinary light microscopy. *Starch/Stärke* 25: 119-123.

Han, X. Z. and Hamaker, B. R. 2002. Association of starch granule properties with starch ghosts and remnants revealed by confocal laser scanning microscopy. *Cereal Chem.* 79: 892-896.

Hanashiro, I., Abe, J., and Hizukuri, S. 1996. A periodic distribution of the chain length of amylopectin as revealed by high-performance anion-exchange chromatography. *Carbohydr. Res.* 283: 151-159.

Harrigan, K. A. 1997. Particle size analysis using automated image analysis. *Cereal Foods World.* 42: 30-35.

Hedley, C. L. 2000 In: *Carbohydrates in Grain Legume Seeds. Improving Nutritional Quality and Agronomic Characteristics.* C. L. Hedley, J. Cunninghamp, and A. Jones eds. p1-13. CABI Publishing, Oxon, UK

Helbert, W., Schülein, M., and Henrissat, B. 1996. Electron microscopic investigation of the diffusion of *Bacillus licheniformis* α-amylase into corn starch granules. *Int. J. Bio. Macromol.* 19:165-169.

Hermansson, A. M., and Svegmark, K. 1996. Developments in the understanding of starch functionality. *Trends Food Sci. Tech.* 7: 345-353.

Hisukuri, S., Takeda, Y., Maruta, N., Juliano, B. O. 1989. Molecular structures of rice starch. *Carbohydr. Res.* 189: 227-235.

Hizukuri, S. 1986. Polymodal distribution of the chain lengths of amylopectins and its significance. *Carbohydr. Res.* 147: 342-347.

Hizukuri, S. 1985. Relationship between the distribution of the chain length of amylopectin and the crystalline structure of starch granules. *Carbohydr. Res.* 141: 295-206.

Hizukuri, S. 1996. Starch: analytical aspects. In: *Carbohydrates in Food.* A. C. Eliasson ed. p.347-429. Marcel Dekker.

Hizukuri, S., and Maehara, Y. 1990. Fine structure of wheat amylopectin: the mode of A to B chain binding. *Carbohydr. Res.* 206: 145-159.

Hizukuri, S., and Takagi, T. 1984. Estimation of the distribution of molecular weight for amylose by the low-angle laser-light-scatting technique combined with high-performance gel chromatography *Carbohydr. Res.* 134: 1-10.

Hizukuri, S., Kaneko, T., and Takeda, Y.1983. Measurement of the chain length of amylopectin and its relevance to the origin of crystalline polymorphism of starch granules. *Biochem. Biophys. Acta* 760: 188-191.

Hizukuri, S., Takeda, Y., Abe, J., Hanashiro, I., Matsunobu, G., and Kiyota, H. 1997. Analytical developments: molecular and microstructural characterization. In: *Starch Structure and Functionality*. P. J. Frazier, P. Richmond, and A. M. Donald eds. p.121-128. The Royal Society of Chemistry, Cambridge.

Hizukuri, S., Takeda, Y., Yasuda, M., and Suzuki, A. 1981. Multi-branched nature of amylose and the action of debranching enzymes. *Carbohydr. Res.* 94: 205-213.

Holló, J. and Hoschke, A. 1993. Bioconversion of starch. *Pol. J. Food Nutri. Sci.* 2: 5-37.

Hood, L. F. and Liboff, M. 1983. Starch ultrastructure. In: *New frontiers in food microstructure.* D. B. Bechtel ed. p.341-370. American Association of Cereal Chemists. St. Paul, Minnesota.

Hoover, R. 2000. Acid-treated starches. *Food Res. Int.* 16: 369-392.

Hoover, R. 2001. Composition, molecular structure, and physicochemical properties of tuber and root starches: a review. *Carbohydr. Polym.* 45: 253-267.

Hoover, R. and Manuel, H. 1996. The effect of heat-moisture treatment on the structure and physicochemical properties of normal maize, waxy maize, dull waxy maize, and amylomaize V starches. *J. Cereal Sci.* 23: 153-162.

Hoover, R. and Sosulski, F. W. 1991. Composition, structure, functionality, and chemical modification of legume starches: a review. *Can. J. Physiol. Pharmacol.* 69: 79-92.

Hoover, R., and Manuel, H. 1995. A comparative study of the physicochemical properties of starches from two lentil cultivars. *Food Chem.* 53: 275-284.

Hoover, R., and Vasanthan, T. 1994. The effect of annealing on the physicochemical properties of wheat, oat, potato and lentil starches. *J. Food Biochem.* 17: 303-325.

Hoover, R., Hannouz, D. and Sosulski, F. W. 1988. Effects of hydroxypropylation on thermal properties, starch digestibility and freeze-thaw stability of field pea (Pisum sativum cv Trapper) starch. *Starch/Stärke* 40: 383-387.

Hoover, R., Li, Y. X., and Senanayake, N. 1997. Physicochemical characterization of mung bean starch. *Food Hydrocol.* 11: 401-408.

Hoover, R., Smith, C., Zhou, Y., and Ratnayake, R. M. W. S. 2003. Physicochemical properties of Canadian oat starches. *Carbohydr. Polym.* 52: 253-261.

Hoover, R., Swamidas, G. and Vasanthan, T. 1993. Studies on the physicochemical properties of native, defatted, and heat-moisture treated pigeon pea (*Cajanus cajan* L) starch. *Carbohydr. Res.* 246: 185-203.

Hoseney, R. C. 1986. Cereal starch. In: *Principles of Cereal Science and Technology*. p.33-68. American Association of Cereal Chemists, St. Paul, MN.

Huber, K. C., and BeMiller, J. N. 1997. Visualization of channels and cavities of corn and sorghum starch granules. *Cereal Chem.* 74: 537-541.

Huber, K. C., and BeMiller, J. N. 2000. Channels of maize and sorghum starch granules. *Carbohydr. Polym.* 41: 269-276.

Imberty, A., and Pérez, S, 1988. A revisit to the three-dimensional structure of B-type starch. *Biopolymers* 27: 1205-1221.

Imberty, A., Buléon, A., Tran, V., and Pérez, S. 1991. Recent advances in knowledge of starch structure. *Starch/Stärke* 43: 375-384.

Imberty, A., Chanzy, H., Pérez, S., Buléon, A., and Tran, V., 1988. The double-helical nature of the crystalline part of A-starch. *J. Mol. Biol.* 201: 365-378.

Inouchi, N., Glover, D. V., and Fuwa, H. 1987. Chain length distribution of amylopectins of several single mutants and the normal counterpart, and sugary-1 phytoglycgen in maize (*Zea mays* L.). *Starch/Stärke* 39: 259-266.

Inouchi, N., Glover, D. V., Sugimoto, Y., and Fuwa, H. 1984. Developmental changes in starch properties of several endosperm mutants of maize. *Starch/Stärke* 36: 8-12.

Jacobs, H. and Delcour. J. 1998. Hydrothermal modifications of granular starch, with retention of the granular structure: a review. *J. Agric. Food Chem.* 46:2895-2906.

Jacobs, H., Eerlingen, R. C., Rouseu, N., Colonna, P., and Delcour, J. A. 1998. Acid hydrolysis of native and annealed wheat, potato and pea starches — DSC melting features and chain length distributions of lintnerized starches. *Carbohydr. Res.* 308: 359-371.

Jadhav, S. J., Lutz, S. E., Ghorpade, V. M., and Salunkhe, D. K. 1998. Barley: chemistry and value-added processing. *Crit. Rev. Food Sci. Nutr.* 38: 123-171.

Jane, J. and Chen, J. F. 1992. Effects of amylose molecular size and amylopectin branch chain length on paste properties of starch. *Cereal Chem.* 69: 60-65.

Jane, J. L. and Robyt, J. F. 1984. Structure studies of amylose-V complexes and retrograded amylose by action of alpha-amylases, and a new method for preparing amylodextrins. *Carbohydr. Res.* 132: 105-118.

Jane, J., and Shen, J. 1993. Internal structure of the potato starch granule revealed by chemical gelatinization. *Carbohydr. Res.* 247: 279-290.

Jane, J., Chen, Y. Y., Lee, L. F., McPherson, A. E., Wong, K. S., Radosavljevic, M., and Kasemsuwan, T. 1999. Effects of amylopectin branch chain length and amylose content on the gelatinization and pasting properties of starch. *Cereal Chem.* 76: 629-637.

Jane, J., Kasemsuwan, T., and Chen, J. F. 2002. Phosphorus in rice and other starches. *Cereal Foods World.* 41: 827-832.

Jane, J., Kasemsuwan, T., Leas, S., Zobel, H., and Robyt, J. F. 1994. Anthology of starch granule morphology by scanning electron microscopy. *Starch/Stärke* 46: 121-129.

Jane, J., Shen, L., Chen, J., Lim, S., Kasemsuwan, T., and Nip, W. K.1992b. Physical and chemical studies of taro starches and flours. *Cereal Chem.* 69: 528-535.

Jane, J., Wong, K., and McPherson, A. E. 1997. Branch-structure difference in starches of A- and B-type X-ray patterns revealed by their Naegeli dextrins. *Carbohydr. Res.* 300: 219-227.

Jane, J., Xu, A., Radosavljevic, M., and Seib, P. A. 1992a. Location of amylose in normal starch granules. I. Susceptibility of amylose and amylopectin to cross-linking reagents. *Cereal Chem.* 69: 405-409.

Jenkins, P. J. and Donald, A. M. 1997. The effect of acid hydrolysis on native starch granule structure. *Starch/Stärke* 49: 262-267.

Jenkins, P. J. and Donald, A. M. 1998. Gelatinization of starch: a combined SAXS/WAXS/DSC and SANS study. *Carbohydr. Res.* 308: 133-147.

Jenkins, P. J., and Donald, A. M. 1995. The influence of amylose on starch granule structure. *Int. J. Biol. Macromol.* 17: 315-321.

Jenkins, P. J., Cameron, R. E., and Donald, A. M. 1993. A universal feature in the structure of starch granules from different botanical sources. *Starch/Stärke* 45: 417-420.

Jenkins, P. J., Cameron, R. E., Donald, A. M., Bras, W., Derbyshire, G. E., Mant, G. R., and Ryan, A. J. 1994. In situ simultaneous small and angle X-ray scattering: a new technique to study starch gelatinization. *J. Polym. Sci. Polym. Phys. Educ.* 32: 1579-1583.

Kainuma, K. and French, D. 1971. Nägeli amylodextrin and its relationship to starch granule structure. I. Preparation and properties of amylodextrins from various starch types. *Biopolymers* 10: 1673-1680.

Kainuma, K., and French, D. 1972. Naegeli amylodextrin and its relationship to starch granule structure. II. Role of water in crystallization of B-starch. *Biopolymers* 11: 2241-2250.

Kalichevsky, M. T., Orford, P. D., and Ring, S. G. 1990. The retrogradation and gelation of amylopectin from various botanical sources. *Carbohydr. Res.* 198: 49-55.

Kalra, S. and Jood, S. 1998. Biological evaluation of protein quality of barley. *Food Chem.* 61: 35-39.

Karim, A. A., Norziah, M. H., and Seow, C. C. 2000. Methods for the study of starch retrogradation. *Food Chem.* 71: 9-36.

Karkalas, J., Tester, R. F., and Morrison, W. R. 1992. Properties of damaged starch granules. I. Comparison of a micromethod for the enzymic determination of damaged starch with the standard AACC and Farrand methods. *J. Cereal Sci.* 16: 237-251.

Karlsson, R., Olered, R., and Eliasson, A. C. 1983. Changes in starch granule size distribution and starch gelatinization properties during development and maturation of wheat, barley and rye. *Starch/Stärke* 35: 335-340.

Kasemsuwan, T. and Jane, J. 1996. Quantitative method for the survey of starch phosphate derivatives and starch phospholipids by ^{31}P nuclear magnetic resonance spectroscopy. *Cereal Chem.* 73: 702-707.

Kasemsuwan, T., and Jane, J. 1994. Location of amylose in normal starch granules. II. Locations of phosphodiester cross-linking revealed by phosphorus-31 nuclear magnetic resonance. *Cereal Chem.* 71: 282-287.

Kassenbeck, P. 1975. Electron microscope contribution to the study of fine structure of wheat starch. *Starch/Stärke* 27: 217-227.

Kassenbeck, P. 1978. Beitrag zur kenntnis der verteilung von amylose und amylopektin in stärkrkörnern (Contribution to the knowledge on distribution of amylose and amylopectin in starch granules). *Starch/Stärke* 30: 40-46.

Katz, J. R. and Van Itallie, T. B. 1930. The physical chemistry of starch and bread making. V. All varieties of starch have similar retrogradation spectra. *Z. Phys. Chem. Abt. A.* 150: 90-100.

Kawabata, A., Sawayama, S., Nagashima, N., del Rosario, R. R., and Nakamura, M. 1984. Some physico-chemical properties of starches from cassava, arrowroot and sago. *J. Jpn. Soc. Starch Sci.* 31: 224-232.

Keagy, P. M., Knuckles, B. E., Yokoyama, W. H., Kahlon, T. S., and Hudson, C. A. 2001. Health-promoting properties of a high beta-glucan fraction. *Nutrition Today*, 36: 121-124.

Kim, H. R., and Eliasson A. C. 1993. The influence of molar substitution on the thermal transition properties of hydroxypropyl potato starches. *Carbohydr. Polym.* 22:31-35.

Kimura, A. and Robyt, J. F. 1995. Reaction of enzymes with starch granules: kinetics and products of the reaction with glucoamylase. *Carbohydr. Res.* 277: 87-107.

Knutson, C. A. 1986. A simplified colorimetric procedure for determination of amylose in maize starches. *Cereal Chem.* 63: 89-92.

Knutson, C. A. 1990. Annealing of maize starches at elevated temperatures. *Cereal Chem.* 67: 376-384.

Knutson, C. A., Cluskey, J. E., and Dintzis, F. R. 1982a. Properties of amylose-iodine complexes prepared in the presence of excess iodine. *Carbohydr. Res.* 101: 117-128

Knutson, C. A., Khoo, U., Cluskey, J. E., and Inglett, G. E. 1982b. Variation in enzyme digestibility and gelatinization behavior of corn starch granule fractions. *Cereal Chem.* 59: 512-515.

Komiya, T, Yamada, T., and Nara, S. 1987. Crystallinity of acid treated corn starch. *Starch/Stärke* 39: 308-311.

Komiya, T. and Nara, S. 1986. Changes in crystallinity and gelatinization phenomena of potato starch by acid treatment. *Starch/Stärke* 38: 9-13.

Kuipers, A. G. J., Jacobsen, E., and Visser, R. G. F. 1994. Formation and deposition of amylose in the potato tuber starch granule are affected by the reduction of granule-bound starch synthase gene expression. *Plant Cell* 6: 43-52.

Kulp, K. 1973. Characteristics of small-granule starch of flour and wheat. *Cereal Chem.* 50: 666-679.

Kurakake, M., Tachibana, Y., Masaki, K., and Komaki, T. 1996. Adsorption of alpha-amylase on heat-moisture treated starch. *J. Cereal Sci.* 23, 163-168.

Lai, V. M. F., Lu, S., and Lii, C. 2000. Molecular characteristics influencing retrogradation kinetics of rice amylopectins. *Cereal Chem.* 77: 272-278.

Langton, M., and Hermansson, A. M. 1989. Microstructural changes in wheat starch dispersions during heating and cooling. *Food Microstructure* 8: 29-39.

Lauro, M., Forssell, P. M., Suortti, M. T., Hulleman, S. H. D., and Poutanen, K. S. 1999. α-amylolysis of large barley starch granules. *Cereal Chem.* 76, 925-930.

Lauro, M., Ring, S. G., Bull, V. J., and Poutanen, K. 1997. Gelation of waxy barley starch hydrolysates. *J. Cereal Sci.* 26: 347-354.

Lauro, M., Suortti, T., Autio, K., Linko, P., and Poutanen, K. 1993. Accessibility of barley starch granules to α-amylase during different phases of gelatinization. *J. Cereal Sci.* 17, 125-136.

Leach, H. W. and Schoch, T. J. 1961. Structure of the starch granule. II. Action of various amylases on granular starches. *Cereal Chem.* 38: 34-46.

Leach, H. W., McCowan, L. D., and Schoch, T. J. 1959. Structure of starch granules. I. Swelling and solubility patterns of various starches. *Cereal Chem.* 36: 534-544.

Lee, Y. E., and Osman, E. M. 1991. Correlation of morphological changes of rice starch granules with rheological properties during heating in excess water. *J. Kor. Agric. Chem. Soc.* 34: 379-385.

Leloup, V. M., Colonna, P., and Ring, S. G. 1991. α-Amylase adsorption on starch: crystallites. *Biotechnol. Bioeng.* 38: 127-134.

Leloup, V. M., Colonna, P., Ring, S. G., Roberts, K., and Wells, B. 1992. Microstructure of amylose gels. *Carbohydr. Polym.* 18: 189-197.

Li, J. H., Vasanthan, T., Hoover, R., and Rossnagel, B. G. 2003. Starch from Hull-less Barley: Ultrastructure and Distribution of Granule-bound Proteins. *Cereal Chem. 80:524-532.*

Liakopoulou-Kyriakides, M, Karakatsanis, A., Stamatoudis, M., and Psomas, S. 2001. Synergistic hydrolysis of crude corn starch by α-Amylases and glucoamylases of various origins. *Cereal Chem.* 78:603-607.

Lii, C. Y., Tsai, M. L., and Tseng, K. H. 1996. Effect of amylose content on the rheological property of rice starch. *Cereal Chem.* 73: 415-420.

Lim, S. T., Kasemsuwan, T., and Jane, J. 1994. Characterization of phosphorus in starch by^{13}P nuclear magnetic resonance spectroscopy. *Cereal Chem.* 71: 488-493.

Lineback, D. R. 1984. The starch granule — organization and properties. *Baker Dig.* 58; 16-21.

Liu, H. and Lelievre, J. 1993. A model of starch gelatinization linking differential scanning calorimetry and birefringence measurements. *Carbohydr. Polym.* 20: 1-5.

Liu, H., Lelievre, J., and Ayoung-Chee, W. 1991. A study of starch gelatinization using differential scanning calorimetry, X-ray, and birefringence measurements. *Carbohydr. Res.* 210: 79-87.

LMC International, 2003. The structure of the world starch market. http://europa.eu.int/ comm /agriculture/eval/reports/amidon/chap1.pdf. (accessed in September).

Lorenz, K., and Collins, F. 1995. Physicochemical characteristics and functional properties of starch from a high-β-glucan waxy barley. *Starch/Stärke* 47: 14-18.

Lowy, G. D. A., Sargeant, J. G., and Schofield, J. D. 1981. Wheat starch granule protein: the isolation and characterization of a salt-extractable protein from starch granules. *J. Sci. Food Agric.* 32: 371-377.

Lund, D. 1984. Influence of time, temperature, moisture, ingredients, and processing conditions on starch gelatinization. In: *Critical Reviews in Food Science and Nutrition*. T. E. Furia ed. Vol. 20, p.249-274. CRC Press, Boca Raton, Florida.

MacGregor, A. W. 1979. Isolation of large and small granules of barley starch and a study of factors influencing the adsorption of barley malt α-amylase by these granules. *Cereal Chem.* 56: 430-434.

MacGregor, A. W. and Ballance, D. L. 1980. Hydrolysis of large and small starch granules from normal and waxy barley cultivars by alpha-amylases from barley malt. *Cereal Chem.* 57: 397-402.

MacGregor, A. W. and Morgan, J. E. 1986. Hydrolysis of barley starch granules by alpha-amylases from barley malt. *Cereal Foods World* 31: 688-693.

MacGregor, A. W., and Morgan, J. E. 1984. Structure of amylopectin isolated from large and small starch granules of normal and waxy barley. *Cereal Chem.* 61: 222-228.

MacGregor, S. 1998. Composition of barley related to food uses. Presented at International Food Barley Program, Canadian International Grains Institute in Winnipeg, Manitoba, Canada.

Mäkelä, M. J., and Laakso, S. 1984. Studies on oat starch with a celloscope: granule size and distribution. *Starch/Stärke* 36: 159-163.

Mäkelä, M. J., Korpela, T., and Laakso, S. 1982. Studies of starch size and distribution in 33 barley varieties with a celloscope. *Starch/Stärke* 34: 329-334.

Manelius, R. and Bertoft, E. 1996. The effect of Ca^{2+}-Ions on the α-amylolysis of granular starches from oats and waxy-maize. *J. Cereal Sci.* 24: 139-150.

Manelius, R., Nurmi, K., and Bertoft, E. 2000. Enzymatic and acidic hydrolysis of cationized waxy maize starch granules. *Cereal Chem.* 77: 345-353.

Manelius, R., Qin, Z., Åvall, A.-K., Andtfolk, H., and Bertoft, E. 1997. The mode of action on granular wheat starch by bacterial α-amylase. *Starch/Stärke* 49: 142-147.

Maningat, C. C. and Juliano, B. O. 1979. Properties of lintnerized starch granules from rices differing in amylose content and gelatinization temperature. *Starch/Stärke* 31: 5-10.

Manners, D. J. 1989. Recent developments in our understanding of amylopectin structure. *Carbohydr. Polym.* 11: 87-112.

Manners, D. J. and Matheson, N. K. 1981. The fine structure of amylopectin. *Carbohydr. Res.* 90: 99-110.

Matveev, Y. I., van Soest, J. J. G., Nieman, C. Wasserman, L. A., Protserov, V. A., Ezernitskaja, M., and Yuryev, V. P. 2001. The relationship between thermodynamic and structural properties of low and high amylose maize starches. *Carbohydr. Polym.* 44: 151-160.

Matveev, Yu. I., Elankin, N. Yu., Kalistrova, E. N., Danilenko, A. N., Niemann, C., and Yuryev, V. P. 1998. Estimation of contributions of hydration and glass transition to heat capacity changes during melting of native starches in excess water. . *Starch/Stärke* 50: 141-147.

McDonald, A. M. L., Stark, J. R., Morrison, W. R., and Ellis, R. P. 1991. The composition of starch granules from developing barley genotypes. *J. Cereal Sci.* 13: 93-112.

McPherson, A. E. and Jane, J. 1999. Comparison of waxy potato with other root and tuber starches. *Carbohydr. Polym.* 40: 57-70.

Miles,M. J., Morris, V. J., Orford, P. D., and Ring, S. G. 1985. The roles of amylose and amylopectin in the gelation and retrogradation of starch. *Carbohydr. Res.* 135: 271-281.

Moon, M. H., and Giddings, J. C. 1993. Rapid separation and measurement of particle size distribution of starch granules by sedimentation/steric field-flow fractionation. *J. Food Sci.* 58: 1166-1171.

Morell, M. K., Samuel, M. S., and O'Shea, M. G. 1998. Analysis of starch structure using fluorophore-assisted carbohydrate electrophoresis. *Electrophoresis* 19: 2603-2611.

Morgan, K. R., Furneaux, R. H., Larsen, N. G. 1995. Solid-state NMR studies on the structure of starch granules. *Carbohydr. Res.* 276: 387-399.

Morris, V. J. 1990. Starch gelation and retrogradation. *Trends Food Sci. Tech.* 7: 2-6.

Morrison, W. R. 1988. Lipids in cereal starches: a review. *J. Cereal Sci.* 8: 1-15.

Morrison, W. R. 1993. Cereal starch granule development and composition. In: *Seed Storage Compounds: Biosynthesis, Interactions and Manipulation*. P. R. Shewry and K. Stobart eds. p.175-190. Clarendon Press, Oxford.

Morrison, W. R. 1995. Starch lipids and how they relate to starch granule structure and functionality. *Cereal Foods World* 40: 437-446.

Morrison, W. R. 1996. Barley lipids. In: *Barley Chemistry and Technology*, A. W. McGregor and R. S. Bhatty eds. p.199-246. American Association of Cereal Chemists, St. Paul, MN.

Morrison, W. R., and Gadan, H. 1987. The amylose and lipid contents of starch granules in developing wheat endosperm. *J. Cereal Sci.* 5: 263- 275.

Morrison, W. R., and Karkalas, J. 1990. Starch. In: *Methods in Plant Biochemistry* Vol. 2. Carbohydrates. P. M. Dey and J. B. Harborne eds. p.323-352. Academic Press, London.

Morrison, W. R., and Laignelet, B. 1983. An improved colorimetric procedures for determining apparent and total amylose in cereal and other starches. *J. Cereal Sci.* 1: 9-20.

Morrison, W. R., and Scott, D. C. 1986. Measurement of the dimensions of wheat starch granule populations using a coulter counter with 100-channel analyzer. *J. Cereal Sci.* 4: 13-21.

Morrison, W. R., and Tester, R. F. 1994a. Properties of damaged starch granules. II. Crystallinity, molecular order and gelatinization of ball-milled starches. *J. Cereal Sci.* 19: 209- 217.

Morrison, W. R., and Tester, R. F. 1994b. Properties of damaged starch granules. IV. Composition of ball-milled wheat starches and fractions obtained on hydration. *J. Cereal Sci.* 20: 69-77.

Morrison, W. R., Law, R. V., and Snape, C. E. 1993b. Evidence for inclusion complexes of lipids with V-amylose in maize, rice and oat starches. *J. Cereal Sci.* 18: 107-109.

Morrison, W. R., Milligan, T. P., and Azudin, M. N. 1984. A relationship between the amylose and lipid contents of starches from diploid cereals. *J. Cereal Sci.* 2: 257-271.

Morrison, W. R., Scott, D. C., and Karkalas, J. 1986. Variation in the composition and physical properties of barley starches. *Starch/Stärke* 38: 374-379.

Morrison, W. R., Tester, R. F., Gidley, M. J., and Karkalas, J. 1993c. Resistance to acid hydrolysis of lipid-complexed amylose and lipid-free amylose in lintnerised waxy and non-waxy barley starches. *Carbohydr. Res.* 245: 289-302

Morrison, W. R., Tester, R. F., Snape, C. E., Law, R., and Gidley, M. J. 1993a. Swelling and gelatinization of cereal starches. IV. Some effects of lipid-complexed amylose and free amylose in waxy and normal barley starches. *Cereal Chem.* 70: 385-391.

Mu-Forster, C., and Wasserman, B. P. 1998. Surface localization of zein storage proteins in starch granules from maize endosperm. *Plant Physiol.* 116: 1563-1571.

Muhr, A. H., Blanshard, J. M. V., and Bates, D. R. 1984. The effect of lintnerization on wheat and potato starch granules. *Carbohydr. Polym.* 4: 399-425

Muhrbeck, P. 1991. On crystallinity in cereal and tuber starches. *Starch/Stärke* 43: 347-348.

Myers, A. M., Morell, M. K., James, M. G., and Ball, S. G. 2000. Recent progress toward understanding biosynthesis of the amylopectin crystal. *Plant physiol.* 122: 989-997.

Nara, S., Takeo, H., and Komiya, T. 1981. Studies on the accessibility of starch by deuteration. *Starch/Stärke* 33: 329-331.

Newman, R. K. and Newman, C. W. 1991. Barley as a food grain. *Cereal Foods World.* 36: 800-805.

Nigam, P. and Singh, D. 1995. Enzyme and microbial systems involved in starch processing. *Enzyme Microb. Technol.* 17: 770-778.

Nilan, R. A. and Ullrich, S. E. 1993. Barley: taxonomy, origin, distribution, production, genetics, and breeding. In: *Barley Chemistry and Technology*, A. W. MacGregor and R. S. Bhatty eds. P1-29. American Association of Cereal Chemists, St. Paul.

Noda, T., Takahata, Y., Sato, T., Suda, I., Morishita, T., Ishiguro, K., and Yamakawa, O. 1998. Relationships between chain length distribution of amylopectin and gelatinization properties within the same botanical origin for sweet potato and buckwheat. *Carbohydr. Polym.* 37: 153-158.

Nordin, P. Moser, H., Rao, G., Girl, N., and Liang, T. 1970. Labeling of starch granules by bombardment with tritium atoms. *Starch/Stärke* 22: 256-261.

Oates, C. G. 1997. Towards an understanding of starch granule structure and hydrolysis. *Trends Food Sci.* Tech. 8: 375-380.

Ohtani, T., Yoshino, T., Hagiwara, S., and Maekawa, T. 2000. High-resolution imaging of starch granule structure using atomic force microscopy. *Starch/Stärke* 52: 150-153.

Oosteregetel, G. T., and van Bruggen, E. F. J. 1993. The crystalline domains in potato starch granules are arranged in a helical fashion. *Carbohydr. Polym.* 21: 7-12

Oostergetel, G. T., and van Bruggen, E. F. J., 1989. On the origin of low angle spacing in starch. *Starch/Stärke* 41: 331-335.

Orford, P. D., Ring, S. G. Carroll, V., Miles,M. J., and Morris, V. J..1987. The effect of concentration and botanical source on the gelation and retrogradation of starch. *J. Sci. Food Agric.* 39: 169-177

Oscarsson, M., Andersson, R., Salomonsson, A. C., and Åman, P. 1996. Chemical composition of barley samples focusing on dietary fiber components. *J. Cereal Sci.* 24: 161-170.

Parker, M. L. 1985. The relationship between A-type and B-type starch granules in the developing endosperm of wheat. *J. Cereal Sci.* 3: 271-278.

Parker, R. and Ring, S. G. 2001. Aspects of the physical chemistry of starch. *J. Cereal Sci.* 34: 1-17.

Perera, C., Lu, Z., and Jane, J. 2001. Comparison of physicochemical properties and structures of sugary-2 cornstarch with normal and waxy cultivars. *Cereal Chem.* 78: 249-256.

Peterson, D. M. and Qureshi, A. A. 1993. Genotype and environment effects on tocols of barley and oats. *Cereal Chem*. 70:157-162.

Pfannemüeller, B. 1987. Influence of chain length of short monodisperse amylose on the formation of A- and B-type X-ray diffraction patterns. *Int. J. Biol. Macromol*. 9: 105-108.

Planchot, V., Colonna, P., Gallant, D. J., and Bouchet, B. 1995. Extensive degradation of native starch granules by alpha-amylase from *Aspergillus fumigatus*. *J. Cereal Sci*. 21: 163-171.

Prentice, R. D. M., and Stark, J. R. 1992. Granule residues and "ghosts" remaining after heating A-type barley-starch granules in water. *Carbohydr. Res*. 227: 121-130.

Radosta, S., Kettlitz, B., Schierbaum, F., and Gernat, C. 1991.Studies on rye starch properties and modification. Part II. Swelling and solubility behaviour of rye starch granules. *Starch/Stärke* 44: 8-14.

Raeker, M. Ö., Gaines, C. S., Finney, P. L., and Donelson, T. 1998. Granule size distribution and chemical composition of starches from 12 soft wheat cultivars. *Cereal Chem.* 75: 721-728.

Rahaman, S., Kosar-Hashemi, B., Samuel, M. S., Hill, A., Abbott, D. C., Skerritt, J. H., Preiss, J., Appels, R., and Morell, M. K. 1995. The major proteins of wheat endosperm starch granules. *Aust. J. Plant Physiol.* 22: 793-803.

Raja, K. C. M. 1994. Modified properties of lintnerized cassava and maize starches. *Carbonhydr. Polym*. 24: 85-90.

Ratnayake, W. S., Hoover, R., and Warkentin, T. 2002. Pea starch: composition, structure and properties — a review. *Starch/Stärke* 34: 217-234.

Ratnayake, W. S., Hoover, R., Shahidi, F., and Perera, C., and Jane, J. 2001. Composition, molecular structure, and physicochemical properties of starches from four field pea (*Pisum sativum* L.) cultivars. *Food Chem.* 74: 189-202.

Reilly, P. J. 1985. Enzyme degradation of starch. In: *Starch Conversion Technology*. G. M. A. van Beynum and J. A. Roels eds. p.101-142. Marcel Dekker, New York.

Rickard, J. E., Asaoka, M., and Blanshard, J. M. V. 1991. The physico-chemical properties of cassava starch. *Trop. Sci.* 31: 189-207.

Ring, S. G. 1985. Some studies on starch gelation. *Starch/Stärke* 37: 80-83.

Ring, S. G., Colonna, Panson, K, J., Kalicheversky, M. T., Miles, M. J., Morris, V. J., and Orford, P. D. 1987. The gelation and crystallization of amylopectin. *Carbohydr. Res.* 162: 277-293.

Robin, J. P., Mercier, C., Charbonnière, R., and Guilbot, A. 1974. Lintnerized starches. Gel filtration and enzymatic studies of insoluble residues from prolonged acid treatment of potato starch. *Cereal Chem.* 51: 389-406.

Robyt, J. F. 1984. Enzymes in the hydrolysis and synthesis of starch. In: *Starch Chemistry and Technology*. R. L. Whistler, J. N. BeMiller, and E. F. Paschall eds. p87-123. Academic Press, Orlando, Florida.

Robyt, J. F. and French, D. 1970. The action patterns of porcine pancreatic α-amylase in relationship to the substrate site of the enzyme. *J. Biol. Chem.* 245: 1917-1927.

Rohwer, R. G. and Klem, R. E. 1984. Acid-modified starch: production and uses. In: *Starch Chemistry and Technology*. R. L. Whistler, J. N. BeMiller, and E. F. Paschall eds. p.529-541. Academic Press, Orlando, Florida.

Röper, H. 1996. Starch: present use and future utilization. In: *Carbohydrates as Organic Raw Materials III*. H. van Bekkum, H. Röper, and F. Voragen eds. p.17-35. VCH Verlagsgesellschaft Weinheim.

Röper, H. 2002. Renewable raw material in Europe – Industrial utilization of starch and sugar. *Starch/Stärke* 54: 89-99.

Russell, P. L. 1987. The ageing of gels from starches of different amylose/amylopectin content studied by differential scanning calorimetry. *J. Cereal Sci.* 6: 147-158.

Salomonsson, A. C., and Sundberg, B. 1994. Amylose content and chain profile of amylopectin from normal, high amylose and waxy barleys. *Starch/Stärke* 46: 325-328.

Salunkhe, D. K., Chavan, J. K., and Kadam, S. S. 1985. Post-harvest Biotechnology of Cereals. p.308-320. CRC Press, Boca Raton, Florida.

Sanders, E. B., Thompson, D. S., and Boyer, C. D. 1990. Thermal behavior during gelatinization and amylopectin fine structure for selected maize genotypes as expressed in four inbred lines. *Cereal Chem.* 67: 594-602.

Sargeant, J. G. 1980. Alpha-amylase isoenzymes and starch degradation. *Cereal Res. Commun.* 8: 77-86

Sarko, A. and Wu, H. H. 1978. The crystal structures of A-, B-, and C-polymorphs of amylose and starch. *Starch/Stärke* 30: 73-78.

Sarko, A., and Zugenmaier, P. 1980. Crystal structures of amylose and its derivatives: a review. *ACS Symp. Ser.* 141: 459-482.

Sasaki, T, and Matsuki, J., 1998. Effect of wheat starch structure on swelling power. *Cereal Chem.* 75: 525-529.

Sasaki, T., Yasui, T., and Matsuki, J. 2000. Effect of amylose content on gelatinization, retrogradation, and pasting properties of starches from waxy and nonwaxy wheat and their F1 seeds. *Cereal Chem.* 77: 58-63.

Saskatchewan Agriculture and Food, 2003. http://www.agr.gov.sk.ca/DOCS/crops/cereals/Hulless.asp.(accessed in September).

Schierbaum, F., Radosta, S., Richter, M., Kettlitz, B., and Gernat, C. 1991. Studies on rye starch properties and modification. Part I. Composition and properties of rye starch granules. *Starch/Stärke* 43: 331-339.

Schoch, T. J. 1969. Mechanochemistry of starch. *Wallerstein Lab. Commun.* 32: 149-172.

Schulman, A. H., Tomooka, S., Suzuki, A., Myllärinen, P., and Hizukuri, S. 1995. Structural analysis of starch from normal and shx (shrunken endosperm) barley (*Hordeum vulgare* L.). *Carbohydr. Res.* 275: 361-369.

Schwatz, D. 1982. Amylose distribution in the starch granule of maize endosperm. *Maydica* 27: 54-57.

Seguchi, M., and Yamada, Y. 1989. Study of proteins extracted from the surface of wheat starch granules with sodium dodecyl sulfate. *Cereal Chem.* 66: 193-196.

Shamekh, S., Forssell, P., Suortti, T., Autio, K., and Pontanen, K.1999. Fragmentation of oat and barley starch granules during heating. *J. Cereal Sci.* 30: 173-182.

Shannon, J. C., and Garwood, D. L. 1984. Genetics and physiology of starch development. In: *Starch: Chemistry and Technology*. R. L. Whistler, J. M. BeMiller, and E. F. Paschall eds. p.25-86. Academic Press, Orlando, Florida.

Shi, Y. C., and Seib, P. A. 1992. The structure of four waxy starches related to gelatinization and retrogradation. *Carbohydr. Res.* 227: 131-145.

Shi, Y. C., and Seib, P. A. 1995. Fine structure of maize starches from four wx-containing genotypes of the W64A inbred line in relation to gelatinization and retrogradation. *Carbohydr. Polym.* 26: 141-147.

Shi, Y. C., Capitani, T., Trzasko, P., and Jeffcoat, R. 1998. Molecular structure of a low-amylopectin starch and other high-amylose maize starches. *J. Cereal Sci.* 27: 289-299.

Shibanumn, K., Takeda, Y., Hizukuri, S., and Shibata, S. 1994. Molecular structures of some wheat starches. *Carbohydr. Polym.* 25: 111-116.

Shiotsubo, T. and Takahashi, K. 1984. Differential thermal analysis of potato starch gelatinization. *Agric. Biol. Chem.* 48: 9-17.

Shuey, W. C. and Tipples, K. H. 1980. In: *The Amylograph Handbook*. American Association of Cereal Chemists., St. Paul, MN

Shukla, T. P. 2003. Global corn and starch conversion business. http://www. frienterprises. com/GlobalCornProcessing.pdf. (accessed in September).

Sievert, D. and Pomeranz, Y. 1989. Enzyme-resistant starch. I. Characterization and evaluation by enzymatic, thermomechanical, and microscopic methods. *Cereal Chem.* 66: 342-347.

Singh, V. and Ali, S. Z. 2000. Acid degradation of starch. The effect of acid and starch type. *Carbohydr. Polym.* 41: 191-195.

Skerritt, J. H., Frend, A. J., Robson, L. G., and Greenwell, P. 1990. Immunological homologies between wheat gluten and starch granule proteins. *J. Cereal Sci.* 12: 123-136.

Song, Y. and Jane, J. 2000. Characterization of barley starches of waxy, normal, and high amylose varieties. *Carbohydr. Polym.* 41: 365-377.

Sosulski, F. W., Yook, C., and Arganosa, G. C. 1997. Functional properties of cationic pea starch. In: *Starch Structure and Functionality*. P. J. Frazier, A. M., Donald, and P. Richmond eds. p.36-41. The Royal Society of Chemistry, Cambridge, UK.

Soulaka, A. B., and Morrison, W. R. 1985. The amylose and lipid contents, dimensions, and gelatinisation characteristics of some wheat starches and their A- and B-granule fractions. *J. Sci. Food Agric.* 36: 709-718.

Sowa, S. M. H., and White, P. J. 1992. Characterization of starch isolated from oat groats with different amounts of lipid. *Cereal Chem*. 69: 521-527.

Stelwagen, P., Lehmussaari, A., and Vaara, T. 1988. The application of enzymes in grain processing. A paper presented at The 1st International Symposium Enzymes in the Forefront of Food and Feed Industries. Espoo, Finland.

Stoddard, F. L. 1999. Survey of starch particle-size distribution in wheat and related species. *Cereal Chem*. 76: 145-149.

Svegmark, K., and Hermansson, A. M. 1991. Distribution of amylose and amylopectin in potato starch pastes: effects of heating and shearing. *Food Structure*. 10: 117-129.

Swinkels, J. J. M. 1985a. Composition and properties of commercial native starches. *Starch/Stärke* 37: 1-5.

Swinkels, J. J. M. 1985b. Sources of starch, its chemistry and physics. In: *Starch Conversion Technology*. G. M. A. Van Beynum and J. A. Roels eds. p15-46, Marcel Dekker, New York.

Szejtli, J. 1991. Helical and cyclic structures in starch chemistry. *ASC Symp. Ser.*, 458:2-10.

Tabada, S., and Hizukuri, S. 1971. Studies on starch phosphates. Part 2. Isolation of glucose-3-phosphate and maltose phosphate by acid hydrolysis of potato starch. *Starch/Stärke* 23: 267-272.

Takeda, C., Takeda, Y., and Hizukuri, S. 1993b. Structure of the amylopectin fraction of amylomaize. *Carbohydr. Res*. 246: 273-281.

Takeda, Y., and Hizukuri, S. 1982. Location of phosphate groups in potato amylopectin. *Carbohydr, Res*. 102: 321-327.

Takeda, Y., Hizukuri, S., and Juliano, B. O. 1987b. Structures of rice amylopectin with low and high affinities for iodine. *Carbohydr. Polym.* 168: 79-88.

Takeda, Y., Maruta, Hizukuri, S., and Juliano, B. O. 1989. Structures of indica rice starches (IR48 and IR64) having intermediate affinity for iodine. *Carbohydr. Res.* 187: 287-294.

Takeda, Y., Shitaozono, T., and Hizukuri, S. 1988. Molecular structure of corn starch. *Starch/Stärke* 40: 51-54.

Takeda, Y., Takeda, C., Mizukami, H., and Hanashiro, I. 1999. Structures of large, medium and small starch granules of barley grain. *Carbohydr. Polym.* 38: 109-114.

Takeda, Y., Tomooka, S., and Hizukuri, S. 1993a. Structures of branched and linear molecules of rice amylose. *Carbohydr. Res.* 246: 267-272.

Tang, H., Ando, H., Watanabe, K., Takeda, Y., and Mitsunaga, T. 2000. Some physicochemical properties of small-, medium-, and large-granule starches in fractions of waxy barley grain. *Cereal Chem.* 77: 27-31.

Tang, H., Ando, H., Watanabe, K., Takeda, Y., and Mitsunaga, T. 2001a. Fine structures of amylose and amylopectin from large, medium, and small waxy barley starch granules. *Cereal Chem.* 78: 111-115.

Tang, H., Ando, H., Watanabe, K., Takeda, Y., and Mitsunaga, T. 2001b. Physicochemical properties and structures of large, medium and small granule starches in fractions of normal barley endosperm. *Carbohydr. Res.* 330: 241-248.

Tatge, H., Marshall, J., Martin, C., Edwards, E. A., and Smith, A. M. 1999. Evidence that amylose synthesis occurs within the matrix of the starch granule in potato tubers. *Plant Cell Environ.* 22: 543-550.

Temelli, F. 2001. Potential food applications of barley beta-glucan concentrate. *Barley Country,* Alberta Barley Commission, Vol. 10.

Tester, R. E. and Morrison, W. R. 1994. Properties of damaged starch granules. V. Composition and swelling of fractions of wheat starch in water at various temperatures. *J. Cereal Sci.* 20: 175-181.

Tester, R. E., and Morrison, W. R. 1990b. Swelling and gelatinization of cereal starches. II. Waxy rice starches. *Cereal Chem.* 67: 558-563.

Tester, R. F. 1997. Starch: the polysaccharide fractions. In: *Starch Structure and Functionality.* P. J. Frazier, A. M. Donald, and P. Richmond eds. p.163-171. The Royal Society of Chemistry, Cambridge.

Tester, R. F. and Debon, S. J. J. 2000. Annealing of starch — a review. *Int. J. Biol. Macromol.* 27: 1-12.

Tester, R. F., and Karkalas, J. 1996. Swelling and gelatinization of oat starches. *Cereal Chem.* 73: 271-277.

Tester, R. F., and Morrison, W. R. 1990a. Swelling and gelatinization of cereal starches. I. Effects of amylopectin, amylose and lipids. *Cereal Chem.* 67: 551-557.

Tester, R. F., and Morrison, W. R.1992. Swelling and gelatinization of cereal starches. III. Some properties of waxy and nonwaxy barley starches. *Cereal Chem.* 69: 654-658.

Tester, R. F., Debon, S. J. J., Qi, X., Sommerville, M. D., Yousuf, R., and Yusuph, M. 2001. Amylopectin crystallization in starch. In*: Starch Advances in Structure and Function*, T. L. Barsby, A. M. Donald, and P. J. Frazier eds. p.97-102. The Royal Society of Chemistry, Cambridge.

Textor, S. D., Hill, G. A., Macdonald, D. G., and St. Denis, E. 1998. Cold enzyme hydrolysis of wheat starch granules. *Can. J. Chem. Eng.* 76: 87-93.

Tharanathan, R. N., and Ramadas Bhat, U. 1988. Scanning electron microscopy of chemically treated black gram (*Phaseolus mango*) and ragi (*Eleusine coracana*) starch granules. *Starch/Stärke*, 40, 378-382.

Thiewes, H. J. and Steeneken, P. A. M. 1997. Comparison of Brabender viskograph and the rapid visco analyzer. 1. Statistical evaluation of the pasting profile. *Starch/Stärke* 49: 85-92.

Tian, S. J., Rickard, J. E., and Blanshard, J. M. V. 1991. Physicochemical properties of sweet potato starch. *J. Sci. Food Agric.* 57: 459-491.

Tibelius, C. and Trenholm, H. L. 1996. Coproducts and near coproducts of fuel ethanol fermentation from grain. Prepared for Agriculture and Agri-Food Canada, Canadian green plan ethanol program. Ottawa, ON.

Trommsdorff, U., Tomka, I. 1995. Structure of amorphous starch. 1. An atomistic model and X-ray scattering study. *Macromolecules* 28: 6128-6137.

Tsai, M. L., Li, C. F., Lii, C. Y. 1997. Effects of granular structures on the pasting behaviors of starches. *Cereal Chem.* 74: 750-757.

Umeki, K. and Kainuma, K. 1981. Fine structure of nageli amylodextrin obtained by acid treatment of defatted waxy maize starch — structural evidence to support the double-helix hypothesis. *Carbohydr. Res.* 96: 143-159.

Valetudie, J. C., Colonna, P., Bouchet, B., and Gallant, D. J. 1993. Hydrolysis of tropical tuber starches by bacterial and pancreatic α-amylases. *Starch/Stärke*, 45, 270-276.

van Soest, J. J. G., de Wit, D., Tournois, H., and Vliegenthart, J. F. G. 1994. Retrogradation of potato starch as studied by fourier transform infrared spectroscopy. *Starch/Stärke* 46: 453-457.

Vasanthan, T. 1994. Effect of physical modification on starch structure and physicochemical properties. Ph.D. Thesis, Memorial University of Newfoundland.

Vasanthan, T. and Bhatty, R. S. 1996. Physicochemical properties of small- and large-granule starches of waxy, regular, and high-amylose barleys. *Cereal Chem*. 73, 199-207.

Vasanthan, T., and Hoover, R. 1992. A comparative study of the composition of lipids associated with starch granules from various botanical sources. *Food Chem*. 43: 19-27.

Vasanthan, T., Bergthaller, W., Driedger, D., Yeung, J., and Sporns, P. 1999. Starch from Alberta potatoes: wet-isolation and some physicochemical properties. *Food Res. Int*. 32: 355-365.

Vasanthan, T., Bhatty, R. S., Tyler, R. T., and Chang, P. 1997. Isolation and cationization of barley starches at laboratory and pilot scale. *Cereal Chem*. 74: 25-28.

Villareal, C. P., Cruz, N. M. de la, and Juliano, B. O. 1994. Rice amylose analysis by near-infrared transmittance spectroscopy. *Cereal Chem*. 71: 292-296.

Virtanen, T., Autio, K., Suortti, T., and Poutanen, K. 1993. Heat-induced changes in native and acid-modified oat starch pastes. *J. Cereal Sci*. 17: 137-145.

Waigh T. A., Perry, P., Riekel, C., Gidley, M. J., and Donald, A. M. 1998. Chiral side-chain liquid-crystalline polymeric properties of starch. *Macromolecules* 31: 7980-7984.

Waigh, T. A., Hopkinson, I., Donald, A. M., Butler, M. F., Heidelbach, F., and Riekel, C. 1997. Analysis of the native structure of starch granules with X-ray microfocus diffraction. *Macromolecules* 30: 3813-3820.

Wang, J., Jiang, G., Vasanthan, T., and Sporns, P. 2000. MALDI-MS characterization of maltooligo/polysaccharides from debranched starch amylopectin of corn and barley. *Starch/Stärke* 51: 243-248.

Wang, Y. J., White, P., and Pollak, L. 1993. Physicochemical properties of starches from mutant genotypes of the Oh43 inbred line. *Cereal Chem.* 70: 199-203.

Watanabe, T. and French, D. 1980. Structural features of naegeli amylodextrins as indicated by enzymic degradation. *Carbonhydr. Res.* 84: 115-123.

White, P. J., Abbas, I. R., and Johnson, L. J. 1989. Freeze-thaw stability and refrigerated-storage retrogradation of starches. *Starch/Stärke* 41: 176-180.

Wolf, B. W., Bauer, L. L., and Fahey Jr., G. C. 1999. Effects of chemical modification on in vitro rate and extent of food starch digestion: an attempt to discover a slowly digested starch. *J. Agric. Food Chem.* 47, 4178-4183.

Wootton, M., Panozzo, J., and Hong, S.-H. 1998. Differences in gelatinization behavior between starches from Australian wheat cultivars. *Starch/Stärke* 50: 154-158.

World Crops and Cropping Systems, 2003. http://mckenna.cses.vt.edu/cses/3444 /3444 lecl2.html. (accessed in September)

Wu, H. C. H. and Sarko, A. 1978a. The double-helical molecular structure of crystalline B-amylose. *Carbohydr. Res.* 61: 7-25.

Wu, H. C. H. and Sarko, A. 1978b. The double-helical molecular structure of crystalline A-amylose. *Carbohydr. Res.* 61: 27-40.

Xue, Q., Wang, L., Newman, R. K., Newman, C. W., and Graham, H. 1997. Influence of the hulless, waxy starch and short-awn genes on the composition of barleys. *J. Cereal Sci.* 26: 251-257.

Yamaguchi, M., Kainuma, K., and French, D. 1979. Electron microscopic observations of waxy maize starch. *J. Ultrastruct. Res.* 69: 249-261.

Yasui, T., Matsuki, J., Sasaki, T., and Yamamori, M. 1996. Amylose and lipid contents, amylopectin structure, and gelatinization properties of waxy wheat (*Triticum aestivum*) starch. *J. Cereal Sci*. 24: 131-137.

Yoshimoto, Y., Takenouchi, T., and Takeda, Y. 2002. Molecular structure and some physicochemical properties of waxy and low-amylose barley starches. *Carbohydr. Polym*. 47: 159-167.

Yoshimoto, Y., Tashiro, J., Takenouchi, T., and Takeda, Y. 2000. Molecular structure and some physicochemical properties of high-amylose barley starches. *Cereal Chem*. 77: 279-285.

Young, A. H. 1984. Fractionation of starch. In: *Starch: Chemistry and Technology*. R. L. Whistler, J. N. BeMiller, E. F. Paschall eds. p. 249-283. Academic Press, Orlando, Florida.

Yuan, R. C., Thompson, D. S., and Boyer, C. D. 1993. Fine structure of amylopectin in relation to gelatinization and retrogradation behavior of maize starches from three wx-containing genotypes in two inbred lines. *Cereal Chem*. 70: 81-89.

Yun, S. H., and Matheson, N. K. 1992. Structural changes during development in the amylose and amylopectin fractions (separated by precipitation with concanavalin A) of starches from maize genotypes. *Carbohydr. Res*. 227: 85-101.

Yuryev, V. P., Kalistratova, E. N., van Soest, J. G. J., and Niemann, C. 1998. Thermaldynamic properties of barley starches with different amylose content. Starch/Stärke 50: 463-466.

Zeleznak, K. J., and Hoseney, R. C. 1987. The glass transition in starch. *Cereal Chem*. 64: 121-124.

Zeng, M., Morris, C. F., Batey, I. L., and Wrigley, C. W. 1997. Sources of variation for starch gelatinization, pasting, and gelation properties in wheat. *Cereal Chem*. 74: 63-71.

Zheng, G. H., Han, H. L., and Bhatty, R. S. 1998. Physicochemical properties of zero amylose hull-less barley starch. *Cereal Chem*. 75: 520-524.

Ziegler, G. R., Thompson, D. B., and Casasnovas, J. 1993. Dynamic measurement of starch granule swelling during gelatinization. *Cereal Chem*. 70: 247-251.

Zobel, H. F. 1992. Starch granule structure. In: *Developments in Carbohydrate Chemistry*. R. J. Alexander and H. F. Zobel eds., p. 1-36. American Association of Cereal Chemistry, St. Paul, MN.

Zobel, H. F. 1984. Gelatinization of starch and mechanical properties of starch pastes. In: *Starch Chemistry and Technology*. R. L. Whistler, J. N. BeMiller, and E. F. Paschall eds. 2nd Ed. p.183-247. Academic Press, Orlando.

Zobel, H. F. 1988a. Starch crystal transformations and their industrial importance. *Starch/Stärke* 40: 1-7.

Zobel, H. F. 1988b. Molecules to granules — a comprehensive starch review. *Starch/Stärke* 40: 44-50.

CHAPTER 2

Granule Morphology, Composition and Amylopectin Structure[1]

2.1 Introduction

Barley is a grass belonging to the family Poaceae, the tribe Triticeae, and the genus Hordeum (Nilan and Ullrich, 1993). Cultivated barley *(Hordeum vulgare* L.*)* is the fourth largest cereal grain crop produced worldwide and the most under utilized cereal grain in terms of human consumption (Bhatty, 1993). About 90% of barley grain is used in alcoholic beverage production and as a livestock feed. Barley is an excellent source of complex carbohydrates, which constitute about 80% of barley grain weight (Szczodrak et al., 1992). Starch is the largest single component in barley grain, representing up to 65% of the kernel dry weight. Hull-less or naked barley (HB) production in Canada is estimated to be between 300,000 and 350,000 ha with an estimated grain production of about 800,000 t in 1998 (Bhatty, 1999). Canada is the leading producer and the major source of published information on HB. Several two- and six-rowed cultivars of HB have been registered in Canada in the last 15 years, including waxy and zero-amylose types (Bhatty, 1995; Bhatty and Rossnagel, 1997). HB cultivars were developed first for use in swine and poultry feeds and later for use in human foods as a source of dietary fiber. HB has been used for the preparation of food malt, production of ethanol, extraction and enrichment of β-glucan, preparation of native and modified starches and preparation of bran and flour for use in bakery products (Bhatty, 1995, 1999). In Canada, the emphasis now is to extend the use of HB in food and non-food industries, including the malting and brewing industries (Bhatty, 1999). HB contains 60-75% starch (Bhatty, 1997). Amylose content in HB starches varies from 0 to 40% (Zheng et al., 1998). Granule size varies from large lenticular to small spherical (Vasanthan and Bhatty, 1995). HB genotypes [normal (20-30% amylose), waxy (1-5% amylose), zero-amylose and high-amylose (30-45%)] have been developed via traditional breeding practices. Recently, several new HB genotypes have been developed at the Crop Development Centre, University of Saskatchewan. A preliminary study showed that starch granules from these new genotypes of HB differed widely in composition, granule morphology, and physicochemical characteristics. Therefore, a study of the structure-property relationships of these starches is needed to understand their functionality in food systems. With this information and available genetic variation, it should be possible to produce HB starches, which are designed for specific uses in food industry.

---

[1] A version of this chapter was published in *Food Chemistry*, 2001, 74: 395-405.

The intent of this study was to characterize the granule morphology, composition, and amylopectin structure of starches from 10 genotypes of HB grown at Saskatoon, Saskatchewan in 1998 and compare the aforementioned barley starch properties to those of commercial maize starches. This is of importance because maize starches are currently used in North America in a number of food and industrial applications.

2.2 Materials and methods

2.2.1 Materials

Four registered cultivars (CDC Alamo, CDC Candle, CDC Dawn, and Phoenix) and six breeding lines (SB 94912, SB 94917, SR 93102, SB 94860, SB 94893, and SB 94897) of HB grown and harvested at Saskatoon in 1998 were obtained from the Crop Development Centre, University of Saskatchewan, Saskatoon, SK. The barley grains were ground in a UDY cyclone sample mill (UDY Lab Equipment and Supplies, Ft. Collins, CO) equipped with a 0.5 mm screen. Commercial waxy and regular maize starches (A.E. Staley Manufacturing Company, Decatur, IL) were used for comparison. Isoamylase (EC 3.2.1.68, debranching enzyme) and Maltoheptaose (DP7, internal standard) were obtained from Sigma Chemical Co. (St. Louis, MO) and Sep-pak C18 cartridges were from Waters Corp. (Milford, MA). Macro-sep centrifuge concentrators (30K) were from Filtron Tech Corp. (Northborough, MA); Sephadex G-10 (desalting columns) from Amersham Pharmacia Biotech AB, (Uppsala, Sweden); and 2,5-dihyroxybenzoic acid (matrix) was from Aldrich Chemical Co. (Milwaukee, WI).

2.2.2 Starch isolation

Starch was isolated from ground barley grains according to the method of Wu et al., (1979). Ground barley flour was blended with 0.06M NaOH (1:15-20 w/v) in a Waring blender for 5 min. The slurry was stirred at room temperature (24°C) for 2 h with an overhead stirrer, and then passed through two layers of cheesecloth. Additional 0.06M NaOH was used during filtration. The filtrate was centrifuged at 7,500xg for 15 min and the supernatant was decanted. The residue was washed with 0.06M NaOH and centrifuged twice. The upper brown layer of the residue was removed and discarded.

The lower brown layer on the top of the white starch layer in the centrifuge bottle was scraped with a spatula and recovered by washing and gravity settling and added back to the main stock starch. The crude starch was washed three more times with distilled water, neutralized with 1M HCl, and finally washed with 95% ethanol. The starch was dried overnight at 40°C, ground, and screened through a No. 60 mesh sieve (W. S. Tyler, Ontario).

2.2.3 Chemical composition of grain and starch

Quantitative estimation of moisture, ash and nitrogen were performed by standard AACC (1983) procedures (Methods 44-15A, 08-01, and 46-10, respectively). Lipids were determined by procedures outlined in an earlier publication (Vasanthan and Hoover, 1992). Apparent and total amylose contents were determined by the method of Chrastil (1987). Starch content was determined using a total starch Megazyme assay kit (Megazyme International Ireland Limited, Wicklow, Ireland). Quantification of β-glucan was performed using an assay kit from Megazyme.

2.2.4 Granule morphology

Granule morphology of native starches was studied by scanning electron microscopy. Starch samples were mounted on circular aluminum studs with double-sided sticky tape and then coated with 12 nm of gold and examined and photographed in a JEOL (JSM 6301FXV) scanning electron microscope (JEOL, Ltd, Tokyo, Japan) at an accelerating voltage of 5 kV. Sample used for transmission electron microscopy was prepared following the method of Garcia et al. (1997) and examined in a Philips CM12 transmission electron microscope (F. E. I. Company, Tacoma, WA) at 60 kV without further staining.

2.2.5 Granule size analysis

Granule size distribution was evaluated by a BioQuant system IV image analyzer (BioQuant R and M, Biometrics, Inc. Nashville, TN) equipped with an image acquisition system and a computer processor. Five hundred starch granules were observed for each sample. Granule size was expressed in terms of the diameter of image surface. The weight of starch granules was derived from the volume of the granules. The volume of granules was calculated assuming spherical particles.

2.2.6 Molecular characterization of amylopectin

Starch (100 mg) was dispersed in 9 ml distilled water and heated in a boiling water bath for 1 h. After being cooled to room temperature, 1ml sodium acetate buffer (pH 3.5) and 1ml isoamylase solution (30,000U) were added to the above starch solution in sequence. The mixture was incubated in a shaker bath at 40°C for 48 h to complete the debranching reaction. The debranched starch solution was boiled for 5 min to inactivate the enzymes, cooled, and then 10 ml solution were filtered through a Sep-pak C18 cartridge at a flow rate of 1 ml/min. The filtrate was then put into a 30K Macro-sep concentrator and centrifuged at 5,000xg for 90 min. The 30K Macro-sep filtrate (2 ml) was loaded on a Sephadex G10 desalting column (1.8x13 cm). A flow rate of 0.7 ml/min was maintained as 1 ml fractions were collected. Sample fractions (No. 10 to 17) were combined and made up to 10 ml. This sample solution was used for matrix-assisted laser desorption/ionization mass spectrometry (MALDI-MS) analysis following the procedure of Wang et al. (1999).

2.2.7 Statistical analysis

All measurements are means of two independent samples analyzed by the Statistical Analysis System for Windows Version 8 (SAS Institute, Cary, NC). Levels of significance used were at $P < 0.1$, $P < 0.05$, and $P < 0.01$.

2.3 Results and discussion

2.3.1 Chemical composition of barley grains

The chemical composition of 10 genotypes of HB grains is presented in Table 2-1. Starch, β-glucan, protein, lipids, and ash contents were in the ranges of 56.0-64.7%, 3.7-7.7%, 11.5 - 14.2%, 4.7-6.8%, and 1.8-2.4%, respectively. These values are within the ranges reported for registered Canadian (Bhatty and Rossnagel, 1998) and USA (Oscarsson et al., 1997; Czuchajowska et al., 1992) barley cultivars. Starch content was negatively correlated with protein content ($r = -0.84$, $P < 0.01$). The β-glucan content of normal starch HB grains was 3.65 and 4.44%, respectively, in CDC Dawn and Phoenix. However, in all other genotypes the β-glucan content was higher than 5.9%. β-Glucan content showed no correlation with amylose content. Bhatty (1999) reported that the β-glucan content in 10 different Canadian HB cultivars was positively correlated with total dietary fiber content ($r = 0.81$, $P < 0.01$) and soluble fiber ($r = 0.86$, $P < 0.01$). Other studies have shown that the β-glucan content of barley is influenced by cultivar and growth environment (Lee et al., 1997; Perez-Vendrell et al., 1996). The

Table 2-1 Chemical composition of hull-less barley grains

Genotype	Starch type[a]	Starch (% db)	β-Glucan (% db)	Protein (% db)	Lipids (% db)	Ash (% db)	Other[b] (% db)
CDC Alamo	Waxy (Zero amylose)	58.47	7.27	13.82	6.57	1.94	9.87
CDC Candle	Waxy	64.73	6.38	11.78	6.13	1.86	6.77
SB 94912	Waxy	59.66	7.14	12.99	6.06	1.77	10.25
SB 94917	Waxy (Compound granules)[c]	58.19	7.41	12.93	6.81	2.10	10.73
SR 93102	Normal amylose (Compound granules)[c]	59.87	5.94	12.80	5.72	1.78	11.90
SB 94860	Normal amylose (Compound granules)[c]	61.02	6.25	13.15	5.34	1.90	10.33
Phoenix	Normal amylose	63.73	4.44	12.57	5.60	1.82	9.40
CDC Dawn	Normal amylose	64.61	3.65	11.53	5.19	1.78	10.59
SB 94893	High amylose	55.95	7.04	14.20	4.81	2.36	13.26
SB 94897	High amylose	56.58	7.67	13.98	4.69	2.33	12.61
LSD[d]		1.30	0.45	0.23	0.32	0.18	

[a] Based on amylose content

[b] Mainly dietary fiber components, including pentosans, cellulose, lignin, uronic acid and low molecular weight carbohydrates (Bhatty, 1999)

[c] Some of the starch granules appeared to be a cluster of a few irregular compound starch granules under scanning electron microscopy (Figures 2-1 and 2-3).

[d] Least significant difference at $P < 0.05$

ash content of the high-amylose HB genotypes, SB 94893 and SB 94897, was higher than that of the other HB genotypes (Table 2-1). The HB genotypes showed a broad range of crude protein levels (11.5-14.2%). High levels of protein are due to a concentration effect caused by the lack of hull and/or are the result of breeding for increased protein content in feed barley (Edney et al., 1992). The genotypes used in this study were grown at the same location in Saskatchewan. Therefore, the observed variation in protein content (Table 2-1) cannot be attributed to soil type, climatic conditions or applied nitrogen fertilizer. Lipid contents of HB were in the range of 4.7-6.8% and in the order of waxy > normal > high-amylose starch types.

2.3.2 Isolation and chemical composition of HB starches

Average yield and extraction efficiency of isolated starches were 44.4% of the total grain weight (dry basis) and 70.9%, respectively. Waxy HB genotypes with a high β-glucan content (6.4-7.4%) gave lower starch yields (42.1%) and extraction efficiencies (68.0%). The low values for protein (N x 6.25, 0.2-0.4%) and ash (0.06-0.40%) contents showed that the starches were of high purity. Isolated starches contained 95-98% starch. β-Glucan levels were very low (0.01-0.06%; Table 2-2). Free lipids [obtained by extraction with $CHCl_3$-CH_3OH (CM)] ranged from 0.1 to 0.3%. However, variation in bound lipid content [obtained by extraction of CM residues with hot n-propanol-water (PW)] was higher (0.3-1.7%). Bound lipid content was positively correlated ($r = 0.92$, $P < 0.01$) with total amylose content. It is plausible that both free and bound lipids may be present on the granule surface as well as within the granule interior. The bound lipids probably represent: (1) lipids that are present in the form of

Table 2-2 Chemical composition of hull-less barley and maize starches

Genotype	Starch (% db)	Amylose (% db)[a]		Lipid (% db)[b]		Protein (% db)	Ash (% db)	β-Glucan (% db)
		Apparent	Total	CM	PW			
CDC Alamo	97.80	0	0	0.22	0.34	0.26	0.06	0.06
CDC Candle	96.88	3.81	4.31	0.18	0.75	0.25	0.19	0.06
SB 94912	98.08	4.42	6.44	0.14	0.65	0.26	0.31	0.02
SB 94917	97.57	4.03	4.60	0.15	0.48	0.38	0.24	0.04
SR 93102	96.94	24.61	27.64	0.16	1.11	0.42	0.30	0.04
SB 94860	96.09	22.95	29.03	0.20	1.32	0.43	0.31	0.06
Phoenix	96.50	23.80	25.84	0.18	0.90	0.30	0.20	0.03
CDC Dawn	96.67	22.49	23.64	0.11	0.80	0.36	0.20	0.03
SB 94893	96.63	38.63	44.52	0.17	1.69	0.43	0.42	0.01
SB 94897	96.48	33.90	41.73	0.12	1.22	0.41	0.36	0.02
Waxy maize	97.07	0	0.62	0.23	0.27	0.21	0.09	–
Normal maize	98.21	21.59	24.45	0.29	0.93	0.33	0.07	–
LSD[c]	1.13	0.64	1.11	0.05	0.09	0.03	0.06	0.02

[a] Apparent and total amylose determined by I_2 binding before and after removal of bound lipids by hot 1- propanol-water 2:3:1 v/v.

[b] Lipids extracted from native starch by chloroform-methanol (CM) 2:1 v/v at 25°C (mainly free lipids) and by hot 1-propanol-water (PW) 3:1 (v/v) from the residue left after CM extraction (mainly bound lipids), respectively.

[c] Least significant difference at $P < 0.05$.

V-amylose-lipid inclusion complexes (Morrison, 1981); and (2) lipids that are trapped between starch chains (Morrison, 1981).

The apparent and total amylose contents of HB starches ranged from 0-39% and 0-45%, respectively (Table 2-2) and the amounts of amylose complexed with native lipids (total amylose-apparent amylose) ranged from 0.5 to 7.8%.

2.3.3 Granule morphology

HB starch granules consist mostly of a mixture of large lenticular granules and smaller, irregularly shaped granules (Figure 2-1). Maize starch granules are angular and more uniform in size with polyhedral faces (Figure 2-1). "Pin holes" and equatorial grooves or furrows were present on large granules of HB and maize starches (Figure 2-2). Starches of SB 94917, SR 93102 and SB 94860 consisted of small irregularly shaped granules (Figure 2-1), large oval shaped granules (Figures 2-1 and 2-2), and very large "dumbbell" shaped and compound granules (clusters of a few granules but looked like single granules) (Figures 2-3 and 2-4). Compound granules were more predominant in SB 94917 and SR 93102 than in SB 94860 (Figure 2-1).

2.3.4 Granule size distribution

Granule size distributions of the starches are presented in Figure 2-5 and size variation of small (≤10 μm) and large (>10 μm) starch granules are presented in Table 2-3. HB starches showed a bimodal size distribution in the diameter range of 2-30 μm, whereas the maize starches showed a relatively narrow and uniform size distribution. The average granule size of HB starches (6.2-9.8 μm) was smaller than that for the maize

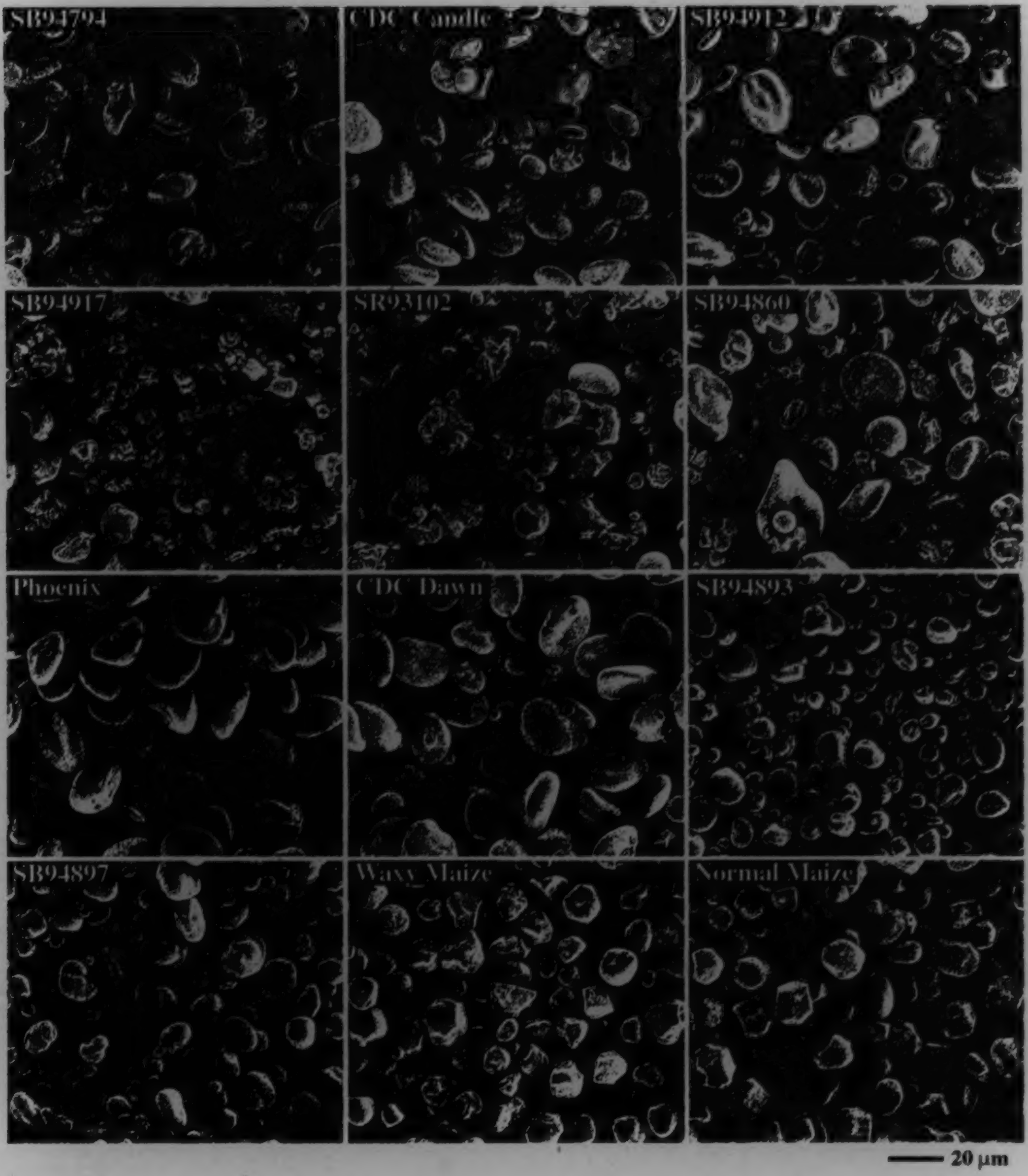
SB94794
CDC Candle
SB94912
SB94917
SR93102
SB94860
Phoenix
CDC Dawn
SB94893
SB94897
Waxy Maize
Normal Maize
20 μm

Figure 2-1 Scanning electron micrographs of hull-less barley and maize starches (Magnification X450).

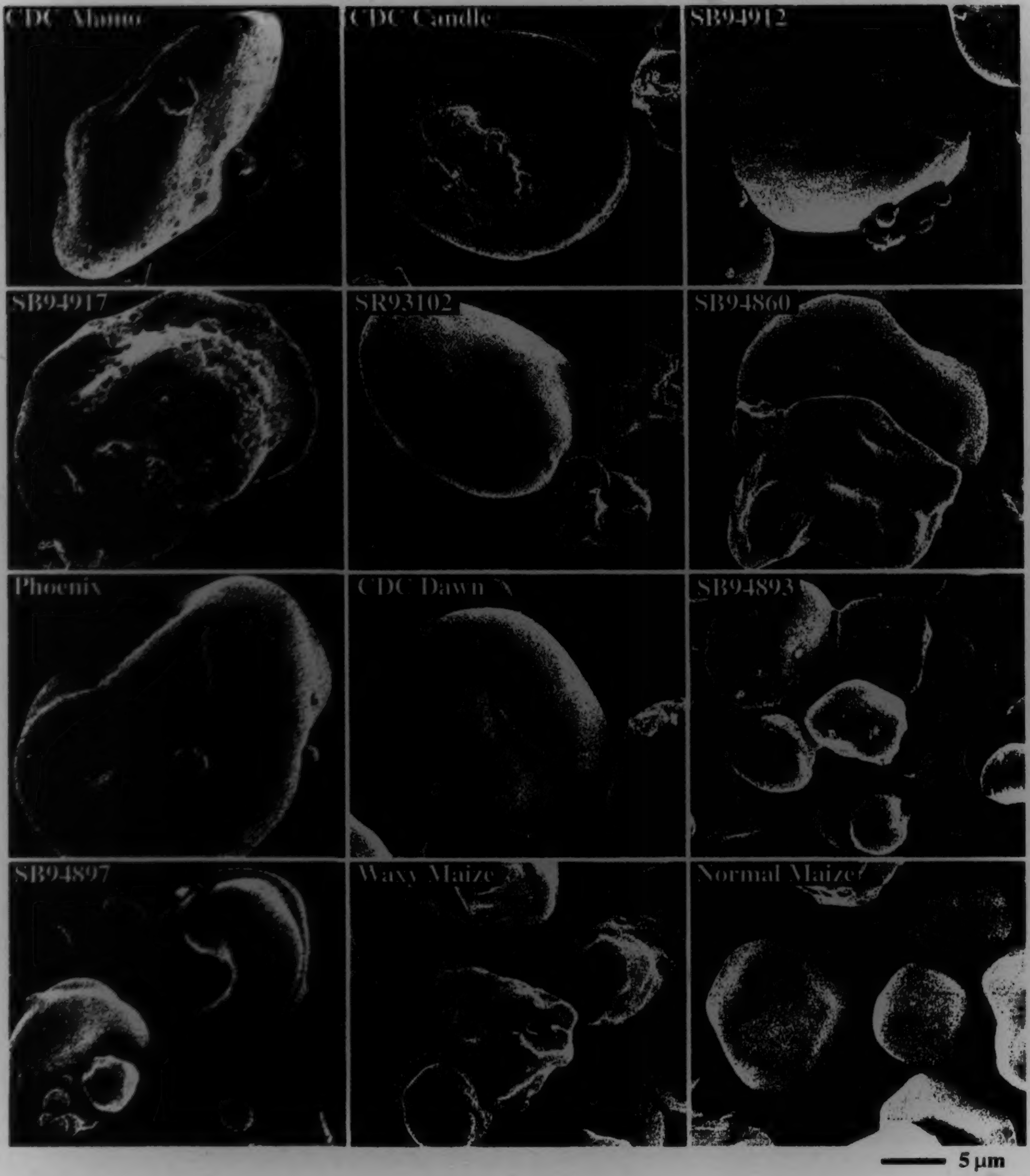
CDC Alamo
CDC Candle
SB94912
SB94917
SR93102
SB94860
Phoenix
CDC Dawn
SB94893
SB94897
Waxy Maize
Normal Maize
5 µm

Figure 2-2 Scanning electron micrographs of hull-less barley and maize starches (Magnification X2200).

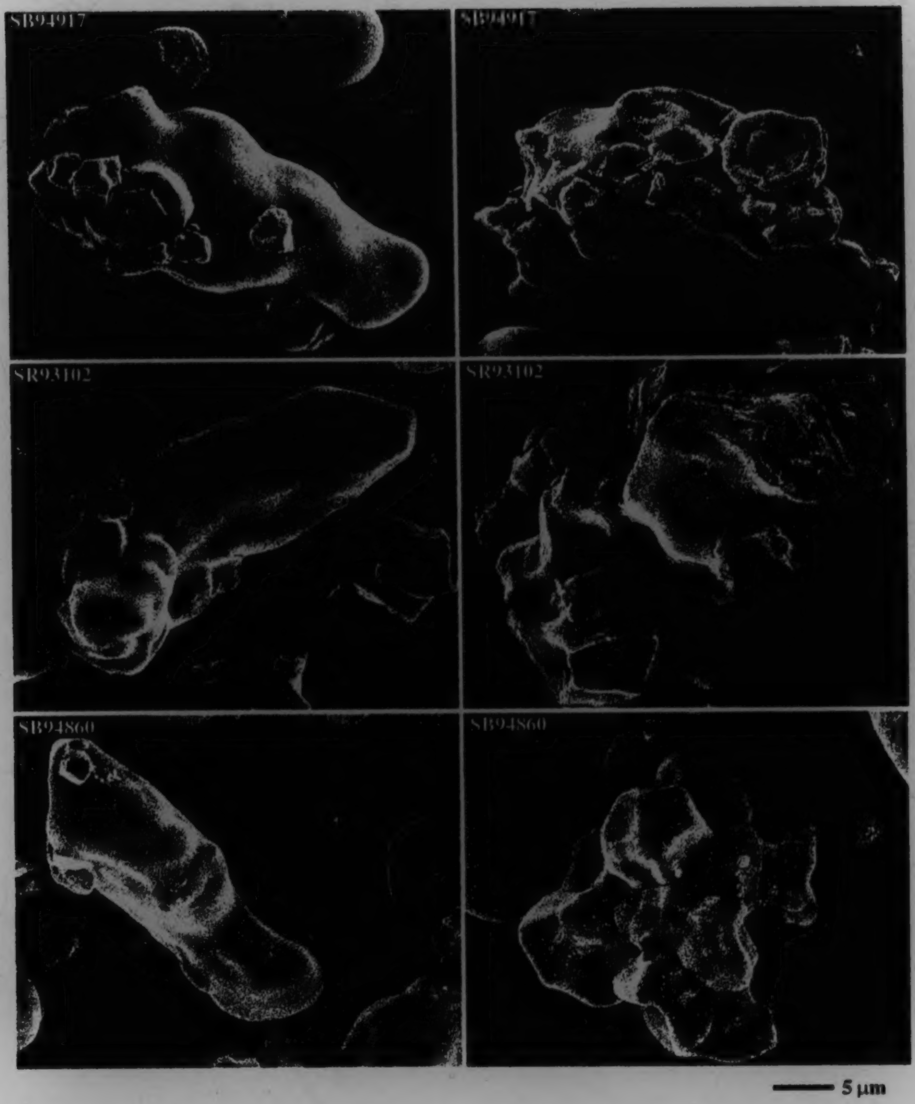
SB94917
SB94917
SR93102
SR93102
SB94860
SB94860
5 μm

Figure 2-3 Scanning electron micrographs of hull-less barley starches from SB 94917, SR 93102, and SB 94860 (Magnification X2000).

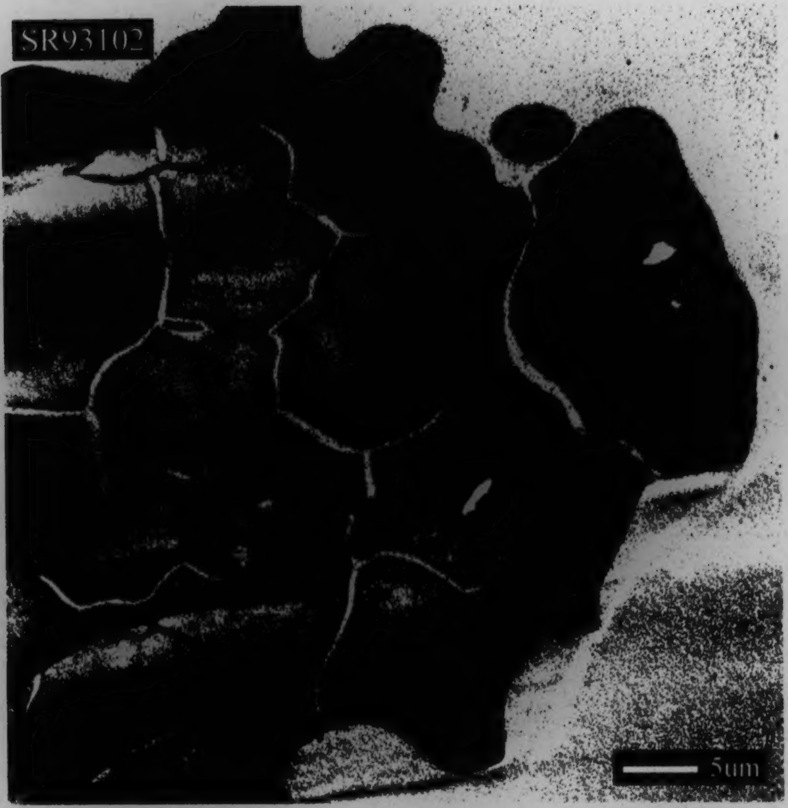

Figure 2-4 Transmission electron micrograph of compound hull-less barley starch granules from SR 93102 (Magnification X7200).

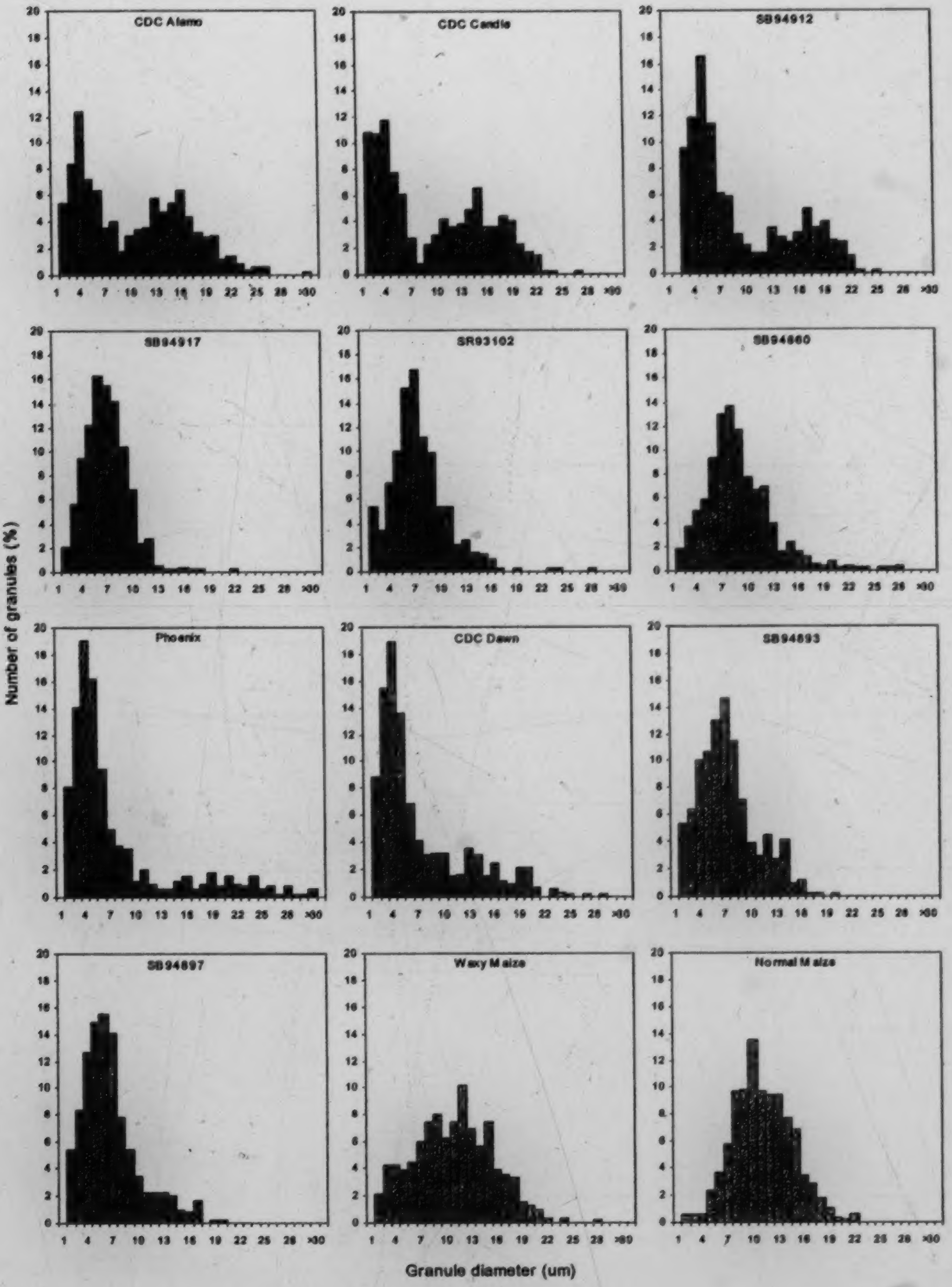

Figure 2-5 Granule size distribution of hull-less barley and maize starches.

Table 2-3 Granule size and size distribution of hull-less barley and maize starches

Genotype	Average diameter (μm)			Number (%)		Weight (%)	
	Mean	Small[a]	Large	Small	Large	Small	Large
CDC Alamo	9.8	4.5	15.6	52.1	47.9	4.6	95.4
CDC Candle	9.1	4.0	15.4	55.9	44.1	4.5	95.5
SB 94912	8.8	5.0	16.2	66.3	33.7	7.9	92.1
SB 94917	6.4	6.0	12.2	92.9	7.1	66.9	33.1
SR 93102	6.9	5.9	12.7	84.8	15.2	41.1	58.9
SB 94860	8.4	6.5	13.5	71.7	28.3	24.7	75.3
Phoenix	7.1	4.2	18.8	80.6	19.5	7.8	92.2
CDC Dawn	6.7	4.2	15.6	77.3	22.7	11.0	89.0
SB 94893	6.8	5.5	12.6	82.8	17.2	37.8	62.2
SB 94897	6.2	5.2	13.2	87.5	12.5	39.3	60.7
Waxy maize	10.6	6.3	13.9	46.8	53.2	9.9	90.1
Normal maize	10.3	7.7	13.2	46.7	53.3	16.0	84.0

[a] Granule diameter ≤ 10 μm.

(10.3-10.6 μm) (Table 2-3) and wheat (Raeker et al., 1998; Stoddard, 1999) starches. The proportions of small and large granules by total number and by total weight differed among genotypes. In compound waxy and compound normal HB starches (SB 94917, SB 94860, and SR 93102), small granules of SB 94917 (waxy) constituted the largest proportion of the total number of starch granules (93%) and total weight (67%). The proportion of small granules by weight in compound normal (SB 94860 and SR 93102), high-amylose (SB 94893 and SB 94897) and normal (Phoenix and CDC Dawn) HB starches were 25-41%, 38-39% and 8-11%, respectively. Large granules from waxy (CDC Alamo, CDC Candle, and SB 94912) and normal (Phoenix and CDC Dawn) HB starches constituted 34-48% and 20-23% of the total number of starch granules, respectively, and made up 89-96% of the total starch weight. Small granules from high-amylose HB starches constituted 83-88% of the total number of starch granules, but accounted for only 38-39% of the total starch weight (Table 2-3).

The proportion of small granules by number was correlated with total amylose content ($r = 0.59$, $P < 0.1$). The average granule diameter was negatively correlated with total amylose content ($r = -0.65$, $P < 0.05$). The correlations mentioned above have also been reported for other barley starches (Czuchajowska et al., 1992; Szczodrak and Pomeranz, 1991; Morrison et al., 1986).

2.3.5 Amylopectin structure

The MALDI-MS spectrum and chain length distribution of debranched amylopectin from high-amylose (SB 94893) HB starch are presented in Figure 2-6. Debranched amylopectins of all HB starches had nearly similar chain length distributions, with the highest peak at degree of polymerization (DP) 12 (Table 2-4, Figure 2-6). The

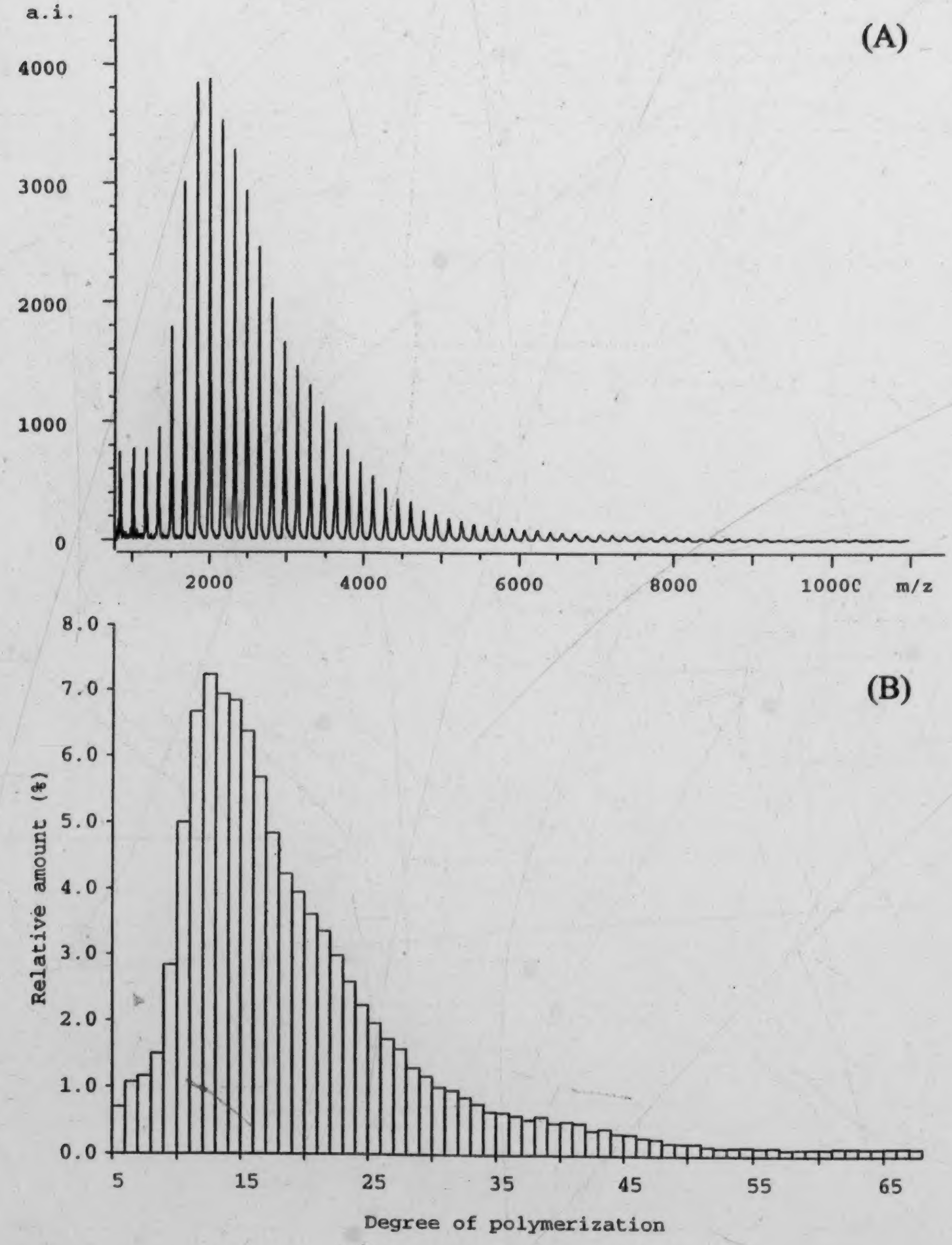

Figure 2-6 MALDI-MS spectrum (A) and chain length distribution (B) of debranched hull-less barley starch (SB 94893).

Table 2-4 Chain length distribution of debranched amylopectins of hull-less barley and maize starches

Genotype	Peak DP[a]	CL[b]	BP[c] (%)	Chain length distribution (%)		
				DP 5-17	DP 18-34	DP 35-67
CDC Alamo	12	18.1	5.5	57.4	38.0	4.5
CDC Candle	12	17.6	5.7	58.8	36.3	4.9
SB 94912	12	19.5	5.1	57.1	34.2	8.7
SB 94917	12	22.7	4.4	48.2	35.8	16.1
SR 93102	12	20.4	4.9	53.8	34.2	12.0
SB 94860	12	21.6	4.6	50.1	36.0	13.8
Phoenix	12	19.3	5.2	59.1	31.4	9.5
CDC Dawn	12	19.4	5.2	57.4	33.8	8.8
SB 94893	12	19.1	5.3	56.9	35.0	8.2
SB 94897	12	20.2	5.0	52.6	36.1	10.6
Waxy maize	14	18.5	5.4	59.2	34.0	6.8
Normal maize	13	19.5	5.2	57.2	33.4	9.4
LSD[d]		1.4	0.4	7.0	5.4	2.1

[a] Degree of polymerization.

[b] Average chain length.

[c] Branch points.

[d] Least significant difference at $P < 0.05$.

corresponding DP values for normal and waxy maize starches were 13 and 14, respectively. The average chain length (CL) and degree of branching were in the range 17.6-22.7% and 4.4-5.7%, respectively, for the HB starches. The corresponding values for the maize starches were 18.5 and 5.4% (waxy maize) and 19.5 and 5.2% (normal maize). The short (DP 5-17) and long (DP ≥ 35) chains ranged from 48.2-59.2% and 3.0-16.1%, respectively, for the HB starches. The corresponding values for the maize starches were 59.2 and 6.8% (waxy) and 57.2 and 9.4% (normal).

Average CL was correlated with small granule size ($r = 0.81$, $P < 0.01$), the proportion of small granules by number ($r = 0.71$, $P < 0.05$), the proportion of small granules by weight ($r = 0.78$, $P < 0.01$), the short chains ($r = -0.92$, $P < 0.01$), and long chains ($r = 0.99$, $P < 0.01$), indicating that amylopectins of small granule high-amylose and compound HB starches contained a larger proportion of long chains. Salomonson and Sundberg (1994) and Cheetham and Tao (1997) also reported relationships between amylose content and amylopectin branch chain length for barley and maize starches, This study has shown that the amylose/amylopectin ratio and branch chain length have high correlation with granule size and size distribution in HB starches.

2.4 Conclusion

This study showed that starches from ten hull-less barley genotypes differed in chemical composition, morphology, granule size, size distribution and amylopectin branch chain length distribution. The total amylose content and amylopectin branch chain length were highly correlated with starch granule size and size distribution in this set of HB genotypes.

2.5 References

AACC. 1983. *Approved Methods of the AACC,* 8th ed., St. Paul: Am. Assoc. Cereal Chem.

Bhatty, R. S. 1993. Non-malting uses of barley. In: *Barley: Chemistry and Technology* A. W. MacGregor and R. S. Bhatty eds. p.355-417. St. Paul: Am. Assoc. Cereal Chem.

Bhatty, R. S. 1995. Hull-less barley bran: A potential new product from an old grain. *Cereal Foods World*, 40: 819-824.

Bhatty, R. S. 1997. Milling of regular and waxy starch hull-less barleys for the production of bran and flour. *Cereal Chem.*, 74: 693-699.

Bhatty, R. S. 1999. The potential of hull-less barley. *Cereal Chem.*, 76: 589-599.

Bhatty, R. S. and Rossnagel, B. G. 1997. Zero amylose lines of hull-less barley. *Cereal Chem.*, 74: 190-191.

Bhatty, R. S. and Rossnagel, B. G. 1998. Comparison of pearled and unpearled Canadian and Japanese barleys. *Cereal Chem.*, 75: 15-21.

Cheetham, N. W. H. and Tao, L. 1997. The effect of amylose content on the molecular size of amylose and on the distribution of amylopectin chain length in maize starch. *Carbohydr. Polym.* 33: 251-261.

Chrastil, J. 1987. Improved colorimetric determination of amylose in starches of flours. *Carbohydr. Res.*, 159: 154-158.

Czuchajowska, Z., Szczodrak, J., and Pomeranz, Y. 1992. Characterization and estimation of barley polysaccharides by near infrared spectroscopy. I. Barleys, starches, and β-D glucans. *Cereal Chem.*, 69: 413-418.

Edney, M. J., Tkachuk, R., and MacGregor, A. W. 1992. Nutrient composition of the hull-less barley cultivar, condor. *J. Sci. Food Agric.*, 60: 451-456.

Garcia, V., Colonna, P., Bouchet, B., and Gallant, D. J. 1997. Structural changes of cassava starch granules after heating at intermediate water contents. *Starch/Stärke,* 49: 171-179.

Lee, C. J., Horsley, R. D., Manthey, F. A., and Schwarz, P. B. 1997. Comparison of β-glucan content of barley and oat. *Cereal Chem.*, 74: 571-575.

Morrison, W. R. 1981. Starch lipids — a reappraisal. *Starch/Stärke*, 33: 408-410.

Morrison, W. R., Scott, D. C., and Karkalas, J. 1986. Variation in the composition and physical properties of barley starches. *Starch/Stärke*, 38: 374-379.

Nilan, R. A. and Ullrich, S. E. 1993. Barley: taxonomy, origin, distribution, production genetics and breeding. In: *Barley: Chemistry and Technology*, A. W. MacGregor and R. S. Bhatty eds. p.1-129. St. Paul: Am. Assoc. Cereal Chem.

Oscarsson, M., Parkkonen, T., Autio, K., and Aman, P. 1997. Composition and microstructure of waxy, normal and high amylose barley samples. *J. Cereal Sci.*, 26: 259-264.

Perez-Vendrell, A. M., Brufau, J., Molinocano, J. L., Francesh, M., and Guasch, J. 1996. Effects of cultivar and environment on β-(1—›3) (1—›4)-D-glucan content and acid extract viscosity of Spanish barleys. *J. Cereal Sci.*, 23: 285-292.

Raeker, M. O., Gaines, C. S., Finney, P. L., and Donelson, T. 1998. Granule size distribution and chemical composition of starches from 12 soft wheat cultivars. *Cereal Chem.*, 75: 721-728.

Salomonsson, A. C. and Sundberg, B. 1994. Amylose content and chain profile of amylopectin from normal high amylose and waxy barleys. *Starch/Stärke*, 46: 325-328.

Stoddard, F. L. 1999. Survey of starch particle size distribution in wheat and related species. *Cereal Chem.*, 76: 145-149.

Szczodrak, J. and Pomeranz, Y. 1991. Starch and enzyme-resistant starch from high-amylose barley. *Cereal Chem.*, 68: 589-596.

Szczodrak, J., Czuchajowska, Z., and Pomeranz, Y. 1992. Characterization and estimation of barley polysaccharide by near-infrared spectroscopy. II. Estimation of total β-D glucans. *Cereal Chem.*, 72: 379-384.

Vasanthan, T. and Bhatty, R. S. 1995. Starch purification after pin milling and air classification of waxy, normal, and high amylose barleys. *Cereal Chem.*, 72: 379-384.

Vasanthan, T. and Hoover, R. 1992. A comparative study of the composition of lipids associated with starch granules from various botanical sources. *Food Chem.*, 43: 19-27.

Wang, J., Jiang, G., Vasanthan, T., and Sporns, P. 1999. MALDI-MS characterization of maltooligo/polysaccharides from debranched starch amylopectin of corn and barley. *Starch/Stärke*, 51: 243-248.

Wu, Y. V., Sexson, K. R., and Sanderson, J. E. 1979. Barley protein concentrate from high-protein, high-lysine varieties. *J. Food Sci.*, 44: 1580-1583.

Zheng, G. H., Han, H. L., and Bhatty, R. S. 1998. Physicochemical properties of zero amylose hull-less barley starch. *Cereal Chem.*, 75: 520-524.

CHAPTER 3

Thermal, Rheological and Acid Hydrolysis Characteristics[1]

3.1 Introduction

Studies on barley starches (Kang et al., 1985; Morrison et al., 1986; Tester and Morrison, 1992; Morrison et al., 1993; Lorenz and Collins, 1995; Vasanthan and Bhatty, 1996; Czuchajowska et al., 1998; Song and Jane, 2000; Yoshimoto et al., 2000) have revealed that starches from different genotypes vary widely in structure, composition and properties. However, similar studies have not been carried out on hull-less barley (HB) starches. In a previous study, the granule morphology, chemical composition, granule size distribution and amylopectin structure of starches from ten HB genotypes grown at Saskatoon, Saskatchewan, were evaluated (Chapter 2). These starches differed with respect to their amylose content, bound lipid content, proportion of small granules, granule morphology, and amylopectin structure. Compound granules were found in certain genotypes, which were clusters of a few granules but looked like single granules. This study was undertaken to characterize structure-property relationships for these same HB genotypes. At present in North America, maize starch is extensively used in a number of food and industrial applications. Therefore, this study was also intended to compare barley starches to waxy and normal maize starches.

---

[1] A version of this chapter was published in *Food Chemistry*, 2001, 74: 407-415.

3.2 Materials and methods

3.2.1 Materials

Barley samples from four registered cultivars (CDC Alamo, CDC Candle, CDC Dawn, and Phoenix) and six breeding lines (SB 94912, SB 94917, SR 93102, SB 94860, SB 94893, and SB 94897) of HB grown and harvested at Saskatoon in 1998 were obtained from the Crop Development Centre, University of Saskatchewan, Saskatoon, SK. Commercial waxy and normal maize starches were purchased from A. E. Staley Manufacturing Company (Decatur, IL).

3.2.2 Starch isolation

Starch was isolated from barley grain according to the method of Wu et al. (1979).

3.2.3 Gelatinization characteristics

Starch gelatinization was studied using a Mettler (TA 4000) differential scanning calorimeter (DSC) (Mettler-Toledo, Switzerland). Water (15µl) was added with a microsyringe to starch (5mg, db) in aluminum DSC pans, which were then hermetically sealed and allowed to stand overnight at room temperature (24°C). The scanning temperature range and the heating rate were 30-110°C and 10°C/min, respectively. The thermograms were recorded with water as reference. Indium was used for calibration.

3.2.4 Brabender viscoamylography

Pasting characteristics (6% w/v, pH 6.5) of the starches were determined using a viscoamylograph (Viskograph-E, C.W. Brabender Instruments, Inc., South Hackensack, NJ) equipped with a 700 cm/g cartridge and operating at a bowl speed of 75 rpm. The starch slurry was heated from 30 to 96°C at a rate of 1.5°C/min, maintained at 96°C for 30 min, and then cooled to 51°C at 1.5°C/min.

3.2.5 Swelling power and solubility

Swelling power and solubility were carried out by heating 3% starch slurry (w/v) at 60, 65, 70, 80, 90°C, respectively, for 30 min according to the method of Li and Corke (1999). Swelling power was defined as the residue weight after centrifugation (2000 xg, 15 min). Solubility was calculated as percentage by dry weight of supernatant based on total sample weight.

3.2.6 Acid hydrolysis

The starches were hydrolyzed with 2.2N HCl at 35°C (1.0 g starch/40 ml acid) for 18 days in a shaking water bath at 35°C. Details of the procedure have been described elsewhere (Vasanthan and Bhatty, 1996).

3.2.7 Statistical analysis

Data reported are means of at least duplicate determinations. Data were analyzed using the SAS System for Windows Version 8 (SAS Institute Inc., Cary, NC). Levels of significance levels used were at $P < 0.1$, $P < 0.05$, and $P < 0.01$.

3.3 Results and discussion

3.3.1 Gelatinization characteristics

The gelatinization transition temperatures [onset (T_o), mid-point (T_p), and conclusion (T_c)] and gelatinization enthalpy (ΔH) are presented in Table 3-1. T_o, T_p, T_c, T_c-T_o, and ΔH were in the ranges of 50.1-56.1°C, 58.1-64.5°C, 71.0-75.8°C, 17.9-24.0°C, and 9.6-14.2 J/g of amylopectin, respectively, in HB starches. Compound HB starches (SB 94917, SB 94860, and SR 93102) exhibited a lower T_o (50.1-51.2°C) and a wider T_c-T_o (21.9-24.0°C) than other HB starches. Compound waxy HB starch (SB 94917) exhibited the lowest ΔH (9.6 J/g of amylopectin), whereas the highest ΔH (13.5-14.2 J/g of amylopectin) was recorded for compound normal starches (SR 93102 and SB 94860) (Table 3-1). T_o, T_p, T_c, T_c-T_o and ΔH were 59.8°C, 66.9°C, 77.8°C, 18.0°C, and 15.5 J/g of amylopectin, respectively, for normal maize starch. The corresponding values for waxy maize starch were 60.6°C, 67.1°C, 78.1°C, 17.6°C, and 13.3 J/g of amylopectin. Correlation analysis (Table 3-2) with previous data (Chapter 2) showed that T_o was positively correlated with starch granule size ($r = 0.63$, $P < 0.05$), short branch chains (DP5-17) ($r = 0.67$, $P < 0.05$), and negatively correlated with small granule (diameter ≤ 10 µm) size ($r = -0.64$, $P < 0.05$), the proportion of small granules by number ($r = -0.70$, $P < 0.05$) and by weight ($r = -0.70$, $P < 0.05$), long branch chains (DP ≥ 35) ($r = -0.78$, $P < 0.01$) and average branch chain length ($r = -0.75$, $P < 0.05$). T_c-T_o was positively correlated with small granule size ($r = 0.86$, $P < 0.01$), the proportion of small granules by number ($r = 0.57$, $P < 0.1$) and by weight ($r = 0.86$, $P < 0.01$), long branch chains ($r = 0.78$, $P < 0.01$), and average branch chain length ($r = 0.84$, $P < 0.01$) and negatively correlated with short branch chains (DP5-17) ($r = -0.91$,

Table 3-1 Thermal characteristics[a] of hull-less barley and maize starches

Genotype	Starch type	T_o (°C)	T_p (°C)	T_c (°C)	T_c-T_o (°C)	ΔH (J/g)
CDC Alamo	Zero-amylose waxy	54.5	61.8	74.5	20.0	12.6
CDC Candle	Waxy	55.4	61.9	73.8	18.4	13.1
SB 94912	Waxy	56.1	62.1	75.8	19.7	13.1
SB 94917	Compound waxy	50.5	64.5	74.5	24.0	9.6
SR 93102	Compound normal	50.1	59.9	72.0	21.9	13.5
SB 94860	Compound normal	51.2	60.9	73.5	22.4	14.2
Phoenix	Normal	53.1	59.1	71.0	17.9	12.8
CDC Dawn	Normal	52.0	58.1	72.5	20.5	12.7
SB 94893	High-amylose	53.0	62.3	74.3	21.3	11.8
SB 94897	High-amylose	53.3	61.7	74.4	21.2	12.2
Waxy maize	Waxy	60.6	67.1	78.1	17.6	13.3
Normal maize	Normal	59.8	66.9	77.8	18.0	15.5
LSD[b]		0.8	0.9	1.1	1.6	1.7

[a] T_o, onset temperature; T_p, peak temperature; T_c, conclusion temperature; T_c-T_o, gelatinization temperature range; ΔH, gelatinization enthalpy in J/g of amylopectin

[b] Least significant difference at $P < 0.05$.

$P < 0.01$). ΔH was negatively correlated with the proportion of small granules by weight ($r = -0.65$, $P < 0.05$) and T_p ($r = -0.62$, $P < 0.05$).

The influence of granule size on ΔH was also reported by Tang et al. (2000) for waxy barley starch. They showed that ΔH decreased with decreasing granule size. Significant correlations between average branch chain length and T_o have also been reported for other starches (Shi and Seib, 1992; Yuan et al., 1993; Wang et al., 1993; Jane et al., 1999). Cooke and Gidley (1992) suggested that ΔH primarily reflects the loss of double helical order rather than loss of X-ray crystallinity, while Tester and Morrison (1990) postulated that the DSC endotherm gives a measure of crystallite quality (effectively double helix length) from T_p and overall crystallinity (quality x quantity) from ΔH. Biliaderis et al.(1980) suggested that T_c-T_o is influenced by the degree of branching of amylopectin (the greater the degree of branching, the wider the melting temperature range). It is likely that T_c-T_o could also indicate the degree of heterogeneity of the starch crystallites. This study indicated that T_c-T_o (Table 3-2) was influenced to a large extent by the proportion of small granules (Chapter 2). For instance, starches containing a high proportion of small granules (compound and high amylose HB starches) exhibited the widest T_c-T_o (Table 3-1). Smaller granules have been shown to contain more amylose (Czuchajowska et al., 1992; Chapter 2), longer ($DP \geq 35$) amylopectin branches (Chapter 2), and lower ΔH (Tang et al., 2000). This suggests that the DSC endotherm of small granule starches could be influenced by the interplay of: (1) disordering of double helices of short chains from amylopectin; (2) disordering of double helical chains formed by interaction between amylose and amylopectin chains (average chain length > 17.9) (Chapter 2); and (3) disordering of V-helix residues of amylose-lipid complexes [the bound lipid content in SB 94917, SR 93102, SB 94860, SB 94893, and SB 94897 was higher than that in other starches used in this study (Chapter 2)]. It is likely that differences in size, form and order of double helices and single V-helix residues of amylose-lipid complexes are the factors responsible for the broad melting endotherm of small granule starches.

Jenkins (1994) has shown, by small angle X-ray scattering studies on normal maize, waxy maize and high-amylose maize starches, that amylose acts to disrupt the packing of the amylopectin double helices within the crystalline lamellae. A reduction in crystalline lamellae was observed with an increase in amylose content. It was postulated that the disrupting effect of amylose on amylopectin could be due to co-crystallization between amylose and amylopectin or to penetration of amylose into the amorphous regions of the cluster (where the branch points are located). This suggests that the energy (ΔH) required for unraveling and melting of the double helices within the crystalline lamella may decrease with increasing amylose content. Recently, Hoover and Manuel (1996) have shown that the ΔH of maize starches (waxy maize > normal maize > high-amylose maize) is influenced by their amylose content. In this study, ΔH followed the order: compound normal > waxy > normal > high-amylose ≈ zero-amylose > compound waxy, indicating that those other factors, such as the proportion of small granules, may also reflect differences in ΔH.

3.3.2 Swelling power and solubility

The swelling power (SP) and solubility of the starches are presented in Figures 3-1 and 3-2, respectively. Compound waxy (SB 94917) and waxy (CDC Candle and SB 94912) HB exhibited a two-stage swelling pattern, whereas a single-stage swelling pattern was

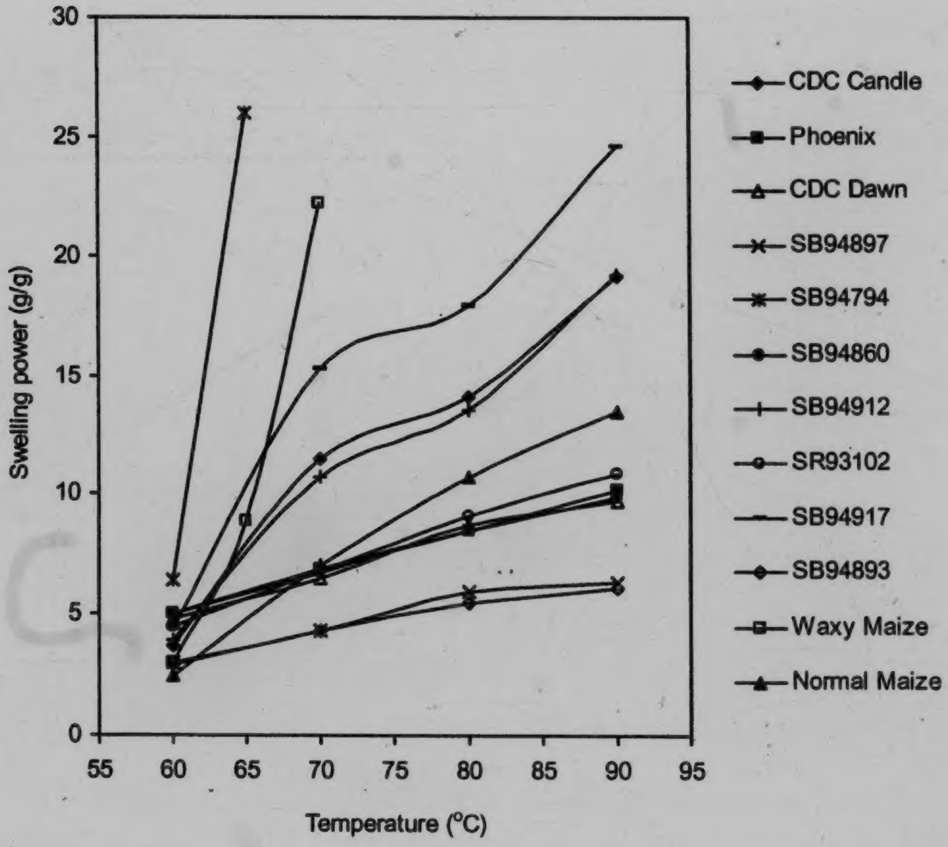

Figure 3-1 Swelling power of hull-less barley and maize starches.

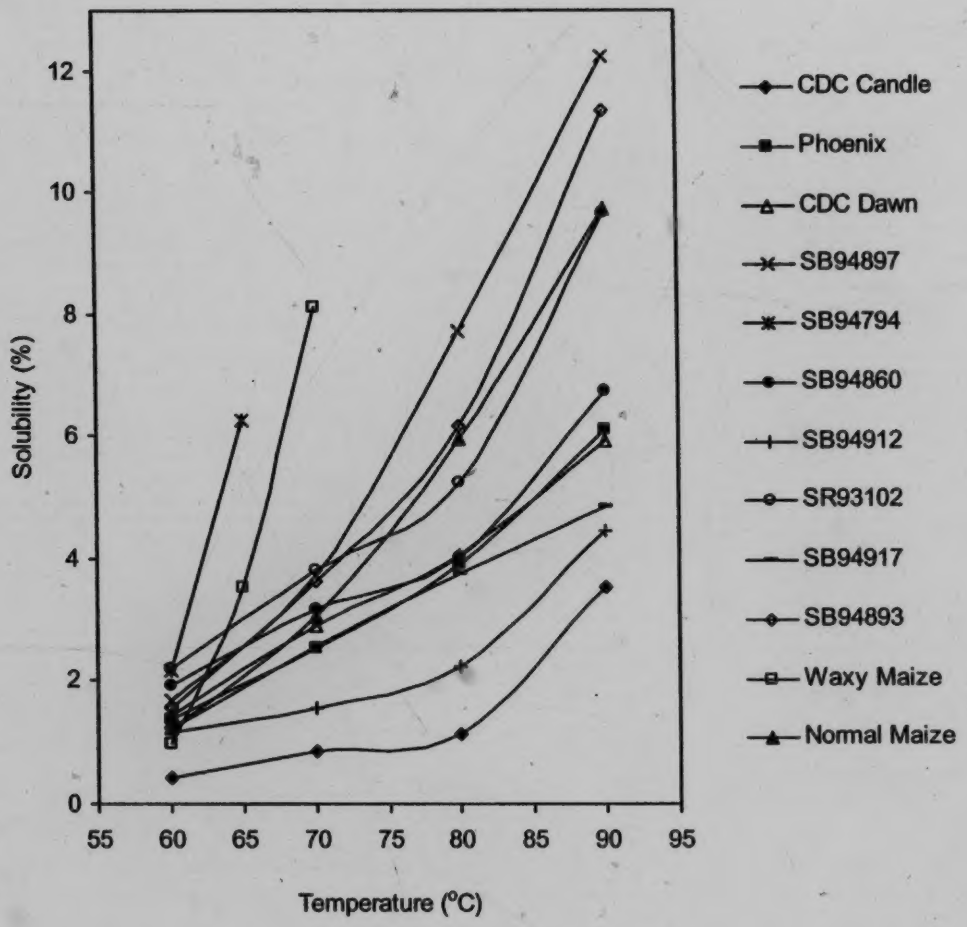

Figure 3-2 Solubility curves of hull-less barley and maize starches.

shown by the other starches (Figure 3-1). SP increased with a rise in temperature from 60 to 90°C. The increase in SP was very rapid for zero-amylose (CDC Alamo) HB and waxy maize starch, and occurred at relatively low temperatures (60-70°C) (Figure 3-1). SP of the other starches at higher temperatures (> 70°C) followed the order: compound waxy HB (SB 94917) > waxy HB (CDC Candle) ≈ waxy HB (SB 94912) > normal maize > compound normal HB (SR 93102) ≈ normal HB (Phoenix) ≈ normal HB (CDC Dawn) > high-amylose HB (SB 94897) ≈ high-amylose HB (SB 94893). The increase in SP (within the temperature range 60-70°C) was rapid for compound waxy HB (SB 94917), waxy HB (CDC Candle), and waxy HB (SB 94912) starches, but was gradual for normal HB, high-amylose HB and normal maize starches (Figure 3-1).

A rapid increase in solubility occurred at lower temperatures (< 70°C) for zero-amylose (CDC Alamo) and waxy maize starches (Figure 3-2). However, the increase in solubility was gradual for the other starches. At 90°C, the solubility followed the order: high-amylose HB (SB 94897) > high-amylose HB (SB 94893) > normal maize > compound normal HB (SR 93102) > compound normal HB (SB 94860) > normal HB (Phoenix) > normal HB (CDC Dawn) > compound waxy HB (SB 94917) > waxy HB (SB 94912) > waxy HB (CDC Candle). Correlation analysis (Table 3-2) showed that SP was negatively correlated with amylose content ($r = -0.94$ at 90°C, $P < 0.01$) and total lipids ($r = -0.81$, $P < 0.01$). Solubility (at 90°C) was positively correlated with amylose content ($r = 0.91$, $P < 0.01$) and total lipids ($r = 0.76$, $P < 0.05$), and negatively correlated with swelling power ($r = -0.78$, $P < 0.05$).

The differences in SP and solubility among the starches can be attributed to the interplay of the following factors: (1) the level of lipid complexed amylose chains (Tester and Morrison, 1992) [high amylose HB (CDC Alamo) > compound normal HB (SB 94860) > high-amylose HB (SB 94893) > compound normal HB (SR 93102) > normal maize > normal HB (Phoenix) > waxy HB (SB 94912) > normal HB (CDC Dawn) > waxy maize > compound waxy (SB 94917) > waxy HB (CDC Candle) (Chapter 2); (2) the molar proportion of amylopectin unit chains of DP 6-24 (Shi and Seib, 1992) [DP5-17 and DP18-34 ranged from 48.2-59.1% and 31.4-38.0%, respectively, in the starches used in this study (Chapter 2)]; (3) the total amylose content (Sasaki and Matsuki, 1998) [SB 94893 > SB 94897 > SB 94860 > SR 93102 > Phoenix > normal maize > CDC Dawn > SB 94912 > SB 94917 > CDC Candle > waxy maize > CDC Alamo (Chapter 2)]; and (4) the extent of interaction between starch chains within the amorphous and crystalline domains (Hoover and Manuel, 1996).

Several researchers have shown that cereal starch granules do not show complete swelling until amylose has been leached from the granule (Bowler et al., 1980; Doublier, 1981). Hermannson and Svegmark (1996) have shown by microscopy that the swelling pattern of potato amylopectin starch differs from that of normal potato starch. They showed that potato amylopectin starch does not exhibit structures typical of swollen gelatinized granules (at 60°C), instead it transforms immediately into a macromolecular solution. This indicates that amylose restraints swelling and maintains the integrity of swollen granules. Furthermore, lipid-complexed amylose chains have been shown to restrict both granular swelling and amylose leaching (Tester and Morrison, 1992). Thus, the differences in SP (Figure 3-1) and solubility (Figure 3-2) between: (1) zero-amylose (CDC Alamo) and waxy maize starches; (2) zero-amylose and the other waxy HB starches (SB 94917, SB 94912, and CDC Candle); (3) the waxy HB starches; and (4) waxy and normal HB starches can be explained. It is unlikely that the molar proportion of amylopectin chains DP5-17 is a major factor influencing SP and solubility, since this parameter did not differ significantly among the starches (Chapter 2).

3.3.3 Pasting properties

The Brabender viscoamylograms of HB and maize starches are presented in Figure 3-3. Zero-amylose (CDC Alamo) and waxy HB starches (CDC Candle, SB 94912, and SB 94917) exhibited lower pasting temperatures (63.0-64.5°C), higher peak viscosities (640-1142BU), and higher viscosity breakdown (424-843BU) (during the holding cycle at 96°C) than did normal HB starches. The corresponding values for normal (SR 93102, SB 94860, Phoenix, and CDC Dawn) HB starches were 82.5-88.1°C, 75-125BU and 4-24BU, respectively. Similar differences were found between waxy and normal maize starches (Figure 3-3).

Pasting temperature was correlated with amylose content ($r = 0.98$, $P < 0.01$), total lipid ($r = 0.84$, $P < 0.01$), SP ($r = -0.96$, $P < 0.01$), and solubility ($r = 0.84$, $P < 0.01$) (Table 3-2). Peak temperature was correlated with amylose ($r = 0.67$, $P < 0.1$), total lipid ($r = 0.64$, $P < 0.1$) and the proportion of amylopectin chains of DP18-34 ($r = -0.67$, $P < 0.1$) (Table 3-2). The peak viscosity was negatively correlated with amylose ($r = -0.96$, $P < 0.01$), total lipid ($r = -0.79$, $P < 0.05$), SP ($r = 0.95$, $P < 0.01$), solubility ($r = -0.75$, $P < 0.1$) and the proportion of amylopectin chains of DP 18-34 ($r = -0.73$, $P < 0.05$) (Table 3-2). Viscosity breakdown during the holding cycle at 96°C was negatively correlated with amylose ($r = -0.95$, $P < 0.01$), total lipid ($r = -0.78$, $P < 0.05$) and solubility ($r = -$

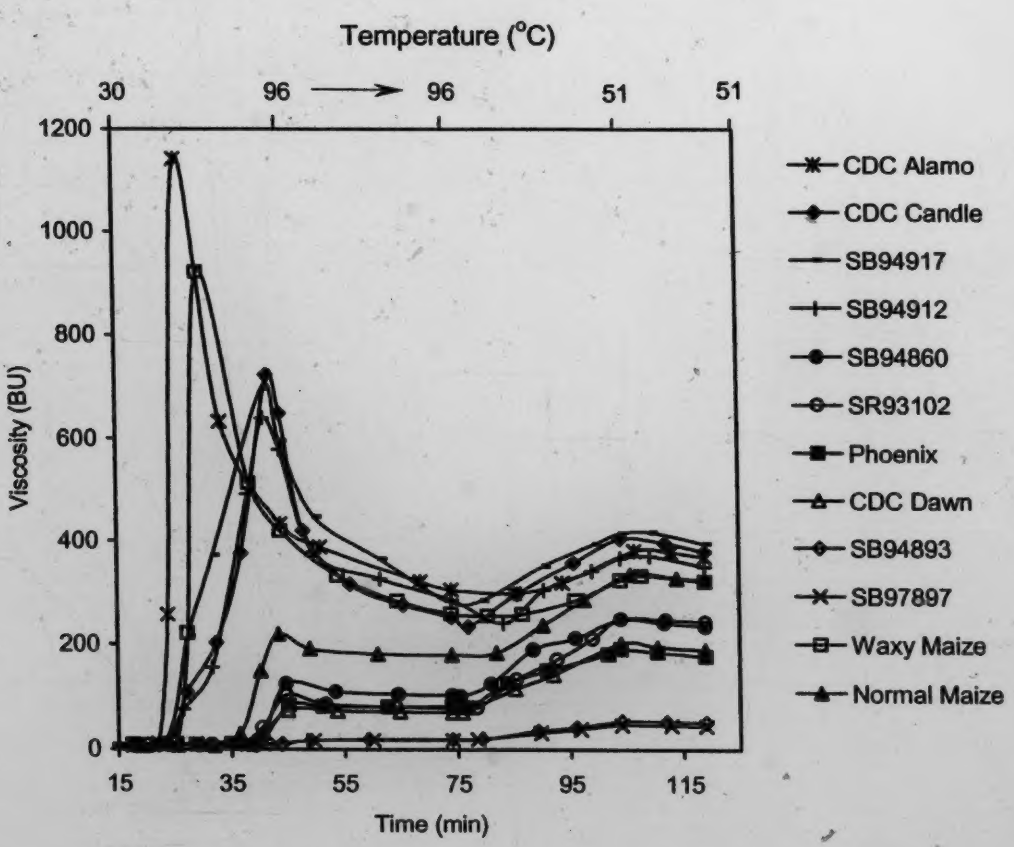

Figure 3-3 Pasting properties of hull-less barley and maize starches.

Table 3-2 Correlations (r value[a]) between physicochemical properties[b] and structural characteristics[c] of hull-less barley starches

	Amylose	Lipids	BL	SGS	GS	SGN	SGW	T_o	T_p	T_c	T_c-T_o	ΔH	SP	S	AH	DP5-17	DP18-34	DP≥35
Lipids	0.90***																	
BL	0.92**	1.00***																
SGS	0.31	0.42	0.42															
GS	-0.65**	-0.38	-0.43	-0.28														
SGN	0.59*	0.37	0.42	0.49	-0.96***													
SGW	0.30	0.24	0.26	0.74**	-0.69**	0.81***												
T_o	-0.36	-0.28	-0.28	-0.64**	0.63**	-0.70**	-0.70**											
T_p	-0.32	-0.16	-0.17	0.38	0.12	0.04	0.51	0.14										
T_c	-0.31	-0.19	-0.18	0.18	0.34	-0.25	0.12	0.48	0.76**									
T_c-T_o	0.17	0.17	0.18	0.86***	-0.44	0.57*	0.86***	-0.73**	0.44	0.25								
ΔH	0.14	0.28	0.25	-0.10	0.47	-0.49	-0.65**	0.20	-0.62**	-0.29	-0.44							
SP	-0.94***	-0.81***	-0.83***	-0.01	0.37	-0.22	0.12	0.16	0.57	0.39	0.11	-0.41						
S	0.91***	0.76**	0.80***	0.34	-0.61*	0.57	0.43	-0.29	-0.05	-0.04	0.29	-0.01	-0.78**					
AH	-0.98***	-0.88***	-0.90***	-0.28	0.66**	-0.59*	-0.30	0.36	0.35	0.36	-0.13	-0.20	0.94***	-0.93***				
DP5-17	-0.11	-0.09	-0.10	-0.85***	0.37	-0.55	-0.81***	0.67**	-0.47	-0.21	-0.91***	0.36	-0.21	-0.16	0.09			
DP18-34	-0.31	-0.16	-0.18	0.20	0.45	-0.43	0.12	0.15	0.58*	0.64**	0.33	-0.11	0.21	0.11	0.33	-0.32		
DP≥35	0.24	0.17	0.19	0.79***	-0.60***	0.77***	0.78***	-0.78***	0.19	-0.11	0.78***	-0.32	0.17	0.10	-0.23	-0.87***	-0.19*	
CL	0.17	0.10	0.11	0.81***	-0.53	0.71**	0.78***	-0.75**	0.28	0.01	0.84***	-0.37	0.21	0.08	-0.14	-0.92***	-0.06	0.99***
PT	0.98***	0.84***	0.86***	0.22	-0.66**	0.56*	0.23	-0.41	-0.46	-0.40	0.15	0.17	-0.96***	0.84***	-0.95***	-0.67	-0.33	0.20
PV	-0.96***	-0.79**	-0.83**	-0.21	0.65*	-0.59	-0.10	0.56	0.72**	0.74**	-0.06	-0.38	0.95***	-0.75*	0.95***	0.08	0.73**	-0.46
TP	0.67*	0.64*	0.71*	0.22	-0.64*	0.61	0.25	-0.39	-0.34	-0.45	0.09	0.16	-0.96***	0.72*	-0.74**	-0.18	-0.67*	0.52
BD	-0.95***	-0.78**	-0.82**	-0.24	0.68*	-0.63*	-0.16	0.58	0.67*	0.72**	-0.10	-0.33	0.93***	-0.76**	0.94***	0.13	0.73**	-0.51
SB	0.20	0.44	0.48	0.34	-0.23	0.26	0.33	-0.18	0.12	0.04	0.23	0.16	0.30	0.09	-0.39	-0.27	-0.10	0.33

[a] *,**, and *** = significant at $P < 0.1$, 0.05, and 0.01, respectively.

[b] BL, bond lipids extracted by hot 1-propanol-water; SGS, small granule size (average small granule diameter); GS, granule size (average granule diameter); SGN, proportion of small granules (granule diameter ≤10 μm) by number; SGW, proportion of small granules by weight; T_o, onset temperature; T_p, peak temperature; T_c, conclusion temperature; T_c-T_o, transition temperature range; ΔH, enthalpy; SP, swelling power at 90°C; S, solubility at 90°C; AH, extent of acid hydrolysis after 12 days; PT, pasting temperature; PV, peak viscosity; TP, pasting peak temperature; BD, breakdown; SB, setback; DP5-17, DP18-34, and DP≥35, degree of polymerization 5-17, 18-34, and ≥ 35, respectively; CL, average chain length of debranched amylopectin.

[c] See Chapter 2.

0.76, P < 0.05), and positively correlated with the proportion of amylopectin chain length of DP 18-34 (r = 0.73, P < 0.05) and SP (r = 0.93, P < 0.01). Waxy HB and waxy maize starches showed higher peak viscosity than normal and high amylose starches (Figure 3-3). It can be attributed to trace quantities of amylose and bound lipids in waxy genotypes (Chapter 2). This seems plausible, since the highest viscosity was shown by zero amylose HB starch.

The difference in the extent of breakdown in viscosity between the waxy and non-waxy HB starches (Figure 3-3) can be explained on the basis of differences in SP [waxy HB > non-waxy HB (Figure 3-2)] and the extent of amylose leaching [non-waxy HB > waxy HB (Figure 3-3)]. The granules of waxy HB starches would be highly susceptible to disintegration during the holding period (at 96°C), due to direct contact between highly swollen granules. However, granules of non-waxy HB starches would be more resistant to disintegration due to lower granular swelling (Figure 3-2) and less friction between swollen granules as the granules would be surrounded by a network of leached amylose chains, which would hinder granule-granule contact.

3.3.4 Acid hydrolysis

The acid hydrolysis patterns of the starches are presented in Figure 3-4. A relatively high rate of solubilization was observed during the first 10 days, followed by a slower rate thereafter. At the end of the 10th day of hydrolysis (corresponding mainly to the degradation of the amorphous region of the granule), zero-amylose (CDC Alamo), compound waxy HB (SB 94917), waxy HB (CDC Candle), normal HB (Phoenix), compound normal HB (SB 94860), normal HB (CDC Dawn), high-amylose HB (SB

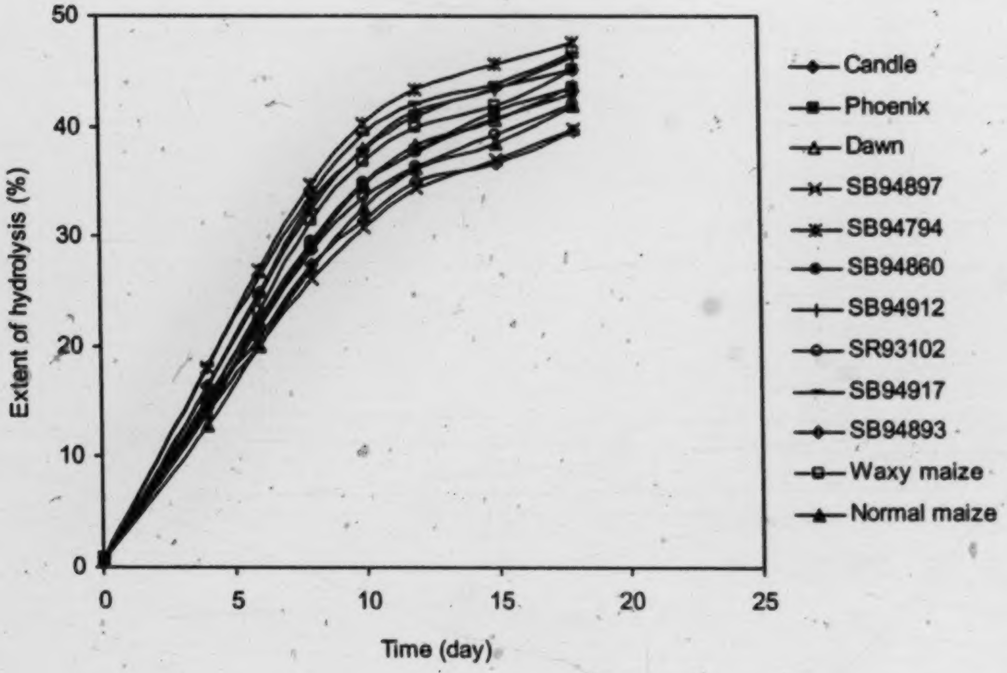

Figure 3-4 Acid hydrolysis (2.2 N HCl at 35°C) of hull-less barley and maize starches.

94893), and high-amylose HB (SB 94897) were hydrolyzed to the extent of 40.2%, 39.3%, 37.8%, 34.8%, 34.9%, 34.7%, 31.5%, and 30.9%, respectively. Corresponding values for normal maize and waxy maize were 32.6% and 36.8%, respectively. Differences in the extent of hydrolysis between the starches were more pronounced beyond the 10th day (corresponding to the degradation of the crystalline region). The extent of hydrolysis at the end of the 18th day of hydrolysis followed the order: CDC Alamo (47.6%) > SB 94917 (46.6%) > SB 94912 (46.2%) > CDC Candle (45.1%) > CDC Dawn (43.7%) = Phoenix (43.6%) > SB 94860 (43.0%) > SR93102 (42.0%) > SB 94893 (39.6%) = SB 94897 (39.7%). Among the maize starches, waxy maize was hydrolyzed (45.1%) to a greater extent than was normal maize (42.0%).

Correlation analysis (Table 3-2) indicated that the extent of acid hydrolysis was negatively correlated with total lipids ($r = -0.88$, $P < 0.01$) and amylose content ($r = -0.98$, $P < 0.01$), solubility ($r = -0.93$, $P < 0.01$), and positively correlated with granule size ($r = 0.66$, $P < 0.05$), ΔH ($r = 0.82$, $P < 0.01$), and SP ($r = 0.94$, $P < 0.01$). No correlation was found with amylopectin branch chain length (Table 3-2).

Differences in the extent and rate of hydrolysis between starches during the initial stages (1-10 days) of hydrolysis has been mainly attributed to differences in: (1) granule size [small granules are hydrolyzed faster and to a greater extent than larger granules (Vasanthan and Bhatty, 1996)]; (2) the amount of lipid-complexed amylose chains [lipid complexed amylose chains resist degradation by H_3O^+ (Morrison et al., 1993)]; (3) double helical content [Morrison et al., 1993 showed, by ^{13}C/CP/MAS-NMR, that double helix content increased (due to retrograded free amylose) on Lintnerization of non-waxy barley starches, but was little changed for waxy barley starches]; and (4) the extent of interaction between starch chains (Hoover and Manuel, 1996) within the amorphous domains of the granule [presence of double helices and close packing of non-helical amylose chains within the amorphous regions will hinder the conformational transformation (chair –› half chair) required for expulsion of protonated glycosidic oxygens (Hoover and Manuel, 1996; Hoover, 2000)].

In this study, the observed differences cannot be explained solely on the basis of small granule content (SB 94917 > SB 94897 > SR 93102 > SB 94893 > Phoenix > CDC Dawn > SB 94860 > SB 94912 > CDC Candle > CDC Alamo > waxy maize ≈ normal maize), level of amylose - lipid complexes (SB 94897 > SB 94860 > SB 94893 > SR 93102 > normal maize > Phoenix > SB 94912 > CDC Dawn > CDC Candle > waxy maize ≈ SB 94917 > CDC Alamo), double helical content, or amylose-amylose interactions. It can be postulated that the observed differences in hydrolysis between the starches during the first 10 days of hydrolysis are probably influenced by the interplay of the above factors.

The hydrolysis pattern beyond the 10th day (Figure 3-4) suggests that the starches differed with respect to the organization of the double helical chains within their crystalline domains. To account for the slower hydrolysis rate of the crystalline domains of the starch granule, two hypotheses have been proposed (Kainuma and French, 1971; French, 1984). First, the dense packing of starch chains within the starch crystallites does not readily allow the penetration of H_3O^+. Second, acid hydrolysis of a glucoside bond requires a change in conformation (chair –› half chair) of the D-glycopyranosyl unit. Obviously, if the crystalline structure immobilizes the sugar conformation then this transition (chair –› half chair) would be difficult. This transition would become even more difficult if crystallites are formed by association between linear amylose chains. (AM-AM) and/or between amylose and the outer branches of amylopectin (AM-AP). The lower extent of hydrolysis observed for the high amylose (SB 94893 and SB 94897) HB starches (Figure 3-4) reflect crystallites formed by association between AM-AM and AM-AP chains.

3.4 Conclusion

This study has shown that the physicochemical properties of HB starches are influenced to different extents by the interplay of: (1) small granule size; (2) proportion of small granules by number and weight; (3) level of amylose - lipid complexes; (4) amylose content; (5) magnitude of interaction between starch chains within the amorphous and crystalline domains; and (6) double helical content.

3.5 References

Biliaderis, C. G., Maurice, T. J., and Vose, J. R. 1980. Starch gelatinization phenomena studied by differential scanning calorimetry. *J. Food Sci.*, 45: 1669-1674.

Bowler, P., Williams, M. R., and Angold, R. E. 1980. A hypothesis for the morphological changes which occur on heating lenticular wheat starch in water. *Starch/Stärke*, 33: 186-189.

Cooke, D. and Gidley, M. J. 1992. Loss of crystalline and molecular order during starch gelatinization: Origin of the enthalpic transition. *Carbohydr. Res.*, 227: 103-112.

Czuchajowska, Z., Szczodrak, J., and Pomeranz, Y. 1992. Characterization and estimation of barley polysaccharides by near-infrared spectroscopy. I. Barleys, starches, and β-D-glucans. *Cereal Chem.*, 69: 413-418.

Czuchajowska, Z., Klamczynski, A., Paszczynska, B., and Baik, B. K. 1998. Structure and functionality of barley starches. *Cereal Chem.*, 75: 747-754.

Doublier, J. L. 1981. Rheological studies on starch — flow behaviour of wheat starch pastes. *Stärke,* 33: 415-420.

French, D. 1984. Organization of starch granules. In: *Starch Chemistry and Technology*. R. L. Whistler, J. N. BeMiller, and E. F. Paschall eds. p.183-247. New York: Academic Press.

Hermannsson, A. M. and Svegmark, K. 1996. Developments in the understanding of starch functionality. *Trends Food Sci. Technol.,* 7: 345-353.

Hoover, R. and Manuel, H. 1996. The effect of heat-moisture treatment on the structure and physicochemical properties of normal maize, waxy maize, dull waxy maize and amylomaize V starches, *J. Cereal Sci.*, 23: 153-162.

Hoover, R. 2000. Acid treated starches. *Food Res. Int.* 16: 369-392.

Jane, J., Chen, Y. Y., McPherson, A. E., Wong, K. S., Radosavljevic, M., and Kasemsuwan, T. 1999. Effects of amylopectin branch chain length and amylose content on the gelatinization and pasting properties of starch. *Cereal Chem.*, 76: 629-637.

Jenkins, P. J. 1994. X-ray and neutron scattering studies of starch granule structure. Ph.D. Thesis, University of Cambridge, U.K.

Kang, M. Y., Sugimoto, Y., Kato, I., Sakamoto, S., and Fuwa, H. 1985. Some properties of large and small granules of barley (*Hordeum vulgarie*. L) endosperm. *Agric. Biol. Chem.*, 49: 1291-1297.

Kainuma, K. and French, D. 1971. Nageli amylodextrins and its relationship to starch granule structure. I. Preparation and Properties of amylodextrins from various starch types. *Biopolymers,* 10: 1673-1678.

Li, J. S. and Corke, H. 1999. Physicochemical properties of normal and waxy Job's tears (*Coix lachryma-Jobi* L.) starch. *Cereal Chem.*, 76: 413-416.

Lorenz, K. and Collins, F. 1995. Physicochemical characteristics and functional properties of starch from a high β-glucan waxy barley. *Starch/Stärke,* 47: 14-18.

Morrison, W. R., Scott, D. C. and Karkalas, J. 1986. Variation in the composition and physical properties of barley starches. *Starch/Stärke,* 38: 374-379.

Morrison, W. R., Tester, R. F., Snape, C. E., Law, R. and Gidley, M. J. 1993. Swelling and gelatinization of cereal starches IV. Some effects of lipid-complexed amylose and free amylose in waxy and normal barley starches. *Cereal Chem.* 70: 385-391.

Morrison, W. R., Tester, R. P., Gidley, M. J., and Karkalas, J. (1993). Resistance to acid hydrolysis of lipid-complexed amylose and lipid-free amylose in lintnerized waxy and non-waxy barley starches. *Carbohydr Res.* 245, 289-302.

Sasaki, T. and Matsuki, J. 1998. Effect of wheat structure on swelling power. *Cereal Chem.*, 75; 525-529.

Shi, Y. C. and Seib, P. A. 1992. The structure of four waxy starches related to gelatinization and retrogradation. *Carbohydr Res.*, 227: 131-145.

Song, Y. and Jane, J. 2000. Characterization of barley starches of waxy, normal and high amylose varieties. *Carbohydr Polym.*, 41: 365-377.

Tang, H., Ando, H, Watanabe, K., Takeda, Y., and Mitrunga, T. 2000. Some physicochemical properties of small-, medium-, and large-granule starches in fractions of waxy barley grain. *Cereal Chem.*, 77: 27-31.

Tester, R. F. and Morrison, W. R. 1992. Swelling and gelatinization of cereal starches. III. Some properties of waxy and normal nonwaxy barley starches. *Cereal Chem.*, 69: 654-658.

Tester, R. F. and Morrison, W. R. 1990. Swelling and gelatinization of cereal starches. II. Waxy rice starches. *Cereal Chem.*, 67: 558-563.

Vasanthan, T. and Bhatty, R. S. 1996. Physicochemical properties of small and large granule starches of waxy, regular and high amylose barleys. *Cereal Chem.*, 73: 199-207.

Wang, Y. J., White, P., and Pollak, L. 1993. Physicochemical properties of starches from mutant genotypes of oh43 inbred line. *Cereal Chem.*, 70: 199-203.

Wu, Y. V., Sexson, K. R. and Sanderson, J. E. 1979. Barley protein concentrate from high-protein, high-lysine varieties. *J. Food Sci.*, 44: 1580-1583.

Yoshimoto, Y., Tashiro, J., Takenouchi, T., and Takeda, Y. 2000. Molecular structure and some physicochemical properties of high-amylose barley starches. *Cereal Chem.*, 77: 279-285.

Yuan, R. C., Thompson, D. B., and Boyer, C. D. 1993. Fine structure of amylopectin in relation to gelatinization and retrogradation behavior of maize starches from three wax-containing genotypes in two inbred lines. *Cereal Chem.*, 70: 81-89.

CHAPTER 4

Ultrastructure and Distribution of Granule-bound Proteins[1]

4.1 Introduction

Starch is a unique carbohydrate polymer existing as discrete granules with different shape, size and composition among various plant sources. It is mainly composed of amylose and amylopectin molecules. These molecules form semi-crystalline and inter-crystalline amorphous regions in alternating layers, also known as granule growth rings (Figure 4-1) (French, 1984), within the starch granules. The fine structure of starch molecules and the degree of association between starch components differ among starch sources and among genotypes within a source.

A number of techniques, such as differential scanning calorimetry (DSC), X-ray diffractometry, nuclear magnetic resonance (NMR), chromatography, mass spectrometry and electron microscopy, in combination with cytochemical techniques, have been used to study the structure of starches. Of these, only the latter enables a direct visualization of starch granule morphology and ultrastructure, with or without the need for prior physical, chemical, and enzymatic treatments (Kassenbeck, 1975, 1978; Yamaguchi et al., 1979; Nikuni, 1978; Gallant and Bouchet, 1986; Oostergetel and Bruggen, 1989; Fannon et al., 1993; Planchot et al., 1995; Helbert and Chanzy, 1996; Helbert et al., 1996; Garcia et al., 1997; Atkin et al., 1998a,b). Previous studies

---

[1] A version of this chapter was published in *Cereal Chemistry*, 2003, 80: 524-532.

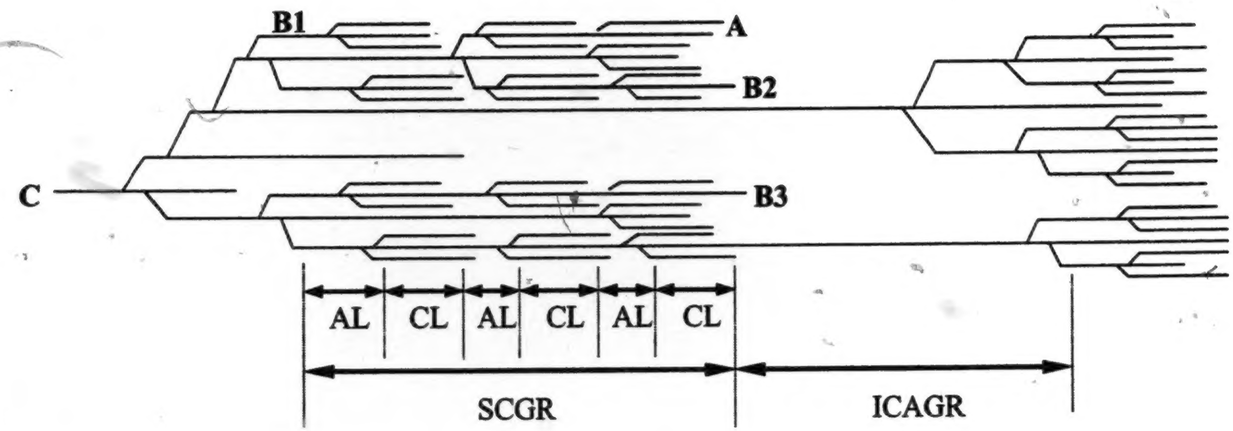
B1
A
B2
C
B3
AL
CL
AL
CL
AL
CL
SCGR
ICAGR

Figure 4-1 Schematic diagram of amylopectin structure showing growth rings and areas for amorphous and crystalline lamellae formation. AL, amorphous lamellae; CL, crystalline lamellae; SCGR, semi-crystalline growth ring; ICAGR, inter-crystalline amorphous growth ring.

(Chapter 2 and 3) indicated that the composition, granule structure, amylopectin chain length profile and physicochemical properties of hull-less barley (HB) starches differ among genotypes. However, the relationship between ultrastructure of HB starches from different genotypes and their reactivity towards hydrolyzing and modifying agents have not been explored. As starch hydrolysis and chemical modifications are widely used in commercial processes, a study of the ultrastructure of barley starches varying in amylose content could pave the way for research geared to understanding the relationship between starch ultrastructure and the degree of accessibility of chemical reagents and hydrolyzing enzymes into the granule interior. Such a study would enable food processors to control modifying reactions, as one path to developing novel derivatized products from barley starches.

Starch granule-bound proteins are a minor component in native starch, which may influence starch physicochemical properties, such as digestibility, swelling, solubilization, retrogradation, and granular integrity (Appelqvist and Debet, 1997). A number of researchers have extracted and identified proteins in cereal (wheat, maize, barley, rice, millet, and sorghum) starch granules (Lowy et al., 1981; Greenwell and Schofield, 1986; Goldner and Boyer, 1989; Seguchi and Yamada, 1989; Sulaiman and Morrison 1990; Rahman et al., 1995; Mu et al., 1998; Darlington et al., 2000; Baldwin, 2001). However, the majority of the true starch granule-bound proteins are integral proteins, which may be associated with amylopectin (Prentice et al., 1992; Appelqvist and Debet, 1997). There is a paucity of information on the localization and distribution of surface and bound proteins in HB starch granules. Therefore, the objective of this study was to investigate granule ultrastructure and the distribution of granule-bound proteins in starches isolated from waxy (zero-amylose), normal, and high-amylose types of HB.

4.2 Materials and methods

4.2.1 Starch source

Waxy (zero-amylose, CDC Alamo), normal (CDC Dawn), and high-amylose (SB 94893) HB (grown in the same location and harvested at Saskatoon, SK, in 1998) were obtained from the Crop Development Centre, University of Saskatchewan, SK. The barley grains were dry ground in a UDY cyclone sample mill equipped with a 0.5 mm screen. Starch was isolated from ground barley grain as described previously (Chapter 2). Waxy and normal maize starches were purchased from A. E. Staley Manufacturing Co., Decatur, IL. High-amylose maize starch (Amylomaize VII) was purchased from American Maize-Products Co., Hammond, IN.

4.2.2 Starch localization

The periodic acid-thiosemicarbazide-silver protenate method (PATAg) described by Garcia et al. (1997) was used after modification. Starch granule samples were fixed in 3% glutaraldehyde in 0.1M sodium cacodylate buffer (pH 7.2) for 2 h at room temperature (24°C) and then for 6 h at 4°C. Fixed samples were pre-embedded in agar aqueous solution (3%), cut into small cubes (1mm^3), and re-fixed for 1 h. After fixation, the sample cubes were washed in buffer (x2) and in distilled water (x2) for 20 min. For blocking residue-free aldehyde, the washed sample cubes were immersed in a saturated 2,4-dinitrophenyl-hydrazine in 15% acetic acid solution for 1 h at room temperature. After washing (x4) in distilled water for 15 min, the sample cubes were oxidized in a 1% aqueous periodic acid solution for 45 min, washed again as above, and then immersed in saturated aqueous thiosemicarbazide solution for 24 h. The sample cubes were washed again and stained in 1% aqueous silver nitrate solution for three days in darkness with daily changes of the staining solution. The stained cubes were rinsed with distilled water, dehydrated in an ethanol series (30 to 100%), and then embedded in EMbed 812 resin (EMS Inc., Fort Washington, PA). Controls of oxidative reaction were performed in parallel by substituting the periodic acid with 10% H_2O_2 (bleaching reagent).

4.2.3 Protease treatment prior to starch localization

Starch samples were hydrolyzed with protease (Megazyme E-BSPRT, 20µl/100mg starch) in MES-TRIS buffer (pH8.2) for 1.5 h at 50°C according to the procedure described for the total dietary fibre assay (Megazyme Int. Ireland, Ltd., Wicklow, Ireland). The treated samples were washed (x3) in distilled water, and then localized for starch as described above.

4.2.4 Protein localization

Starch granules were fixed in a mixture of glutaraldehyde (3%) and paraformaldehyde (4%) in 0.1M phosphate buffer (pH 7.0) for 1 h at room temperature and 2 h at 4°C. The samples were then thoroughly washed in 0.1M phosphate buffer (x3) and in distilled water (x2). The samples were incubated in ammoniacal silver nitrate (AS) solution (MacRae and Meetz, 1970) for 5 min followed by washing (x3) in distilled water. The AS solution was prepared just before use by gradual addition of 10% silver nitrate solution to concentrated ammonium hydroxide until the appearance of a slight persistent turbidity. The samples were then placed in a 3% paraformaldehyde in 0.1M phosphate buffer for 5 min until the appearance of a yellow-brown color. After washing (x3), the samples were pre-embedded in 3% agar solution and dehydrated in a graded series of ethanol. The samples were finally dehydrated with 100% ethanol and embedded in EMbed 812 resin.

4.2.5 Transmission electron microscopy

The embedded sample blocks were randomly cut into thin sections (90-100 nm) with a diamond knife in an ultramicrotome (MT 4000, RMC, Tucson, AZ). The ultra-thin sections collected on collodion-coated copper grids were observed and photographed with a transmission electron microscope (TEM) (Philips CM12, F.E.I. Company, Tacoma, WA) at 60kV without further staining. For each sample, six blocks were cut and three grids from each block were observed. Each grid contained 5-8 thin sections. Each thin section had about 20-50 granules. Hundreds of thin sections were examined. All images taken from thin sections were carefully compared. The granule growth rings were measured using image analysis software (Analysis Pro, Soft Imaging System Corp., Lakewood, CO).

4.2.6 Scanning electron microscopy

Starch (120 mg) was suspended in 0.1M phosphate buffer (10 ml) containing 0.006M NaCl at pH of 6.9. Alpha-amylase (26.5 µl, 8 units/mg starch) from porcine pancreas (EC 3.2.1.1, Sigma Chemical Co., St. Louis, MO) was added. The starch was hydrolyzed in a water bath at 37°C for 1h, centrifuged (1,700 x g) for 5 min, washed with distilled water (x3) and 100% ethanol (x2), then dried at 40°C overnight. The dried starch sample was mechanically cracked with a mortar and pestle, mounted on circular aluminum studs with double-sided sticky tape, coated with 12 nm gold, and examined and photographed in a scanning electron microscope (JSM 6301FXV, JEOL, Tokyo, Japan) at an accelerating voltage of 5 kV.

4.3 Results

4.3.1 Starch granule structure

The periodic acid - thiosemicarbazide - silver protenate (PATAg) reaction produced an excellent electron dense contrast for revealing starch granule inner structure (Figure 4-2 A, C, E). There exist two populations of granules, A (large) and B (small), in HB starches. Our attention was focused mainly on A-granules, as they are large and elliptical in shape, represent the major granule population (weight/volume) of starch (Chapter 2), and are easily observed under TEM. Ultrathin sections of A-granules from zero-amylose (CDC Alamo), normal (CDC Dawn), and high-amylose (SB 94793) starches exhibited different structural features. The above starch granules showed two distinct regions (Figure 4-2 A, C, E): 1) a central region with a loose filamentous network, and 2) a dense relatively uniform peripheral region with growth rings. Waxy (zero-amylose) starch granules showed the smallest central region, whereas high-amylose starch granules showed the largest central region. Similar structural features were observed in waxy, normal, and high-amylose maize starches (Figure 4-3). Scanning electron micrographs of enzyme (α-amylase) hydrolyzed HB starches (Figure 4-4) also showed differences in the size of the central region, suggesting that the size of the filamentous central region increases with increasing amylose content. Under

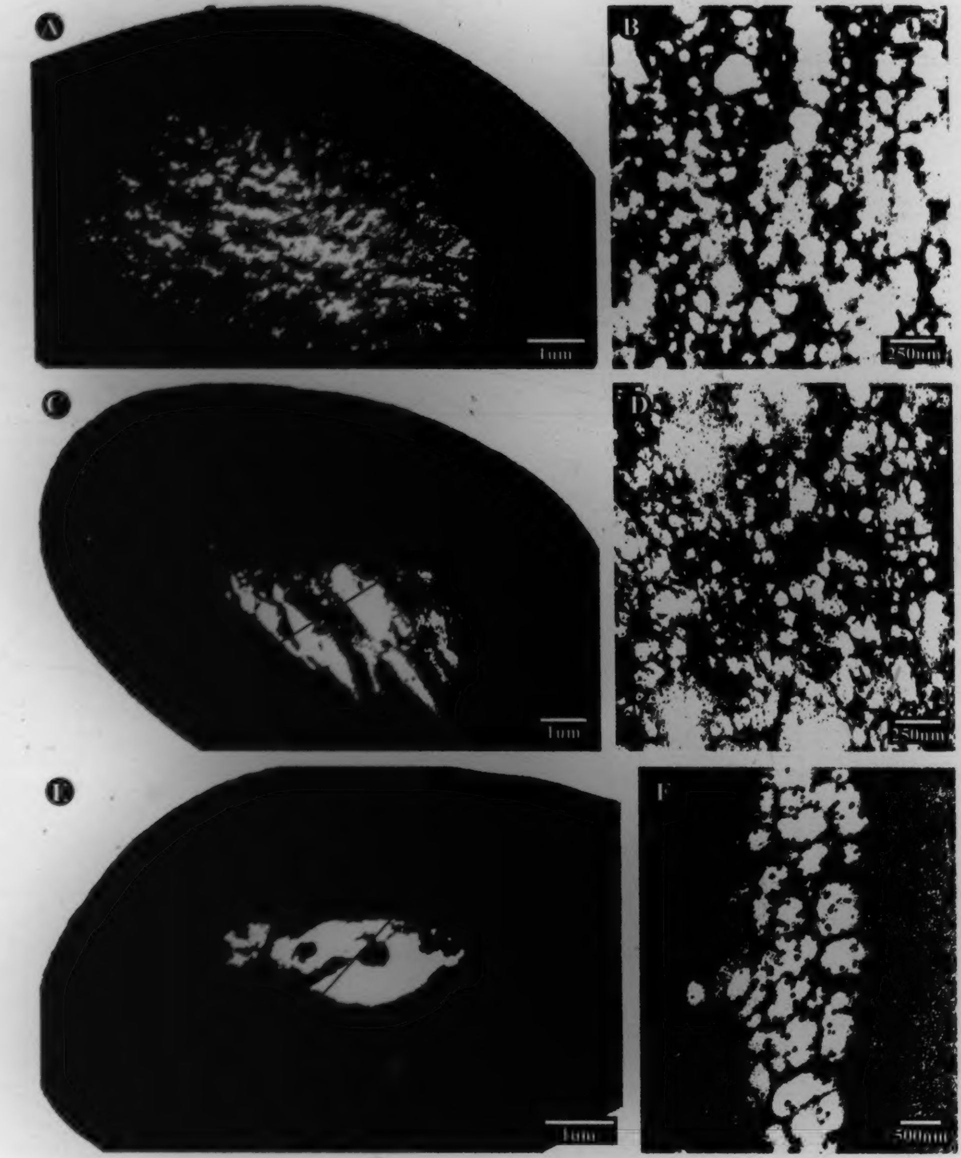

Figure 4-2 Transmission electron micrographs of ultrathin sections of HB starch granules treated with PATAg. A and B, high-amylose (SB 94893); C and D, normal (CDC Dawn); E and F, waxy (CDC Alamo). Lines in A, C and E indicate the size of the central region of granules. Micrographs B (x34K), D (x34K), and F (x18K) show magnified central regions of A, C, and E, respectively.

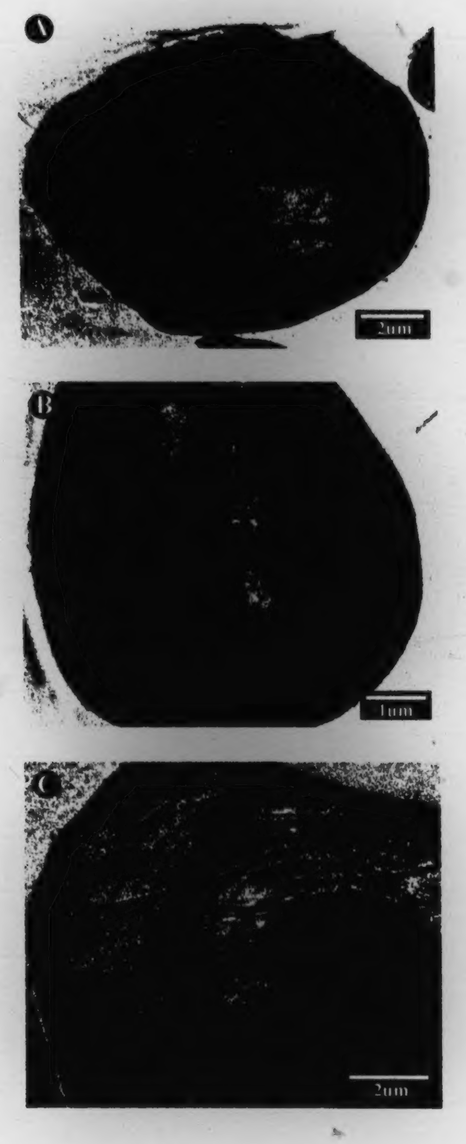

Figure 4-3 Transmission electron micrographs of ultrathin sections of maize starch granules treated with PATAg. A, high-amylose; B, normal; C, waxy. Folds are artifacts, caused by mounting on the grids or high viscosity embedding medium.

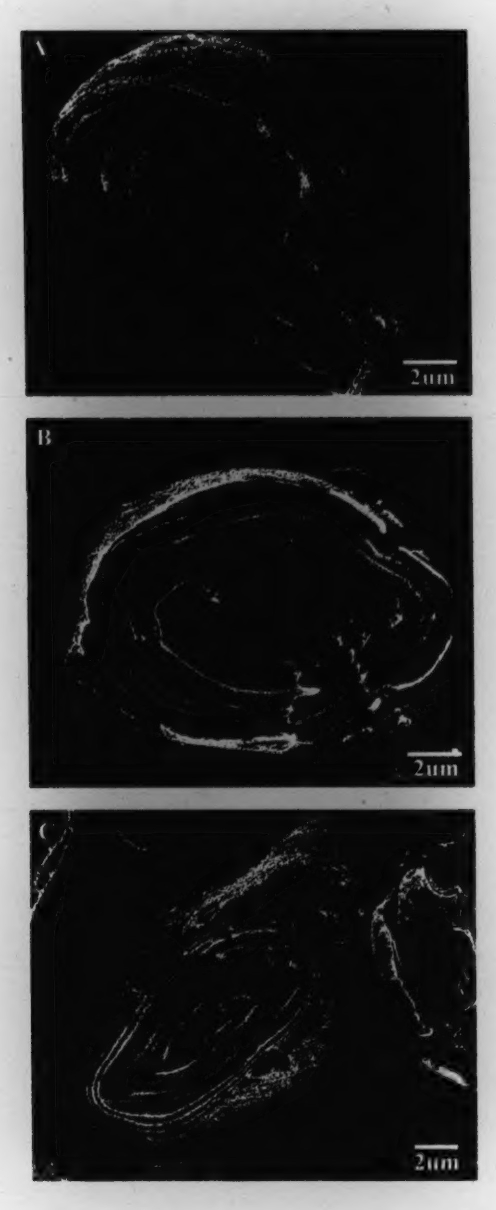

Figure 4-4 Scanning electron micrographs of HB starch granules hydrolyzed by alpha-amylase from porcine pancreas at 37°C for 1h and cracked mechanically. A, high-amylose (SB 94893); B, normal (CDC Dawn); C, waxy (CDC Alamo).

high magnification (Figure 4-2 B, D, F), the filamentous network in the central region of native waxy starch granules appeared to be more loosely packed than those of normal and high-amylose native starch granules. The filamentous network was present surrounding clear areas, and large silver-stained particles were found deposited beside the network in waxy starch granules (Figure 4-2 F). However, in non-waxy starch granules (Figure 4-2 B, D), large silver particles were randomly deposited beside and inside the filamentous network. This difference in the structure of the starch granule central region between waxy and non-waxy starches may be due to variations in amylose content. Treatment of high-amylose HB starch and normal maize starch with protease (before fixation/staining) resulted in the disappearance of the silver particles (Figure 4-5), suggesting that these silver particles could be stained proteins.

4.3.2 Growth rings

Growth rings (semi-crystalline rings [lighter rings] and inter-crystalline amorphous rings [darker rings]) of the starch granules were clearly visualized in the peripheral regions of the starch granules. The growth rings varied in number and size depending on the genotype (Figure 4-2 A, C, E). Artifacts, such as swelling, shrinkage and/or stretching may occur during section preparation, but it was not noticeable. The number and width of the semi-crystalline growth rings and inter-crystalline amorphous growth rings in HB starch granules measured from transmission electron micrographs are presented in Table 4-I. The width of granule growth rings decreased with increasing amylose content. Furthermore, growth rings present closer to the granule surface were narrower in width than those present within the granule interior (Figure 4-2 A, C, E, and Figure 4-3). A similar measurement on maize starches was impossible because the width of the

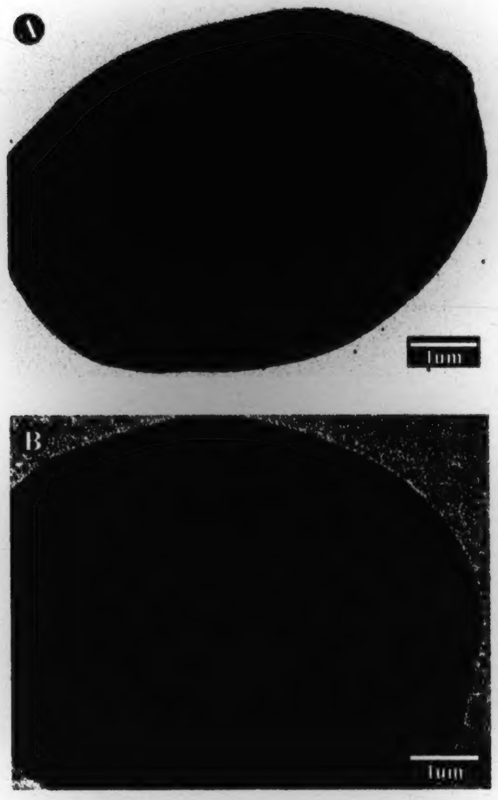

Figure 4-5 Transmission electron micrographs of ultrathin sections of high-amylose barley starch granule (A) and normal maize starch granule (B) hydrolyzed by protease.

Table 4-1 Widths of granule growth rings[a] of hull-less barley starches

Starch type	Semi-crystalline growth ring width (nm)		Inter-crystalline amorphous growth ring width (nm)	
	Range	Average	Range	Average
Waxy	165-380	261	55-150	93
Normal	65-310	167	25-150	72
High-amylose	70-270	193	50-85	69

[a] 20 granules from each starch were measured.

semi-crystalline rings and inter-crystalline amorphous rings varied substantially across the granule (Figure 4-3). This is perhaps due to irregular granule shapes. In addition, the intensity and density of silver-stained particles appeared unevenly in the granules. Large silver-stained particles were mainly located in the central region and on both sides of the inter-crystalline amorphous rings in the peripheral region (Figure 4-2).

4.3.3 Proteins in starch granules

The ammoniacal silver (AS) reaction produced discrete electron dense particles (localized proteins), which were unevenly distributed both on the edge and inside area of embedded native starch granules (Figure 4-6). This suggests that proteins associated with starch granules are located both on the granule surface (surface proteins) and within the interior (integral proteins). Integral proteins accounted for a large proportion of the total proteins based on the particle density (visual evaluation). Compositional analysis (Chapter 2) results had shown that the protein contents of waxy, normal, and high-amylose HB starches were 0.26%, 0.33%, and 0.42%, respectively. The location of dense particles in both of the central and peripheral regions of the granule (Figure 4-6) suggests that integral proteins are probably present within these regions. The density of silver particles (proportional to the protein content) increased with an increase in amylose content (waxy < normal < high-amylose).

4.4 Discussion

4.4.1 Architecture of starch granules

The PATAg reaction enabled a clear visualization of the granule ultrastructure but did not distinguish between amylose and amylopectin within the starch granules. The

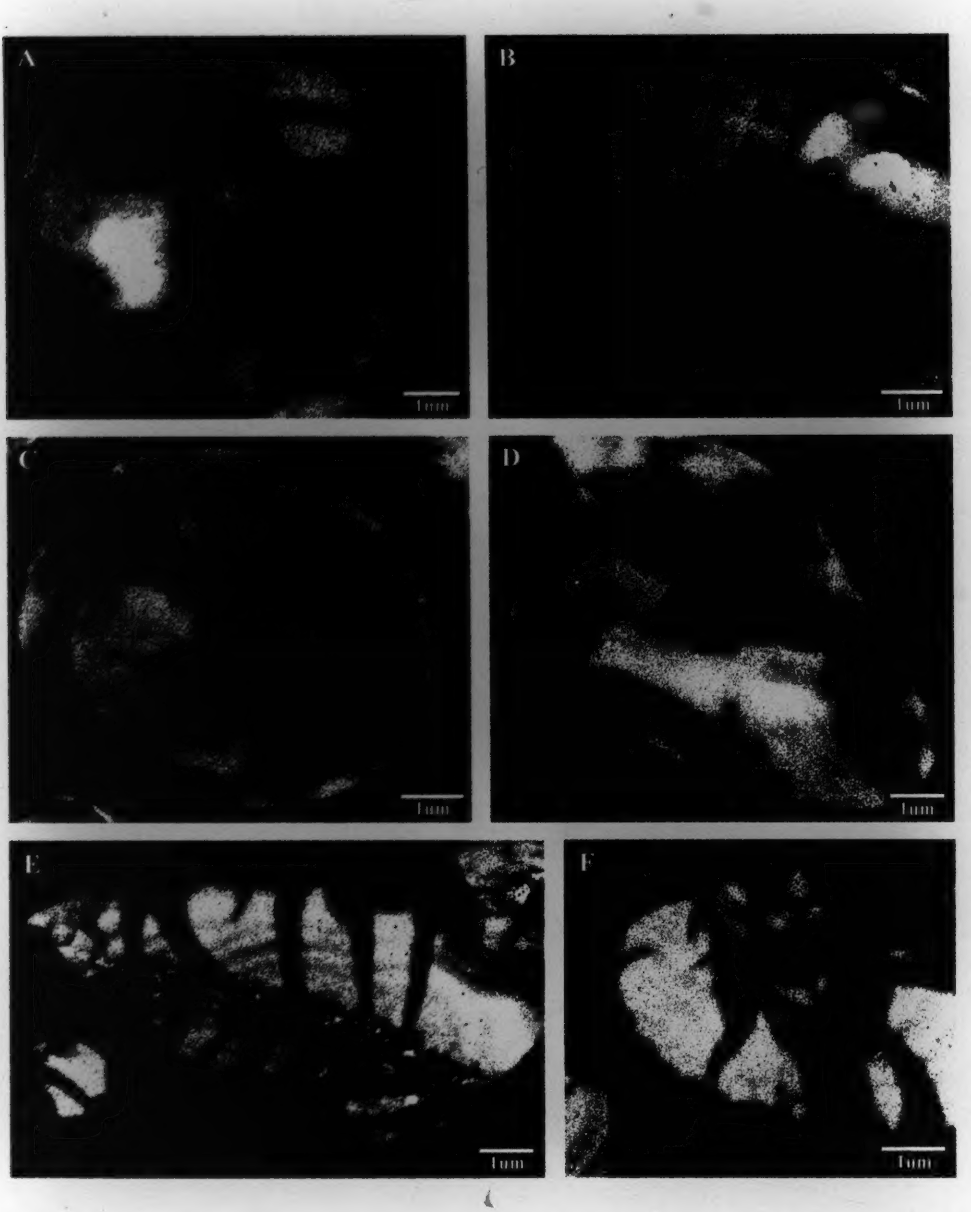
A
B
1um
1um
C
D
1um
1um
E
F
1um
1um

Figure 4-6 Transmission electron micrographs of ultrathin sections of HB starch granules treated with AS. A and B, high-amylose (SB 94893); C and D, normal (CDC Dawn); E and F, waxy (CDC Alamo).

alternating densely and loosely packed regions and the central filamentous region represent three distinct inner structural features of starch granules. The densely packed semi-crystalline regions (lighter growth rings) are mainly formed from ordered double-helical amylopectin lamellae and amorphous amylopectin lamellae (Figure 4-1), whereas the central filamentous region is completely amorphous. A ^{13}C CP/MAS NMR study (Gidley and Bociek, 1985) suggested that amylopectin double helices (not involved in crystal formation) are located in amorphous rings together with lipid-complexed amylose, lipid-free amylose and some proteins (Morrison, 1995). Seguchi and Kanenaga (1997) studied wheat starch granules using remazolbrilliant blue dye staining and an aqueous sodium dodecyl sulfate extraction procedure with contrast light microscopy and reported that the central region (surrounded by concentric circles) was different from other inner regions (concentric circles surrounded by "skirt" area) of wheat starch granules. Helbert et al. (1996) showed that the central region of (immuno-gold labeled) maize starch granules was degraded by α-amylase more readily than the outer region. Localization of amylose and amylopectin using enzyme-gold labeling (Atkin et al., 1999) and iodine staining (Seguchi et al., 2000) studies revealed that both linear amylose and branched amylopectin co-exist in the central region of the granules of non-waxy maize and potato starches, whereas only amylopectin is present within the central region of waxy maize and waxy wheat starch granules. These studies confirmed that an amorphous central region exists in most native starch granules. Research has shown that amylose is concentrated in the center of granules in maize (Schwartz, 1982) and potato (Tatge, 1999) starches. Tatge (1999) observed that the size of the amylose region increased as the granule grew and the increase in size was greater in potato with higher levels of granule-bound starch synthase. This suggests that the size of the central region is closely related to the amylose content and is also associated with the content and distribution of starch synthesis enzymes. The present study indicated that in HB starch granules, the central region increased in size and the growth rings decreased in width with increasing amylose content. These structural variations could influence the enzymatic digestion, hydration, and chemical reactions of starch. Further research along this line of investigations is warranted.

4.4.2 Growth rings

For HB starches, the average widths (Table 4-1) of semi-crystalline growth rings are: waxy (260 nm) > high-amylose (190 nm) ≈ normal (170 nm). The average width of crystalline and amorphous lamellae (Figure 4-1) has been shown to range from 9-12 nm (French, 1984). Therefore, the average number of crystalline and amorphous lamellae in the semi-crystalline growth rings of HB starches could be estimated to follow the order: waxy (22 – 29) > high-amylose (16 – 21) ≈ normal (14 – 19). The width and the number of growth rings varied with amylose content. The smaller width of growth rings in non-waxy starch granules may be attributed to amylose synthesis that interrupts formation of the semi-crystalline region. Thus, the greater width of growth rings in waxy starch granules may be due to the very low amylose content.

Furthermore, in starch granules, the semi-crystalline growth rings are formed by associations between A-chains (A-chain clusters) of amylopectin that arise from B1-chains, which in turn arise from B2/B3-chains (Figure 4-1). Determination of the amylopectin branch chain length distribution of HB starches (Chapter 2) had shown that the waxy type had a lower proportion of longer chains (DP 35 – 67) when compared to normal and high-amylose types. This indicated that waxy barley amylopectin has a lower proportion of B2/B3 branch chains, suggesting that the crystalline lamellae of waxy HB starch may be packed more loosely and thus were more open than those of normal and high-amylose starches. Such an open structure in waxy barley starch may be related to its higher swelling (during pasting) and higher initial rate of enzyme and acid hydrolysis (Chapter 3; Vasanthan and Bhatty, 1996).

4.4.3 Starch granule-bound proteins

As minor components, two types of starch granule-bound proteins, namely surface proteins and integral proteins are present in native starch granules. Surface proteins on cereal starch granules have molecular weights in the range 5-30 kDa and are readily removed by repeated washing with water (Darlington et al., 2000), sodium dodecyl sulfate (SDS) (Greenwell and Schofield, 1986; Seguchi and Yamada 1989; Rahman et al., 1995), NaCl (Lowy et al., 1981), and thermolysin (Mu-Forster and Wasserman, 1998) at sub-gelatinization temperatures. Major surface proteins account for about 8% of total starch proteins in wheat starch (Lowy et al., 1981). Integral proteins, which are embedded within the starch matrix, can be extracted by gelatinizing starch granules in the presence of SDS (Lowy et al., 1981; Mu et al., 1998). SDS gel electrophoresis showed that the integral proteins are the three major starch synthases (60 kDa granule-bound starch synthase I, 76 kDa starch synthase I, and 85 kDa starch-branching enzyme IIb) in maize starch (Mu-Forster et al., 1996) and wheat (Rahman et al., 1995) whilst the other two proteins (100 kDa and 105 kDa) are only present in wheat and absent in other cereal starches. Granule-bound starch synthase, also known as waxy protein, is correlated with the synthesis of amylose. Waxy mutants of cereals lack this functional protein (Goldner and Boyer, 1989). By using fluorescence-labeling, Han and Hamaker (2001) showed that granule-bound starch synthase (GBSS) is concentrated in the granule rings of normal potato, maize, and wheat starches, but not in waxy potato and waxy maize starches. However, protein bands other than GBSS were also identified by sodium dodecyl sulfate - polyacrylamide gel electrophoresis (SDS-PAGE) but were not labeled by the fluorescence dye. Silver staining is a commonly used staining procedure to stain proteins. In the present study, stained proteins were located in both central and peripheral regions of the granules. With increasing amylose content, more stained proteins were visualized in the central region, indicating the diversity of concentration and distribution of integral proteins and/or enzymes among different genotypes of HB starches, as well as some relevance to starch biosynthesis.

4.4.4 Periodic acid - thiosemicarbazide - silver protenate and ammoniacal silver reactions in starch granules

The periodic acid - thiosemicarbazide - silver protenate (PATAg) method is derived from the periodic acid - Schiff (PAS) light microscopy staining technique and is used for the detection of carbohydrates in cells by electron microscopy (Jewell and Saxton, 1970). A number of tissue components give positive PAS reaction, including polysaccharides, glycoproteins and glycolipids (Pearse, 1968). In the PATAg method, the dialdehydes react with thiosemicarbazide instead of Schiff reagent forming thiosemicarbazones, which effectively reduce silver proteinate and release metallic silver at the sites of glycol linkages (Hayat, 1989). The PATAg method has been successfully used for electron microscopy investigation of starch granule ultrastructure (Kassenbeck 1975, 1978; Gallant and Bouchet, 1986; Planchot et al., 1995; Gallant et al., 1997). The PATAg reaction produces a very fine reaction product and is almost free of non-specific precipitates (Hayat, 1989), which leads to good contrast in the thin sections of starch granules. However, proteins (mostly enzymes involved in starch synthesis) that are also rich in 1, 2-glycols and amino-substituted alcohol groups have a strong affinity for silver stains and the small silver particles may fuse to form large aggregates after a longer treatment time (Hayat, 1989). These large silver-stained particles disappear when starch granules are treated with protease prior to staining (Figure 4-5), suggesting that the large silver-stained particles in PATAg staining may be the PATAg reaction products with proteins rather than with polysaccharides.

The ammoniacal silver (AS) technique was introduced by MacRae and Meetz (1970) to electron microscopy and successfully applied to identify localized proteins in animal and plant tissues (Souto-Padrón and Souza, 1978; Benchimol et al., 1982; Hayat, 1989; Yoshikawa and Oishi, 1997). Also, it has been used for characterization of protein in SDS-PAGE as one of the routine high sensitivity staining reagents (Bollag and Edelstein, 1991). Proteins could reduce ammoniacal silver nitrate to metallic silver, which are deposited as dark silver particles of variable diameters in the plant/animal specimen (Robards and Wilson, 1993). However, the precise mechanism of binding between silver and polypeptides is poorly understood (MacRae and Meetz, 1970; Troyer, 1980). The treatment of samples with buffered formaldehyde solution is an absolute requirement for the reaction with silver regardless of previous fixation in formalin (Troyer, 1980). Starch granule-bound proteins exist as monomers (Mu-Foster and Wasserman, 1998) and are clearly visualized (appear in the form of electron-dense particles by AS staining). In this study, the density of these silver-stained particles increased with an increase in amylose content (Figure 4-6) and is consistent with the protein content of HB starches (Chapter 2).

A number of studies have reported that surface pores and internal channels (up to 0.4 µm in diameter) are present on the granule surface and within granules (Fannon et al., 1992, 1993; Karathanos and Saravacos, 1993; Huber and BeMiller, 1997, 2000). These surface pores and internal channels provide an entry pathway for enzymes, dyes and reagents diffusing into the granule interior (Kimura and Robyt, 1995; Herbert et al., 1996; Huber and BeMiller, 2000). Therefore, it is possible for protease to pass through the channels to the interior of granules. The observations in this study clearly showed that the dark particles (representing proteins) were greatly reduced in the thin sections of starches from barley and maize after protease treatment.

4.5 Conclusion

Substantial differences in ultrastructure in terms of crystallite formation, the number and size of crystalline and amorphous lamellae, amylopectin chain length, and association with minor components (i.e. protein) exists among HB starch granules. Waxy HB starch had wider inter-crystalline amorphous growth rings, semi-crystalline growth rings, and more open crystalline lamellae than did normal and high-amylose genotypes. Starch granule-bound proteins were mainly located in the granule interior as integral proteins, although there was diversity in the concentration and distribution of proteins among different genotypes of HB. With increasing amylose content, the central region of the starch granule became larger and more protein was present. The structural variations among HB starches as demonstrated in this study could influence their reactivity towards enzymes and modifying reagents.

4.6 References

Appelqvist, I. A. M., and Debet, M. R. M. 1997. Starch-biopolymer interactions — a review. *Food Rev. Int.* 13:163-224.

Atkin, N. J., Abeysekera, R. M., and Robards, A. W. 1998b. The events leading to the formation of ghost remnants from the starch granule surface and the contribution of the granule surface to the gelatinization endotherm. *Carbohydr. Polym.* 36:193-204.

Atkin, N. J., Abeysekera, R. M., Cheng, S. L., and Robards, A. W. 1998a. An experimentally-based predictive model for the separation of amylopectin subunits during starch gelatinization. *Carbohydr. Polym.* 36:173-192.

Atkin, N. J., Cheng, S. L., Abeysekera, R. M., and Robards, A. W. 1999. Localisation of amylose and amylopectin in starch granules using enzyme-gold labeling. *Starch/Stärke* 51:163-172.

Baldwin, P. M. 2001. Starch granule-associated proteins and polypeptides: a review. *Starch/Stärke* 53:475- 503.

Benchimol, M. Elias, C. A. and Souza, W. D. 1982. *Tritrichomonas foetus*: Ultrastructural localization of basic proteins and carbohydrates. *Exp. Parasitol.* 54: 135-144.

Bollag, D. M., and Edelstein, S. J. 1991. *Protein Methods*. Wiley-Liss, Inc.: New York.

Darlington, H. F., Tecsi, L., Harris, N., Griggs, D. L., Cantrell, I. C., and Shewry, P. R. 2000. Starch granule associated proteins in barley and wheat. *J. Cereal Sci.* 32:21-29.

Fannon, J. E., Hauber, R. J., and BeMiller, J. N. 1992. Surface pores of starch granules. *Cereal Chem.* 68:284-288.

Fannon, J. E., Shull, J. M., and BeMiller, J. N. 1993. Interior channels of starch granules. *Cereal Chem.* 70:611-613.

French, D. 1984. Organization of starch granules. In: *Starch Chemistry and Technology*, R. L. Whistler, J. N. Miller, and E. F. Paschall eds. p.183-283. Academic Press, Orlando, Florida.

Gallant, D. J., and Bouchet, B. 1986. Ultrastructure of maize starch granules. A review. *Food Microstruct.* 5:141-155.

Gallant, D. J., Bouchet, B., and Baldwin, P. M. 1997. Microscopy of starch: evidence of a new level of granule organization. *Carbohydr. Polym.* 32:177-191.

Garcia, V., Colonna, P., Bouchet, B., and Gallant, D. J. 1997. Structural changes of cassava starch granules after heating at intermediate water contents. *Starch/Stärke.* 49:171-179.

Gidley, M. J., and Bociek, S. M. 1985. Molecular organization in starches: A ^{13}C CP/MAS NMR study. *J. Am. Chem. Soc.* 107:7040-7044.

Goldner, W. R., and Boyer, C. D. 1989. Starch granule-bound proteins and polypeptides: The influence of the waxy mutations. *Starch/Stärke.* 41:250-254.

Greenwell, P., and Schofield, J. D. 1986. A starch granule protein associated with endosperm softness in wheat. *Cereal Chem.* 63:379-380.

Han, X. Z., and Hamaker, B. R. 2001. Location of starch granule-associated proteins revealed by confocal laser scanning microscopy. *J. Cereal Sci.* 35: 109-116.

Hayat, M. A. 1989. *Principles and Techniques of Electron Microscopy*. The Macmillan Press: Hong Kong.

Helbert, W., and Chanzy, H. 1996. The ultrastructure of starch from ultrathin sectioning in melamine resin. *Starch/Stärke* 48:185-188.

Helbert, W., Schülein, M., and Henrissat, B. 1996. Electron microscopic investigation of the diffusion of *Bacillus licheniformis* α-amylase into corn starch granules. *Int. J. Bio. Macromol.* 19:165-169.

Huber, K. C., and BeMiller, J. N. 1997. Visualization of channels and cavities of corn and sorghum starch granules. *Cereal Chem.* 74:537-541.

Huber, K. C. and BeMiller, J. N. 2000. Channels of maize and sorghum starch granules. *Carbohydr. Polym.* 41: 269-276.

Jenkins, P. J., and Donald, A. M. 1995. The influence of amylose on starch granule structure. *Int. J. Biol. Macromol.* 17:315-321.

Jewell, G. G., and Saxton, C. A. 1970. The ultrastructural demonstration of compounds containing 1, 2-glycol groups in plant cell walls. *Histochem. J.* 2:17-27.

Karathanos, V. T., and Saravacos, G. D. 1993. Porosity and size distribution of starch materials. *J. Food Eng.* 18:259-280.

Kassenbeck, V. P. 1975. Elektronenmikroskopischer Beitrag zur Kenntnis der Feinstruktur der Weizenstärke. *Starch/Stärke.* 27:217-226.

Kassenbeck, V. P. 1978. Beitrag zur Kenntnis der Verteilung von Amylose und Amylopektin in Stärkekörnern. *Starch/Stärke.* 30:40-46.

Kimura, A. and Robyt, J. F. 1995. Reaction of enzymes with starch granules: kinetics and products of the reaction with glucoamylase. *Carbohydr. Res.* 277: 87-107.

Lowy, G. D. A., Sargeant, J. G., and Schofield J. D. 1981. Wheat starch granule protein: The isolation and characterization of a salt-extractable protein from starch granules. *J. Sci. Food Agric.* 32:371-377.

MacRae, E. K., and Meetz, G. D. 1970. Electron microscopy of the ammoniacal silver reaction for histones in the erythropoietic cells of the chick. *J. Cell Biol.* 45:235-245.

Morrison, W. R. 1995. Starch lipids and how they relate to starch granule structure and functionality. *Cereal Foods World* 40:437-446.

Mu, H. H., Mu-Forster, C., Bohonko, M., and Wasserman, B. P. 1998. Heat-induced fragmentation of the maize waxy protein during protein extraction from starch granules. *Cereal Chem.* 75:480-483.

Mu-Forster, C., and Wasserman, B. P. 1998. Surface localization of zein storage proteins in starch granules from maize endosperm. *Plant Physiol.* 116:1563-1571.

Mu-Forster, C., Huang, R., Powers, J. R., Harriman, R. W., Knight, M., Singletary, G. W., Keeling, P. L, Wasserman, B. P. 1996. Physical association of starch biosynthetic enzymes with starch granules of maize endosperm. *Plant Physiol.* 111:821-829.

Nikuni, Z. 1978. Studies on starch granules. *Starch/Stärke* 30:105-111.

Oostergetel, G. T., and Bruggen, E. J. V. 1989. On the origin of a low angle spacing in starch. *Starch/Stärke* 41:331-335.

Pearse, A. G. E. 1968. *Histochemistry: Theoretical and Applied.* Vol.1. Little, Brown and Company: Boston.

Planchot, V., Colonna, P., Gallant, D. J., and Bouchet, B. 1995. Extensive degradation of native starch granules by alpha-amylase from *Aspergillus fumigatus*. *J. Cereal Sci.* 21:163-171.

Prentice, R. D. M., Stark, J. R., and Gidley, M. J. 1992. Granule residues and "ghosts" remaining after heating A-type barley starch granules in water. *Carbohydr. Res.* 227:121-130.

Rahman, S., Kosar Hashemi, B., Samuel, M. S., Hill, A., Abbott, D. C., Skerritt, J. H., Preiss, J., Appels, R., and Morell, M. K. 1995. The major proteins of wheat endosperm starch granules. *Aust. J. Plant Physiol.* 22:793-803.

Robards, A. W., and Wilson, A. J. 1993. *Procedures in Electron Microscopy*. John Wiley and Sons Ltd: Toronto.

Schwartz, D. 1982. Amylose distribution in the starch granule of maize endosperm. *Maydica* 27: 54-57.

Seguchi, M., and Kanenaga, K. 1997. Study of three-dimensional structure of wheat starch granules stained with remazolbrilliant blue dye and extracted with aqueous sodium dodecyl sulfate and mercaptoethanol solution. *Cereal Chem*. 74:548-552.

Seguchi, M., and Yamada, Y. 1989. Study of proteins extracted from the surface of wheat starch granules with sodium dodecyl sulfate. *Cereal Chem*. 66:193-196.

Seguchi, M., Yasui, T., Hosomi, K., and Imai, T. 2000 Study of internal structure of waxy wheat starch granules by KI/I_2 solution. *Cereal Chem*. 77:339-342.

Souto-Padrón, T. and Souza, W. D. 1978. Ultrastructural localization of basic proteins in *Tryanosma cruzi*. *J. Histochem. Cytochem*. 26: 349-358.

Sulaiman, B. D., and Morrison, W. R. 1990. Proteins associated with the surface of wheat starch granules purified by centrifuging through caesium chloride. *J. Cereal Sci*. 12: 53-61.

Tatge, H., Marshall, J., Martin, C., Edwards, E. A., and Smith, A. M. 1999. Evidence that amylose synthesis occurs within the matrix of the starch granule in potato tubers. *Plant Cell Environ*. 22: 543-550.

Troyer, H. 1980. *Principles and Techniques of Histochemistry*. Little, Brown and Company: Boston

Vasanthan, T. and Bhatty, R. S. 1996. Physicochemical properties of small- and large-granule starches of waxy, regular, and high-amylose barleys. *Cereal Chem*. 73: 199-207.

Yamaguchi, M., Kainuma, K., and French, D. 1979 Electron microscopic observations of waxy maize starch. *J. Ultrastruct. Res.* 69:249-261

Yoshikawa, H. and Oishi, K. 1997. Ultrastructural localization of basic proteins of *Blastocystis hominis*. *Protoplasma.* 200: 31-34.

CHAPTER 5

Morphological and Structural Changes in Waxy, Normal and High-amylose Starch Granules during Heating[1]

5.1 Introduction

Starch is stored as discrete semi-crystalline granules in higher plants. Starch consists of two main components: mainly linear amylose and highly branched amylopectin. The amylose content usually varies from 17-65% depending on the botanical origin of the starch. The exact location of amylose within the granule interior and the extent and nature of its interaction with amylopectin is still unclear. The minor starch components include bound and free lipids, proteins and minerals. Starch granules vary in shape, size and composition, depending on their botanical origin (French, 1984). Extracted starches from cereals are used extensively in food and non-food industries. These starches are physically and chemically modified to meet the properties demanded by the industry. A major step during industrial utilization of starch is gelatinization. During gelatinization, starch granules undergo hydration, formation of ghost remnants (derived from the external layers of the granule), swelling (radial and tangential), exudation of amylose and amylopectin (to a limited extent), loss of birefringence, loss of crystallinity and changes in viscosity. Morphological and ultrastructural changes during starch gelatinization have been observed by scanning electron microscopy (SEM) and transmission electron microscopy (TEM) in potato, waxy maize, normal maize, barley, oat, wheat, cassava and in chemically modified maize starches (Bowler et al., 1980;

---

[1] A version of this chapter is in press in *Food Research International*, 2004.

Holmes and Soeldner, 1981; Christianson et al., 1982; Ghiasi et al., 1982; Williams and Bowler, 1982; Varriano-Marston et al., 1985; Langton and Hermansson, 1989; Liu and Zhao, 1990; Fannon and BeMiller, 1992; Svegmark et al., 1993; Garcia et al., 1997; Atkin et al., 1998a; Atkin et al., 1998b). Morphological and structural changes at various temperature and moisture combinations have been shown to influence rheological behaviour and functionality of starch gels (Sterling, 1978; Christianson et al., 1982; Autio, 1990; Lii et al., 1995; Hermansson and Svegmark, 1996).

A study of granule morphological and structural changes during heating is important for establishing structure-functionality relationships in hull-less barley (HB) starches. However, such studies have not been carried out on HB starches. Several HB cultivars have been registered in Canada and a series of HB genotypes with a wide range of amylose content have been developed through a breeding program in Saskatchewan. The variation in composition and structure of HB starches may influence the quality of starch-containing products. Therefore, the choice of starch type and control of processing conditions are very important in subsequent HB starch utilization. The objective of this study was to follow (using SEM and TEM) the morphological and ultrastructural changes of three genotypes (CDC Alamo, CDC Dawn, and SB 94893) of HB starch granules during heat treatment at different temperatures.

5.2 Materials and methods

5.2.1 Materials

Waxy/zero-amylose (CDC Alamo), normal (CDC Dawn), and high-amylose (SB 94893) HB grains grown and harvested at Saskatoon, SK, in 1998 were obtained from the

Crop Development Centre, University of Saskatchewan, SK. The barley grains were ground in a UDY cyclone sample mill (UDY Lab Equipment and Supplies, Ft. Collins, CO) equipped with a 0.5 mm screen. Isopentane was purchased from Sigma Chemical Co. (St. Louis, MO). Starch was isolated form ground barley grain as described previously (Chapter 2).

5.2.2 Sample preparation

Starch samples used for scanning electron microscopy observation consisted of 500 mg starch dispersed in 5 ml of distilled water. Each was heated at different temperatures (50, 55, 65, 80, 90, and 100°C) for 30 min in a water bath with minimal manual mixing. Droplets of starch paste were rapidly frozen by immersing into melting isopentane precooled by liquid nitrogen and then freeze-dried (Labconco 6 Liter Console Freeze Dry System, Labconco Corporation, Kansas City, MI) at -60°C for one day. An unheated starch sample was used as control. Starch samples used for Matrix-assisted laser desorption/ionization-mass spectrometry (MALDI-MS) analysis were prepared by heating starch at 65°C and 100°C, respectively, for 30 min and then centrifuged at 6,000 xg for 10 min. The supernatant and residue were freeze-dried.

5.2.3 Scanning electron microscopy

Fine powder or cracked particles of freeze-dried samples were mounted on circular aluminum studs with double-sided sticky tape and then coated with 10 nm gold. Samples were examined and photographed in a JEOL (JSM 6301 FXB) scanning electron microscope (JEOL Ltd., Tokyo, Japan) at an accelerating voltage of 5 kV.

5.2.4 Transmission electron microscopy

Starch paste samples for transmission electron microscopy were prepared as above and then fixed, embedded, and stained following the periodic acid-thiosemicarbazide-silver reaction method described previously (Chapter 4). Thin sections of 90-100 nm in thickness were randomly cut from the embedded sample blocks with a diamond knife in an RMC MT 4000 ultramicrotome (Boeckeler Instruments, Inc., Tucson, AZ) and examined and photographed with a Philips CM12 transmission electron microscope (F.E.I. Company, Tacoma, WA) at 60 kV without further staining.

5.2.5 Matrix-assisted laser desorption/ionisation mass spectrometry

Debranching of soluble starch samples and matrix-assisted laser desorption/ionisation mass spectrometry (MALDI-MS) analysis were carried out as described previously (Chapter 2).

5.3 Results and discussion

5.3.1 Morphology and ultrastructure of native HB starch granules

The surfaces of native starch granules from waxy, normal and high-amylose HB grains were smooth and uniform with equatorial grooves (Figure 5-1 A, C, E). Randomly distributed pinholes of varying size were present on the surface of larger granules (Figure 5-1 A, C, E). Under transmission electron microscopy, a dense, uniform peripheral region with alternate growth rings (the dark regions correspond to the stained amorphous growth rings whereas the semi-crystalline growth rings were much lighter) and a central region with a filamentous network in the native HB starch granules were clearly observed (Figure 5-1 B, D, F).

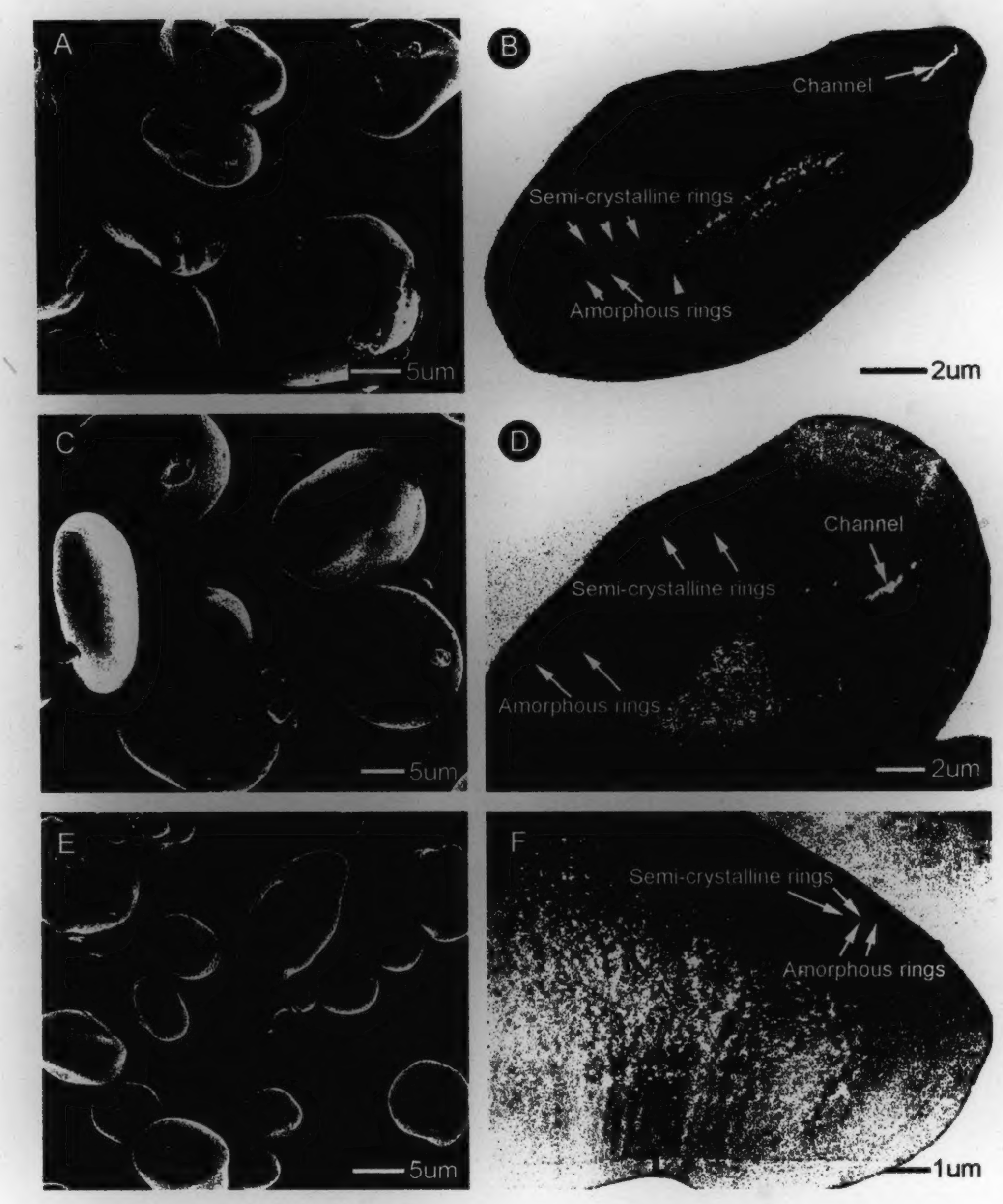
A
5um
B
Channel
Semi-crystalline rings
Amorphous rings
2um
C
5um
D
Channel
Semi-crystalline rings
Amorphous rings
2um
E
5um
F
Semi-crystalline rings
Amorphous rings
1um

Figure 5-1 Scanning (A, C, & E) and transmission electron micrographs (B, D, & F) of native waxy (CDC Alamo) (A & B), normal (CDC Dawn) (C & D), and high-amylose (SB 94893) (E & F) HB starch granules.

5.3.2 Morphological and ultrastructural changes during heating of waxy starch granules

Scanning electron micrographs of waxy HB starch granules heated at different temperatures are presented in Figures 5-2 and 5-3. At 50°C, larger granules displayed ridges on their surfaces (Figure 5-2 A). This suggests uneven granular swelling in the radial and tangential directions. In addition, a small amount of exudate was present on the granular surface (Figure 5-2 B). Morphological changes were more pronounced at 55°C. These changes were as follows: 1) Leaching of exudate increased slightly (Figure 5-2 E); 2) Many of the larger granules were split into two halves at the equatorial grooves (this suggests that the equatorial groove is a region of granule instability) (Figure 5-2 C, E, F), whereas smaller granules remained intact (Figure 5-2 D, E); 3) Many of the granules were fragmented (Figure 5-2 D, E); 4) Granule rings were visible in split granules (Figure 5-2 E, F); 5) Formation of a cavity in the central region of the granule (Figure 5-2 E, F); 6) Formation of a loose filamentous network in the central region of the granules (Figure 5-2 F); and 7) Some of the pinholes were enlarged and split (Figure 5-2 D, F). At 65°C, most granules gelatinized/melted (Figure 5-3 A, B). At 80°C, the gelatinized matrix formed a coarse honeycomb-like structure, which may have been due to ice crystal formation during freezing and freeze-drying (Figure 5-3 C). At 100°C, all granules had already gelatinized and the remnants formed a looser filamentous network (Figure 5-3 D) as compared to those heated at 80°C.

In parallel to SEM, transmission electron micrographs of waxy HB starch granules heated at 65°C, 80°C, and 90°C are presented in Figure 5-4. At 65°C, partly gelatinized starch sections (Figure 5-4 A, B) showed the development of a radially

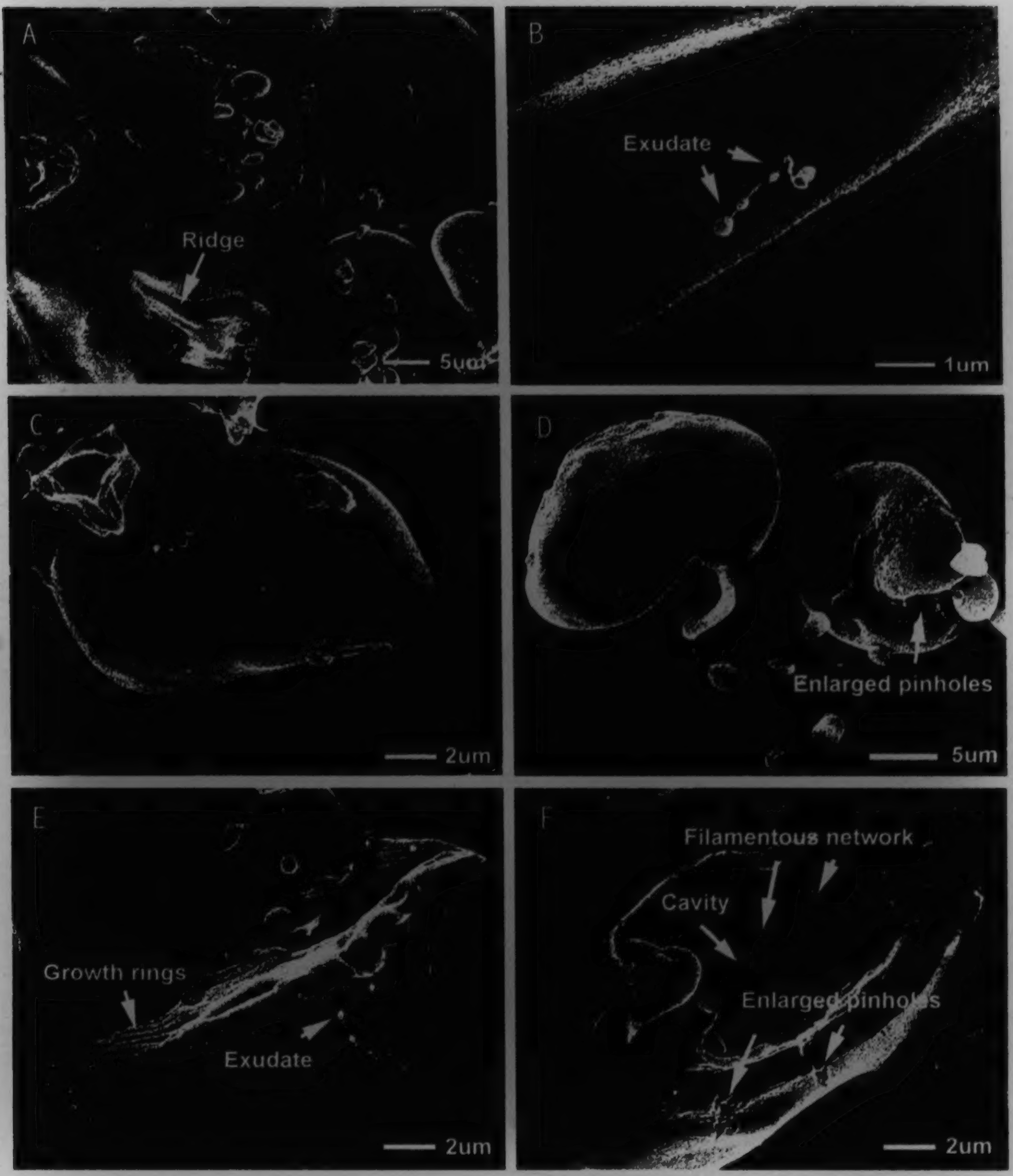
A
Ridge
5um
B
Exudate
1um
C
2um
D
Enlarged pinholes
5um
E
Growth rings
Exudate
2um
F
Filamentous network
Cavity
Enlarged pinholes
2um

Figure 5-2 Scanning electron micrographs of waxy HB starch granules (CDC Alamo) heated in water to various temperatures. A, 50°C; B, C, D, E, and F, 55°C.

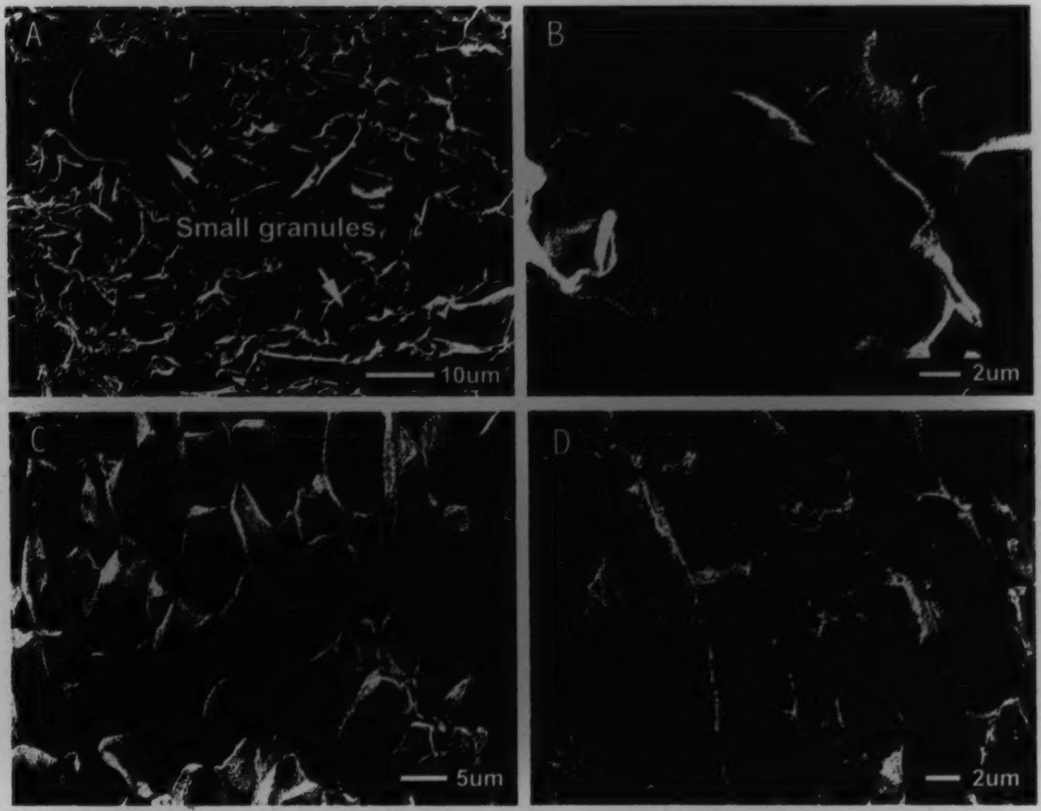
A
Small granules
10um
B
2um
C
5um
D
2um

Figure 5-3 Scanning electron micrographs of waxy HB starch granules (CDC Alamo) heated in water to various temperatures. A and B, 65°C; C, 80°C; D, 100°C.

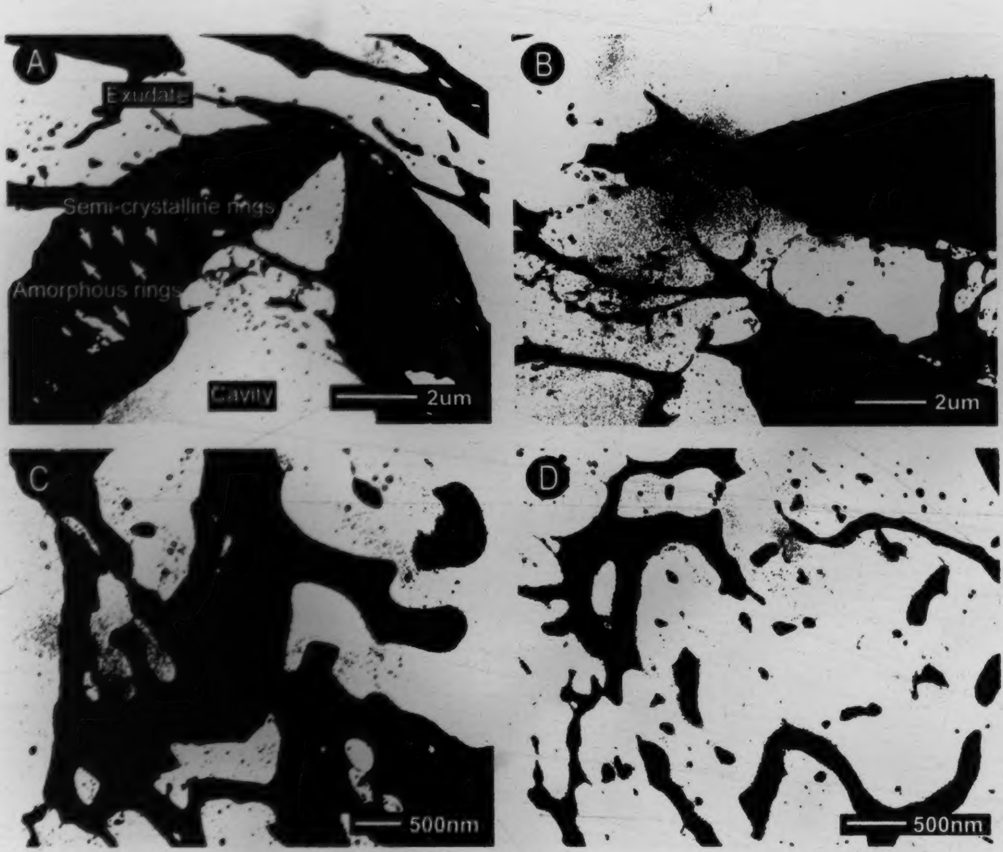
A
Exudate
Semi-crystalline rings
Amorphous rings
Cavity
2um
B
2um
C
500nm
D
500nm

Figure 5-4 Transmission electron micrographs of waxy HB starch granules (CDC Alamo) heated in water to various temperatures. A and B, 65°C; C, 80°C; D, 90°C.

oriented fibrillar network. This could be attributed to melting of starch crystallites, which facilitates entry of silver ions into the regions that were not previously accessible to the stain. Central cavities with a loose network and melting of macromolecules starting from the equatorial groove were again evident at this heating temperature. At 80°C, the granular shape was totally lost and all granules were fully fragmented (Figure 5-4 C). Further heating (90°C) increased the homogeneity of the gelatinized/solubilized amylopectin matrix (no amylose in waxy starch) showing a coarse rod-like or droplet-like structure (Figure 5-4 D). This kind of amylopectin structure is also observed in heated waxy potato (Hermansson and Svegmark, 1996) and heated waxy maize starches (Barron et al., 2001).

5.3.3 Morphological and ultrastructural changes during heating of non-waxy HB starch granules

Scanning electron micrographs of normal and high-amylose HB starches heated to temperatures ranging from 55 to 100°C are presented in Figures 5-5 to 5-8. At 55°C, ridges were present on the larger granules of both normal (Figure 5-5 A) and high-amylose (Figure 5-7 A) HB starches due to fast swelling in the less organized regions of the granules. The ridge structure is also found in heated maize starch granules (Christianson et al., 1982). Leaching of a small amount of exudate (probably amylose) occurred via pinholes at this temperature (Figures 5-5 A, B and 5-7 A). Doublier et al. (1987) and Autio (1990) have shown that in non-waxy cereal starches, amylose is preferentially leached out at low temperatures with the exception of oat starch, where amylose co-leaches with amylopectin (Doublier et al., 1987; Autio, 1990). At 65°C, closely distributed knobs/protrusions (200-400 nm diameter) were present at the dent

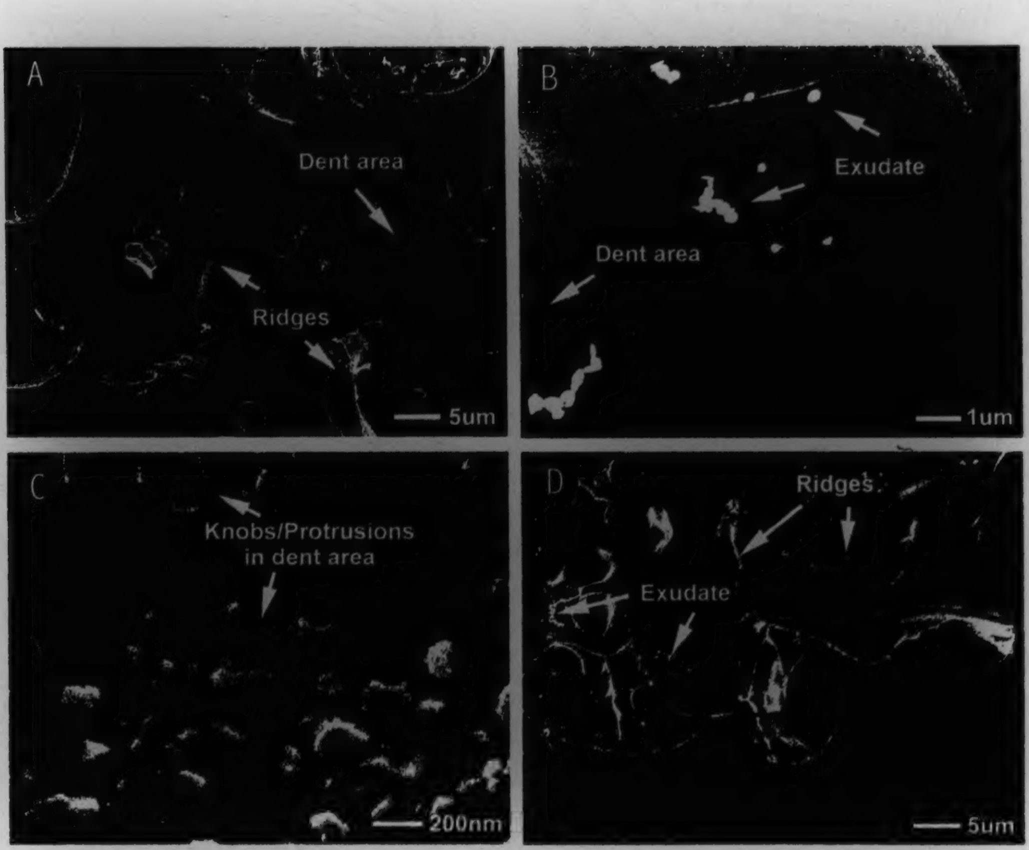
A
Dent area
Ridges
5um
B
Exudate
Dent area
1um
C
Knobs/Protrusions in dent area
200nm
D
Ridges
Exudate
5um

Figure 5-5 Scanning electron micrographs of normal HB starch granules (CDC Dawn) heated in water to various temperatures. A, B, and C, 55°C; D, 65°C.

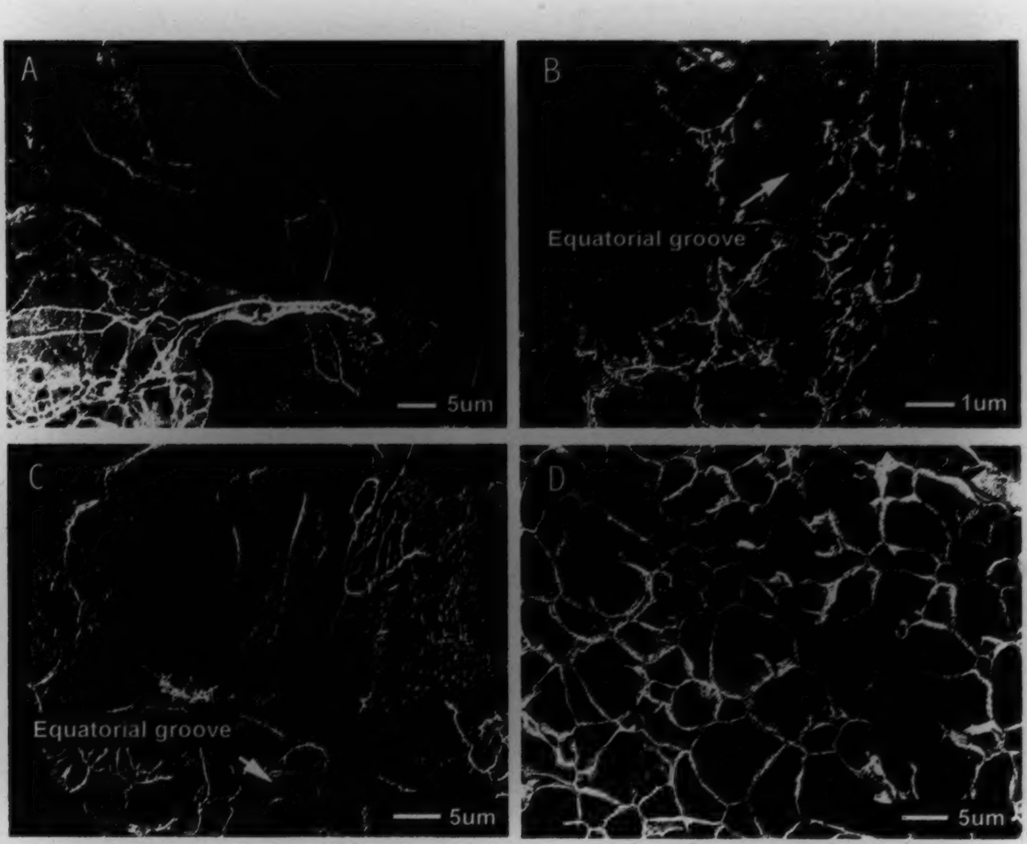
A
5um
B
Equatorial groove
1um
C
Equatorial groove
5um
D
5um

Figure 5-6 Scanning electron micrographs of normal HB starch granules (CDC Dawn) heated in water to various temperatures. A and B, 80°C; C, 90°C; D, 100°C.

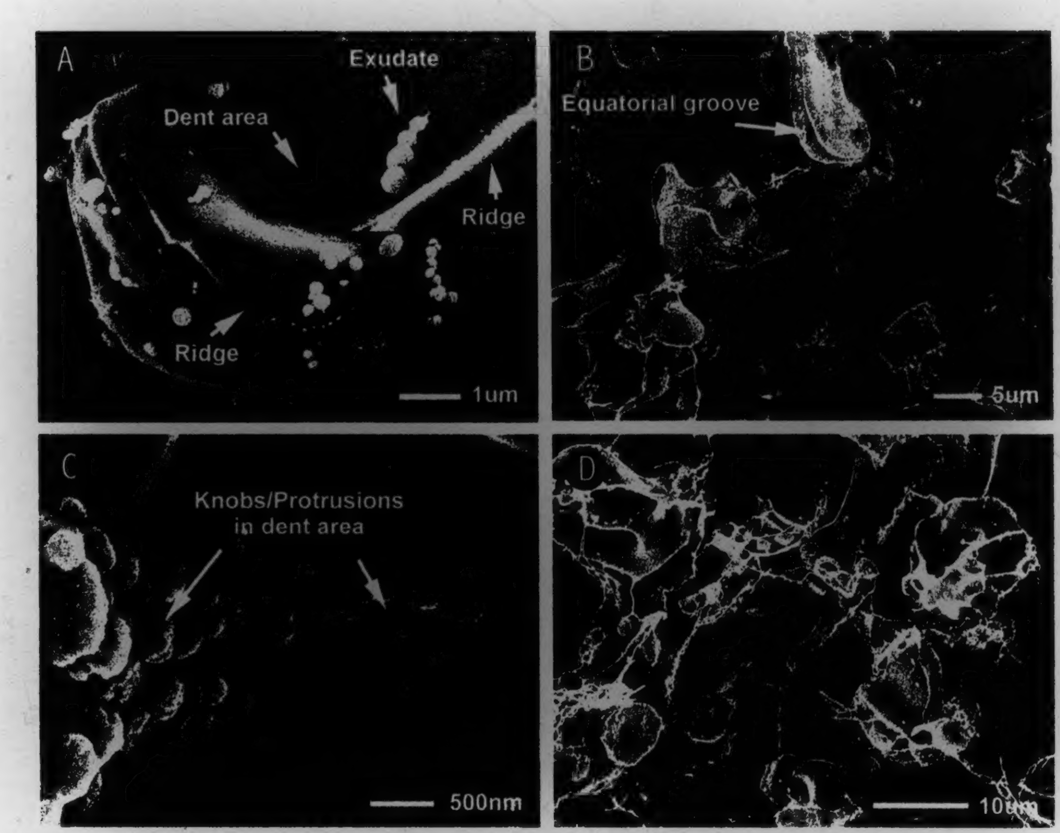
A
Exudate
Dent area
Ridge
Ridge
1um
B
Equatorial groove
5um
C
Knobs/Protrusions
in dent area
500nm
D
10um

Figure 5-7 Scanning electron micrographs of high-amylose HB starch granules (SB 94893) heated in water to various temperatures. A, 55°C; B, 65°C; C and D, 80°C.

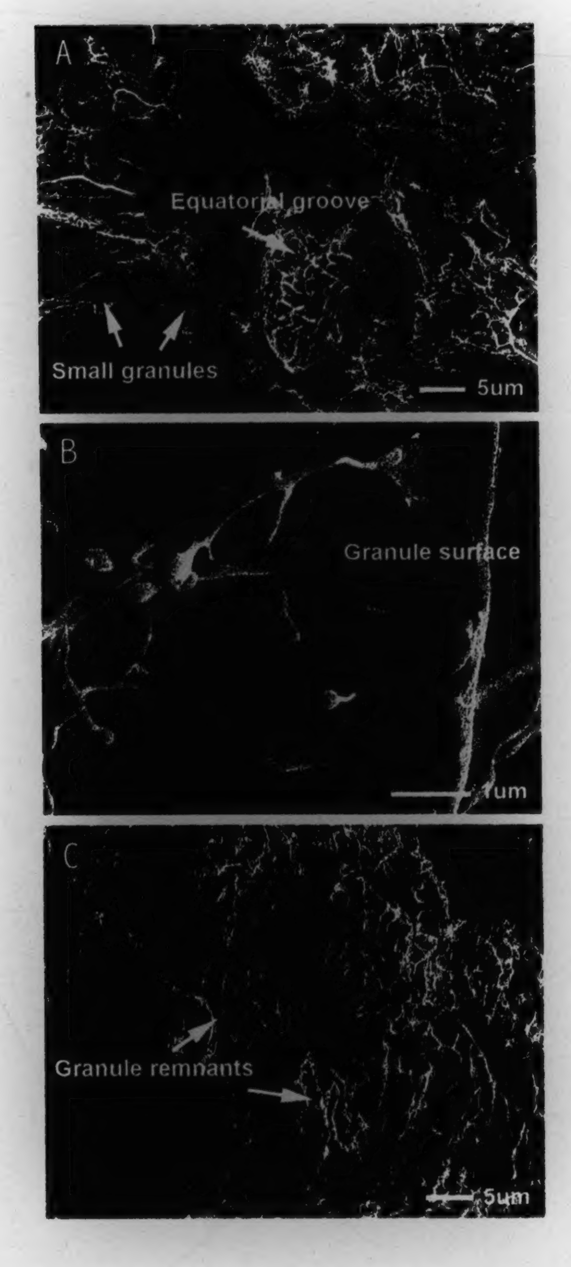
A
Equatorial groove
Small granules
5um
B
Granule surface
1um
C
Granule remnants
5um

Figure 5-8 Scanning electron micrographs of high-amylose HB starch granules (SB 94893) heated in water to various temperatures. A and B, 90°C; C, 100°C.

area of normal HB starch granules (Figure 5-5 B, C). However, in high-amylose HB starch granules, similar knobs/protrusions appeared only at 80°C (Figure 5-7 C). These knobs/protrusions are probably amylopectin side chain clusters and correspond to the blocklet structural model proposed by Gallant et al. (1997). Atkin et al. (1998) showed that amylopectin forms turgid sacs of 400 nm particles during gelatinization of potato and maize starches. The absence of knobs/protrusions on waxy HB starch granule is probably due to the rapid granule splitting that may have occurred at low temperatures (<55°C). When normal and high-amylose HB starch granules were heated to 65°C, most granules became ridged and a large amount of exudate was present on the surfaces of both larger and smaller granules (Figures 5-5 D and 5-7 B). In non-waxy HB starch granules, equatorial grooves were clearly visible during gelatinization (Figures 5-6 B, C, 5-7 B, and 5-8 A). The ridges merged together at higher temperatures (80-90°C) forming melting regions on the granule surface with a honeycomb-like and strand-like structure (Figure 6 A-C). Leaching of starch molecules was more pronounced between 80-90°C (Figures 5-6 B, C, 5-7 D, and 5-8 A, B). Atkin et al. (1998) have shown in studies on potato and Hylon VII maize (amylose content 70%) starches that at high temperatures, both amylose and amylopectin are released from the granule. As a result, the starch solution contains a mixture of dispersed gelatinized amylose and amylopectin in a continuous phase with fragmented "ghost" structures in an excluded phase. In high-amylose starch, a number of small granules were observed, even at 90°C, in the soluble and fragmented matrix (Figure 5-8 A). At 100°C, fragmented and melted normal HB starch remnants formed a coarse honeycomb-like network structure (Figure 5-6 D) and in high-amylose HB starch, the honeycomb-like structure had fine cells (Figure 5-8 C).

Ultrastructural changes of normal (Figure 5-9) and high-amylose (Figure 5-10) HB starches heated to 65°C, 80°C, and 90°C were examined by transmission electron microscopy. Heating at a low temperature (65°C) caused structural changes as follows (Figures 5-9 A and 5-10 A): 1) formation of fine radial fibrillar structure in the peripheral region (sub-surface) of starch granules similar to those of waxy starch granules; 2) leaching of a small amount of strand-like exudate from the fibrillar structure of normal starch but not from high-amylose starch (possibly washed away during sample preparation); 3) distortion of granules (consistent with that observed in scanning electron micrographs); and 4) formation of porous central region of the granule (showing the least organized region to be sensitive to heating). Spherical light "blocklet" structures surrounded with dark amorphous material (probably amylose) in the semi-crystalline region (light ring) was more pronounced in normal starch granules (Figure 5-9 A) than in high-amylose HB starch granules (Figure 5-10 A) at the same heating temperature. The growth rings and fibrillar structure in the peripheral region of granules disappeared at 80°C (Figures 5-9 B and 5-10 B), indicating melting of the semi-crystalline region. More strand-like exudate leached out of granules at this heating temperature (Figure 5-9 B and 5-10 B), which is similar to the gel structure of pure amylose extracted from pea starch (Leloup et al., 1992), and potato starch (Hermansson et al., 1995), as well as gels of wheat, maize, and potato starches (Hermansson et al., 1995). At 90°C, most swollen granules were still relatively intact and did not fragment, showing distinct separated phases (Figures 5-9 C and 5-10 C-E): strands of exudate between the inter space of granule ghosts (granule remnants) with a web-like network in the central regions of the swollen granules. Iodine staining of thin sections of heated granules from wheat, maize, potato, and barley starches (Langton and Hermansson, 1989; Autio, 1990; Shamekh et al., 1999) showed that amylopectin

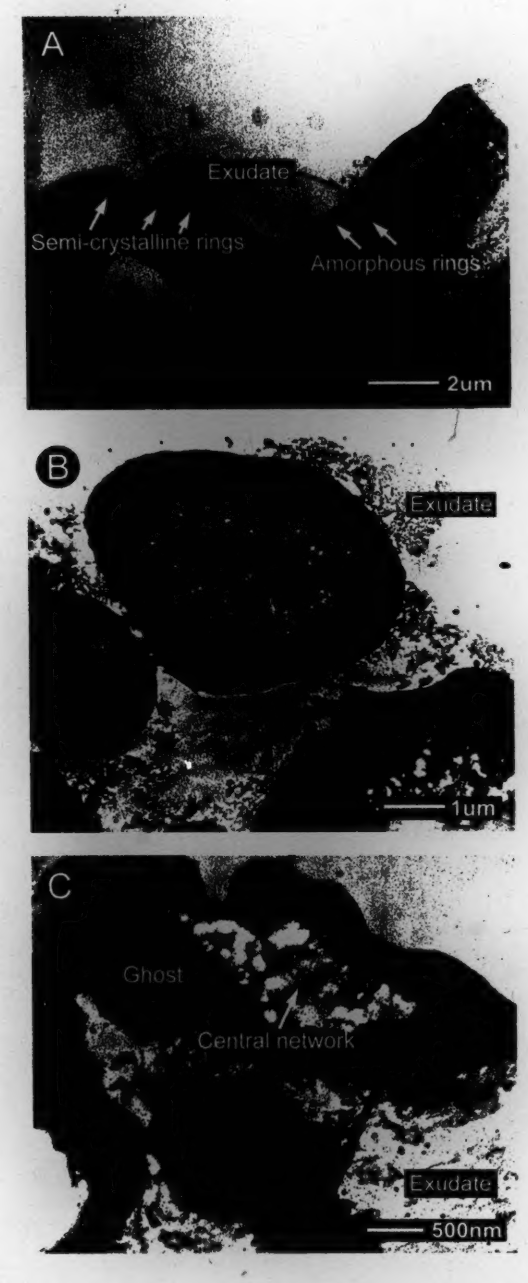
A
Exudate
Semi-crystalline rings
Amorphous rings
2um
B
Exudate
1um
C
Ghost
Central network
Exudate
500nm

Figure 5-9 Transmission electron micrographs of normal HB starch granules (CDC Dawn) heated in water to various temperatures. A and B, 65°C; C, 80°C; D, 90°C.

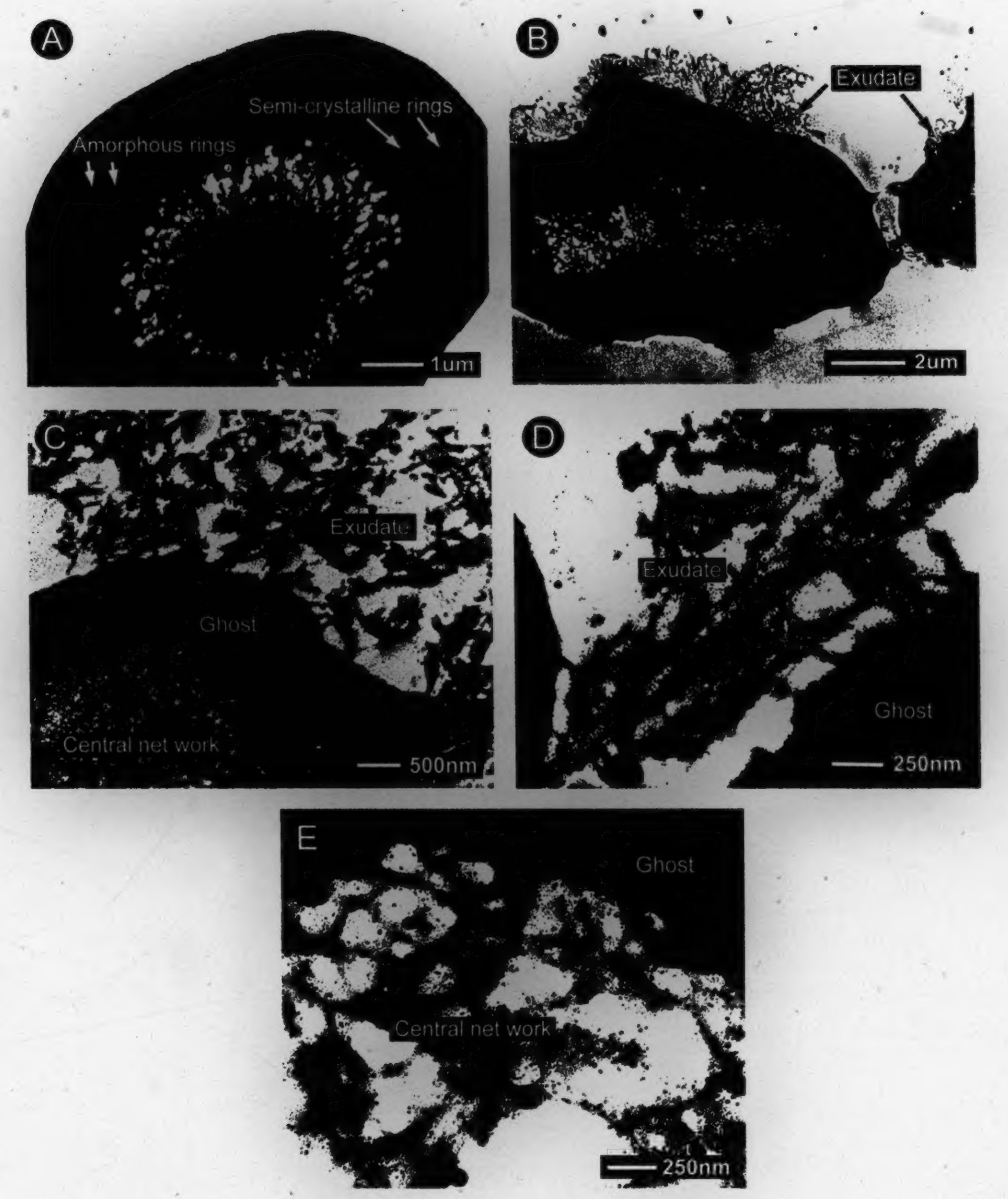
A
Semi-crystalline rings
Amorphous rings
1um
B
Exudate
2um
C
Exudate
Ghost
Central net work
500nm
D
Exudate
Ghost
250nm
E
Ghost
Central net work
250nm

Figure 5-10 Transmission electron micrographs of high-amylose HB starch granules (SB 94893) heated in water to various temperatures. A, 65°C; B, 80°C; C and D, 90°C.

is enriched in ghosts and that amylose is present mainly in the central and external regions of the granule. Langton and Hermansson, (1989) and Svegmark and Hermansson (1991) have shown that shearing results in fragmentation of heated starch granules and facilitates the development of a homogeneous matrix. Bundles of brush-like strands, due to aggregation of amylose molecules on cooling, were observed in the exudate of high-amylose HB starch granules heated to 90°C and cooled (Figure 5-10 C, D). This is in agreement with the model for amylose gel, proposed by Leloup et al. (1992). Amylose aggregation was also observed in wheat starch granules with iodine staining after heating at 95°C for 30 min and cooled to room temperature (Langton and Hermansson, 1989). Solubilized amylopectin may adsorb onto strands of amylose, but does not interfere with the aggregation of amylose into superstrands (Svegmark et al., 1993; Hermansson et al., 1995). Denser and thicker layers of granular ghost in high-amylose starch (Figure 5-10 C) than in normal starch (Figure 5-9 C) at the same heating temperature indicated higher stability of high-amylose starch granules.

Fine particles of diameter 10 nm were present on waxy (Figure 5-11 A), normal and high-amylose (Figure 5-11 B, C) HB starch granule remnants. These were arranged in the form of a chain. The fine particles of 10 nm diameter may correspond to amylopectin clusters. During gelatinization, amorphous macromolecules around blocklets are initially released first, exposing large particles. Further heating facilitates amorphous macromolecules inside the blocklets to become soluble, thus exposing the organized amylopectin clusters.

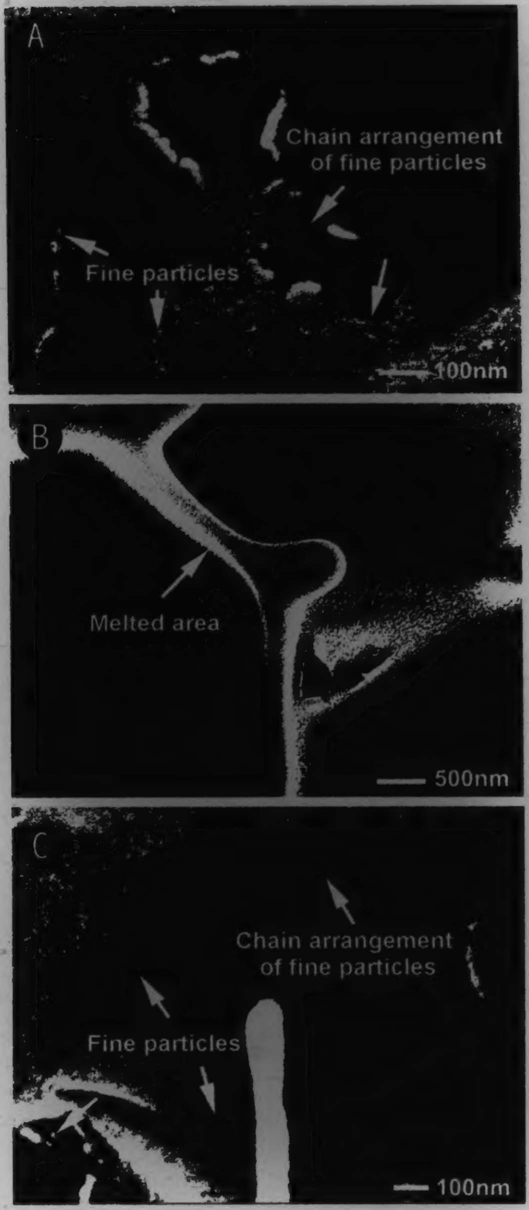
A
Chain arrangement of fine particles
Fine particles
100nm
B
Melted area
500nm
C
Chain arrangement of fine particles
Fine particles
100nm

Figure 5-11 Scanning electron micrographs of HB starch granule remnants heated in water to 100°C. A, waxy (CDC Alamo); B, normal (CDC Dawn); C, high-amylose (SB 94893).

The techniques used during sample preparation such as freezing, freeze drying, dehydration, and staining may cause various artifacts (Bowler et al., 1987; Crang and Klomparens, 1988). For instance, the round-up of strands of exudate, uniform honeycomb-like structures, and the smooth surface of fragments from melted granules (due to solute relocation/case-hardening caused by the concentration of solute onto the crystal interfaces and ice crystal formation), and folds and voids on thin sections of granules (due to embedding and sectioning) could be observed. However, in the present study, the main features of heated starch granules were clearly observed and the diversity of morphology and ultrastructure in different starch types at each heating stage were clearly revealed by the combination of scanning electron microscopy and transmission electron microscopy, with good agreement and complementary information.

5.3.4 Detection of amylopectin in the leached exudates at 65°C and 100°C by MALDI-MS

Soluble fractions of HB starches heated at 65°C and 100°C were separated by centrifugation (6000 xg). However, at 100°C the pastes from waxy and normal HB starches (10%) had high viscosity and consequently, the soluble fraction could not be separated even at higher centrifugal speeds. The chain length distributions of isoamylase debranched amylopectin (soluble and residue fractions) are shown in Figure 5-12. The absence of longer B chains (i.e. B2 and B3 chains) in the detectable branch chains of amylopectin (Figure 5-12 A-C) suggests that amylopectin that leached out at 65°C was of a lower molecular weight. However, at 100°C, the longer amylopectin chains were detectable in the soluble fractions (Figure 5-12 D). This

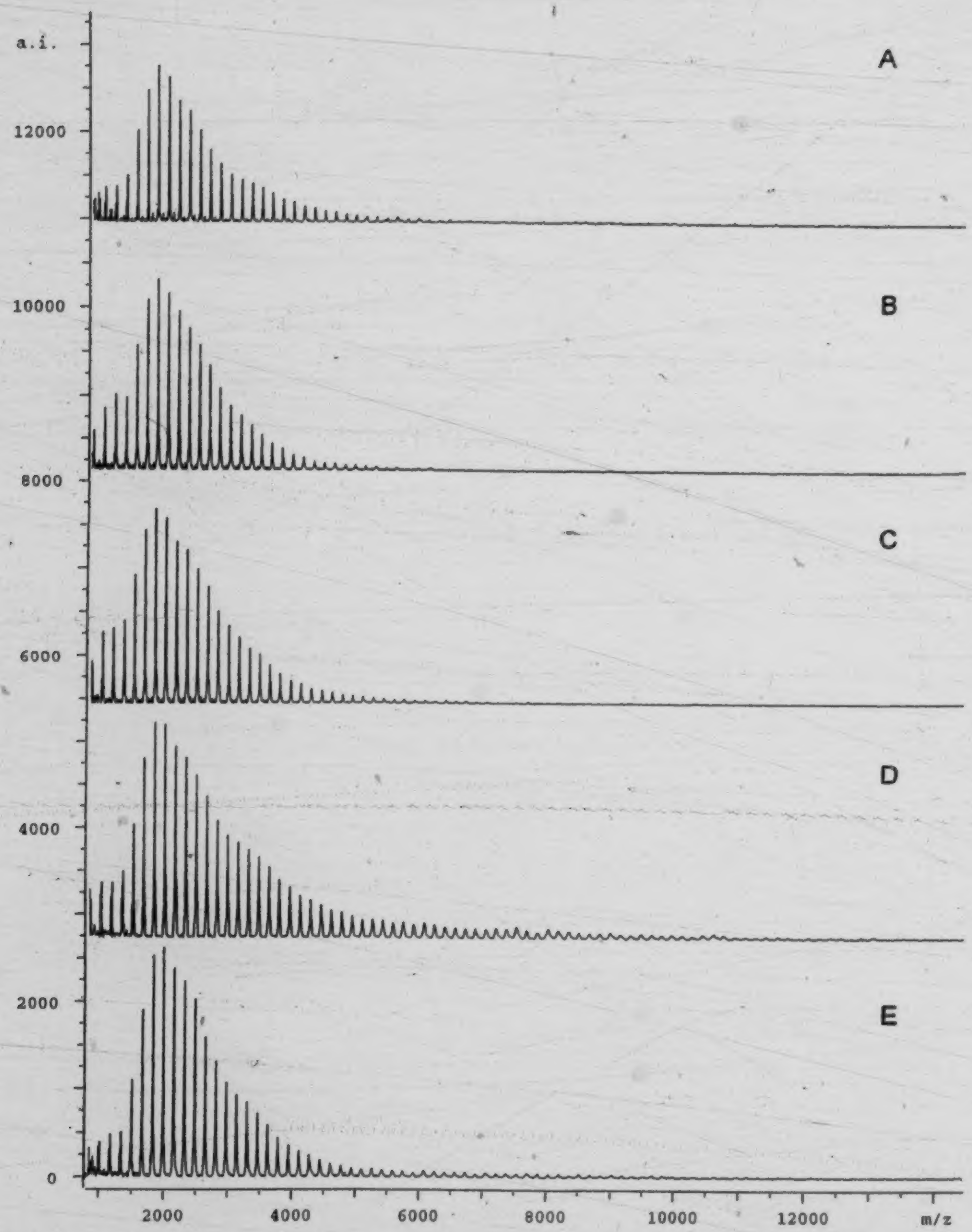

Figure 5-12 MALDI-MS spectra of debranched HB starch heated in water to 65°C and 100°C. A, B and C, soluble fraction centrifuged from the waxy, normal and high-amylose starches, respectively, heated to 65°C; D and E, soluble and residue fraction centrifuged from the high-amylose starch heated to 100°C.

suggests that amylopectin with higher molecular weight was solubilized at higher heating temperatures. All soluble fractions from the three types of starches showed generally similar distributions of branched amylopectin chains at 65°C (Figure 5-12 A-C). The debranched amylopectin chain length distribution in the soluble fraction obtained by heating high-amylose HB starch at 100°C was generally similar to that of the residue obtained at this temperature, suggesting a similar amylopectin structure for the soluble fraction and the residue. In addition, the exudate, which consists of amylose and low molecular weight amylopectin, leached out of the granules through the fibrillar structure, suggesting the presence of a continuous pathway (fine channels) for leaching of the starch components.

5.4 Conclusion

Morphological and structural changes, such as granule swelling/fragmentation, molecular leaching and gelatinization/solubilization, during heating in water varied among the three types of HB starches. Swelling and melting patterns differed substantially between waxy and non-waxy HB starches. High-amylose HB starch showed swelling and melting patterns similar to that of normal HB starch, but these occurred at higher temperatures. Amylopectin in the soluble fraction obtained from the starch-water slurry heated to 65°C showed a similar chain length distribution in all three HB starches. Leaching of amylose and/or low molecular weight amylopectin occurred at 65°C in all three HB starches. Increasing the heating temperature increased leaching of higher molecular weight amylopectin. However, the chain length distribution of amylopectin was generally similar in both the soluble and insoluble fractions of high-amylose HB starch heated to 100°C. The differences in the morphological and structural changes of waxy, normal and high-amylose HB starches during heating in water may potentially influence their functionality during processing. Therefore, HB varieties and heating conditions are important factors for quality control of starch containing products.

5.5 References

Atkin, N. J., Abeysekera, R. M., and Robards, A. W. 1998a. The events leading to the formation of ghost remnants from the starch granule surface and the contribution of the granule surface to the gelatinization endotherm. *Carbohydr. Polym.* 36: 193-204.

Atkin, N. J., Abeysekera, R. M., Cheng, S. L., and Robards, A. W. 1998b. An experimentally-based predictive model for the separation of amylopectin subunits during starch gelatinization. *Carbohydr. Polym.* 36: 173-192.

Autio, K. 1990. Rheological and microstructural changes of oat and barley starches during heating and cooling. *Food Structure,* 9: 297-304.

Autio, K., Poutanen, K., Suortti, T., and Pessa, E. 1992. Heat-induced structural changes in acid-modified barley starch dispersions. *Food Structure*, 11: 315-322.

Barron, C., Bouchet, B., Della Valle, G., Gallant, D. J. and Planchot, V. 2001. Microscopical study of the destructuring of waxy maize and smooth pea starches by shear and heat at low hydration. *J. Food Sci.* 33: 289-300.

Bowler, P., Williams, M. R. and Angold R. E. 1980. A hypothesis for the morphological changes which occur on heating lenticular wheat starch in water. *Starch/Stärke*, 32: 186-189.

Bowler, P., Evers, A. D. and Sargent, J. 1987. Dehydration artifacts in gelatinized starches. *Starch/Stärke*, 39: 46-49.

Christianson, D. D., Baker, F. L., Loffredo, A. R., and Bagley, E. B. 1982. Correlation of microscopic structure of corn starch granules with rheological properties of cooked pastes. *Food Microstructure,* 1: 13-24.

Crang, R. F. E., and Klomparens, K. L. 1988. *Artifacts in Biological Electron Microscopy*. New York and London: Plenum Press.

Doublier, J. L., Paton, D., and Llamas, G. 1987. A rheological investigation of oat starch pastes. *Cereal Chem.* 64: 21-26.

Fannon, J. E., and BeMiller, J. N. 1992. Structure of corn starch paste and granule remnants revealed by low-temperature scanning electron microscopy after cryopreparation. *Cereal Chem.* 69: 456-460.

French, D. (1984). Organisation of starch granules. In: *Starch: Chemistry and Technology*. R. L. Whistler, J. N. BeMiller, and J. F. Paschall eds., 2nd ed. p. 183-247. New York: Academic Press.

Gallant, D. J., Bouchet, B., and Baldwin, P. M. 1997. Microscopy of starch: evidence of a new level of granule organisation. *Carbohydr. Polym.* 32: 177-191.

Garcia, V., Colonna, P., Bouchet, B., and Gallant, D. J. 1997. Structural changes of cassava starch granules after heating at intermediate water contents. *Starch/Stärke*, 49: 171-179.

Ghiasi, K., Hoseney, R. C., and Varriano-Marston, E. 1982. Gelatinization of wheat starch. I. Excess-water systems. *Cereal Chem.* 59: 81-85.

Hermansson, A. –M., and Svegmark, K. 1996. Developments in the understanding of starch functionality. *Trends Food Sci. Technol.* 7: 345-353.

Hermansson, A.-M., Kidman, S., and Svegmark, K. 1995. Starch—a phase-separated biopolymer system. In *Biopolymer Mixtures*. S. E. Harding, S. E. Hill, and J. R. Michell eds., p.225-246. Nottingham University Press.

Holmes, Z. A., and Soeldner, A. 1981. Macrostructure of selected raw starches and selected dispersions. *J. Am. Dietet. Assoc.* 78: 153-157.

Langton M., and Hermansson, A. M. 1989. Microstructural changes in wheat starch dispersions during heating and cooling. *Food Microstructure*, 8: 29-39.

Leloup, V. M., Colonna, P., Ring, S. G., Roberts, K., and Wells, B. 1992. Microstructure of amylose gels. *Carbohydr. Polym.* 18: 189-197.

Lii, C. Y., Shao, Y. Y., and Tseng, K. H. 1995. Gelation mechanism and rheological properties of rice starch. *Cereal Chem.* 72: 393-400.

Liu, J. M., and Zhao, S. L. 1990. Scanning electron microscope study on gelatinization of starch granules in excess water. *Starch/Stärke,* 42: 96-98.

Myllärinen, P., Autio, K., Schulman, A. H., and Poutanen, K. 1998. Heat-induced structural changes of small and large barley starch granules. *J. Int. Brew.* 104: 343-349.

Shamekh, S., Forssell, P., Suortti, T., Autio, K., and Poutanen, K. 1999. Fragmentation of oat and barley starch granules during heating. *J. Cereal Sci.* 30: 173-182.

Sterling, C. (1978). Textural qualities and molecular structure of starch products. *J. Texture Studies,* 9: 225-255.

Svegmark, K., and Hermansson, A.-M. 1991. Distribution of amylose and amylopectin in potato starch pastes: effects of heating and shearing. *Food Structure*, 10: 117-129.

Svegmark, K., Kidman, S., and Hermansson, A.-M. 1993. Molecular structures obtained from mixed amylose and potato starch dispersions and their rheological behavior. *Carbohydr. Polym.* 22: 19-29.

Varriano-Marston, E., Zeleznak, K., and Nowotna, A. 1985. Structural characteristics of gelatinized starch. *Starch/Stärke,* 37: 326-329.

Williams, M. R., and Bowler, P. 1982. Starch gelatinization: A morphological study of triticeae and other starches. *Starch/Stärke,* 34: 221-223.

CHAPTER 6

In vitro Susceptibility of Waxy, Normal, and High-amylose Starches towards Hydrolysis by Alpha-amylases and Amyloglucosidase[1]

6.1 Introduction

In vitro enzyme hydrolysis of starches is not only an important industrial process for production of sweeteners, syrups, and chemicals (e. g. ethanol, acetone, and lactic acid) (Nigam and Singh, 1995), but also as a probe for studying starch ultrastructure (French, 1984; Gallant et al., 1997). Numerous researchers have investigated the enzyme hydrolysis of starches from cereals, roots, tubers, and legumes in terms of enzyme adsorption, action pattern, extent of hydrolysis, degree of crystallinity, and hydrolysis products. The susceptibility of starch to hydrolysis by amylases has been shown to vary with enzyme source and starch origin (Leach and Schoch, 1961; Rasper et al., 1974; Koba et al., 1986; Hoover and Sosulski, 1991; Rickard et al., 1991; Colonna et al., 1992; Gallant et al., 1992; Lauro et al., 1993; Planchot et al., 1995; Gérard et al., 2001; Hoover, 2001).

Electron microscopy (Evers and McDermott, 1970; Gallant et al., 1972; Fuwa et al., 1978, 1979; MacGregor and Ballance, 1980; Valetudie, Colonna et al., 1993; Planchot et al., 1995; Helbert, et al., 1996) has revealed that α-amylase pits the granule surface first, penetrates through pinholes/internal channels and then hydrolyzes the granule from the inside-out. The A-, B- and C-types of starches (as classified according to X-ray diffraction pattern) show different susceptibilities to α-amylase hydrolysis. Generally, A-type (most cereals and tapioca) starches are more readily hydrolyzed by α-amylase than B-type (amylomaize and potato) starches (Gallant et al., 1972; Planchot et al., 1995). Waxy starches are hydrolyzed by α-amylase faster than non-waxy starches (Leach and Schoch, 1961; MacGregor and Ballance, 1980). For a given starch, the rate of hydrolysis is dependent on enzyme type (Valetudie et al., 1993; Planchot et al., 1995), conditions of hydrolysis (e.g. concentration, pH, and temperature) (Franco and Ciacco, 1987), and physical (Lauro et al., 1993; Kurakake et al., 1996) and chemical (Tharanathan and Ramadas Bhat, 1988; Wolf et al., 1999) modification of starch prior to hydrolysis. Kimura and Robyt (1995) have shown that variations in susceptibility of cereal and tuber starches towards amyloglucosidase can be partly explained by differences in their ultrastructure. The ultrastructural features of granule organization include inter-chain association (e.g. amylose-amylose and/or amylose-amylopectin) (Vasanthan and Bhatty, 1996), type and degree of crystallinity (double helical packing) (Gérard et al., 2001), the number of the crystalline and amorphous lamellae in each growth ring (Gallant, Bouchet, and Baldwin, 1997; Chapter 3), and amylose-lipid interaction (Anger et al., 1994; Morrison, 1995; Appelqvist and Debet, 1997; Lauro et al., 1999). Colonna et al. (1988) have shown, in an iodine binding study, that there is no preferential hydrolysis of either amylose or amylopectin by α-amylase. X-ray diffraction has also shown that both amorphous and semi-crystalline regions of barley starch granules are hydrolyzed simultaneously by α-amylase at the initial stage of hydrolysis, and that lipid-complexed amylose was retained in the residue of starches even after about half the starch was solubilized (Lauro et al., 1999). Gérard et al. (2001) further reported that amorphous material co-exists with B-type crystallites in hydrolysis (α-amylase) residues of maize mutant starches (with a wide range of crystallinity levels and various ratios of A-, B-, and V-crystalline types), although the ultimate extent of hydrolysis was highly correlated with the amount of B-type crystallites. These studies suggest that there is a strong molecular association in the residue (mainly in the semi-crystalline regions) of the starch granule.

---

[1] A version of this chapter was published in *Food Chemistry*, 2004, 84: 621-632.

Starch from hull-less barley (HB) has comparable properties with maize starch (Vasanthan and Bhatty, 1996; Chapter 2 and 3). There is great potential for HB starch to replace industrial applications of maize starch, which is currently quite widely used in North America. However, studies on enzyme hydrolysis of HB starches by various amylases and visualization of structural changes during hydrolysis have not been well documented. The objective of this study was two-fold: 1) A comparison of the susceptibility of starches from HB genotypes (waxy, normal, and high-amylose) towards α-amylases and amyloglucosidase and, 2) To obtain an understanding of how HB starch ultrastructure influences the rate and extent of hydrolysis by amylases.

6.2 Materials and methods

6.2.1 Starch sources

Waxy (zero-amylose, CDC Alamo), normal (CDC Dawn), and high-amylose (SB 94893) HB grain (grown at the same location and harvested at Saskatoon, SK, in 1998) was obtained from the Crop Development Centre, University of Saskatchewan, Saskatoon, SK. Barley grain was ground in a cyclone sample mill (UDY Lab Equipment and Supplies, Ft. Collins, CO) equipped with a 0.5 mm screen. Starch was isolated from ground barley grain as described previously (Chapter 2).

6.2.2 Enzymes

α-Amylase (suspension in 2.9M NaCl solution containing 3mM $CaCl_2$, 37 mg protein/ml) from porcine pancreas (EC 3.2.1.1) (PPA), α-amylase (crystallized, lyophilized powder, 2150 units/mg solid) from *Bacillus species* (EC 3.2.1.1) (BAA), and amyloglucosidase (lyophilized powder containing less than 0.02% glucose, 40 units/mg solid) from *Aspergillus niger* (EC 3.2.1.3) (AAG) with specific activities of 1020, 2880, and 42 units/mg protein, respectively, were purchased from Sigma Chemical Co. (St. Louis, MO).

6.2.3 Enzyme hydrolysis

Duplicate samples of starch (120±0.1 mg) were suspended in 10 ml of 0.1M phosphate buffer (pH 6.9) containing 0.006M NaCl. The screw cap tubes containing the starch samples were placed in a constant temperature shaking water bath at 37°C. Then, PPA (16.5 μl, 5 units/mg starch) and BAA (45 μl, 5 units/mg starch) for PPA and BAA hydrolysis, respectively, were added to the starch slurry. Hydrolysis was conducted for 72 h. For AAG hydrolysis, starch (120±0.1 mg) was suspended in 0.05M acetate buffer (pH 4.5) followed by the addition of 0.1 ml of buffered AAG (2.5 units/mg starch). Hydrolysis was conducted for 72 h at 55°C. For all three enzymes, 1 ml aliquots were removed at specified time intervals and centrifuged (1,700 xg) for 5 min. Aliquots of the supernatant were analyzed for soluble carbohydrates (Bruner, 1964). Percentage of hydrolysis was calculated as the amount (mg) of glucose equivalents released per 100 mg of dry starch. The residue was washed with distilled water (x3) and 100% ethanol (x2), and then dried at 40°C. The dried samples were used for electron microscopy.

6.2.4 Quantification of glucose, maltose, and maltotriose

The soluble products of hydrolysis (glucose, maltose, and maltotriose) were analyzed in triplicate by high performance liquid chromatography (HPLC) system equipped with an HP1050 sampler (GMI, Inc., Albertville, MN), a Varian 9090 pump (Varian, Inc., Walnut Creek, CA), an Alltech 500 ELSD Evaporative Light-Scattering Detector (Mandel Scientific Company Ltd., Guelph, ON) and a Supelcosil LC-NH 2-5um column (Supelco, Bellefonte, PA) (Vasanthan et al. (2001). Standard solutions of authentic fructose, glucose, sucrose, maltose, and maltotriose (Sigma Chemical Co., St. Louis, MO) were prepared and used for calibration. Data acquisition and peak integration were performed using Shimadza Class-VP Chromatography Laboratory Automated Software System (Shimadzu Scitific Instruments, Inc., Columbia, MD).

6.2.5 Scanning electron microscopy

The dried starch sample from enzyme hydrolysis was directly mounted on circular aluminum studs with double-sided sticky tape, coated with 12nm gold, then examined and photographed in a JEOL (JSM 6301FXV) scanning electron microscope (JEOL Ltd, Tokyo, Japan) at an accelerating voltage of 5 kV.

6.2.6 Transmission electron microscopy

The periodic acid-thiosemicarbazide-silver reaction (PATAg) method (Garcia et al., 1997) was used to reveal the ultrastructure of starch granules. Heavy metal ions (silver) can bind to oxidized (by periodic acid) starch molecules after specific oxidation of α-glycols at C2-C3 of the anhydro-glucose units of starch and thiosemicarbazide fixation, which gives good contrast on ultra-thin sections of granules under transmission electron microscope. Since oxidation is more efficient in the starch amorphous regions, the silver ions preferentially bind to the amorphous regions of oxidized starch granules, resulting in dark regions in transmission electron microscopy images, whilst semi-crystalline regions appear lighter.

Native starches and starch samples from enzyme hydrolysis were fixed in 3% glutaraldehyde in 0.1M sodium cacodylate buffer (pH 7.2) for 2 h at room temperature and then for 6 h at 4°C. Fixed samples were pre-embedded in agar aqueous solution (3%), cut into small cubes (1mm^3), and re-fixed for 1 h. After fixation, the sample cubes were washed in buffer (x2) and in distilled water (x2) for 20 min. For blocking residue free aldehyde, the washed sample cubes were immersed in a saturated 2,4-dinitrophenylhydrazine in 15% acetic acid solution for 1 h at room temperature. After washing (x4) in distilled water for 15 min, the sample cubes were oxidized in a 1% aqueous periodic acid solution for 45 min, washed again as above, and then immersed in saturated aqueous thiosemicarbazide solution for 24 h. The sample cubes were washed again and stained in 1% aqueous silver nitrate solution for 3 d in darkness with daily changes of the staining solution. The stained cubes were rinsed with distilled water, dehydrated in an ethanol series (30 to 100%), and then embedded in EMbed 812 resin (EMS Inc., Fort Washington, PA). Controls of the oxidative reaction were performed in parallel by substituting the periodic acid with 10% H_2O_2 (bleaching reagent). The embedded sample blocks were randomly cut into 90-100 nm thin sections with a diamond knife in an RMC (Tucson, AZ) MT 4000 ultramicrotome. The ultra-thin sections collected on collodion-coated copper grids were observed and photographed with a Philips CM12 transmission electron microscope (F.E.I. Company, Tacoma, WA) at 60 kV without further staining.

6.3 Results and discussion

6.3.1 Granule morphology of native HB starches

Scanning and transmission electron micrographs of granules from native HB starches are presented in Figure 6-1. The granule size of the three HB starches (Figure. 6-1 A, C, E) ranged from 2 to 30 µm in diameter. Granules were round to oval in shape with smooth surfaces. High-amylose HB starch showed smaller granules compared with waxy and normal HB starches. Numerous pinholes (up to 0.9 µm in diameter) were observed on larger waxy HB starch granules (Figure 6-1 A). A number of tiny pinholes were visible on the surface of normal HB starch granules (Figure 6-1 C). However, pinholes were rarely visible on the surface of high-amylose HB starch granules (Figure 6-1 E). Under the transmission electron microscope, the alternating growth rings (amorphous regions appeared as dark rings and semi-crystalline regions appeared as light rings) of waxy, normal and high-amylose types of HB starches were seen to vary in number and size (Figure 6-1 B, D, F). Some internal channels were also occasionally observed in the thin-sections of waxy (Figure 6-1 B) and normal (Figure 6-1 D) HB starch granules.

6.3.2 Hydrolysis kinetics

The hydrolysis by α-amylase from porcine pancreas (PPA), α-amylase from *Bacillus species* (BAA), and amyloglucosidase from *Aspergillus niger* (AAG) in all three

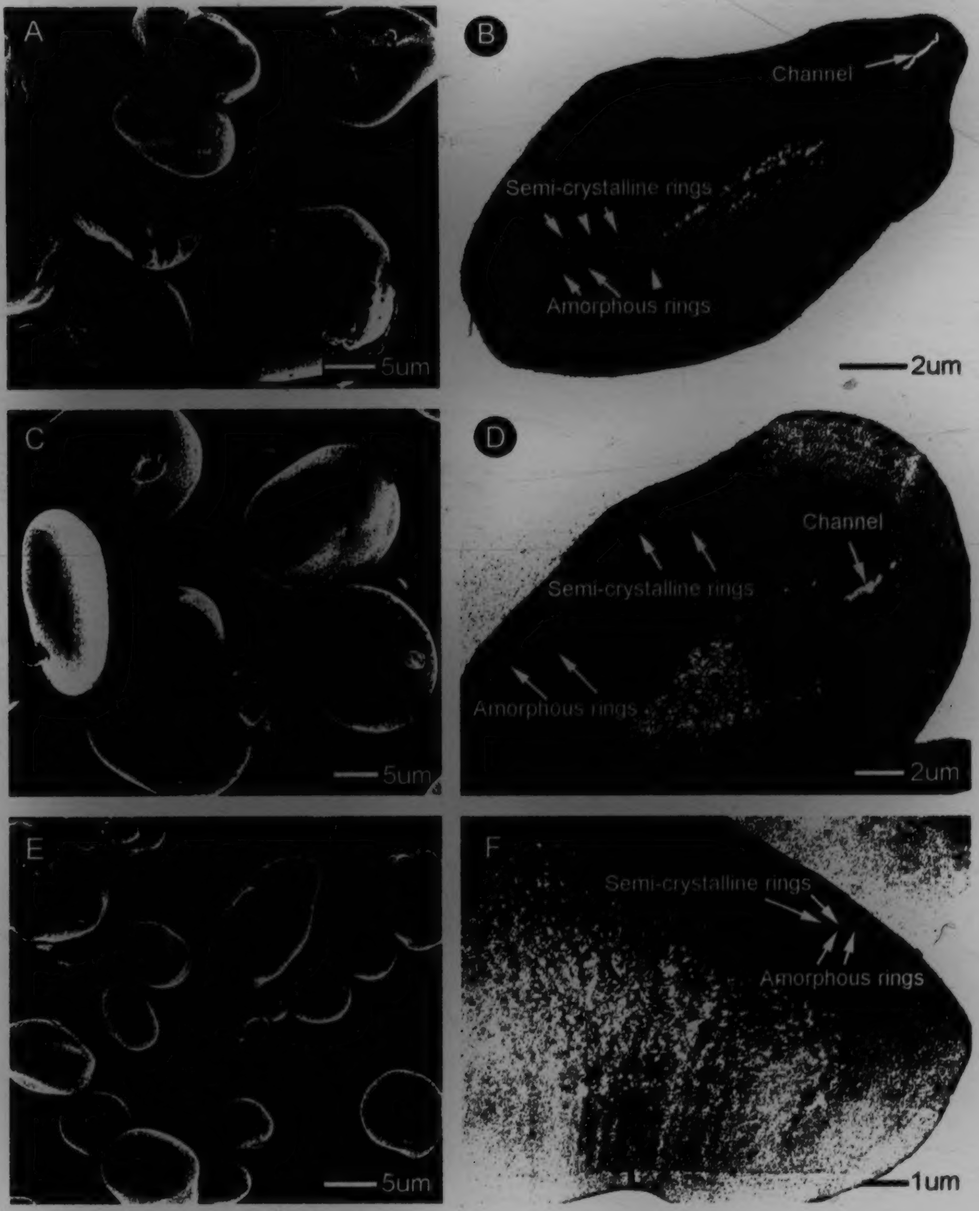
A
B
Channel
Semi-crystalline rings
Amorphous rings
5um
2um
C
D
Channel
Semi-crystalline rings
Amorphous rings
5um
2um
E
F
Semi-crystalline rings
Amorphous rings
5um
1um

Figure 6-1 Scanning (A, C & E) and transmission (B, D & F) electron micrographs of HB starch granules from waxy (CDC Alamo) (A & B), normal (CDC Dawn) (C & D), and high-amylose (SB 94893) (E & F) types.

starches was bi-phasic, with a relatively rapid rate at the initial stage followed by a progressively decreasing rate thereafter (Figure 6-2). The rate of hydrolysis at the initial stage varied with enzyme and starch type. During the time course of hydrolysis, waxy HB starch was more readily hydrolyzed (by all three enzymes) than were the normal and high-amylose HB starches (Figure 6-2 A-C), while normal HB starch showed the lowest hydrolysis rate towards all three enzymes. After 72h, waxy, normal and high-amylose HB starches were hydrolyzed to the extent of 97%, 94%, and 91%, respectively, by PPA. During the same time interval, the degree of hydrolysis by BAA and AAG, respectively, reached 78% and 67% in waxy HB starch, 29% and 30% in normal HB starch, and 37% and 33% in high-amylose HB starch.

Amylase hydrolysis involves an enzyme in solution acting on a solid starch substrate. Thus, the surface area accessible to enzyme and the efficiency of adsorption of enzyme onto this surface are critical kinetic parameters (Bertoft and Manelius, 1992). However, wide variation exists among starches from various origins and different types with respect to enzyme adsorption and hydrolysis rate (Bertoft and Manelius, 1992; Kimura and Robyt, 1995). The rate of hydrolysis may be influenced by both the surface features and internal structure of starch granules. Knutson et al. (1982) studied the PPA hydrolysis of maize starch granule fractions according to granule size. They found that the hydrolysis rate for waxy, normal, and high-amylose maize starches was proportional to the surface area of the granules, which may be closely related to the adsorption of enzyme onto the granule surface (MacGregor, 1979). Pinholes/internal channels, which are naturally occurring features of many starch granules (Huber and BeMiller, 2000), may create preferential sites and specific areas on the granule surface and in the interior for enzyme diffusion and adsorption. Thus, the initial high hydrolysis rate shown by waxy HB starch (Figure 6-2) may be partly due to the presence of pinholes and internal channels. Both normal and high-amylose HB starches have generally similar average granule sizes (6.7-6.8 µm in diameter) (Chapter 2). However, high-amylose HB starch showed a higher rate of hydrolysis by amylases than normal HB starch at the initial stage (Figure 6-2). This is perhaps due to the higher proportion of small granules (≤ 10 µm in diameter, 38% of total weight) in high-amylose HB starch compared to normal HB starch (11% in total weight) (Chapter 2). A high proportion of smaller granules leads to a larger granule surface to volume ratio. Also, microscopic observation (Valetudie et al., 1993) has shown that polyhedric shaped granules of tropical tuber starches (tannia, sweet potato and cassava) are hydrolyzed to a greater extent than spherical granules by α-amylases. Thus, granule morphology may influence the degree of susceptibility of starches to α-amylases.

The composition and concentration of hydrolysis products may also have an inhibitory effect on the rate of hydrolysis. Gradual reduction in the rate of hydrolysis may be partly caused by inhibition due to oligosaccharides on α-amylase activities (Colonna et al., 1992). Colonna et al. (1992) reported that in the oligosaccharide-enzyme complex, the molar ratio between oligosaccharide and enzyme influences the adsorption equilibrium. The concentration increases, during amylolysis, in maltose and maltotriose rather than in glucose or maltotetraose influence the adsorption equilibrium. However, if amyloglucosidase is used in combination with α-amylases, amyloglucosidase can hydrolyze maltose and maltotriose into glucose and thereby continuously transform the reaction products of α-amylolysis (Colonna et al., 1992; Planchot et al., 1995).

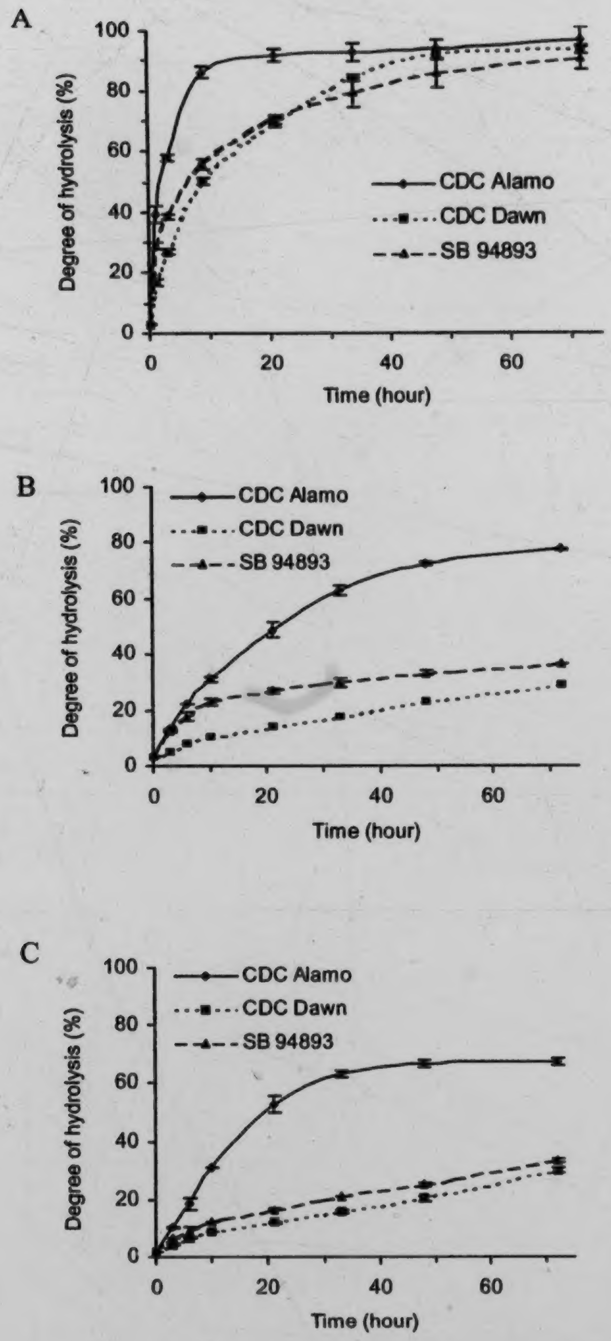

Figure 6-2 Hydrolysis of HB starches from waxy (CDC Alamo), normal (CDC Dawn) and high-amylose (SB 94893) types by PPA (A), BAA (B) and AAG (C).

6.3.3 Scanning electron microscopy

Scanning electron micrographs of the residues left after hydrolysis of waxy, normal and high-amylose HB starches by porcine pancreatic alpha-amylase (PPA) and amyloglucosidase (AAG) are presented in Figures 6-3 to 6-6. The granule surfaces of all three HB starches showed roughened surfaces (Figure 6-3) after 1 h hydrolysis by PPA. In waxy HB starch granules, many of the granules displayed highly perforated surfaces. The erosion areas were roughly circular to oval to elliptical ranging from 0.3-3 µm in diameter and penetrated through several layers of the granule into the interior (Figure 6-3 A). However, some granules were less eroded. Erosion areas with layered structure were less pronounced in granules of normal (Figure 6-3 C) and high-amylose (Figure 6-3 E) HB starches. The extent of erosion was higher in waxy HB starch. Some hollowed granules were present in high-amylose HB starches (Figure 6-3 E). In all three starches, some granules were split open revealing their internal layered structure (Figure 6-3 B, D, F). This may have been due to structural weakness of the granule resulting from hydrolysis along the equatorial groove plane or to mechanical damage during starch isolation. The internal layered structure showed, that in all three starches, the semi-crystalline growth rings gradually became closer from the interior to the surface (Figure 6-3 B, D, F). Furthermore, the size of the central region of hydrolyzed HB starch granule followed the order: waxy < normal < high-amylose (Figure 6-3 B, D, F). Split granules were more frequently observed in waxy HB starch than in normal and high-amylose HB starches. A similar erosion pattern has been reported in wheat starch (Evers and McDermott, 1970; Smith and Lineback, 1976) and legume starches (Tharanathan and Ramadas Bhat, 1988; Bertoft et al., 1993) hydrolyzed by alpha-amylase and amyloglucosidase. Kimura and Robyt (1995) also reported that the

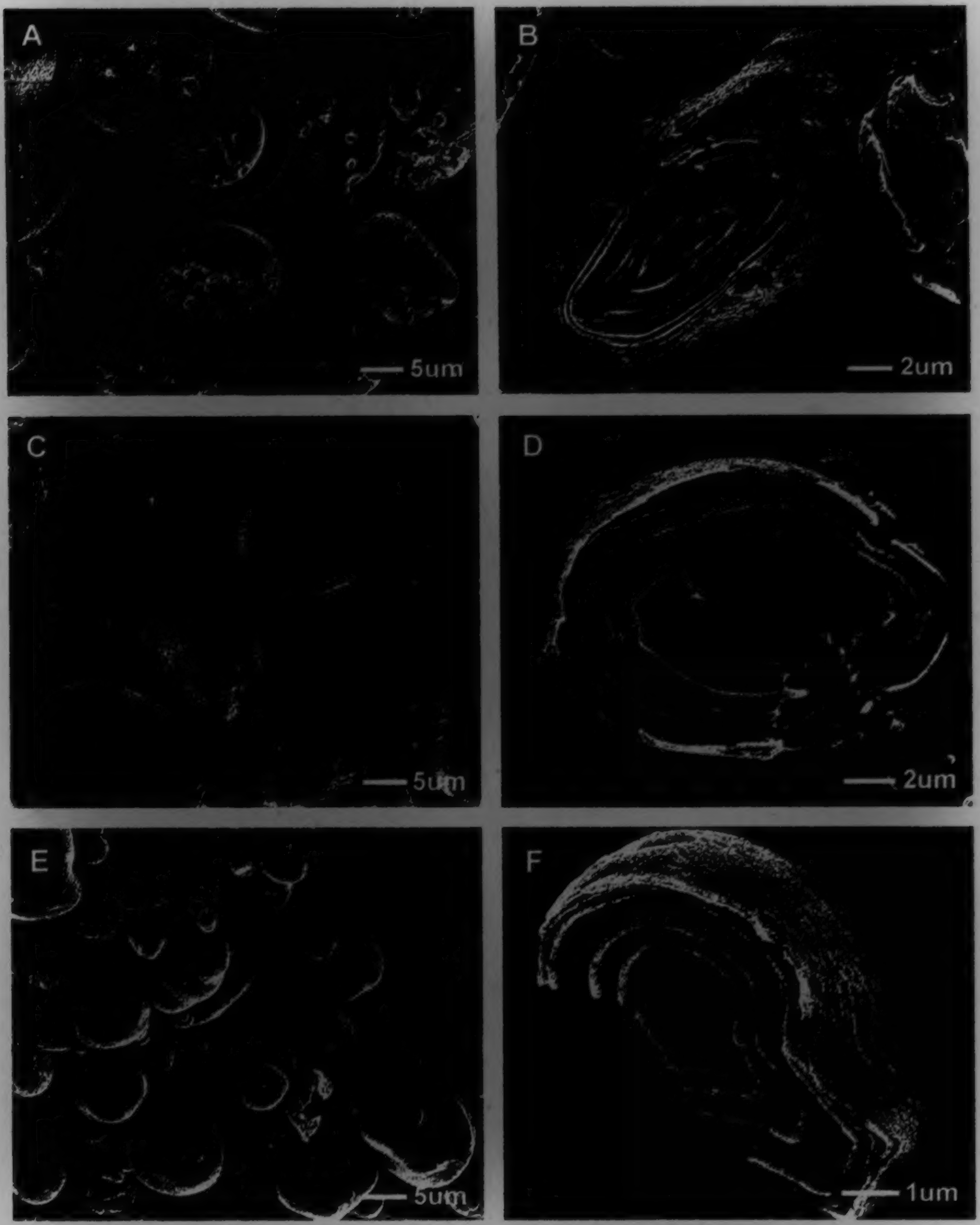
A
5um
B
2um
C
5um
D
2um
E
5um
F
1um

Figure 6-3 Scanning electron micrographs of HB starch granules from waxy (CDC Alamo) (A & B), normal (CDC Dawn) (C & D), and high-amylose (SB 94893) (E & F) types hydrolyzed by PPA at 37ºC for 1h.

number of barley starch granules significantly increased (almost doubled) initially and then decreased during amyloglucosidase hydrolysis.

After 3 h hydrolysis by PPA, erosion was more pronounced in the size and depth of erosion areas rather than increasing the number of erosion areas in all three HB starches (Figure 6-4 A, C, E). Some granules in waxy HB starch were fragmented (Figure 6-4 A). However, granule fragmentation was limited in normal (Figure 6-4 C) and high-amylose (Figure 6-4 E) HB starches. Most of the granules of normal and high-amylose HB starches retained their granular shape and showed a dense shell of varying thickness (Figure 6-4 C, E). After 6 h hydrolysis, waxy HB starch was fragmented and deformed (Figure 6-4 B). However, in normal HB starches, many granules were deformed (Figure 6-4 D). The extent of deformation became more pronounced after 21 h hydrolysis (Figure 6-5 C). Granules of high-amylose HB starch showed thin, granular shells with large hollows between 6 h (Figure 6-4 F) and 21 h hydrolysis (Figure 6-5 D). However, in waxy HB starch, only a small amount of sponge-like residue was left after 21 h hydrolysis (Figure 6-5 A). Under higher magnification (x25 K), the above residue appeared as clustered spherical particles (approximately 100 nm in diameter), showing a layered structure (Figure 6-5 B). This suggests the presence of amylopectin crystals (cluster structure) in the semi-crystalline regions of the granule. The thin shell structure in hydrolyzed granules of normal and high-amylose HB starches suggests that the peripheral regions of these granules are resistant (due to a strong association between amylopectin molecules) to enzyme hydrolysis.

BAA hydrolysis showed a similar action pattern to that of PPA (micrographs not shown). However, AAG hydrolysis showed some different features as depicted in

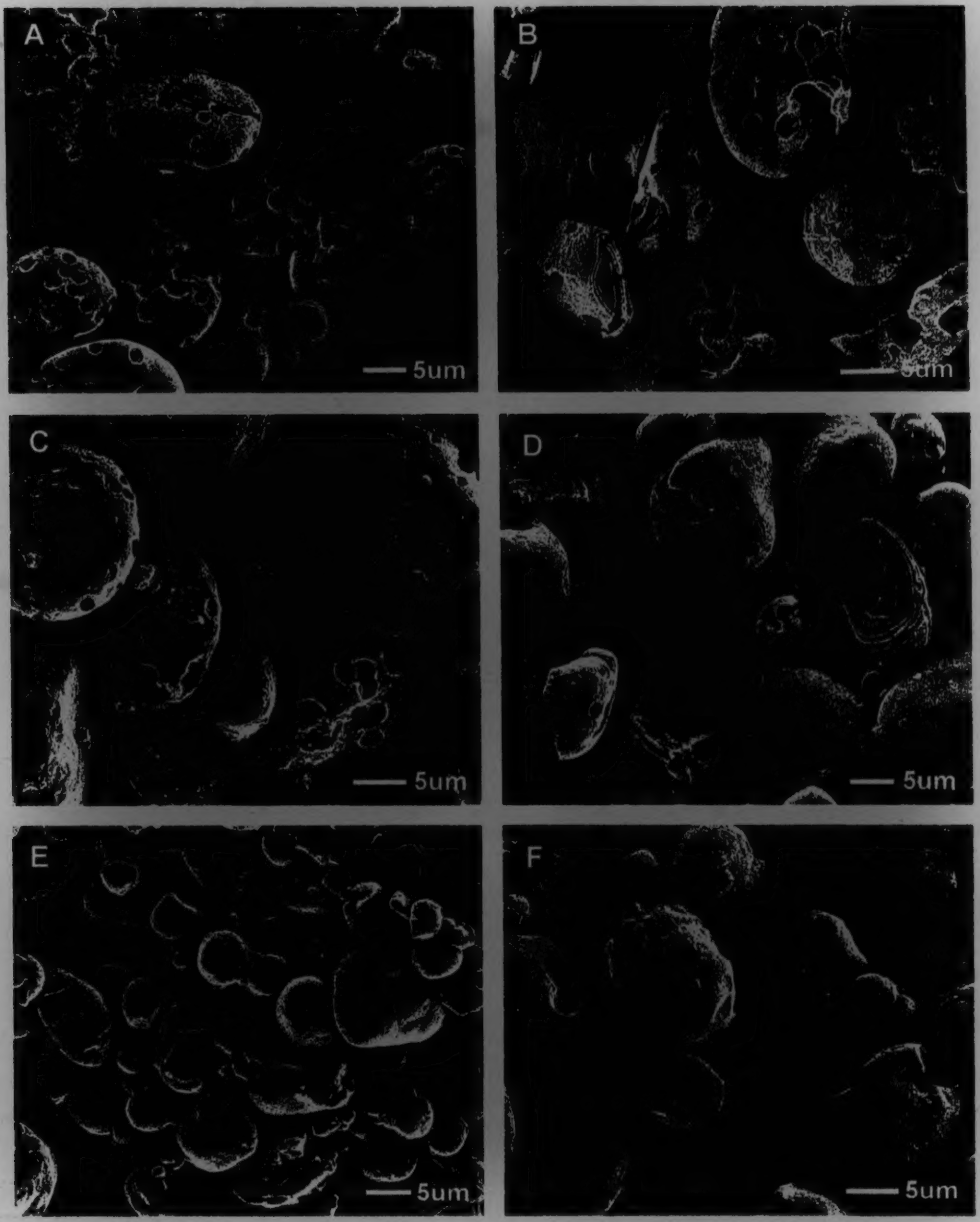

A
5um
B
5um
C
5um
D
5um
E
5um
F
5um

Figure 6-4 Scanning electron micrographs of HB starch granules from waxy (CDC Alamo) (A & B), normal (CDC Dawn) (C & D), and high-amylose (SB 94893) types (E & F) hydrolyzed by PPA at 37°C for 3h (A, C & E) and 6h (B, D & F).

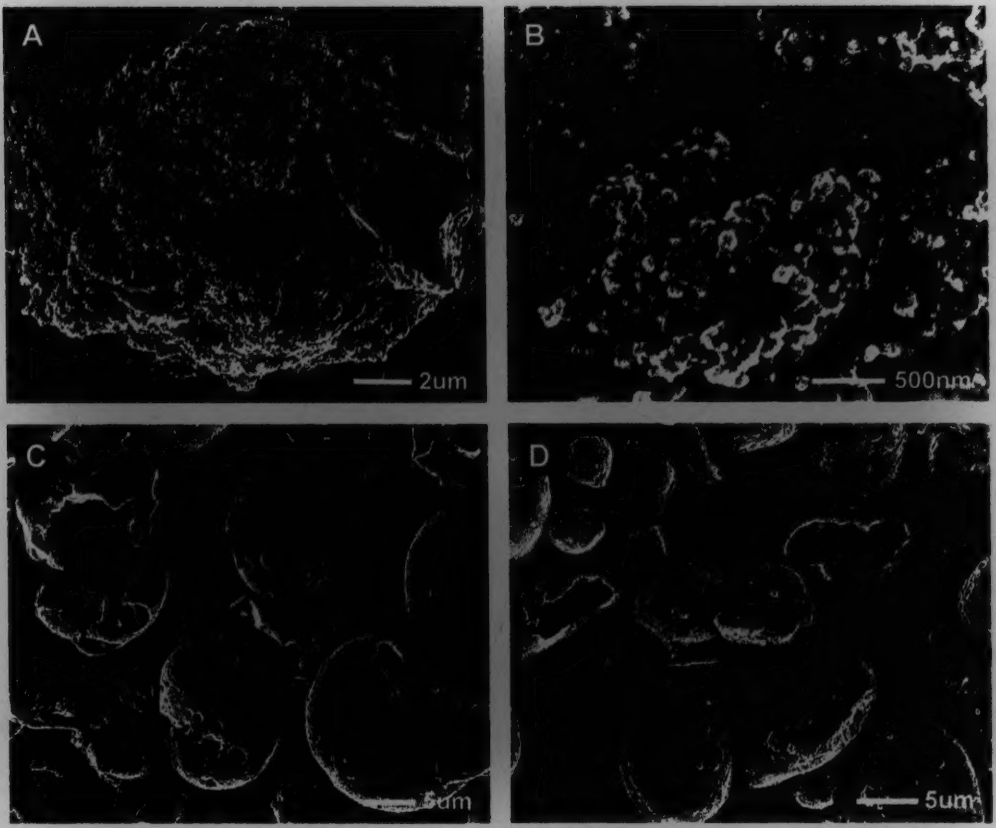
A
2um
B
500nm
C
5um
D
5um

Figure 6-5 Scanning electron micrographs of HB starch granules from waxy (CDC Alamo) (A & B), normal (CDC Dawn) (C), and high-amylose (SB 94893) types (D) hydrolyzed by PPA at 37°C for 21h.

Figure 6-6. After 21 h hydrolysis, wide, shallow and circular pits with internal layered structures were seen in the erosion areas of all three HB starches (Figure 6-6 A-C). The granules of waxy HB starch hydrolyzed by AAG were completely deformed and fragmented (Figure 6-6 A), whereas most granules in normal and high-amylose HB starches were less fragmented and deformed (Figure 6-6 B, C). Granules with thin shells and large hollows were frequently observed in normal and high-amylose HB starches (Figure 6-6 B, C). Compared with PPA hydrolysis, AAG hydrolysis was confined to the tangential direction of the granule (Figure 6-6).

6.3.4 Transmission electron microscopy

Transmission electron micrographs of the residues left after hydrolysis of waxy, normal and high-amylose HB starches by PPA and AAG are presented in Figures 6-7 and 6-8, respectively. After 3 h hydrolysis by PPA, hydrolyzed HB starch granules showed large cavities in their central region (Figure 6-7 A-C), suggesting that rapid hydrolysis may have occurred in the central region. Channels in the peripheral regions of the granule were present in all three native HB starches (Figure 6-7 A-C). These were more pronounced in waxy HB starch (Figure 6-7 A). A number of studies (Leach and Schoch, 1961; Valetudie et al., 1993; Herbert et al., 1996) have shown that channels in the granule periphery provide a pathway for the entry of enzymes into the granule interior. These channels may be derived from inherent surface pores/internal channels in starch granules and enlarged by enzyme hydrolysis (Kimura and Robyt, 1995). Several outer layers of granules were left with a sharp saw-toothed structure on the edge of fragments (Figure 6-7 A-C). These observations suggest that a relatively more rapid hydrolysis (along the tangential direction of granule) occurs in the amorphous

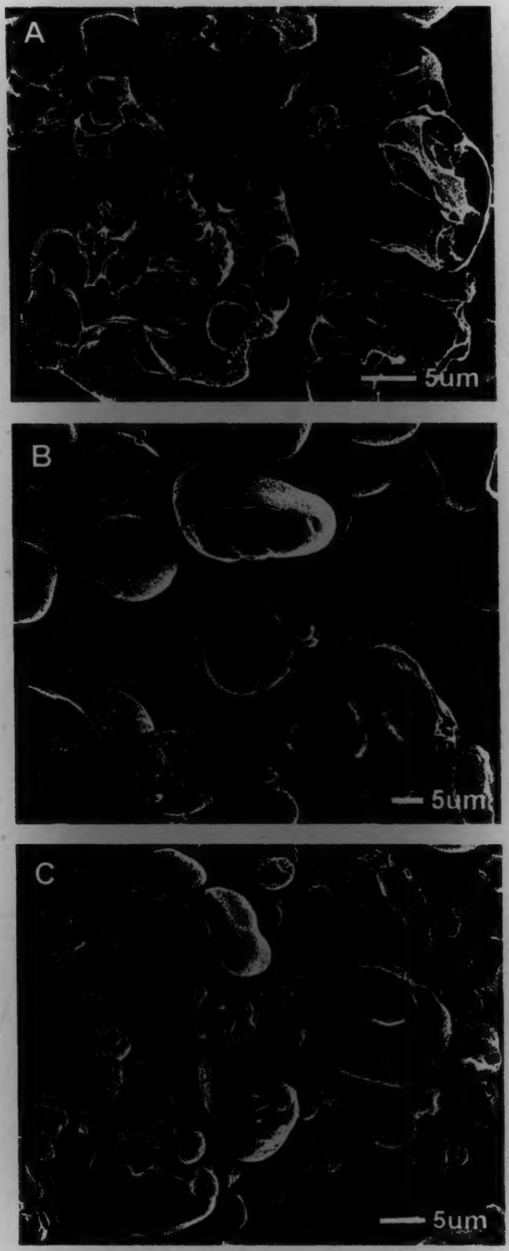

Figure 6-6 Scanning electron micrographs of HB starch granules from waxy (CDC Alamo) (A), normal (CDC Dawn) (B), and high-amylose (SB 94893) types (C) hydrolyzed by AAG at 55°C for 21h.

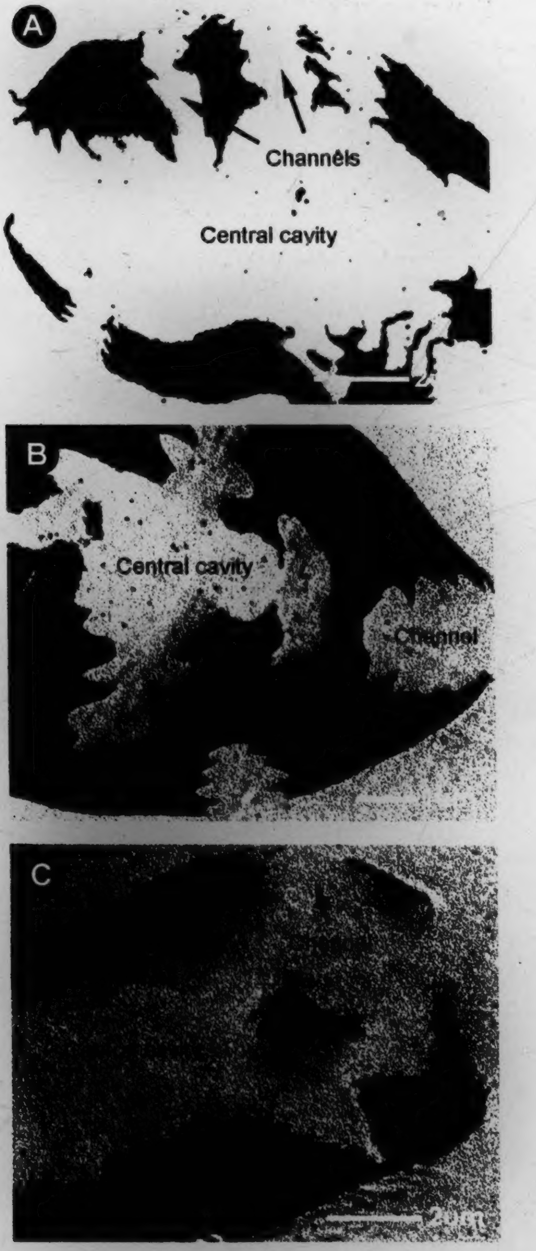
A
Channels
Central cavity
B
Central cavity
Channel
C
2μm

Figure 6-7 Transmission electron micrographs of HB starch granules from waxy (CDC Alamo) (A), normal (CDC Dawn) (B), and high-amylose (SB 94893) types (C) hydrolyzed by PPA at 37°C for 3h.

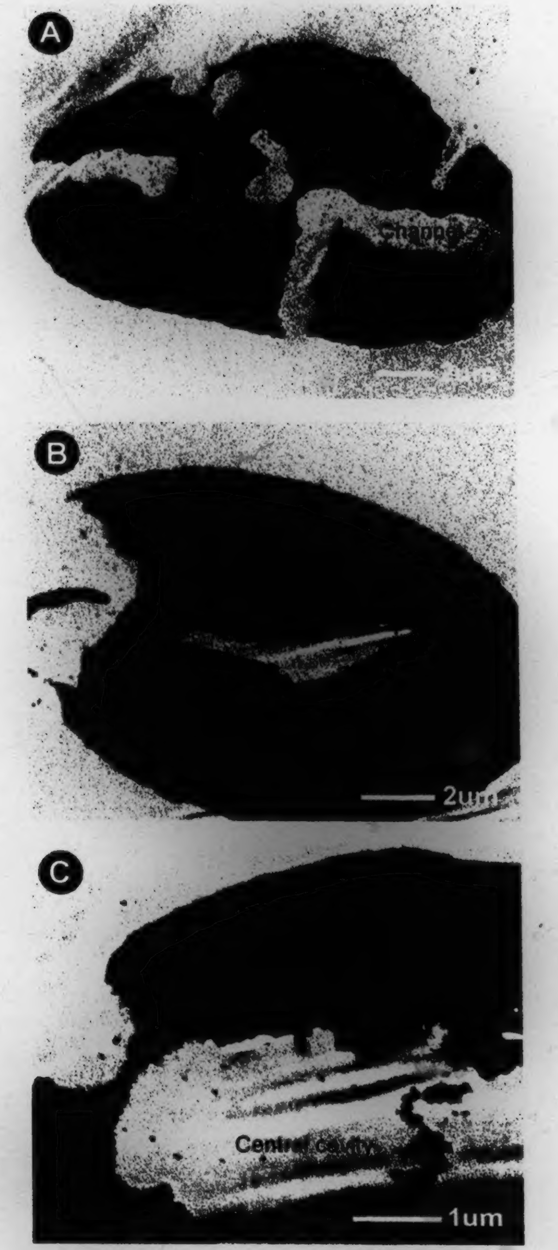
A
Channel
B
2um
C
Central cavity
1um

Figure 6-8 Transmission electron micrographs of HB starch granules from waxy (CDC Alamo) (A), normal (CDC Dawn) (B), and high-amylose (SB 94893) types (C) hydrolyzed by AAG at 55°C for 21h.

region (dark rings) than in the semi-crystalline region (light rings). The hydrolysis patterns of HB starches by PPA and BAA are similar to those of other cereal starches (Gallant et al., 1972; Gallant et al., 1992; Planchot et al., 1995), but differed with respect to some tuber starches (Gallant et al., 1992; Valetudie et al., 1993; Planchot et al., 1995). Valetudie et al. (1993) reported a difference in enzymatic action on yam starch between bacterial and pancreatic α-amylases. A sponge-like structure (numerous radial pores/canals) with bacterial α-amylase was formed in yam starch granules at the initial stage of hydrolysis, and fragmentation occurred at the final stage, whereas, a filamentous structure was retained with the resistant outer layer of granule in the residue of starch hydrolyzed by pancreatic α-amylase.

After 21 h hydrolysis of three HB starches by AAG, erosion areas were present in all three HB starch granules in the form of channels/pits varying in width and depth and central cavities (Figure 6-8 A-C). Channels/pits were present to a greater extent in waxy (Figure 8 A) than in normal and high-amylose HB starches (Figure 6-8 B, C). Channels in waxy HB starch granules were perpendicular to the granule surfaces (Figure 6-8 A). Furthermore, the saw-toothed edges observed during hydrolysis of HB starches by AAG were not as clearly visible (Figure 6-8) as those of PPA and BAA. The above observations suggest that amorphous (dark rings) and crystalline (light rings) regions of all three HB starch granules were hydrolyzed in a similar faction by AAG.

6.3.5 Hydrolysis products

The contents of glucose, maltose, and maltotriose in the hydrolysates of HB starches were determined by HPLC at different time periods of hydrolysis (Figure 6-9). The composition and concentration of soluble products during hydrolysis differed with starch and enzyme type and with the duration of hydrolysis. At the onset of hydrolysis, no sugars were detected by HPLC. When PPA and BAA hydrolysis of three HB starches progressed, glucose, maltose, and maltotriose were produced, whereas only glucose was detected during AAG hydrolysis. In all three starches, AAG hydrolysis (48 h) produced at least 2.8 times more glucose in waxy HB starch than in normal HB starch, and 3.3 times more than in high-amylose HB starches. Hydrolysis (1 h) of three HB starches by PAA produced more maltotriose (0.23-0.31 mg/mg starch, db) than glucose (0.01-0.03 mg/mg starch, db) and maltose (0.11-0.21 mg/mg starch, db) (Figure 6-9 A, C and E). With extensive hydrolysis of the three HB starches, the amount of maltose increased significantly and glucose increased slightly, while maltotriose content decreased greatly. After 72 h hydrolysis, the maltose content (0.52-0.54 mg/mg starch, db) was 2.3-4.3 times more than that of glucose (0.12-0.23 mg/mg starch, db) and maltotriose (0-0.03 mg/mg starch, db). These three sugars accounted for 68-75% of total starch in each starch source. During BAA hydrolysis (Figure 6-9 B, D, F), the contents of glucose, maltose, and maltotriose increased gradually in all three HB starches. However, the amount of maltose increased faster than that of maltotriose in waxy HB starch, whereas the content of maltose was lower than that of maltotriose in normal and high-amylose HB starches. After 72 h hydrolysis, the contents of glucose, maltose, and maltotriose were in the range of 0.01-0.07, 0.17-0.26, 0.17-0.25 mg/mg starch (db), respectively. These three sugars accounted for 40-51% of total starch in each HB starch. In general, the concentration and composition of hydrolysis

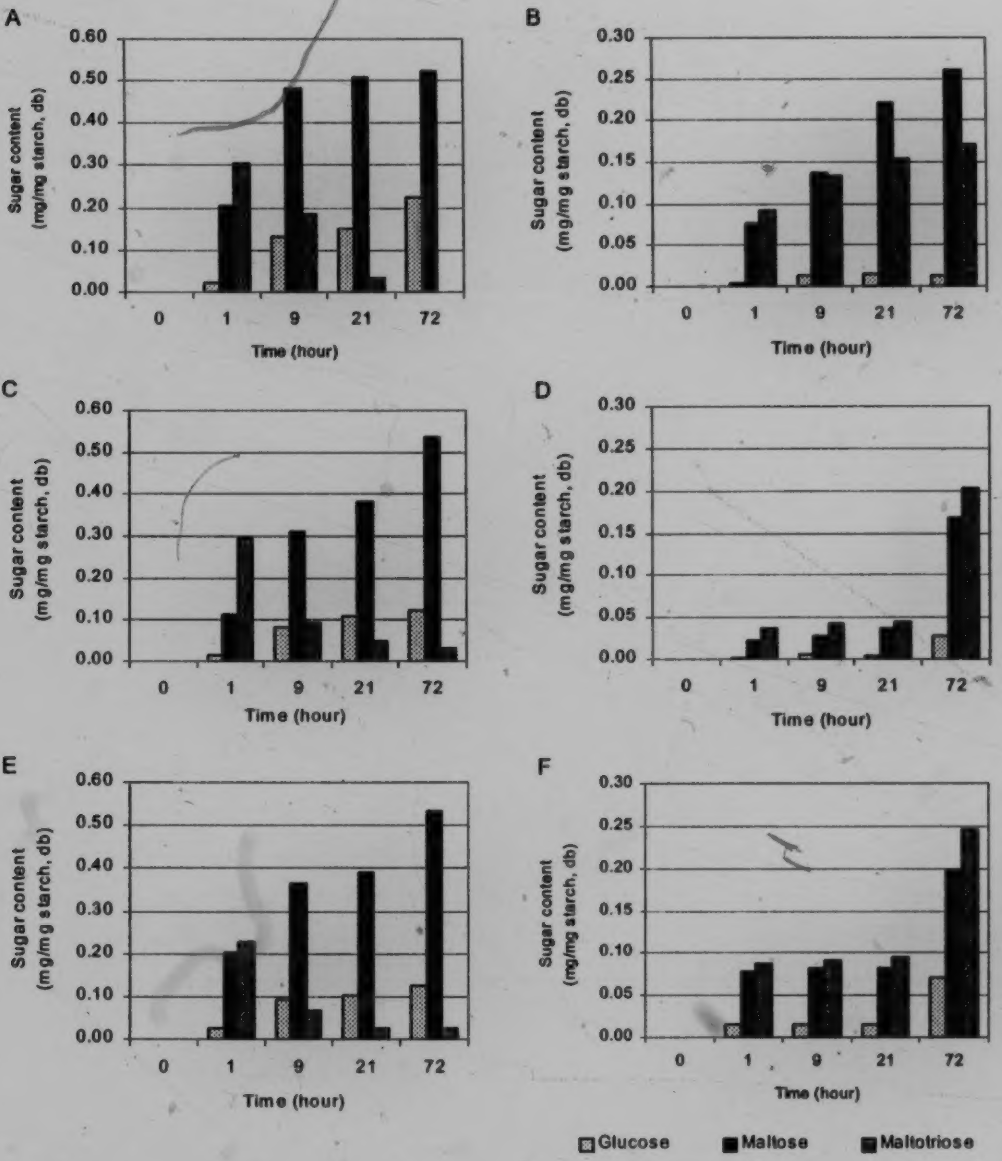

Figure 6-9 The contents of glucose, maltose, and maltotriose produced during HB starch hydrolysis by PPA (A, C, E) and BAA (B, D, F). A and B, waxy (CDC Alamo); C and D, normal (CDC Dawn); E and F, high-amylose (SB 94893).

products (predominantly glucose, maltose, and maltotriose) depended on enzyme source, origin and type of starch, and conditions of hydrolysis.

6.4 Conclusion

In vitro hydrolysis patterns of HB starches were dependent on enzyme source and starch types. Transmission electron microscopy showed the pathway of starch hydrolysis by α-amylase and amyloglucosidase. The rate of hydrolysis by PPA, BAA and AAG in waxy HB starch was higher than those of normal and high-amylose HB genotypes. The outer layers of normal and high-amylose HB starch granules were more resistant to enzyme hydrolysis. The concentration and composition of soluble sugars (glucose, maltose and maltotriose) in hydrolysates varied with enzyme source, starch types and the duration of hydrolysis. The study suggests that both morphological and ultrastructural features influence *in vitro* hydrolysis of HB starches.

6.5 References

Anger, H., Richter, M., Kettlitz, B., and Radosta, S. 1994. Hydrothermische Behandlung von Stärke in Gegenwart von α-Amylase Teil 1: Hydrolyse von Stärke mit α-Amylase in heterogener Phase. *Starch/Stärke*, 46: 182-186.

Appelqvist, I. A. M., and Debet, M. R. M. 1997. Starch-biopolymer interactions — a review. *Food Rev. Int.* 13: 163-224.

Bertoft, E. and Manelius, R. 1992. A method for the study of the enzymatic hydrolysis of starch granules. *Carbohydr. Res.* 227: 269-283.

Bertoft, E., Manelius, R., and Qin, Z. 1993. Studies on the structure of pea starches. Part 1. Initial stages in α-amylolysis of granular smooth pea starch. *Starch/Stärke* 45: 215-220.

Bruner, R. L. 1964. Determination of reducing value. In *Methods of Carbohydrate Chemistry*, R. L. Whistler ed., Vol. 4, p. 67. New York: Academic Press.

Colonna, P., Buléon, A, and Lemarié, F. 1988. Action of *Bacillus subtilis* α-amylase on native wheat starch. *Biotechnol. Bioeng.* 31: 895-904.

Colonna, P., Leloup, V., and Buléon, A. 1992. Limiting factors of starch hydrolysis. *Eur. J. Clin. Nutr.* 42: S17-S32.

Evers, A. D. and McDermott, E. E. 1970. Scanning electron microscopy of wheat starch II. Structure of granules modified by alpha-amylolysis — preliminary report. *Starch/Stärke*, 22: 23-26.

Franco, C. M. L. and Ciacco, C. F. 1987. Studies on the susceptibility of granular cassava and corn starches to enzymatic attack. *Starch/Stärke*, 39: 432-435.

French, D. 1984. Organization of starch granules. In *Starch: Chemistry and Technology*. R. L. Whistler, J. N. Miller, and E. F. Paschall eds., p.183-248. New York: Academic Press.

Fuwa, H., Sugimoto, Y., and Takaya, T. 1979. Scanning electron-microscopy of starch granules, with or without amylase attack. *Carbohydr. Res.* 70: 233-238.

Fuwa, H., Sugimoto, Y., Tanaka, M., and Glover, D. V. 1978. Susceptibility of various starch granules to amylases as seen by scanning electron microscope. *Starch/Stärke*, 30: 186-191.

Gallant, D, Mercier, C. and Guilbot, A. 1972. Electron microscopy of starch granules modified by bacterial α-amylase. *Cereal Chem.* 49: 354-365.

Gallant, D. J., Bouchet, B., and Baldwin, P. M. 1997. Microscopy of starch: evidence of a new level of granule organization. *Carbohydr. Polym.* 32: 177-191.

Gallant, D. J., Bouchet, B., Buléon, A., and Pérez, S. 1992. Physical characteristics of starch granules and susceptibility to enzymatic degradation. *Eur. J. Clin. Nutr.* 46: S3-S16.

Garcia, V., Colonna, P., Bouchet, B., and Gallant, D. J. 1997. Structural changes of cassava starch granules after heating at intermediate water contents. *Starch/Stärke*, 49: 171-179.

Gérard, C., Colonna, P., Buléon, A., and Planchot, V. 2001. Amylolysis of maize mutant starches. *J. Sci. Food Agric.* 81: 1281-1287

Helbert, W., Schülein, M., and Henrissat, B. 1996. Electron microscopic investigation of the diffusion of bacillus licheniformis α-amylase into corn starch granules. *Int. J. Bio. Macromol.* 19:165-169.

Hoover, R., and Sosulski, F. W. 1991. Composition, structure, functionality, and chemical modification of legume starches: a review. *Can. J. Physiol. Pharmacol.* 69: 79-92.

Hoover, R. 2001. Composition, molecular structure, and physicochemical properties of tuber and root starches: a review. *Carbohydr. Polym.* 45: 253-267.

Huber, K. C. and BeMiller, J. N. 2000. Channels of maize and sorghum starch granules. *Carbohydr. Polym.* 41: 269-276.

Kimura, A. and Robyt, J. F. 1995. Reaction of enzymes with starch granules: kinetics and products of the reaction with glucoamylase. *Carbohydr. Res.* 277: 87-107.

Knutson, C. A., Khoo, U., Cluskey, J. E., and Inglett, G. E. 1982. Variation in enzyme digestibility and gelatinization behavior of corn starch granule fractions. *Cereal Chem.* 59: 512-515.

Koba, Y., Saha, B. C. and Ueda, S. 1986. Adsorption on and digestion of raw starch by malt and bacterial alpha-amylases. *J. Jpn. Soc. Starch Sci.* 33: 199-201.

Kurakake, M., Tachibana, Y., Masaki, K., and Komaki, T. 1996. Adsorptions of alpha-amylase on heat-moisture treated starch. *J. Cereal Sci.* 23: 163-168.

Lauro, M., Forssell, P. M., Suortti, M. T., Hulleman, S. H. D., and Poutanen, K. S. 1999. α-amylolysis of large barley starch granules. *Cereal Chem.* 76: 925-930.

Lauro, M., Suortti, T., Autio, K., Linko, P., and Poutanen, K. 1993. Accessibility of barley starch granules to α-amylase during different phases of gelatinization. *J. Cereal Sci.* 17: 125-136.

Leach, H. W. and Schoch, T. J. 1961. Structure of the starch granule. II. Action of various amylase on granular starches. *Cereal Chem.* 38: 34-46.

MacGregor, A. W. 1979. Isolation of large and small granules of barley starch and a study of factors influencing the adsorption of barley malt α-amylase by these granules. *Cereal Chem*. 56: 430-434.

MacGregor, A. W., Ballance, D. L. 1980. Hydrolysis of large and small starch granules from normal and waxy barley cultivars by alpha-amylases from barley malt. *Cereal Chem*. 57: 397-402.

Morrison, W. R. 1995. Starch lipids and how they relate to starch granule structure and functionality. *Cereal Foods World*, 40: 437-446.

Nigam, P. and Singh, D. 1995. Enzyme and microbial systems involved in starch processing. *Enzyme Microb. Technol*. 17: 770-778.

Planchot, V., Colonna, P., Gallant, D. J., and Bouchet, B. 1995. Extensive degradation of native starch granules by alpha-amylase from *Aspergillus fumigatus*. *J. Cereal Sci*. 21: 163-171.

Rasper, V., Perry, G., and Duitschaever, C. L. 1974. Functional properties of non-wheat flour substitutes in composite flours. II. Amylolytic susceptibility of non-wheat starches. *Can. Inst. Food Sci. Technol. J*. 7: 166-174.

Rickard, J. E., Asaoka, M., and Blanshard, J. M. V. 1991. The physico-chemical properties of cassava starch. *Trop. Sci*. 31: 189-207.

Smith, J. S. and Lineback, D. R. 1976. Hydrolysis of native wheat and corn starch granules by glucoamylases from *Aspergillus niger* and *Rhizopus niveus*. *Starch/Stärke*, 28: 243-249.

Tharanathan, R. N., and Ramadas Bhat, U. 1988. Scanning electron microscopy of chemically treated black gram (*Phaseolus mango*) and ragi (*Eleusine coracana*) starch granules. *Starch/Stärke*, 40: 378-382.

Valetudie, J. C., Colonna, P., Bouchet, B., and Gallant, D. J. 1993. Hydrolysis of tropical tuber starches by bacterial and pancreatic α-amylases. *Starch/Stärke*, 45: 270-276.

Vasanthan, T. and Bhatty, R. S. 1996. Physicochemical properties of small- and large-granule starches of waxy, regular, and high-amylose barleys. *Cereal Chem*. 73, 199-207.

Vasanthan, T., Yeung, J., and Hoover, R. 2001. Dextrinization of starch in barley flours with thermostable alpha-amylase by extrusion cooking. *Starch/Stärke*, 53: 616-622.

Wolf, B. W., Bauer, L. L., and Fahey Jr., G. C. 1999. Effects of chemical modification on in vitro rate and extent of food starch digestion: an attempt to discover a slowly digested starch. *J. Agric. Food Chem*. 47: 4178-4183.

CHAPTER 7

Conclusions and Recommendations

Starches were extracted from ten HB genotypes [waxy (CDC Alamo, CDC Candle, SB 94912, and SB 94917), normal (Phoenix, CDC Dawn, SR 93102, and SB 94860), and high-amylose (SB 94893 and SB 94897)] and their composition and physicochemical properties were determined. The morphological and ultrastructural changes during heating in water at various temperatures and the susceptibility of starches towards amylolysis were also examined.

Starch content in HB grains ranged from 56 to 65%. The purity of the isolated starches was greater than 96%. Average starch yield and extraction efficiency were 44% and 71%, respectively. The starches from all genotypes consisted of a mixture of large lenticular and small irregularly shaped granules. The granules of most starches were intact, whereas in others (SB 94917, SR 93102, and SB 94860) they were compound (clustered). The proportions of small (diameter ≤ 10μm) and large (diameter > 10μm) granules by total number and by total weight differed among genotypes. Bound lipid content was positively correlated ($r = 0.92$, $P < 0.01$) with total amylose content. Free and bound lipid content ranged from 0.1-0.3% and 0.3-1.7%, respectively. The apparent and total amylose contents ranged from 0-39% and 0-45%, respectively. The amounts of amylose complexed with native lipids (total amylose - apparent amylose) ranged from 0.5-7.8%. The proportion of small granules was positively correlated with total amylose content ($r = 0.59$, $P < 0.1$). However, the average granule diameter was negatively correlated ($r = -0.65$, $P < 0.05$) with total amylose content. The debranched amylopectins of all starches exhibited the highest peak in the MALDI-MS spectrum at degree of polymerization (DP) 12. The average chain length (CL) and degree of branching ranged from 17.6-22.7 anhydro-glucose units and 4.4-5.5%, respectively. The proportion of short (DP 5-17) and long (DP ≥ 35) chains ranged from 58.2-59.1% and 3.0-12.8%, respectively. The study showed that amylose/amylopectin ratio and amylopectin branch chain length were highly correlated with starch granule size and size distribution in this set of barley genotypes.

Gelatinization, granular swelling, amylose leaching, viscosity and acid susceptibility characteristics of ten HB starches were monitored by DSC, swelling power, solubility, Brabender viscoamylography, and hydrolysis with 2.2N HCl (at 35°C), respectively. DSC data showed that T_o, T_p, T_c, T_c-T_o, and ΔH ranged from 50.1-56.1°C, 58.1-64.5°C, 71.0-75.8°C, 17.9-24.0°C and 9.6-14.2 J/g of amylopectin, respectively. In compound waxy (SB 94917) and compound normal (SR 93102 and SB 94860) starches, T_o and T_c-T_o were lower and higher, respectively, than that of the other starches. ΔH followed the order: compound normal > waxy > normal ≈ zero amylose > high amylose > compound waxy. Swelling power (SP) followed the order: zero amylose > waxy > compound normal > normal > high amylose. A rapid increase in solubility occurred at lower temperatures (< 70°C) for zero-amylose HB starch; however, this increase was gradual for the other starches. At 90°C, solubility followed the order: high-amylose > compound normal > normal > waxy. Zero-amylose and waxy HB starches exhibited lower pasting temperatures, higher peak viscosities, and higher viscosity breakdown than did normal HB starches. The extent of acid hydrolysis followed the order: zero-amylose > compound waxy > waxy > normal > compound normal > high-amylose. High correlations were observed between physicochemical properties and structural characteristics of HB starches.

Scanning electron microscopic (SEM) and transmission electron microscopic (TEM) studies of the structure of waxy, normal, and high-amylose starch granules showed two distinct regions of different sizes within granules: 1) densely packed granule growth rings (which varied in size and number depending on the genotype), and 2) a loose filamentous network located in the central region of the granule. Granule ring width decreased with increasing amylose content. In all three genotypes, the growth rings closer to the granule surface were narrower in width than those in the granule interior. Waxy starch had wider inter-crystalline amorphous growth rings, semi-crystalline growth rings, and more open crystalline lamellae than did normal and high-amylose starches. Granule bound proteins (mainly integral proteins) were located in the central and peripheral (growth ring) regions of the granule.

Morphological and ultrastructural changes in waxy, normal and high-amylose HB starch granules heated in water to various temperatures were examined by SEM and TEM. Swelling and gelatinization/solubilization patterns of waxy HB starch were different from those of non-waxy HB starches. Waxy HB starch granules were split into two halves with a large cavity in the central region of the granule and started melting at the equatorial grooves during heating in water to 55°C, whilst only a small amount of molecules leached out of granules. Heating resulted in rapid fragmentation of granules at temperatures exceeding 55°C. With increasing temperature, the extent of release of the exudate became more pronounced while swollen starch granules remained intact in non-waxy HB starches. Knobs/protrusions (200-400 nm diameter) were present on the granule surfaces of non-waxy HB starches during gelatinization, but were not present on the granule surface of gelatinized waxy HB starch. Ghost structure was formed and embedded in exudate/soluble matrix with a web network within ghosts at

90-100°C. Bundles of brush-like strands in the exudate of high-amylose starch were formed after heating. Fine particles (~10 nm diameter) arranged into chains were present on the granule remnants of all three types of barley starches. MALDI-MS analysis showed that the distribution of branched chains in leached (at 65°C) amylopectin was similar in both waxy and non-waxy HB starches. An increase in heating temperature from 65°C to 100°C increased the molecular size and branch chain length of the leached amylopectin fraction from high-amylose HB starch. The chain length distribution of amylopectin was identical in both the soluble and insoluble fractions obtained by heating high-amylose HB starch in water to 100°C.

The susceptibilities of waxy (CDC Alamo), normal (CDC Dawn), and high-amylose (SB 94893) HB starches to porcine pancreatic alpha-amylase (PPA), *Bacillus* species alpha-amylase (BAA), and *Aspergillus niger* amyloglucosidase (AAG) were determined. Scanning and transmission electron micrographs showed that the patterns of enzyme hydrolysis (surface erosion, endoerosion, and erosion at the equatorial groove plane) were dependent on the enzyme source and starch type. The outer layers of normal and high-amylose HB starch granules were more resistant to enzyme hydrolysis. The hydrolysis rates of waxy HB starch by the three amylases at 37°C were significantly higher than those of normal and high-amylose HB starches. The degree of hydrolysis by PPA, after 72 h, reached 91-97% in all three starches. However, BAA and AAG showed significantly less hydrolysis in normal (< 30%) and high-amylose (< 37%) HB starches than in waxy HB starch (> 67%). Glucose, maltose, and maltotriose contents of the hydrolysates, collected at different time intervals, were determined by HPLC. The concentration and composition of soluble sugars in hydrolysates varied with enzyme source, starch type, and conditions of hydrolysis. The study suggested that both morphological and ultrastructural features influence *in vitro* hydrolysis, and that the ultrastructure of waxy HB starch may be more open than those of normal and high-amylose HB starches.

In general, starches, from the ten hull-less barley genotypes studied, differed in chemical composition, morphology, granule size, size distribution and amylopectin branch chain length distribution. The physicochemical properties of HB starches were differently influenced by the interplay of: 1) small granule size; 2) proportion of small granules by number and weight; 3) level of amylose-lipid complexes; 4) amylose content; 5) magnitude of interaction between starch chains within the amorphous and crystalline domains; and 6) double helical content. Substantial differences in ultrastructure in terms of crystallite formation, the number and size of crystalline/amorphous lamellae, amylopectin chain length, and association with minor components (i.e. protein) exist among HB starch granules. Based on the series of studies presented in this thesis, an ultrastructural model of the HB starch granule was perceived schematically and presented in Figure 7-1. The model agrees with the physicochemical characteristics of the HB starches investigated in this research. The schematic diagram illustrates the following: (1) In all HB starches, the growth ring width decreases gradually from the center to the periphery of the granule indicating a lower number of (amorphous and crystalline) lamellae layers at the periphery of the granule. The central region becomes larger with an increase in amylose content (possibly due to more interspersed amylose in the central region of the granule). (2) In waxy or zero-amylose HB starches, the lower percentage of longer amylopectin B-chains (primarily B3 or more) that connect amylopectin clusters and the absence of amylose leads to a more open granule ultrastructure. Such an open structure would have a higher

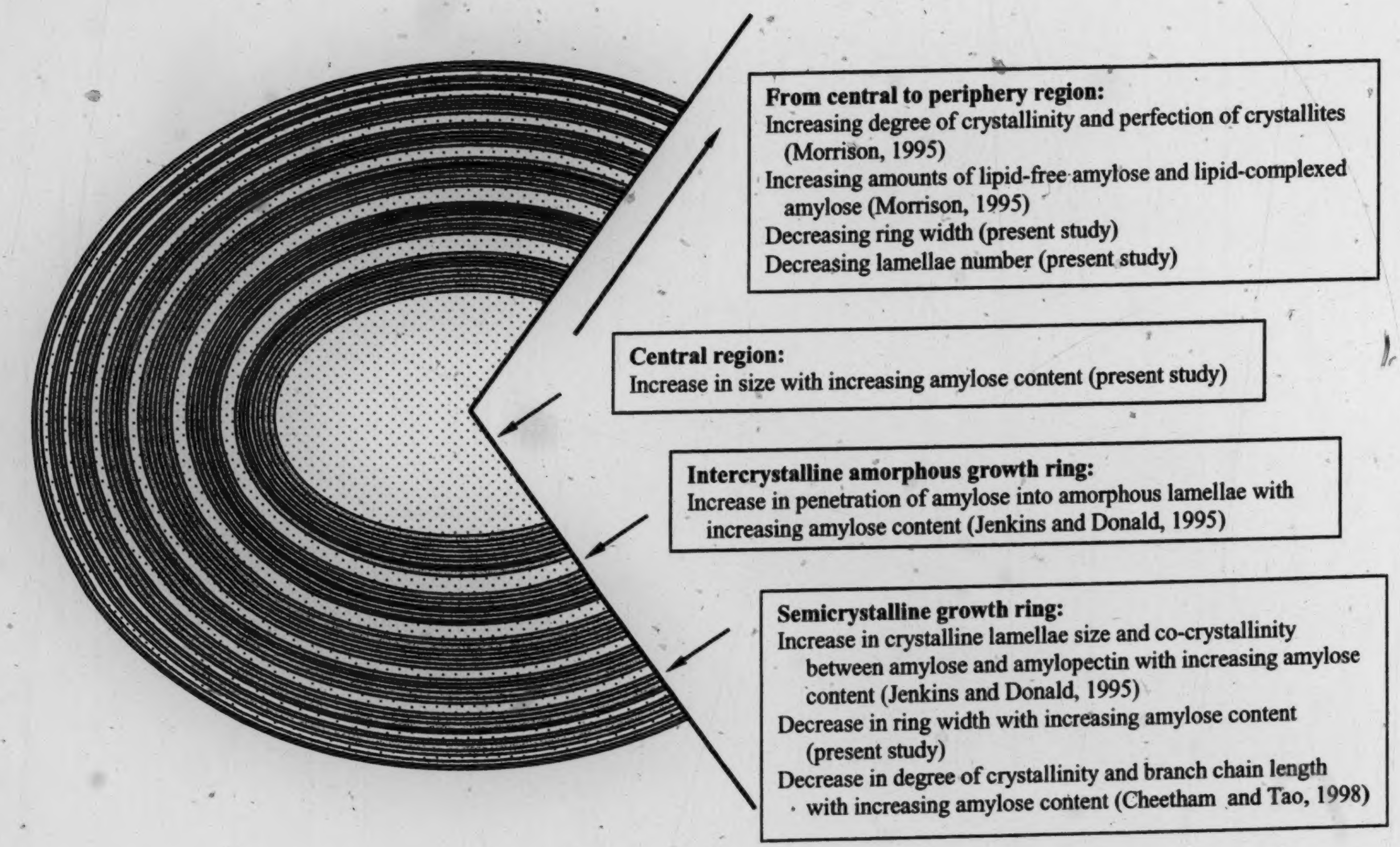

From central to periphery region:
Increasing degree of crystallinity and perfection of crystallites (Morrison, 1995)
Increasing amounts of lipid-free amylose and lipid-complexed amylose (Morrison, 1995)
Decreasing ring width (present study)
Decreasing lamellae number (present study)

Central region:
Increase in size with increasing amylose content (present study)

Intercrystalline amorphous growth ring:
Increase in penetration of amylose into amorphous lamellae with increasing amylose content (Jenkins and Donald, 1995)

Semicrystalline growth ring:
Increase in crystalline lamellae size and co-crystallinity between amylose and amylopectin with increasing amylose content (Jenkins and Donald, 1995)
Decrease in ring width with increasing amylose content (present study)
Decrease in degree of crystallinity and branch chain length with increasing amylose content (Cheetham and Tao, 1998)

Figure 7-1 Schematic diagram of a HB starch granule detailing the ultrastructural features.

tendency to bind water (higher swelling) during heating/gelatinization and would have an increased susceptibility towards acid and enzyme hydrolysis as compared to non-waxy HB starches that have a more compact structure; (3) In non-waxy starches, a higher degree of co-crystallization is likely at the periphery of the granules. This would explain the higher resistance of these granules towards heating and acid/enzyme hydrolysis.

Most of the image observations of HB starch granule ultrastructure presented in this thesis were based on large granules. Further research is needed to reveal the structural differences between large and small granules. Also, studies on the location and distribution of amylose within large and small starch granules are important. In addition, studies on the interactions of HB starch with other food components such as protein, hydrocolloids, lipids, and β-glucan in complex systems are needed to expand HB starch applications in food and non-food industries. Understanding starch properties in the presence of other components and their interaction is very important for better control and for improving the texture and other quality attributes of starch-based foods. The mixed systems of starch plus other components may have unique properties and provide processing advantages to improve existing products and to develop new novel products for food and non-food industries.

7.1 References

Cheetham, N. W. H. and Tao, L. 1998. Variation in crystalline type with amylose content in maize starch granules: an X-ray powder diffraction study. *Carbohydr. Polym.* 36: 277-284.

Jenkins, P. J., and Donald, A. M. 1995. The influence of amylose on starch granule structure. *Int. J. Biol. Macromol.* 17: 315-321.

Morrison, W. R. 1995. Starch lipids and how they relate to starch granule structure and functionality. *Cereal Foods World.* 40: 437-446.

PUBLICATIONS

Li, J. H., Vasanthan, T., Hoover, R., and Rossnagel, B. 2004. Starch from hull-less barley: V. In-vitro susceptibility of waxy, normal, and high-amylose starches towards hydrolysis by alpha-amylases and amyloglucosidase. *Food Chemistry*. 84: 621-632.

Li, J. H., Vasanthan, T., Hoover, R., and Rossnagel, B. 2004. Starch from hull-less barley: IV. Morphological and structural changes in waxy, normal and high-amylose starch granules during heating. *Food Research International*. (In press)

Li, J. H., Vasanthan, T., Hoover, R., and Rossnagel, B. 2003. Starch from hull-less barley: III. Ultra-structure and distribution of granule-bound proteins. *Cereal Chemistry*. 80: 524-532.

Li, J. H. and Vasanthan, T. 2003. Hypochlorite oxidation of field pea starch and its suitability for noodle making using an extrusion cooker. *Food Research International*. 36: 381-386.

Vasanthan, T., Jiang, G. S., Yeung, J., and Li, J. H. 2002. Dietary fibre profile of barley flour as affected by extrusion cooking. *Food Chemistry*. 77: 35-40.

Li, J. H., Vasanthan, T., Rossnagel, B., and Hoover, R. 2001. Starch from hull-less barley: I. Granule morphology, composition, and amylopectin structure. *Food Chemistry*. 74: 395-405.

Li, J. H., Vasanthan, T., Rossnagel, B., and Hoover, R. 2001. Starch from hull-less barley: II. Thermal, rheological and acid hydrolysis characteristics. *Food Chemistry*. 74: 407-415.

APPENDIX A

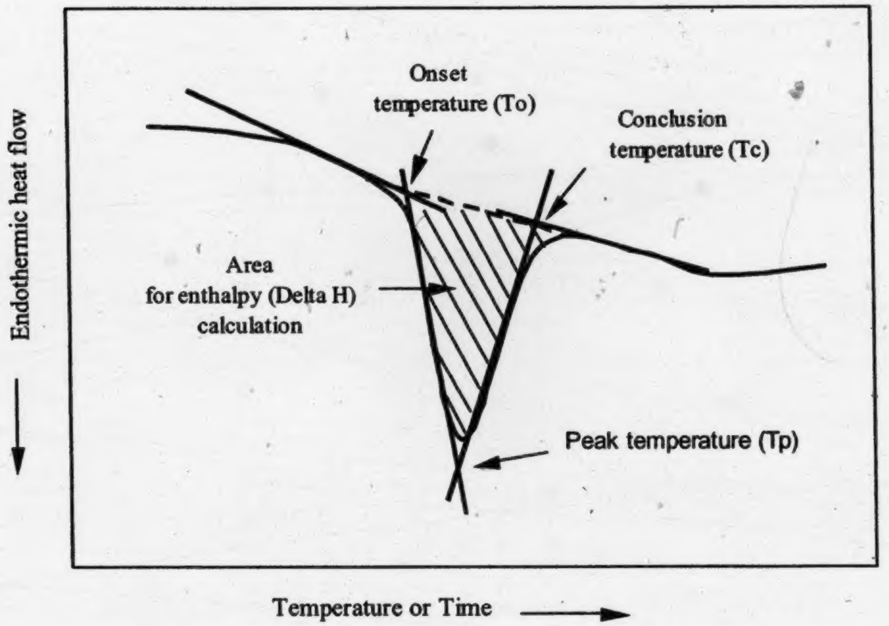
Onset
temperature (To)
Conclusion
temperature (Tc)
Area
for enthalpy (Delta H)
calculation
Peak temperature (Tp)
Endothermic heat flow
Temperature or Time

DSC thermogram showing measurement of thermal parameters

APPENDIX B

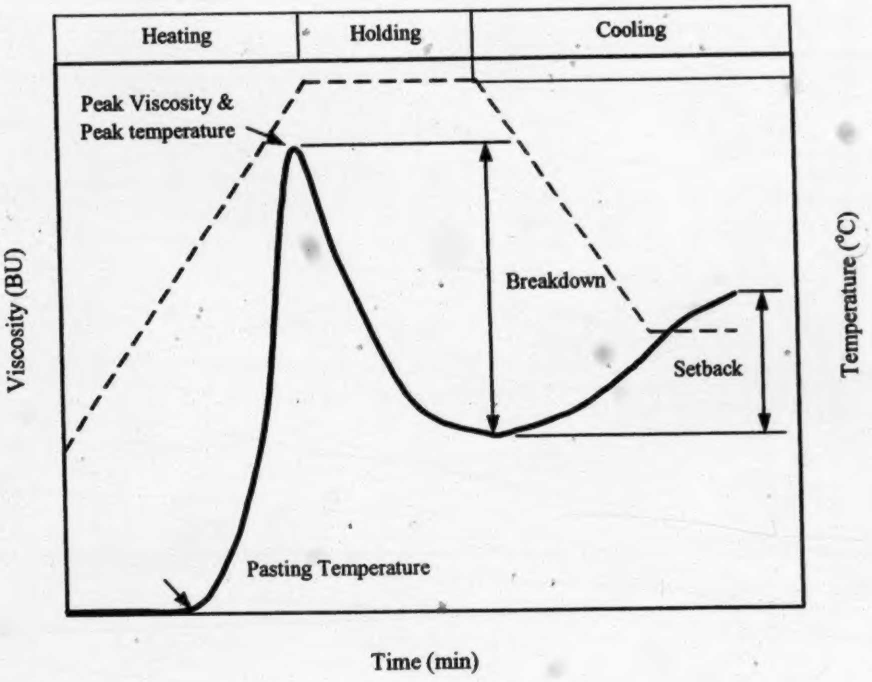
Heating
Holding
Cooling
Peak Viscosity &
Peak temperature
Breakdown
Setback
Pasting Temperature
Viscosity (BU)
Temperature (°C)
Time (min)

A pasting cycle curve showing definition of pasting parameters.